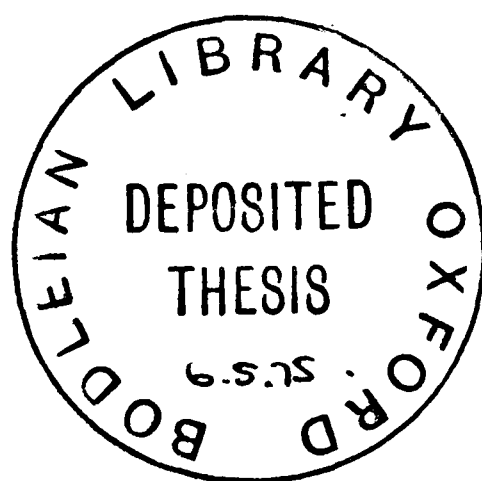


Thesis Submitted for the Degree of Doctor of Philosophy
in the University of Oxford

STRONTIUM ISOTOPE STUDIES
OF SEDIMENTARY ROCKS

by

Adrian H. Bath



Keble College

and

Department of Geology and Mineralogy

Oxford University

1974

ABSTRACT

The present investigation has been undertaken in an attempt to clarify the effects of the physico-chemical conditions encountered during burial diagenesis and very low-grade metamorphism on the Rb-Sr systems of the various components of argillaceous sediments. Two methods of study have been used: (a) comparison of Rb-Sr data from suites of variably metamorphosed argillites, and (b) an investigation of the mobility of Rb and Sr in a clay-water system under metamorphic conditions simulated in the laboratory.

A suite of Lower Silurian (Upper Llandovery) mudstones (clay fraction consisting of mixed-layer illite-smectite+kaolinite) gives whole-rock Rb-Sr isotope data which form a non-linear array on an isochron diagram. A best-fit line through all data points represents an age of ca. 510 m.y., which may be compared with an estimate of ca. 420 m.y. for the true stratigraphic age. This is interpreted as reflecting the multi-component nature of the sediment, the components ranging from detrital minerals (e.g. kaolinite and possibly illite) and partially transformed mixed-layer minerals, to authigenic phases (e.g. calcite). This interpretation is amplified by data from within-sample size-fractions, whose Rb-Sr model ages decrease towards the estimated age of deposition as the grain size decreases.

In contrast, a suite of folded and cleaved shales (illite + chlorite clay assemblage), of identical stratigraphic age, yields a whole-rock Rb-Sr isochron age of 382 ± 12 m.y. ($\lambda = 1.39 \times 10^{-11} \text{ yr}^{-1}$), i.e. significantly younger than deposition. A period of Sr-isotope homogenization throughout the section sampled, followed by a closure at ca. 382 m.y. of the system to further redistribution of Rb or Sr on a scale greater than that of intergranular distances, is inferred. This age is concordant with previous ages from the southern Caledonides, and it

is suggested that the Rb-Sr system responded to metamorphic recrystallization of metastable degraded clay minerals to a stable illite + chlorite paragenesis in the presence of a continuous fluid phase. Furthermore, whole-rock samples from thin meta-bentonite bands within these shales, though frequently separated by many metres of clastic sediment, define a perfect Rb-Sr isochron corresponding to 298 ± 7 m.y. This date, significantly younger than the 382 ± 12 m.y. date yielded by the subjacent shales, is considered to reflect a further episode of metamorphic recrystallization concurrent with the superposition of the Hercynian structural trends now observed in these strata. The disparity between this response from bentonites and the maintenance of closed system behaviour by the subjacent shales is tentatively explained as being due to the survival of a metastable assemblage in the bentonites through the earlier Caledonian metamorphism. Kinetic and thermodynamic factors, and the role of a fluid phase, which are relevant to this interpretative problem are discussed.

Rb-Sr studies of size-fractions separated from two samples of these shales reveal a remobilisation of Sr over intergranular distances subsequent to the whole-rock system closure at ca. 382 m.y. Model ages for these fractions decrease with grain-size, from a maximum close to the whole-rock age to ages close to 300 m.y. for the 0.2-1 μm fractions. Further data from clay fractions from several samples yield a Rb-Sr isochron age which is indistinguishable from that from the whole-rocks, but give a significantly lower initial $^{87}\text{Sr}/^{86}\text{Sr}$ ratio. Both of these sets of data reflect a systematic depletion of radiogenic ^{87}Sr in the finer fractions; models to interpret this grain-size effect are discussed.

In the second part of this investigation, a degraded clay assemblage has been subjected to an experimental simulation of conditions experienced during deep burial or low-grade metamorphism. The dependences of the

rates of exchange of Rb and Sr from clay to fluid on three parameters: temperature, time, and fluid composition, have been studied. Experimental runs were carried out in the presence of 1 molar Na^+ , K^+ and Mg^{2+} brines at temperatures of 315°C , 340°C and 360°C for durations of up to 306 hours. Exchange of Rb and Sr between clay and fluid, the rate-determining process in Sr-isotope homogenization in sedimentary systems, has been measured by means of isotope dilution analysis of the fluids on completion of experimental runs. Changes in the nature of the solid phases during experiments have also been monitored. The measured rates of Rb and Sr exchange show contrasting dependences on fluid composition. These observations, and the rate dependence on temperature, are discussed in relation to two basic models for the exchange processes.

Finally, the feasibility of obtaining useful chronostratigraphic information from whole-rock Rb-Sr studies on sediments has been tested on two successions which present particular stratigraphic problems.

The Longmyndian succession in Shropshire has previously been considered to be late Precambrian. Fine-grained whole-rock samples from three lithological groups, near to the base of the succession, yield well-defined isochrons. One such isochron, from the Burway Group, corresponds to an age of 529 ± 6 m.y., with an initial $^{87}\text{Sr}/^{86}\text{Sr}$ ratio of $0.7061 \pm .0001$. This enables a maximum limit of ca. 600 m.y. to be placed on the depositional age of these sediments, i.e. considerably younger than had previously been assumed.

Argillaceous horizons in the Cambrian successions of the Harlech Dome and the Caernarvonshire Slate Belt in North Wales were sampled, each suite of samples yielding an Rb-Sr isochron. The lower horizon sampled in the Harlech Dome, the Llanbedr Slates, gave a whole-rock Rb-Sr age of 467 ± 40 m.y.; whilst the fossiliferous Middle Cambrian Clogau Shales from the same succession gave an age of 409 ± 20 m.y. The

Purple Slate group from Nantlle in Caernarvonshire gave an Rb-Sr age of 393 ± 22 m.y. The latter two, statistically indistinguishable, ages are considered to date Caledonian metamorphism and folding. The former age of ca. 467 m.y. from the unfossiliferous ? Lower Cambrian Llanbedr Slates suggests that local recrystallization of clay minerals was induced prior to the regional metamorphism at ca. 400 m.y. This may have been due either to diagenetic recrystallization, or more probably to the temporary thermal effects of mid-Ordovician dyke intrusion. The suggested equivalence of the Purple Slates at Nantlle and the Llanbedr Slates in the Harlech Dome, is challenged by considerations based on the initial $^{87}\text{Sr}/^{86}\text{Sr}$ ratios on the respective isochrons.

ACKNOWLEDGEMENTS

I thank Dr. R.K. O'Nions for much assistance and active encouragement in all phases of this project; he initially suggested this project, and has given freely of his time in stimulating discussion and the constructive criticism of manuscripts.

I am grateful to Professor E.A. Vincent for allowing me use of the facilities of the Department of Geology and Mineralogy in Oxford. I am indebted to Dr. S. Moorbath, Dr. N.H. Gale and Dr. R.J. Pankhurst for their cooperation and encouragement. The entire staff of the Age and Isotope Research Group in Oxford have always been of every possible assistance, and in particular I thank Dr. Pankhurst (especially for his technical and computing expertise), R.A. Dick, and R. Goodwin for skilled technical assistance. P.N. Taylor, P.J. Hamilton, C.J. Hawkesworth, Miss P. Shreeve, P.C. England, Miss C.M. Shepperd, A.P. Middleton and many other staff and student members of the Department of Geology are thanked for their friendship and help at various times.

The Silurian sections in Shropshire and Pembrokeshire, on which a major part of this study has been based, were brought to my attention by Dr. W.S. McKerrow, whom I gratefully acknowledge for many helpful discussions and help with fieldwork.

Dr. H.F. Shaw introduced me to the practical aspects of determinative clay mineralogy. Special thanks go to Dr. N. Clauer of CNRS, Strasbourg, for stimulating discussions on our several meetings, and also for practical help with some clay fractionations.

I am indebted to the typist, who typed this thesis almost faultlessly, despite a seemingly illegible manuscript. For photographic work on some diagrams, I thank J.R. McAvoy and S. Baker.

This study was undertaken with the financial support of the British Petroleum Research Fellowship fund in the University of Oxford, which I

very gratefully acknowledge. Finally, I should like to thank Professor E.A. Vincent for his encouragement throughout the years in which I have been associated with the Department of Geology and Mineralogy in Oxford.

CONTENTS

	<u>Page</u>
Abstract	ii
Acknowledgements	vi
Contents	viii
List of Tables	xii
List of Figures	xiii
CHAPTER 1. INTRODUCTION	1
1.1 Previous Work	2
1.2 Aims of Recent Study	5
1.3 Rb-Sr Dating - a Brief Survey	6
CHAPTER 2. Rb-Sr ISOTOPE AND MINERALOGICAL INVESTIGATION OF LLANDOVERY SEDIMENTS	11
2.1 Outline Geological History of Sample Localities	11
2.1.1 Welsh Borderland	11
2.1.2 Pembrokeshire	12
2.2 Details of Sample Collection	19
2.2.1 Buildwas, Shropshire	19
2.2.2 Marloes, Pembrokeshire	20
2.3 Mineralogical Analysis	21
2.3.1 Whole-rock and clay mineralogies	21
2.3.2 Illite crystallinity measurements	27
2.4 Rb-Sr Study on Whole-Rock Samples	30
2.5 Sr-Isotopes in Calcite Leachates	37
2.6 Rb-Sr Study on Size-Fractionated Samples	40
2.6.1 Within-sample size fractions	40
2.6.2 Between-sample clay fractions	43
2.7 Intercalated Bentonites	43

	<u>Page</u>
CHAPTER 3. THE BEHAVIOUR OF Rb AND Sr IN ARGILLACEOUS SYSTEMS - AN INTERPRETATION OF THE ISOTOPIC AND MINERAL- OGICAL DATA	48
3.1 Introductory Comment	48
3.2 Buildwas - an Example of Unmetamorphosed Palaeozoic Argillites	49
3.2.1 Interpretation of Rb-Sr data from whole-rock samples	49
3.2.2 Within-sample size fractions	51
3.2.3 Between-sample clay fractions	53
3.3 Marloes - an Example of Folded and Slightly Meta- morphosed Palaeozoic Shales	53
3.3.1 Interpretation of Rb-Sr data from whole-rock samples	53
3.3.2 Within-sample size fractions	59
3.3.3 Between-sample clay fractions	61
3.3.4 Whole-rock data from bentonites	63
3.4 Discussion of Behaviour of Sr and Rb in Sediments	65
3.4.1 Weathering, halmyrolysis and deposition	65
3.4.2 Burial and early diagenesis	66
3.4.3 Low-grade metamorphism	71
CHAPTER 4. AN EXPERIMENTAL INVESTIGATION OF FACTORS INFLUENCING Rb-Sr SYSTEMS DURING DIAGENESIS	81
4.1 Introduction	81
4.2 Experimental Details	82
4.2.1 Starting material	82
4.2.2 Fluid composition	83
4.2.3 Reactor assembly	83
4.2.4 Analytical techniques	85
4.2.5 Hydrothermal experimental conditions	86

	<u>Page</u>
4.3 Results	87
4.3.1 Post-experiment solid phases	87
4.3.2 Rb and Sr exchanged with fluid	89
4.4 Discussion of Results	96
4.4.1 Time-dependence	96
4.4.2 Dependence on fluid composition and temperature	96
4.5 Discussion of Interpretational Models	99
4.5.1 Volume diffusion from lattice	99
4.5.2 Dissolution kinetics and equilibria	104
4.5.3 Conclusions	105
CHAPTER 5. Rb-Sr STUDIES ON SEDIMENTS FROM THE LONG MYND, SHROPSHIRE	107
5.1 Introduction	107
5.2 The Longmyndian Succession	107
5.2.1 Geological setting and structure	107
5.2.2 Previous geochronological evidence	108
5.3 Sample Description	112
5.4 Whole-Rock Rb-Sr Isotope Data	115
5.5 Interpretation	120
5.5.1 Isochron ages	120
5.5.2 Maximum depositional age - discussion	122
5.6 Stratigraphical Implications	123
CHAPTER 6. Rb-Sr STUDIES ON CAMBRIAN SLATES FROM NORTH WALES	126
6.1 Introduction	126
6.2 Geological Setting	128
6.2.1 Harlech Dome	128
6.2.2 Caernarvonshire Slate Belt	132
6.3 Sample Collection and Description	135
6.3.1 Harlech Dome	135
6.3.2 Caernarvonshire Slate Belt	136

	<u>Page</u>
6.4 Whole-Rock Rb-Sr Data	137
6.5 Interpretation and Discussion	143
6.6 Conclusion	146
CHAPTER 7. CONCLUDING SUMMARY	147
7.1 The Significance of Rb-Sr Data from Sediments	147
7.2 Isotope Techniques in Experimental Investigations	150
7.3 Future Work	151
APPENDIX A. Techniques for Crushing and Size-Fractionation of Argillaceous Rocks	152
APPENDIX B. X-ray Diffraction Techniques of Determinative Mineralogy	157
B.1 Whole-rock mineralogy	158
B.2 Clay-fraction mineralogy	159
B.2.1 Sample mounting	162
B.2.2 Classification and estimation of clay mineralogy	164
APPENDIX C. Crystallinity Index Measurements and Standards	172
APPENDIX D. Chemistry of Rb & Sr Separations for Mass- Spectrometric Analysis	174
D.1 Extraction of unspiked Sr for isotopic analysis	174
D.2 Extraction of spiked Rb & Sr for isotope dilution analysis	175
APPENDIX E. Computations	178
E.1 Rb/Sr ratios by XRF	178
E.2 $^{87}\text{Sr}/^{86}\text{Sr}$ ratios from mass-spectrometric measurements	180
E.3 Sr concentrations & $^{87}\text{Sr}/^{86}\text{Sr}$ ratios by isotope dilution	181
E.4 Rb concentrations by isotope dilution	182
E.5 Isochron regression	183
APPENDIX F. Diffusion coefficient computations	184
References	186

LIST OF TABLES

<u>Table</u>		<u>Page</u>
2.1	Coarse-grained mineralogy of Upper Llandovery rocks	23
2.2	$^{87}\text{Sr}/^{86}\text{Sr}$ for Eimer and Amend SrCO_3 standard	33
2.3	Rb-Sr data for Upper Llandovery sediments from Buildwas	34
2.4	Rb-Sr data for Upper Llandovery sediments from Marloes	35-36
2.5	Sr-isotope data for calcite leachates	39
2.6	I.D. data for size-fractions from Buildwas & Marloes samples	42
2.7	I.D. data for clay-fractions from Buildwas & Marloes samples	44
2.8	Clay mineralogy of bentonites from Marloes	46
2.9	Rb-Sr data for bentonites from Marloes	47
3.1	Comparison of Rb-Sr data for WR & clays of Marloes samples	79
4.1	Summary of clay phase changes in experiments at 360°C	90
4.2(a)	List of experimental conditions	91
4.2(b)	Analytical data for Sr exchange	92
4.2(c)	Analytical data for Rb & ^{87}Sr exchange	93
4.3	Empirical diffusion coefficients from experiments	100
5.1	Lithologic succession of the Longmyndian	110
5.2	Summary of mineralogical characteristics of Longmyndian samples	114
5.3	Rb-Sr analytical data from Longmyndian samples	116
6.1	Stratigraphic sequence of the Harlech Dome	131
6.2	Stratigraphic sequence of the Slate Belt at Nantlle	134
6.3	Rb-Sr whole-rock data from Harlech Dome samples	138
6.4	Rb-Sr whole-rock data from Slate Belt samples	139
B.1	Data for estimation of coarse-grained phases by XRD	160
B.2	Identification of clay minerals by XRD	165
B.3	Comparison of intensity factors for clays used by several authors	168
D.1	Concentrations & compositions of Sr and Rb 'spike' solutions	176

LIST OF FIGURES

<u>Figure</u>		<u>Page</u>
2-1	Regional map showing Buildwas and Marloes	12
2-2	Geological sketch-map of area around Buildwas, Shropshire	13
2-3	Comparison of estimated max. overburdens at Buildwas and Marloes	15
2-4	Geological sketch-map of Pembrokeshire	16
2-5	Map of the major structures in S. Wales	18
2-6	Diffraction patterns of clay from sample DD7d	24
2-7	Diffraction patterns of clay from sample MS9	25
2-8	Clay-fraction mineralogy of Buildwas & Marloes samples	26
2-9	Illite crystallinity index scale	29
3-1	Rb-Sr data from Buildwas whole-rock samples on isochron diagram	50
3-2	Rb-Sr model ages against mean particle size for DD9, MS1 & MS6	52
3-3	Rb-Sr data from Buildwas clay fractions on isochron diagram	54
3-4	Rb-Sr data from Marloes Sands shales on isochron diagram	55
3-5	Rb-Sr data from Deadman's Bay shales on isochron diagram	56
3-6	Rb-Sr data from Marloes size-fractions on isochron diagram	60
3-7	Rb-Sr data from Marloes clay fractions on isochron diagram	62
3-8	Rb-Sr data from Marloes bentonites on isochron diagram	64
3-9	Activity diagrams for phases in argillaceous sediment at 300°C	74
4-1	Diffraction patterns of clay before & after experimental runs at 360°C	88
4-2	Graph demonstrating correlation between exchange of ^{87}Sr and Rb	95
4-3	Mean rates of Rb & Sr exchange plotted against duration	97
4-4	Rates of Rb & Sr exchange as a function of brine composition	98
4-5	Arrhenius plots for Sr & Rb exchange between reactant and 1M NaCl	103

	<u>Page</u>
5-1 Geological sketch-map of part of the Long Mynd, Shropshire	109
5-2 Whole-rock Rb-Sr isochron from Burway Gp., Longmyndian	117
5-3 Whole-rock Rb-Sr isochron from Synalds Gp., Longmyndian	118
5-4 Whole-rock Rb-Sr isochron from Lightspout Gp., Longmyndian	119
6-1 Geological sketch-map of North Wales	127
6-2 Geological sketch-map of Harlech Dome area	129
6-3 Simplified geological map & section of Slate Belt outcrop near Nantlle	133
6-4 Whole-rock Rb-Sr isochron from Clogau Shales, Harlech Dome	140
6-5 Whole-rock Rb-Sr isochron from Llanbedr Slates, Harlech Dome	141
6-6 Whole-rock Rb-Sr isochron from Purple Slates, Nantlle	142
A-1 Sedimentation nomographs	156
B-1 Clay mineral groups involved in this study	161
B-2 Apparatus for producing oriented clay mineral mounts for XRD	163
B-3 Diffractograms of clay from DD 7d after various treatments	171
C-1 Illustration of illite crystallinity index standards	173

CHAPTER 1

INTRODUCTION

In recent years radiometric dating has assumed a major rôle in elucidating the timing and nature of processes operative during crustal development. The radiometric dates obtained from igneous and metamorphic rocks can often be interpreted as the time of magmatic crystallization or cooling below certain threshold temperatures subsequent to reheating episodes. In other cases, particularly those of low-grade metamorphic and sedimentary rocks, a detailed knowledge of the behaviour of the relevant parent-daughter system under the conditions experienced by the rocks is prerequisite to an interpretation of the radiometric dates.

Historically, dating (in the stratigraphic sense) of sedimentary rocks has been the preserve of the palaeontologist. Various attempts have been made to put numerical age limits on divisions, based predominantly on observed faunal changes, of the Phanerozoic time-scale (see Harland et al., 1971). The indirect nature of those investigations in which radiometric dates have been obtained on associated igneous rocks has produced an unsatisfactory and incomplete time-scale. Interpretation of these radiometric ages has required not only a knowledge of the behaviour of the parent-daughter system, but also an elucidation of the field-relations between the radiometrically-dated igneous rocks and the stratigraphically-relevant sedimentary strata. The uncertainties are further compounded by the diversity of parent-daughter systems used in investigations (K-Ar, Rb-Sr, U-Pb, etc.) and the multitude of laboratories contributing frequently discordant data.

There is, at present, a major requirement for radiometric methods of dating directly not only fossiliferous Phanerozoic sedimentary rocks but also unfossiliferous sediments which occur in the Phanerozoic and particularly in the Proterozoic and the Archaean.

1.1 Previous Work

Glaucouite, considered by many authors (e.g. Grim, 1953) to be a universally authigenic mineral, was the first component of sedimentary rocks for which the possibilities of radiometric dating were considered. The K-Ar method (Wasserburg et al., 1956) and the Rb-Sr method (Herzog et al., 1958) were both tried. These and subsequent data from other authors have shown, however, that radiometric dates from glaucouites tend to be consistently lower than independent estimates of formational age. Hurley et al. (1960) suggested that the susceptibility of glaucouite to diagenetic modification, as well as the possibility of diffusive loss of radiogenic products, may explain the poor reliability of the dates from this mineral.

Much of the early work in this field was confined to the K-Ar parent-daughter system. Despite the suitability of potassium-rich illitic shales for investigation by this method, the inherent problems associated with K-Ar dating - particularly the uncertainty concerning the behaviour of the gaseous daughter nuclide under different thermal régimes - have always made difficult the interpretation of data (e.g. Evernden et al., 1961; Hower et al., 1963; Harper, 1964).

Initial attempts to date sediments by the Rb-Sr isochron method were encouraging, indicating a close approach to closed system behaviour in many of the sediments studied (Compston & Pidgeon, 1962; Whitney & Hurley, 1964). However, these early investigations, and more recent ones (e.g. Bofinger et al., 1970), were concerned chiefly with the stratigraphic significance of such radiometric dates; the approach taken, and the precision of data then possible, permitted little to be inferred concerning the detailed behaviour of the Rb-Sr system.

The studies of Rb-Sr systems in sedimentary rocks and in pelitic metamorphic rocks are naturally related to one another. Indeed, it has been a common feature of studies on sediments (Compston & Pidgeon, 1962; Peter-

man, 1966; Obradovich & Peterman, 1968; Allsopp et al., 1968; Faure & Kovach, 1969; Bofinger et al., 1970) that the interpretation of radiometric data is made difficult, and often ambiguous, by the complex tectonic histories of the regions studied. Conversely, Rb-Sr data from pelites has been used as a tool in elucidating the chronologies of tectonic events in structurally complex regions (Hunziker, 1970; Clauer & Bonhomme, 1970; Gebauer & Grünfelder, 1973). These studies have also contributed towards an understanding of the behaviour of Rb-Sr systems under various metamorphic conditions.

More recent attempts to obtain whole-rock Rb-Sr isochrons from unmetamorphosed or only slightly metamorphosed sediments have met with some success (Moorbath, 1969; Pringle, 1973; O'Nions et al., 1973). These investigations were all on shales from Proterozoic or very early Palaeozoic successions which are of special stratigraphic interest. The colinearity of data, generally of much higher precision than earlier researches, was of special significance, since it confirmed that in many cases the Rb-Sr system in argillaceous sediments has satisfied conditions for an isochron. These authors assumed that the fulfillment of isochron conditions was a result of processes occurring during diagenesis, and that the radiometric ages are close to, and minima for, the true depositional ages. In one case (O'Nions et al., *op. cit.*) considerations based on the value of the initial ratio $(^{87}\text{Sr}/^{86}\text{Sr})_0$ have enabled a maximum limit to be placed on the depositional age. It is worth noting that promising results have recently been obtained (Moorbath et al., 1973) using the Pb-Pb dating method on a metamorphosed sedimentary iron formation in the Archaean of West Greenland. Several whole-rock samples yield Pb-isotope data consistent with an isochron age of 3760 ± 70 m.y., interpreted by the authors to reflect a metamorphic event.

In recent years, the success of whole-rock Rb-Sr studies on argillaceous sediments has prompted more detailed investigations into the behaviour of

the parent-daughter system in the various components of sediments. This has, to a large extent, coincided with a revision of ideas concerning clay mineral transformations during burial and diagenesis (see, for example, Dunoyer de Segonzac, 1970; Perry & Hower, 1970). The distinction between illite polytypes, specifically the 1Md and 2M polytypes (Velde & Hower, 1963), and their potential significance with respect to the illite's genetic history, have been used frequently as an aid to the interpretation of isotopic data (e.g. Hower et al., 1963; Bofinger et al., 1970; Brookins & Chaudhuri, 1973; Hofmann et al., 1974).

Although the technique of studying pure mineral separates, widely used in investigations of igneous and metamorphic rocks, is not generally available for studying argillaceous sediments, the technique of size fractionation which concentrates certain components has been developed. This not only permits the assessment of Rb-Sr behaviour as a function of particle size and clay mineralogy (Hofmann et al., 1974), but it also enables the contribution of coarse-grained minerals (some of which may be detrital) to the Rb-Sr system to be assessed (Clauer, 1973). Another technique by which the Rb-Sr system within specific phases has been investigated is that of acid leaching (Bofinger et al., 1968; Chaudhuri & Brookins, 1969; Clauer, 1973) which preferentially removes calcite.

An understanding of the behaviour of the Rb-Sr system during sediment transport, deposition and early burial is clearly necessary before behaviour at later stages of burial and diagenesis can be elucidated. Evidence has been obtained which demonstrates the absence of a significant degree of Sr-isotope equilibration between sea-water and recent deep-sea sediments (Dasch, 1969) or even between the connate waters and sediment in deep-sea cores of Late Mesozoic age (Hofmann et al., 1972). Indeed, this absence of equilibration has been utilised to advantage in attempting to distinguish between oceanic regions of different sediment provenance (Biscaye & Dasch, 1971).

Investigations of materials buried to greater depths than those available from deep-sea cores, are possible in some oil-well cores. Perry & Turekian (1974) have established that, even at depths of over 5000 m. under a normal geothermal gradient, total Sr equilibration between all mineral phases and pore-fluids has still not been induced.

There still remains an important gap in observations of the behaviour of Rb-Sr systems of argillaceous sediments during deposition, burial, diagenesis and metamorphism. Unfortunately, this gap is occupied by the processes of most significance to an eventual full understanding of Rb-Sr isochron dates from ancient sediments. For the present, we are restricted to inferences based on detailed studies of sediments which satisfy isochron conditions, comparison with sediments which do not satisfy these conditions, and predictions based on our present knowledge of the physico-chemical processes of sediment burial.

1.2 Aims of Present Study

It is apparent from the preceding section that, despite the ever-growing number of radiometric dates obtained on sediments, ambiguity and uncertainty still surrounds their interpretation. This interpretation has often been hampered by the low level of data precision at which an assessment of data concordance (i.e. colinearity on an isochron diagram) has been made.

The first part of the present study is aimed at an investigation of behaviour of the Rb-Sr system in various components of argillaceous sediments during burial, diagenesis, and very low-grade metamorphism. The approach adopted involves a study of suites of Lower Silurian argillites of essentially identical stratigraphic age but with different post-depositional histories. As well as whole-rock samples, fractions separated on a particle size criterion have been studied since these may yield additional information helpful in the elucidation of the Rb-Sr systematics. The isotope

investigations of the sediments are accompanied by detailed mineralogical studies, particularly of the clay fractions, in order to assess the relationships between mineralogical changes and Rb-Sr systematics.

The second part of this study complements the field-based investigation, and is concerned with simulation in the laboratory of conditions experienced by sediments during deep burial. Unmetamorphosed fine-grained sediments are subjected to these controlled conditions, and the perturbation of the Rb-Sr system investigated. By varying the physical and chemical conditions, it is possible to define some of the parameters which control the behaviour of the Rb-Sr system during burial and diagenesis. The present work can only be viewed as a preliminary study, and much additional work is required in this area.

Finally, the extent of our current understanding of Rb-Sr systematics within sedimentary rocks is applied to suites of sediments which pose some particular stratigraphic problems. Samples from the Longmyndian succession in Shropshire (previously considered to be of Precambrian age, > 600 m.y.), and from the Harlech Dome and slate belt regions of North Wales, are investigated by Rb-Sr methods.

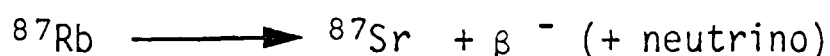
1.3 Rb-Sr dating - a brief survey

It is worthwhile at this stage to summarise briefly the theory and principles of the rubidium-strontium isochron method of dating. Comprehensive treatments of this subject are given by Nicolaysen (1961), Hamilton (1965) and Faure & Powell (1972), and only the salient points will be presented here.

Rubidium and strontium occur in detectable, trace quantities in virtually all rocks. In silicate minerals, they substitute predominantly for their more abundant, smaller Groups I and II cogeners - K^+ in 8- and 12-fold coordination, and Ca^{++} in 8-fold coordination respectively. Therefore argillaceous sediments, which generally contain plagioclase as well as

layer-lattice clay minerals, are found to contain moderate amounts of these two elements. Taylor (1965) has compiled average trace element concentrations for various lithologies, and has estimated mean contents of 140 ppm Rb and 300 ppm Sr for shales. An augmented Sr content is observed in calcareous shales.

Naturally-occurring rubidium has two isotopes: ^{87}Rb and ^{85}Rb , with the atomic ratio $^{87}\text{Rb}/^{85}\text{Rb} = 0.3829$. (This is the figure used in the Oxford laboratory, though Nier, 1950, originally measured it as 0.3856). The former nuclide, ^{87}Rb , undergoes spontaneous decay by β -emission to ^{87}Sr :



Strontium has four naturally-occurring isotopes: ^{88}Sr , ^{87}Sr , ^{86}Sr , and ^{84}Sr . Due to the radiogenic nature of some ^{87}Sr , natural strontium does not have a constant isotopic composition. However, the relative proportions of the non-radiogenic isotopes are constant, $^{86}\text{Sr}/^{88}\text{Sr}$ being 0.1194 and $^{86}\text{Sr}/^{84}\text{Sr}$ being 17.61 (Nier, 1938). The most primitive (i.e. non-radiogenic) strontium yet analysed is that from the Angra dos Reis (ADOR) achondrite, with a measured $^{87}\text{Sr}/^{86}\text{Sr}$ ratio of 0.69884 ± 4 (Papanastassiou, 1970).

The rate of decay of a radioactive nuclide to a daughter product is described by the first-order rate law, being of a spontaneous nature. Thus the rate of decay of the parent is proportional to the number (N) of parent atoms:

$$\frac{dN}{dt} = -\lambda N$$

where λ is the first-order rate constant, known in this specific case as the radioactive decay constant. Integration of this rate equation between the limits ($N = N_0$ at $t = 0$) and (N at time t) yields:

$$N = N_0 e^{-\lambda t}$$

This law is the basis of all radiometric dating methods.

In the present case, that of the ^{87}Rb - ^{87}Sr parent-daughter system, the

number, N_0 , of parent ^{87}Rb atoms at time zero (i.e. t million years ago) is represented by:

$$N_0 = {}^{87}\text{Rb} + {}^{87}\text{Sr} - {}^{87}\text{Sr}_0$$

where ${}^{87}\text{Rb}$ = no. of ^{87}Rb atoms measured now. (N)

${}^{87}\text{Sr}$ = total no. of ^{87}Sr atoms measured now (i.e. radiogenic + non-radiogenic)

${}^{87}\text{Sr}_0$ = no. of ^{87}Sr atoms present at zero time.

Thus, substituting into the decay law:

$${}^{87}\text{Rb} = ({}^{87}\text{Rb} + {}^{87}\text{Sr} - {}^{87}\text{Sr}_0)e^{-\lambda t}$$

which, rearranged, leads to:

$${}^{87}\text{Sr} = {}^{87}\text{Sr}_0 + {}^{87}\text{Rb} (e^{\lambda t} - 1)$$

Dividing through by the number of ^{86}Sr atoms present (which is constant with time, ^{86}Sr being non-radiogenic), yields an equation in isotopic ratios, which are easily determined:

$$\frac{{}^{87}\text{Sr}}{{}^{86}\text{Sr}} = \frac{{}^{87}\text{Sr}_0}{{}^{86}\text{Sr}} + \frac{{}^{87}\text{Rb}}{{}^{86}\text{Sr}} (e^{\lambda t} - 1)$$

This expression is the formal presentation of the Rb-Sr isochron method of dating rocks, originally proposed by Nicolaysen (1961). It is an expression of the form

$$y = b + mx$$

which represents a straight line of gradient $m [(e^{\lambda t} - 1)]$ and y -intercept $b [(^{87}\text{Sr}/^{86}\text{Sr})_0]$.

Therefore measurements of $^{87}\text{Sr}/^{86}\text{Sr}$ ratios (by mass-spectrometry) plotted against the corresponding $^{87}\text{Rb}/^{86}\text{Sr}$ ratios for a suite of cogenetic rocks or minerals should yield a straight line. The slope of this straight line is proportional to the time, t , which has elapsed since that suite of rocks or minerals last shared a common Sr-isotope composition with a value $(^{87}\text{Sr}/^{86}\text{Sr})_0$.

It is very important to emphasise the assumptions concerning the Rb-Sr system which are implicit in use of the isochron method for dating a suite of rocks:

- (i) the individual samples, whether whole rocks or mineral separates, representing the suite have not undergone any redistribution of Rb or Sr amongst themselves since time t ;
- (ii) the system as a whole has remained closed with respect to Rb and Sr, and has not suffered mass-transfer of these elements (e.g. by metasomatism) in or out of the system since time t .

Conversely, the term 'systematics' can be used to describe the behaviour (particularly the mobility) of the parent and daughter elements - Rb and Sr in this case - under relevant physical and chemical conditions. It is this behaviour which determines the applicability of the Rb-Sr isochron method in different situations.

It is a feature of the isochron method that a good 'spread' of $^{87}\text{Rb}/^{86}\text{Sr}$ ratios from a suite of cogenetic samples is necessary, in addition to precise measurements of this ratio and the $^{87}\text{Sr}/^{86}\text{Sr}$ ratio, in order that a precise assessment of isochron slope (and hence radiometric date) be possible.

A disadvantageous feature of the Rb-Sr method of dating is the present uncertainty in the value for the decay constant of ^{87}Rb , λ . Two values are in current use:

- (i) $\lambda = 1.47 \times 10^{-11} \text{yr}^{-1}$, which was determined directly on rubidium by incorporation of a Rb salt in a scintillation liquid (Flynn & Glendenin, 1959).
- (ii) $\lambda = 1.39 \times 10^{-11} \text{yr}^{-1}$, which has been calculated from cogenetic minerals to be concordant with U-Pb ages.

The latter value is adopted in the present investigations, since this value appears to be the most widely accepted at present. In the present state of uncertainty, uniformity of constant is of paramount importance in order that inter-laboratory comparison of Rb-Sr dates be facilitated. This is not to underestimate the somewhat dubious basis of the chosen value and the need for precise direct physical determinations of λ .

Some idea of the range of ages over which Rb-Sr dating can be applied

with success, is given by the half-life for ^{87}Rb . The half-life, $t_{\frac{1}{2}}$, is the time for the original number of parent nuclide atoms to be halved by radioactive decay. It can be shown to be related to λ thus:

$$t_{\frac{1}{2}} = \frac{\ln 2}{\lambda} = \frac{0.693}{\lambda}$$

Thus ^{87}Rb has a value $t_{\frac{1}{2}} = 5.0 \times 10^{10}$ yr. corresponding to $\lambda = 1.39 \times 10^{-11}$ yr $^{-1}$. Rb-Sr dating may be successfully applied over a range of dates from those in the order of millions of years up to meteorite dates (in the region of 4.6×10^9 yr).

In conclusion, we might re-define the specific problems of Rb-Sr systematics with regard to the proposed radiometric dating of sediments as:

- (a) In which sediment systems, if any, may we expect to observe closed system behaviour such as is required to satisfy the conditions for an isochron?
- (b) Having recognised closed system behaviour subsequent to an instant in geological time, what is the geological significance of this 'event' for the particular system being studied?

CHAPTER 2

Rb-Sr ISOTOPE AND MINERALOGICAL INVESTIGATION OF LLANDOVERY SEDIMENTS

2.1 Outline Geological History of Sample Localities

As previously stated in Chapter 1, the initial part of this study involves a comparison of the Rb-Sr data for Silurian argillaceous sediments from localities which have suffered different post-depositional histories. The two localities selected for study were Buildwas in Shropshire, and Marloes in Pembrokeshire (Fig. 2-1). At both of these localities there are excellent exposures of argillaceous sediments of Upper Llandovery (C₆ zone) age, but which have been subjected to quite different geological histories.

The Lower Palaeozoic rocks of Wales and the Welsh Borderland form one of the classic areas of British geology, and as such are well documented stratigraphically, palaeontologically and sedimentologically.

The major palaeogeographic feature of this area is the Central Wales basin, which developed by subsidence throughout the Lower Palaeozoic. Sporadic periods of uplift and erosion, however, may be inferred from basal Ordovician and Silurian unconformities.

2.1.1. Welsh Borderland

The Upper Llandovery section at Buildwas in Shropshire (Fig. 2-2) is situated on the eastern flank of the Welsh basin. These sediments represent the culmination of a marine transgression to the east throughout Llandovery time (Ziegler et al. 1968). They have been considered, on faunal and sedimentological grounds (Ziegler et al., *op.cit.*; Cocks & Walton 1968), to have been deposited on the seaward limit of the shelf abutting onto the Welsh basin. The strata in this region, east of the Church Stretton fault, have been little affected by post-Silurian tectonic

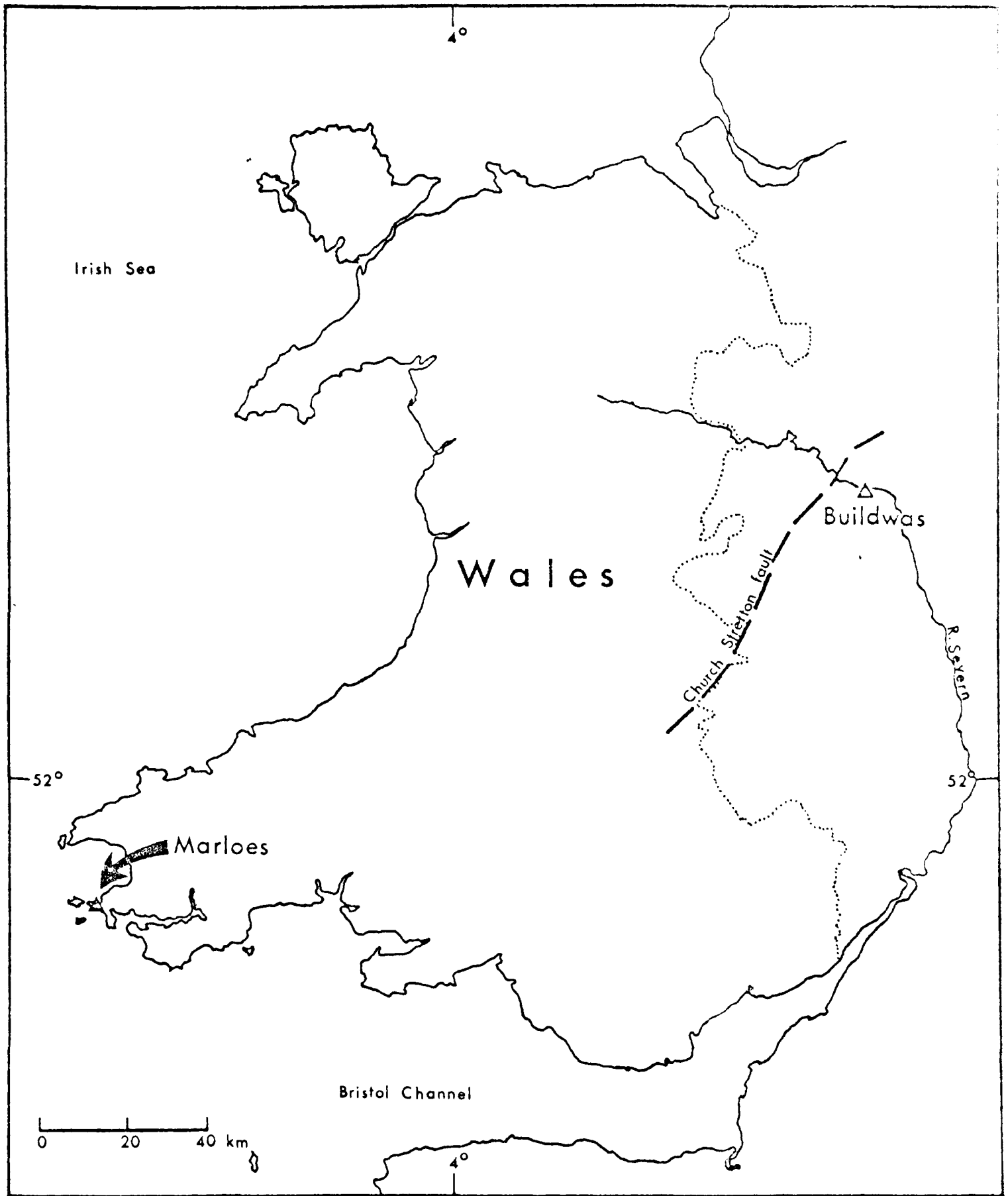
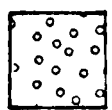
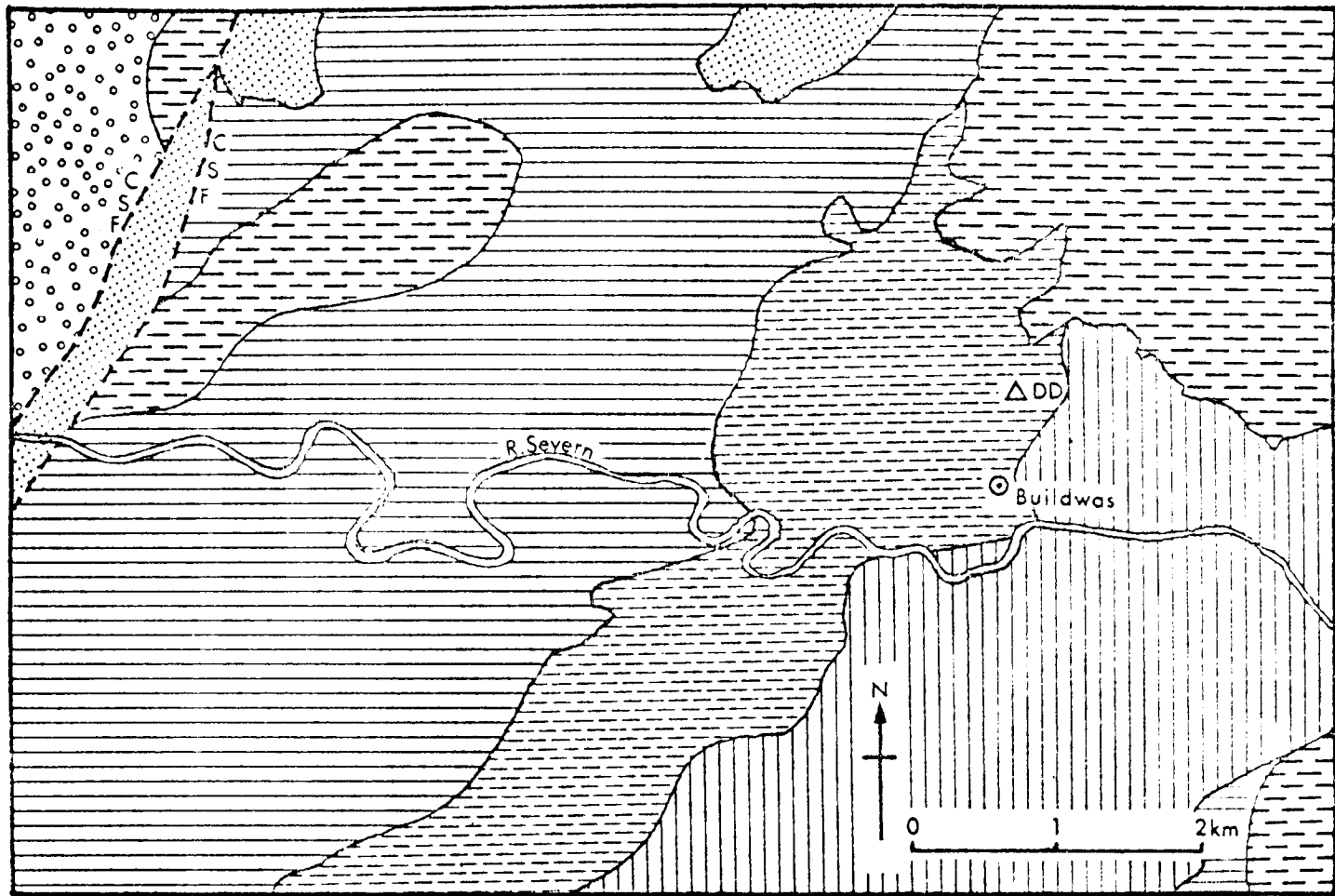
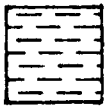


Fig. 2-1. Regional map showing locations of Buildwas and Marloes sampling areas. Also shown is the Church Stretton fault complex.



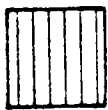
Triassic



Carboniferous



Ludlow



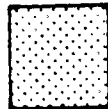
Wenlock



Llandovery



Cambrian



Uriconian extrusives

△ DD Samples locality

CSF Church Stretton fault complex

Fig. 2-2. Geological sketch-map of the area around Buildwas, Shropshire, showing DD sampling locality. For regional location, see Fig. 2-1. (Based on Geological Survey, Sheet 152).

movements. The predominant strike of Silurian outcrops is N.N.E.-S.S.W. (the Wenlock limestone scarp of Wenlock Edge, a major topographic feature of this area, is a good illustration of this trend) with the beds dipping gently to the south-east. A local unconformity between the top of the Silurian and the top of the Lower Carboniferous (Visean) further indicates that the overall structure was imposed during the Caledonian orogeny.

Post-Carboniferous crustal deformation appears to have had little effect on the strata east of the Church Stretton fault, possibly attributable to the relief of stress by movement along this fault-complex (Earp & Hains 1971). The N-S orientation of the resultant forces of Hercynian compression combined with the resistance of the Longmyndian massif to the west of the Church Stretton Fault, may account for the small scale N.E and N.N.E. trending faults and the very small amount of warping (W.N.W. trend) of the Silurian rocks at Buildwas (Cocks & Walton, op.cit.). The maximum thickness of post-Llandovery strata overlying the Llandovery beds at Buildwas, prior to the mid-Devonian uplift of the area, is estimated at 1500-2000 m. (Earp & Hains, op.cit), though it may have been considerably less. Subsequent to this Caledonian uplift, only the 200-300 m. of Middle and Upper Carboniferous strata were deposited, unconformably on the erosional surface of Lower Silurian rocks (illustrated diagrammatically in Fig. 2-3).

2.1.2. Pembrokeshire

The Lower Palaeozoic strata of south-west Wales present a quite different picture, having been deposited to the south of the central trough of the Welsh basin. The Upper Llandovery strata at Marloes in Pembrokeshire (Fig. 2-4), were laid down unconformably on the Skomer Volcanic Group. The Skomer Volcanics represent a period of late Ordovician - early Silurian volcanic activity (Ziegler et al. 1969). Ziegler and co-workers have suggested, on the basis of faunal evidence, that,

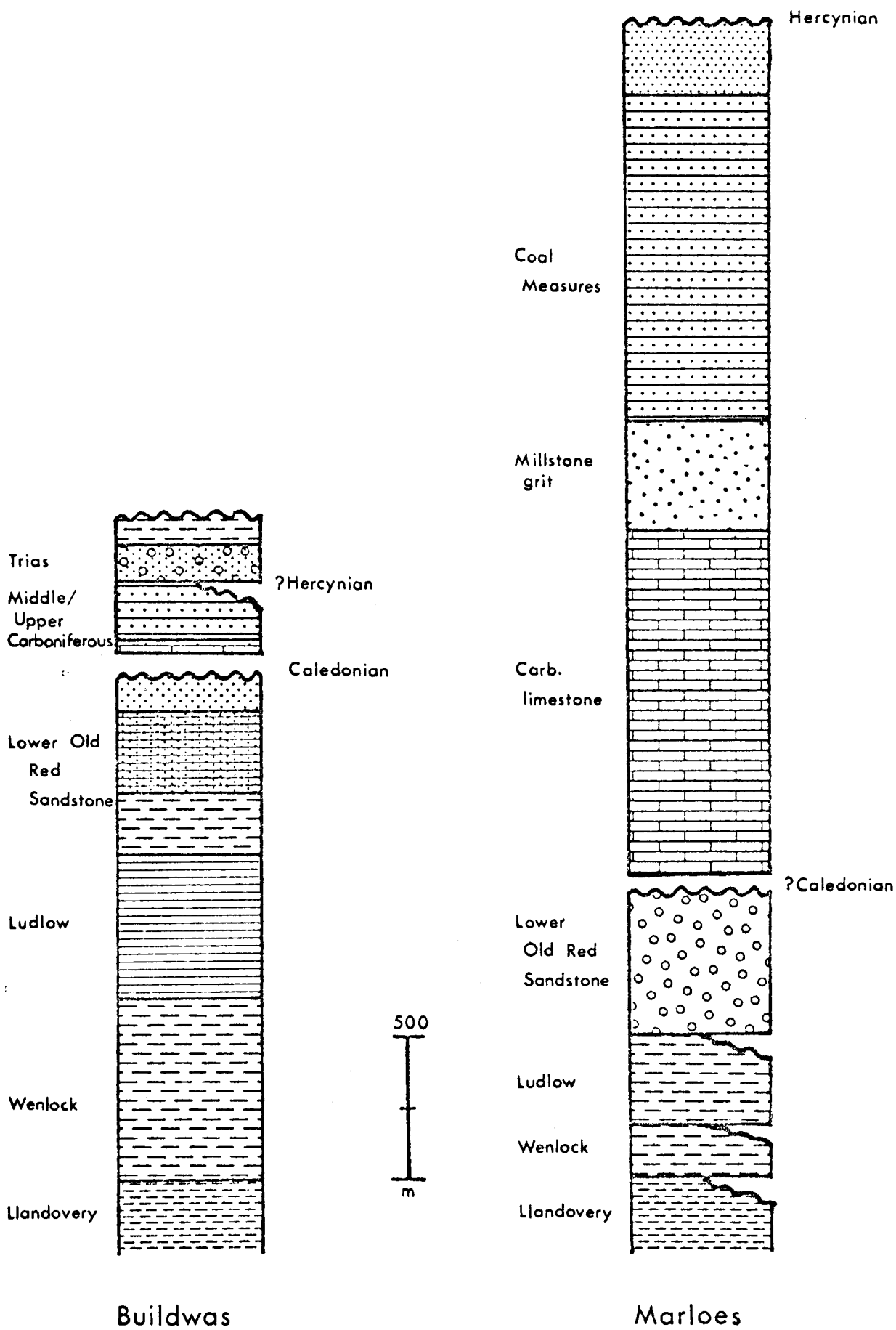


Fig. 2-3. Comparison of estimates of maximum overburden experienced by Llandovery strata in Welsh Borderland (Buildwas) and Pembrokeshire (Marloes). Local unconformities shown are observed in area referred to, but not necessarily in the specific sections investigated in this study.

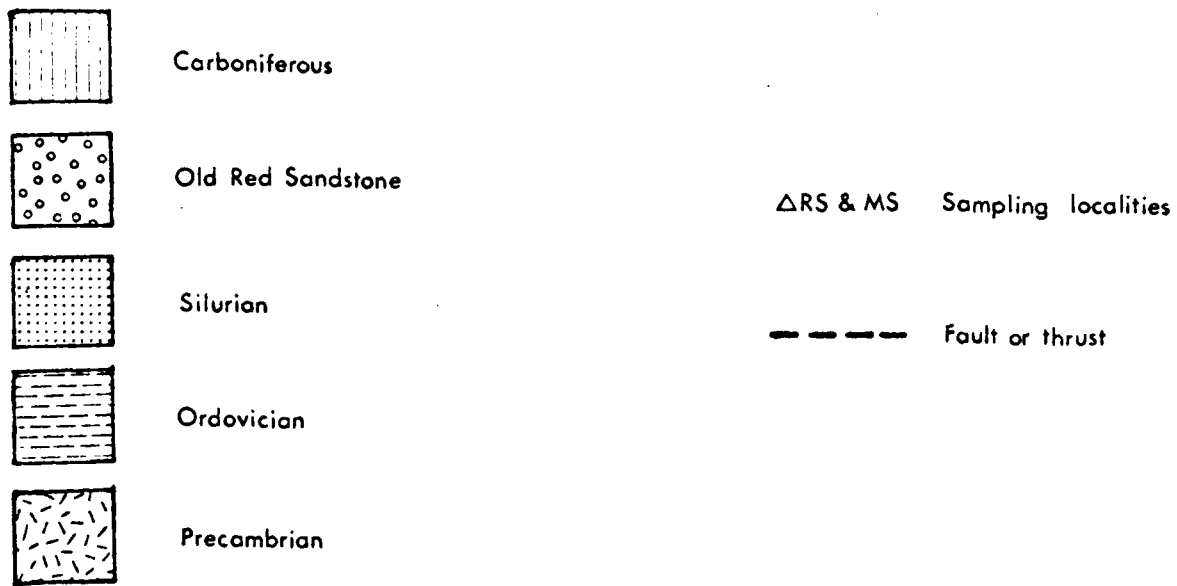
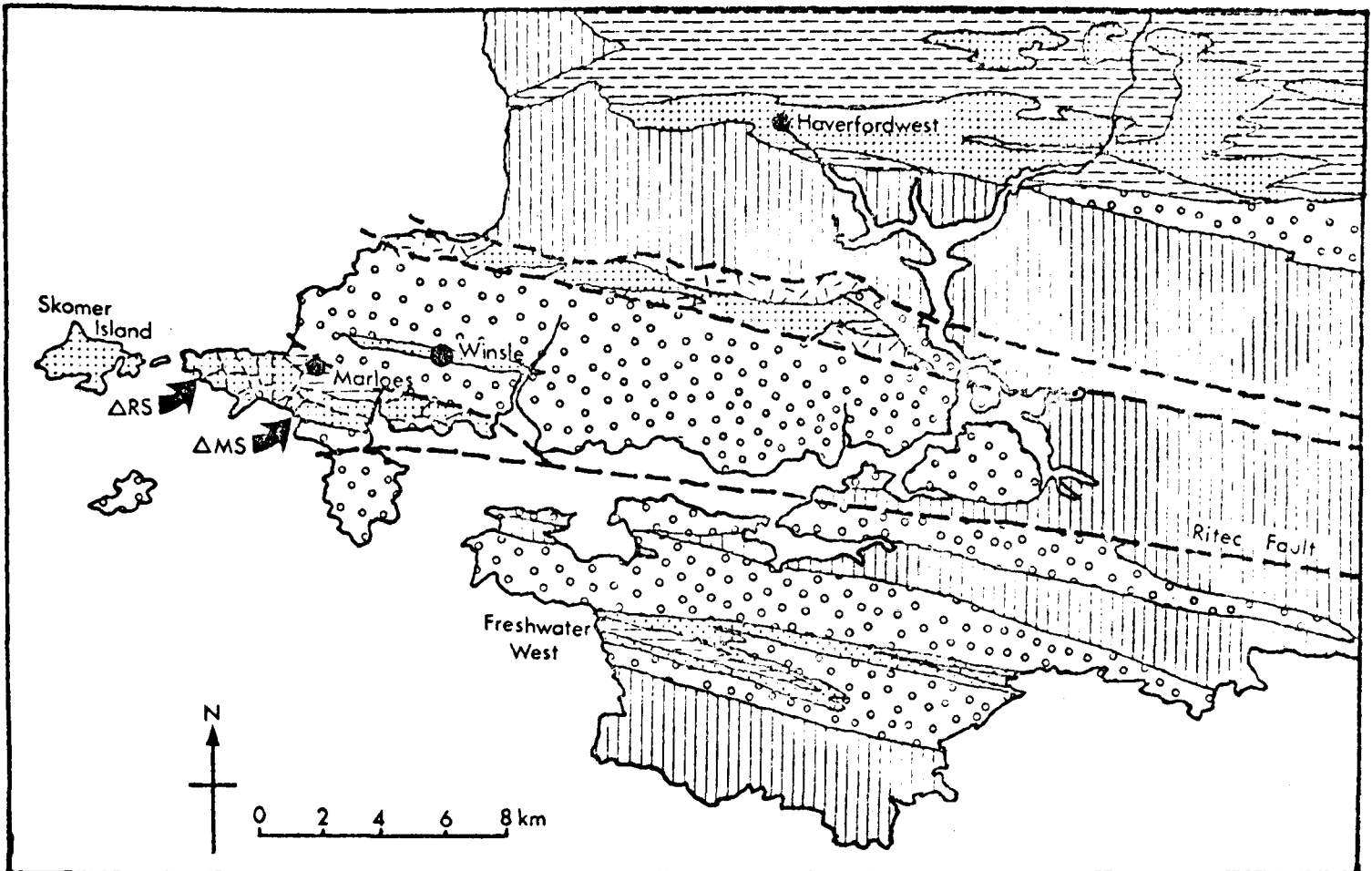


Fig. 2-4. Geological sketch-map of Pembrokeshire, showing Marloes Sands (MS) and Deadman's Bay (RS) sampling localities. For regional location, see Fig.2-1. Note E-W trending faults and thrusts, dividing area into structural blocks, four of which are allocthonous. (After Sanzen-Baker, 1972).

after the cessation of volcanic activity, sedimentation took place in a rapidly deepening shelf environment.

Sedimentation continued in this region throughout the Silurian and into the early Devonian. Although there is no direct evidence in the Marloes Bay section for Caledonian movements prior to the deposition of the Old Red Sandstone rocks, Cantrill et al. (1916) have presented evidence for a strong unconformity between the Silurian and the O.R.S. in the Winsle Inlier (6 km. N.E. of Marloes Bay). On the other hand, Sanzen-Baker (1972) does not recognize such a discontinuity at this locality, but has reiterated the case for end-Silurian uplift on the basis of unconformities in sections in the Freshwater and the Haverfordwest districts (respectively S.E. and N.E. of Marloes Bay). For example, in the Haverfordwest section, basal O.R.S. unconformably overlies Upper Llandovery strata. However, it should be noted that many of these sections are in allocthonous blocks (Sanzen-Baker, *op.cit.*), brought into their present relative positions by Hercynian thrusting. Consequently, these highly variable stratigraphic relations in Pembrokeshire may be accounted for.

As sedimentation continued throughout the Silurian, the deepwater marine conditions gave way to the deltaic and fluvial environments characteristic of Lower Old Red Sandstone. These Lower Old Red Sandstone sediments are unconformably overlain by more continental facies sandstones of the Upper Old Red Sandstone (e.g. at Freshwater West, cf. Fig. 2-4). The mid-Devonian unconformity and the absence of any Middle O.R.S. strata in South Wales has been attributed to a late 'pulse' of Caledonian uplift (George 1970), although it is clear from a map of the major structural trends in this region of South Wales (Fig. 2-5) that a distinction between Caledonian and Hercynian structures is not always possible and, indeed, may not be warranted. Prior to the mid-Devonian crustal movements, it is estimated that the combined thickness of Silurian

and Lower O.R.S. strata overlying the Upper Llandovery sediments in the Marloes section was about 1000 m. (Fig. 2-3).

The Carboniferous succession probably added up to 3000 m. of sediments to the Pembrokeshire section (Fig. 2-3), so that at the end of the Carboniferous the maximum overburden experienced by the Llandovery strata may be estimated at 4000 m. Hercynian compression probably commenced sometime near to the Westphalian stage of the Upper Carboniferous (George 1970). Associated with the strong folding along east-west axes, a considerable amount of faulting and overthrusting took place. This overthrusting is of particular importance with regard to the Marloes section. South-west Pembrokeshire is composed of five structurally separate blocks, four of which (including the one in which the Marloes section is situated) have been thrust into place from the south (Fig. 2-4; Sanzen-Baker 1972). In addition to strike faults (e.g. the high-angle Ritec fault), there is a well-developed fault set approximately normal to the Hercynian structural trends.

In the Marloes Bay section itself, the beds have a virtually constant dip of 50° - 60° to the S.S.E., and form part of a large amplitude monocline.

2.2. Details of Sample Collection

2.2.1. Buildwas, Shropshire

A temporary exposure of Lower Silurian strata in Devil's Dingle, near Buildwas in Shropshire (Grid. ref. SJ/640 055) provided an excellent, accessible section of Upper Llandovery age (Fig. 2-2; Cocks & Walton 1968). The rocks were exposed as a result of excavations associated with the construction of a reservoir for the disposal of slurried ash from the nearby C.E.G.B. power station at Ironbridge.

This Upper Llandovery section comprises a unit known as the Purple (or Hughley) Shale. The so-called Purple Shale is predominantly mud-

stones, with occasional thin, persistent bands of silts, calcareous silts and limestones. The purple mudstones are, to a large extent, homogeneous, although the coarser bands have a pronounced lamination. The degree of compaction and induration of the mudstones is remarkably low.

The thickness of sediments exposed in the section is between 25-30 metres, and samples were taken across the entire exposure. Sampling was confined to the fine-grained mudstones and limestones. Fossiliferous bands (predominantly brachiopods and occasionally corals) were avoided. Descriptions of the mineralogy of these samples (sample numbers prefixed by letters DD) are given subsequently in Table 2.1 and Fig. 2-8.

2.2.2. Marloes, Pembrokeshire

Excellent exposures of Lower Silurian sediments appear in cliff sections on the southern part of the Marloes Peninsula in south-west Wales (Fig. 2-4). The Hercynian thrusting and faulting give rise to a repetition of units along these cliff sections. The unit known as the Coralliferous Series has been shown on faunal evidence to be Upper Llandovery (C_6 zone) to Wenlock in age (Ziegler et al. 1969). Samples were collected from two outcrops of the Coralliferous Series: one at Deadman's Bay (Grid.ref. SM/761 085) (sample numbers prefixed by letters RS), and one at Marloes Sands (Grid. Ref. SM/788 072) (sample numbers prefixed by letters MS).

The former section of the Coralliferous Series, that at Deadman's Bay, has a thickness of 114 m., the basal 22 m. of which consists of conglomerates and coarse-grained beds (Ziegler et al. 1969). The remaining 92 m. of the section, across which samples were collected, consists of siltstones with minor intercalations of sandstone. In addition, there are many (upwards of twenty) thin, persistent bands (between 20-150 mm. thick) which have a grey-green colour. These bands have been identified as bentonites by Ziegler et al. (op. cit.), although, as will be shown later, their mineral assemblage is indistinguishable from that of the surrounding

darker grey terrigenous sediments. The beds in this section dip at 45° to the S.S.E.

The section at Marloes Sands has a thickness of 119 m., 9 m. of which are basal clastics (Ziegler et al., op.cit.). The lithologies comprising this section are similar to those previously described at Deadman's Bay, with the exception that a few calcareous bands are present in this case. Bentonite bands are again present, although an attempt to correlate bands between the Coralliferous Series of Deadman's Bay and that of Marloes Sands has proved unsuccessful (N.J. Hancock, pers. comm.). These rocks, particularly the finer-grained units, have a moderately developed cleavage sub-parallel to bedding, and dip is at 60° to the south.

In parts of both sections, quartz (and occasionally calcite) veining is common. Some of these veins appear to have been deformed and are clearly pre- or syntectonic, whilst others post-date the episode(s) of folding and cleavage development. Samples were not taken adjacent to these regions of hydrothermal fluid activity.

2.3 Mineralogical Analysis

2.3.1. Whole-Rock and Clay Mineralogies

Whole-rock powders and clay-fractions ($<2\mu\text{m}$ estimated spherical diameter) were prepared by the methods outlined in Appendix A. Whole-rock powders were pressed into cavity mounts with random grain orientation, whilst clay fractions were mounted as oriented specimens by the suction-onto-ceramic-tile technique (Shaw 1972; see Appendix B for a full description). The mounted specimens were analysed mineralogically by standard X-ray diffractometry techniques. Clay minerals were differentiated by use of oriented specimens and various treatments such as glycollation and heating. Full details of these techniques, and of the computations of semi-quantitative compositional estimates, are given in Appendix B.

As stated in Appendix B, the inherent structural differences between

coarse-grained phases and the clay minerals prevents a meaningful estimate of relative proportions of all phases (i.e. coarse-grained and clays) in a whole-rock specimen. Thus the analytical results which follow give the relative percentages (by weight) of coarse-grained phases only (i.e. quartz, feldspars, calcite). The relative proportions of clay minerals in the clay-fractions, where investigated, are given separately. However, it is worth bearing in mind that an average non-calcareous shale is composed of 30-40% coarse-grained phases with clays making up the remaining 70-60%. Clearly, calcareous samples may have a considerably lower proportion of clays.

The coarse-grained phases of most samples from the Buildwas section (DD prefix) and from the Marloes Sands section (MS prefix) have been analysed, and the results are presented in Table 2.1. Abundances are rounded to the nearest five percent and are reproducible at this level.

Two significant points arise from the data shown in Table 2.1. Firstly, the presence of calcite in some samples from both sections; the percentage calcite indicates variation in lithology of these samples from slightly calcareous shales to impure limestones. Of particular significance is the absence of potassium feldspar from the samples analysed. In sediments deposited under normal conditions, potassium feldspar would certainly be of detrital origin; thus its appearance would be firm evidence for the presence of a detrital component in the sediment.

The clay fractions (<2 μ m e.s.d.) of six samples from each of the Buildwas and Marloes Sands suites were separated and analysed by XRD. Examples of diffractograms of samples from each locality, and their responses to various treatments, appear in Figs. 2-6 and 2-7. The clay minerals present, and their relative abundances, are shown as histograms in Fig. 2-8.

The most striking contrast between samples from the two localities, apparent in Fig. 2-8, is the important rôle of mixed-layer clays (illite-

<u>Sample</u>	<u>Quartz, %</u>	<u>Plag, %</u>	<u>Calcite, %</u>
<u>Buildwas Mudstones</u>			
DD 4	30	5	65
DD 7A	80	20	nd
DD 7B	90	10	nd
DD 7C	90	10	nd
DD 7D	85	15	nd
DD 7E	80	20	nd
DD 8A	55	15	30
DD 9	85	15	nd
DD 30	75	20	5
DD 33	55	5	40
DD 37	70	10	20
DD 38	85	15	nd
<u>Marloes Shales</u>			
MS 1	75	25	nd
MS 2	85	15	nd
MS 3	90	10	nd
MS 6	75	25	nd
MS 9	90	10	nd
MS 10	65	30	5
MS 12	5	trace	90
MS 16	80	10	10
MS 17	45	5	50
MS 19	55	5	40

Table 2.1. Relative abundances of coarse-grained phases in samples from Upper Llandoverly of Buildwas, Shropshire and Marloes, Pembroke-shire. Determined by semi-quantitative X-ray diffraction method (Schultz, 1964).
(N.B. This analysis omits clay minerals - often the major component.)

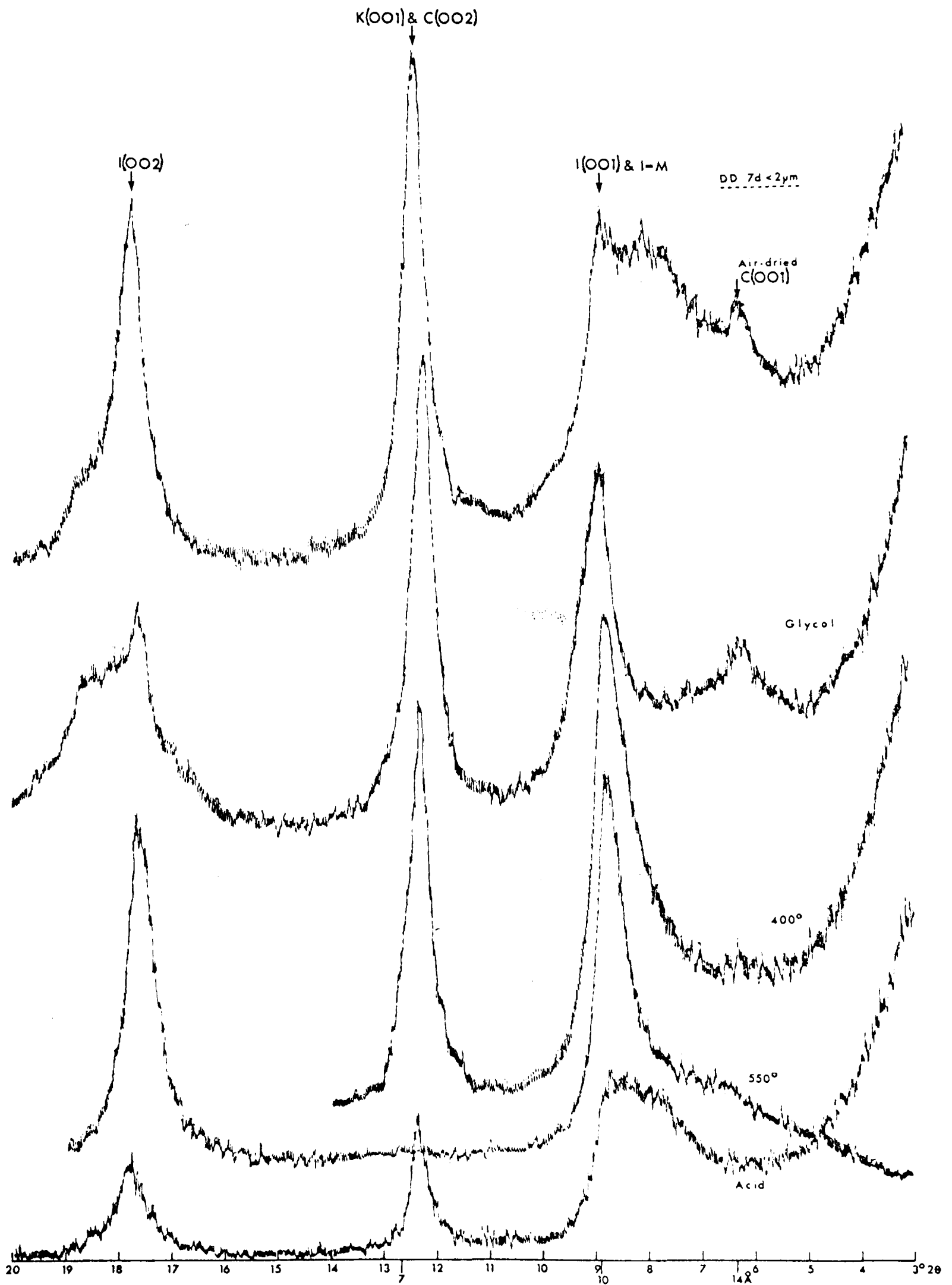


Fig.2-6. Diffractograms of oriented mount of clay-fraction from Buildwas sample DD7d. I = Illite, I-M = mixed-layer phase, C = chlorite, K = kaolinite.

From top: (a) air-dried, (b) glycollated, (c) heated at 400°C for 1hr., (d) heated at 550°C for 1hr., (e) boiled in 10% HCl.

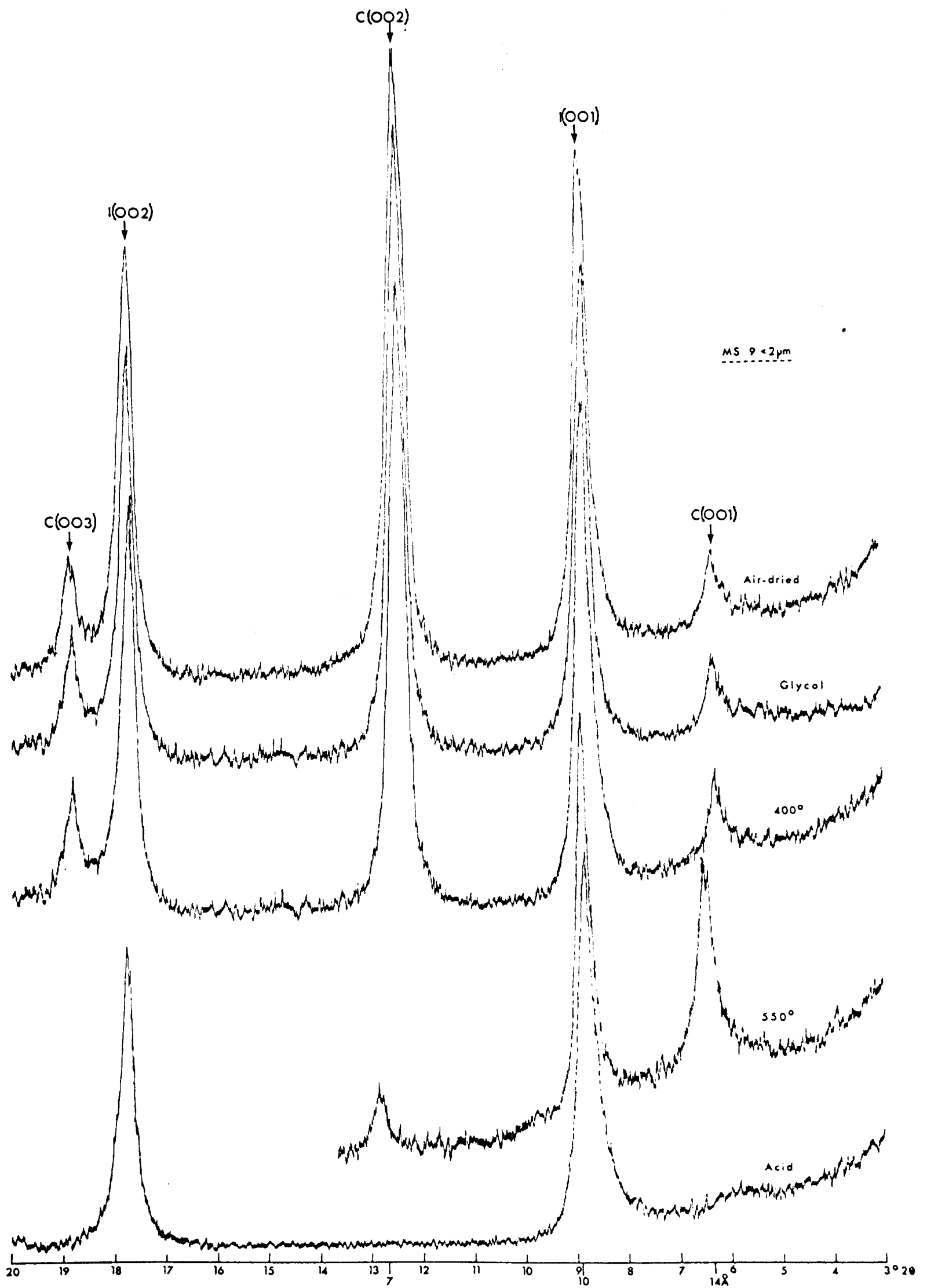


Fig.2-7. Diffractograms of oriented mount of clay-fraction from Marloes sample MS 9. I = Illite, C = chlorite.

From top: (a) air-dried, (b) glycolated, (c) heated at 400°C for 1hr., (d) heated at 550°C for 1hr., (e) boiled in 10% HCl.

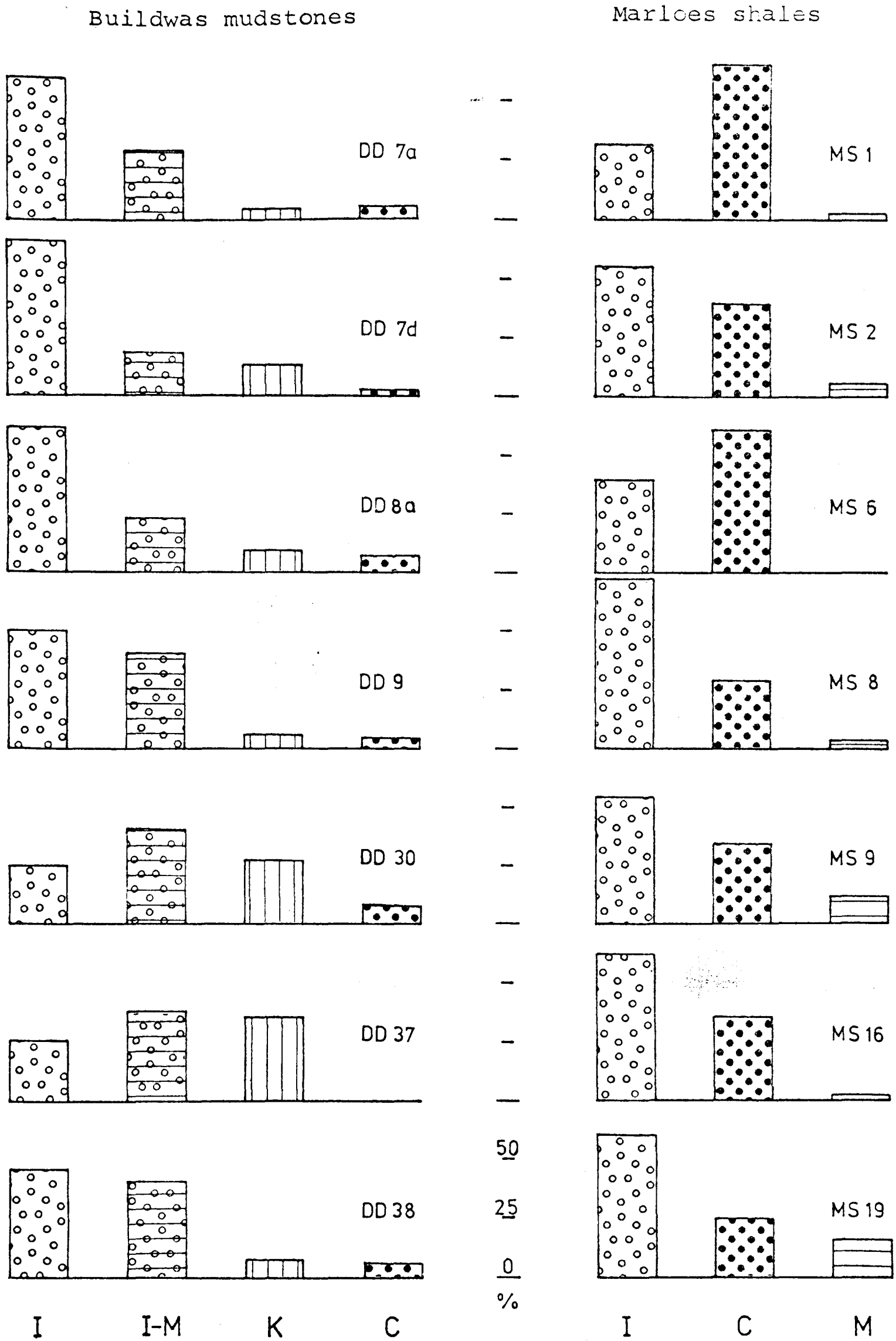


Fig.2.8 Clay fraction mineralogy of Buildwas & Marloes samples. I=illite, I-M=illite-montmorillonite, M=montmorillonite, K=kaolinite, C=chlorite.

smectite) in the Buildwas samples, whereas the clay-fractions of the Marloes samples are dominated by an 'illite-chlorite paragenesis'. Kaolinite is present in minor amounts in Buildwas samples, but absent from Marloes samples. Interpretation of this data will be discussed subsequently in Chapter 3.

2.3.2. Illite Crystallinity Measurements

For many years, it has been recognised that the degree of crystallinity of illite might be used as a measure of the advancement of burial diagenesis (Dunoyer de Segonzac 1970) towards incipient metamorphism (Frey 1970). Use of illite crystallinity as an index of burial processes is based on the structural and chemical changes which are observed to take place in illitic clays during burial (Weaver & Beck 1971). Smectites, which have variable interlayer spacings and are able to expand and incorporate organic molecules (e.g. glycol), undergo 'aggradation' (Millot 1970) during burial. Aggradation involves the assimilation of K^+ cations from pore solutions, and production of mixed-layer clays with an increasing proportion of illitic layers as burial progresses. Therefore these chemical changes are accompanied by structural and morphological changes, such that the crystal perfection will advance towards that of a true 10\AA mica.

The width of the 10\AA peak at half-peak height, measured under standardised conditions, has been used as an index of illite crystallinity (Kubler 1968). Kubler's technique was used in the present study and data were normalised to a set of international standards produced by Professor Kubler. The experimental conditions, and details of the Kubler standards, are given in Appendix C. It should be noted that the illite crystallinity index, defined as half-peak height width, decreases as the crystallinity (i.e. degree of crystal perfection) increases.

The illite crystallinity index has been used as a parameter by which

argillaceous rocks may be classified according to diagenetic advancement. French investigators (see, for example, Kubler 1968) have defined in this way three zones: the Diagenetic Zone, the Anchizone and the Epizone. In this study, to avoid confusion with the general usage of the term 'diagenesis', which normally encompasses all three zones, the first zone is re-named here the Non-metamorphic Zone (after Dunoyer de Segonzac et al. 1968).

The scale of illite crystallinity indices divided into these three zones of diagenesis (Kubler 1968) is shown in Fig. 2-9. On the scale are marked the positions of the three Kubler standards (cf. Appendix C) and the range of crystallinity index (CI) values measured for Marloes samples. The Marloes samples are all seen to be in the Anchizone on this scale:

<u>Sample No.</u>	<u>CI, mm</u>
MS 1	5.5
MS 6	6.3
MS 9	5.5
MS 16	7.5
MS 19	7.7

The diffuse nature of the "10⁰Å" peak on the low-angle side of 10⁰Å for the Buildwas (DD) samples (Fig. 2-6) renders any attempt to assign accurate CI values to the illite meaningless. However, glycollated specimens suggest a CI value in excess of 13, i.e. well down in the Non-metamorphic zone (Fig. 2-9).

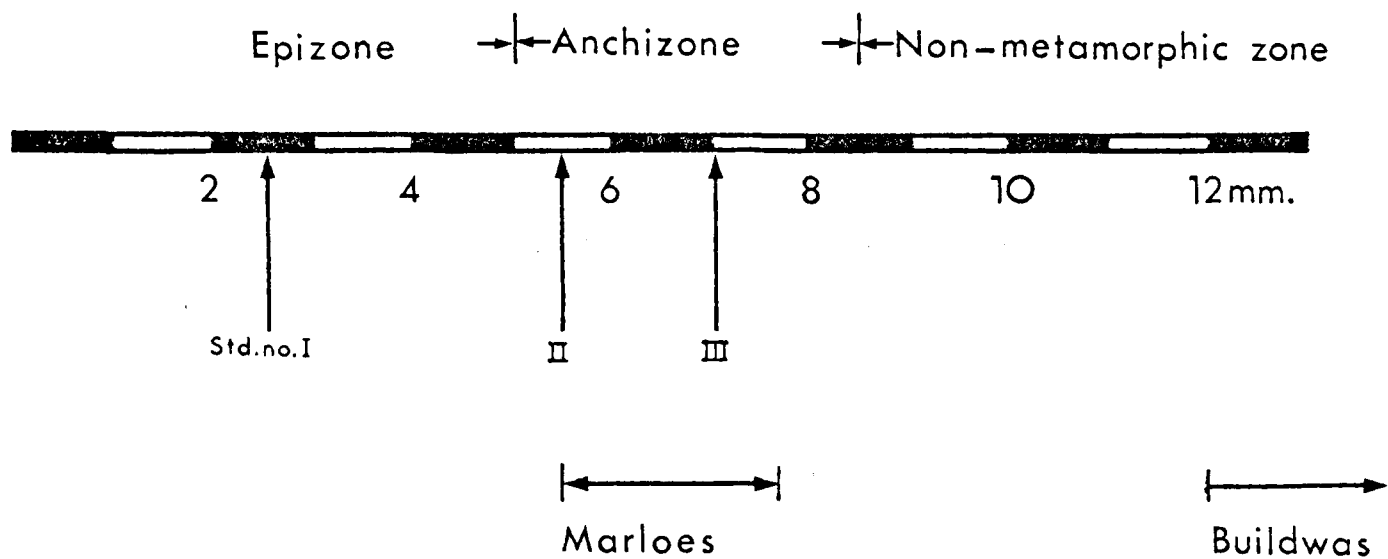


Fig. 2-9. Illite crystallinity index scale according to Kubler (1968). Index is peak width in mm at half-height, recorded on chart speed of 1600 mm hr^{-1} with goniometer speed at $2^\circ 2\theta \text{ min}^{-1}$. Positions of three Kubler standards (cf. Appendix C), and ranges of CI from Buildwas and Marloes sediments are also shown.

2.4. Rb-Sr Study on Whole-Rock Samples

Rb/Sr ratios of whole-rock samples were determined by X-ray fluorescence analysis. Pressed-powder pellets were prepared in duplicate, using the method of dry compaction onto a backing of boric acid.

The method described by Pankhurst & O'Nions (1973) was adopted, whereby a single standard was used. For the purposes of obtaining precise Rb/Sr ratios only, the mass absorption coefficients for Rb $K\alpha$ and Sr $K\alpha$ radiation in each sample are considered identical (due to the predominance in both of the contribution due to Fe K absorption) and therefore cancel out in computation. However, in calculating estimates of Rb and Sr concentrations the relative MAC's between samples and standard are required, and in this case have been assumed to be inversely proportional to mean background intensity. (In more recent investigations, the Mo $K\alpha$ Compton scatter peak intensities have been recorded, and the MAC's assumed to be inversely proportional to this more precisely measured parameter).

An automatic Philips PW 1212 spectrometer in the Department of Geology at the University of Nottingham was used (with the co-operation of Dr. P.K. Harvey). Radiation was provided by a Mo-target X-ray tube operating at 100 kV and 20 mA; the secondary radiation was analysed via a flat crystal spectrometer using a LiF 220 crystal and measured by a scintillation detector with a discrimination circuit optimized for Sr $K\alpha$ radiation. X-ray intensities were measured sequentially at five goniometer positions (background-Sr $K\alpha$ peak - background - Rb $K\alpha$ peak-background), counting times being 40 sec-peak and 20 sec-background. Samples were analysed in batches of four, and each batch was cycled seven times. The standard chosen, AGX (a syenite used in Oxford as an XRF standard), was included in every other batch of four. Pankhurst & O'Nions (op. cit.) have obtained precise analyses for Rb & Sr in AGX by replicate isotope dilution. The mean values obtained are 243.0 ± 0.7 ppm Rb and 175.2 ± 0.3 ppm Sr,

which make this a suitable standard for determinations of Rb/Sr ratios on argillaceous sediments (average 200 ppm Rb, 200 ppm Sr).

Data was recorded on punched tape and processed on the Oxford Elliott 903 computer, using program P2XRF (written by Dr. R.J. Pankhurst). Measured count-rates were corrected for 2 μ sec dead time (estimated), and also for background and inter-peak interference. A more detailed breakdown of the corrections and computations is given in Appendix E.1 in the form of a flow-diagram.

Pankhurst & O'Nions (op. cit.) conclude, from a series of analyses of standard rocks by both isotope dilution and X-ray fluorescence, that the absolute accuracy of Rb/Sr ratios determined by the above XRF technique is in the region of $\pm 0.5\%$ (Rb or Sr concentrations below 50 ppm level demand refined equipment and longer counting times to achieve this degree of accuracy). However, the absolute concentrations of Rb and Sr must be regarded as estimates only, since deviations are at best around $\pm 5\%$.

Analytical results for Buildwas (DD) samples and for the two suites of shales from Pembrokeshire - Deadman's Bay (RS) and Marloes Sands (MS) - appear in Tables 2.3 and 2.4 respectively. Calculated errors in Rb/Sr ratios are little more than 1% at the 2σ level.

Strontium for mass-spectrometric analysis was extracted from whole-rock samples by the procedures described in Appendix D. The extracted strontium was loaded as the dissolved chloride onto single tantalum filaments with one drop of 1M orthophosphoric acid (the latter having been found to stabilize ion emission).

Isotope analyses were performed on a 30 cm. radius mass spectrometer (designed by Dr. N.H. Gale). Emitted ions were accelerated through a potential of 7kV, passed through a series of focussing plates, into the tube assembly, and collected on a Faraday cup arrangement. The source, tube and collector were maintained at a pressure less than 5×10^{-8} torr.

The ion current was recorded across a 10^{10} ohm resistor on a V.G. Chopper amplifier, fed into a Hewlett-Packard voltage-frequency converter, and integrated for 2 sec. on a Börer fast scaler. Peak switching was performed by means of a current switching unit linked to the magnet power supply; a counting delay of 2 sec. was found sufficient to overcome hysteresis effects.

Each cycle consisted of seven measurements, passing through the mass sequence 88-87-86-85½ (baseline) - 85 (Rb-interference) - 84½-88½. The measured ^{88}Sr beam was maintained within the range 10^{-11} - 10^{-10}A ; over a greater range of beam currents, no systematic bias due to voltage coefficient could be detected in $^{88}\text{Sr}/^{86}\text{Sr}$ ratio measured for the Eimer and Amend standard.

Output from the Börer scaler was fed directly into an Elliott 903 computer via an interfacing unit. The data was processed on-line by program P1A7 in batches of ten cycles, the output consisting of a $^{87}\text{Sr}/^{86}\text{Sr}$ ratio corrected for baseline (by interpolation) and normalised to a $^{86}\text{Sr}/^{88}\text{Sr}$ ratio of 0.1194. More refined data was obtained by processing the data, off-line, by program P2ZSR, which corrects for Rb-interference as well as baseline, and in addition permits the selection of data below a chosen level of precision (cf. Appendix E.2).

The Eimer and Amend SrCO_3 isotope standard was analysed several times over the period of time in which these investigations took place. The normalised $^{87}\text{Sr}/^{86}\text{Sr}$ ratios obtained for this standard were consistently within error, as will be seen in Table 2.2.

The Sr-isotope analyses of whole-rock samples from the Welsh Borderland and Pembrokeshire suites are shown, along with Rb/Sr ratios, in Table 2.3 and 2.4 respectively.

The errors associated with isotopic analyses reported here are those calculated at 95% confidence limits on the mean value of the isotope ratios from individual batches of ten scans. The assumption implicit

<u>Date</u>	<u>E & A $^{87}\text{Sr}/^{86}\text{Sr}$ ($\pm 2\sigma$)</u>	<u>No. of cycles</u>
10 Nov 1972	0.70825 \pm 9	100
1 Feb 1973	0.70823 \pm 10	80
8 Oct 1973	0.70830 \pm 7	140
20 Oct 1973	0.70829 \pm 5	140
24 Oct 1973	0.70830 \pm 4	190
18 Dec 1973	0.70827 \pm 4	230
5 Mar 1974	0.70828 \pm 5	270

Table 2.2. $^{87}\text{Sr}/^{86}\text{Sr}$ ratios obtained for Eimer and Amend SrCO_3 standard. (V.G. Chopper amplifier, $10^{10}\Omega$ resistor).

Sample No.	Rb ppm*	Sr ppm*	Rb/Sr±2σ	⁸⁷ Rb/ ⁸⁶ Sr±2σ	⁸⁷ Sr/ ⁸⁶ Sr±2σ
DD 1	151	127	1.192±.016	3.459±.046	0.7348±3
DD 4	27	191	0.141±.002	0.408±.006	0.7122±4
DD 7A	172	150	1.151±.016	3.340±.046	0.7337±3
DD 7B	187	158	1.183±.016	3.433±.046	0.7355±3
DD 7C	177	147	1.196±.016	3.471±.046	0.7349±3
DD 7D	178	144	1.241±.018	3.602±.052	0.7355±3
DD 7E	186	147	1.263±.018	3.666±.052	0.7360±2
DD 8A	50	129	0.389±.008	1.127±.023	0.7191±4
DD 8C	170	165	1.031±.014	2.991±.020	0.7313±6
DD 9	186	155	1.202±.016	3.488±.046	0.7341±3
DD 30	69	93	0.738±.010	2.140±.029	0.7270±3
DD 34	145	140	1.031±.014	2.991±.041	0.7310±3
DD 38	173	155	1.118±.016	3.244±.046	0.7333±5
DD 39	30	156	0.196±.004	0.568±.011	0.7143±2

*Rb & Sr concentrations estimated independently of Rb/Sr ratio;
 estimated precision ± 5%

Table 2.3. Rb-Sr Analytical Data for Upper Llandoverly Sediments from Buildwas, Shropshire.

Sample No.	Rb ppm*	Sr ppm*	Rb/Sr±2σ	⁸⁷ Rb/ ⁸⁶ Sr±2σ	⁸⁷ Rb/ ⁸⁶ Sr±2σ
Deadman's Bay section:					
RS 3	116	59	1.958±.026	5.685±.075	0.7402±2
RS 4	135	51	2.686±.044	7.807±.128	0.75107±8
RS 5	143	50	2.891±.048	8.405±.140	0.75380±12
RS 7	150	67	2.224±.032	6.460±.093	0.74389±14
RS 10	158	98	1.610±.022	4.673±.064	0.73700±12
RS 11	171	111	1.550±.022	4.499±.064	0.7360 ±2
RS 12	170	96	1.773±.026	5.147±.075	0.73877±12
RS 13	166	99	1.681±.024	4.880±.070	0.73769±10
RS 14	169	98	1.724±.024	5.005±.070	0.73840±12
RS 15	157	99	1.588±.024	4.607±.070	0.73576±14
Marloes Sands section:					
MS 1	115	52	2.224±.032	6.458±.093	0.7445±4
MS 2	177	44	3.998±.070	11.639±.204	0.7710±2
MS 3	154	50	3.107±.050	9.034±.145	0.75916±10
MS 4	164	58	2.836±.044	8.242±.128	0.7537±4
MS 5	140	73	1.919±.030	5.570±.087	0.74074±6
MS 6	145	74	1.956±.026	5.677±.075	0.7406±4
MS 7	141	83	1.697±.026	4.924±.075	0.73633±8
MS 9	192	71	2.710±.038	7.875±.110	0.7531±2
MS 10	114	95	1.197±.018	3.470±.052	0.72808±4
MS 11	171	134	1.281±.018	3.715±.052	0.7315±2
MS 12	21	516	0.040±.002	0.116±.006	0.71123±14
MS 13	162	93	1.746±.024	5.066±.070	0.73687±12
MS 14	153	125	1.229±.016	3.564±.046	0.73022±10
MS 15	159	115	1.378±.060	3.996±.174	0.73210±6
MS 16	171	121	1.417±.020	4.110±.058	0.7333±4

Sample No.	Rb ppm*	Sr ppm*	Rb/Sr $\pm 2\sigma$	$^{87}\text{Rb}/^{86}\text{Sr}\pm 2\sigma$	$^{87}\text{Rb}/^{86}\text{Sr}\pm 2\sigma$
MS 17	118	345	0.342 \pm .004	0.990 \pm .011	0.7152 \pm 2
MS 18	175	122	1.442 \pm .020	4.183 \pm .058	0.7338 \pm 4
MS 19	156	184	0.852 \pm .012	2.469 \pm .035	0.7234 \pm 4
MS 20	176	123	1.435 \pm .064	4.162 \pm .185	0.73264 \pm 10
MS 21	11	372	0.031 \pm .002	0.090 \pm .006	0.7118 \pm 4
MS 22	152	90	1.691 \pm .024	4.906 \pm .069	0.7366 \pm 4

* Rb & Sr concentrations estimated independently of Rb/Sr ratio;
estimated precision \pm 5%

Table 2.4. Rb-Sr Analytical Data for Upper Llandovery Sediments from Marloes district, Pembrokeshire.

in taking this to be a significant statistic is that there is no systematic bias of measurements and ratios are therefore normally distributed about their mean. A practical test of the significance of this statistic is provided by the data for the Eimer and Amend standard, shown in Table 2.2. It is apparent from these data that the variances calculated in this manner are meaningful reflections of reproducibility.

2.5. Sr-Isotopes in Calcite Leachates

Acid-leaching experiments were performed in order to evaluate the contribution to Sr-isotope composition of whole-rock samples from the calcite phase in some samples. Calcite is of particular interest since it is undoubtedly authigenic: its isotope composition therefore reflects that of the depositional environment or subsequent conditions.

Clearly, the leaching procedure must be one which excludes, as far as is possible, the leaching of strontium from phases other than calcite. Strontium in the silicate phases might be expected to be more radiogenic than that in the rubidium-free calcite. To a large extent, the elimination of such interference in measured calcite $^{87}\text{Sr}/^{86}\text{Sr}$ ratios is aided by the relatively high Sr content in calcite (an average 660 ppm Sr in the calcite of Palaeozoic limestones was estimated by Kulp et al. 1952). Bofinger et al. (1968) examined, in some detail, the isotope composition of Sr leached from dolomitic Ordovician shales with hydrochloric acid of variable molarity and for different lengths of time. In all their experiments, the above authors found that a relatively Rb-rich component (possibly chlorite) was dissolved to a small extent as well as the Sr-rich carbonate component. However, preferential leaching of radiogenic ^{87}Sr from the Rb-rich component was not observed, and therefore the problem of interference on this account is minimized. In fact, Bofinger et al. (op. cit.) observed a slight decrease in $^{87}\text{Sr}/^{86}\text{Sr}$ of leachate as HCl normality was increased up to 1N, presumably due to increasing the eff-

iciency of dissolving the Sr-rich phase (low $^{87}\text{Sr}/^{86}\text{Sr}$) relative to that of leaching the Rb-rich phase. The conditions chosen for the present study were 5 mins. of leaching by quartz-distilled 1N HCl (the conditions which yielded the lowest $^{87}\text{Sr}/^{86}\text{Sr}$ for leachate in the work of Bofinger and co-workers). Leaching with 0.4N B.D.H. 'Aristar' acetic acid was also tried, to see if the weak acid would produce a lower $^{87}\text{Sr}/^{86}\text{Sr}$ ratio for leachate. Results, however, with the two acids are indistinguishable.

Four samples of calcareous mudstone from Buildwas (DD) and three samples of calcareous shale from Marloes Sands (MS) were treated by the above procedure. 0.5-1.0g. of rock was agitated with an excess of the acid for about 5 mins. and the solution decanted. Any remaining solids were removed by centrifuging, and the solution was evaporated to dryness. Sr was separated from Ca by conventional cation exchange techniques (see Appendix D). In the case of high Ca/Sr ratio samples, a double ion exchange step proved necessary.

The measured Sr-isotope compositions for these calcite leachates are shown in Table 2.5. Also shown, for comparison, are averages of Palaeozoic and modern sea-water strontium analyses (Peterman et al. 1970). Peterman's Palaeozoic sea-water value is based upon analyses of many samples of primary calcite from shelly fauna.

It is clear from Table 2.5 that the $^{87}\text{Sr}/^{86}\text{Sr}$ ratios of Buildwas samples cluster around a mean value which is significantly lower than that of the Marloes samples. This difference will be discussed in the subsequent chapter in the context of the whole-rock Rb-Sr systems.

Sample	$^{87}\text{Sr}/^{86}\text{Sr}$ of calcite leachate ($\pm 2\sigma$)	
DD 4	0.7085 \pm .0002	} 0.7089 \pm 6
DD 8a	0.7092 \pm .0001	
DD 33	0.7088 \pm .0001	
DD 39	0.7087 \pm .0003	
MS 12	0.7106 \pm .0001	} 0.7104 \pm 4
MS 17	0.7102 \pm .0001	
MS 19	0.7104 \pm .0001	
Average Palaeozoic sea-water	0.7078*	
Average Modern sea-water	0.7090*	

* Peterman et al. (1970)

Table 2.5. Strontium isotope data for calcite leachates on Buildwas and Marloes samples.

2.6. Rb-Sr Study on Size-fractionated Samples

2.6.1. Within-sample size fractions

The usual method of investigating Rb-Sr systematics on a small scale (i.e. between mineral phases) in igneous and metamorphic rocks is one of obtaining pure mineral separates and subjecting them to isotope analysis. Such methods are not possible in the case of very fine grained sedimentary rocks. The small crystallite size prohibits the routine separation of pure clay mineral fractions. However, it is possible to obtain fractions, from within a single sample, which differ widely in their Rb and Sr contents, by means of size fractionation. The varying Rb/Sr ratios of different size-fractions reflect the different size ranges and hence abundances of the mineral phases, particularly those of the clay minerals. Smectite crystallites are extremely small, having sub-micron dimensions and apparently breaking down into particles approaching unit-cell thickness; on the other hand, kaolinite is frequently euhedral, dimensions ranging up to, and beyond, the $2\mu\text{m}$ limit assigned somewhat arbitrarily to clay minerals. Illite frequently shows no distinct morphology in electron micrographs, occurring as clusters of sub-micron particles (Grim, 1953).

One sample from Buildwas, DD 9, and two from Marloes, MS 1 & 6, were sub-divided in this manner by means of the centrifugal sedimentation technique described in Appendix A. Five size-fractions of each sample were obtained - $>10\mu\text{m}$, $5-10\mu\text{m}$, $2-5\mu\text{m}$, $1-2\mu\text{m}$, $0.2-1\mu\text{m}$.

Due to the small amounts of material separated by this procedure (less than 1 gram in the case of the finest fractions), Rb and Sr concentrations were measured by means of isotope dilution analysis. Accurately weighed amounts of ^{84}Sr - and ^{87}Rb -enriched 'spike' solutions were added to a known weight of sample prior to decomposition, and Sr & Rb extracted by ion exchange techniques (method fully described in Appendix D.2). The extracted Sr was isotopically analysed using the 30 cm. radius mass spectrometer described earlier in this chapter. In this case,

however, the mass sequence was 88-87-86-85-84-84½ (baseline) - 88½.

Rb was isotopically analysed by similar methods. Rb ions are emitted from the Ta-filament at a considerably lower temperature than those of Sr, hence interference of Sr on Rb peaks may be discounted. Each cycle consisted of five peaks, in the mass sequence 87-85-85-85½-87, the data being processed on-line by program P1A5. Since natural Rb has only two component nuclides, ⁸⁷Rb and ⁸⁵Rb, it is not possible to eliminate fractionation effects by normalization. Consequently, the filament temperature during analysis was maintained as low as possible (Rb ion beam intensity of $\sim 10^{-11}$ A), which resulted in stable ion beams and an 87/85 ratio reproducible to within 0.3% (see Pankhurst & O'Nions 1973).

Rb and Sr concentrations and the unspiked ⁸⁷Sr/⁸⁶Sr ratio for each sample were calculated from the measured Rb and Sr isotope compositions (Programs PS841D and P87RB1D, see Appendix E.3 and E.4).

The analytical data for these three sets of size-fractions are shown in Table 2.6. Errors quoted for Rb/Sr ratios are based on an estimated maximum error of 0.5% (1σ). This estimate is almost certainly a maximum for the isotope dilution method (Pankhurst & O'Nions 1973). Also tabulated are whole-rock (W.R.) analyses for each of the three samples (DD9, MS1 & MS6).

For sample DD9 (Table 2.6), both Rb and Sr are seen to increase with decreasing grain size, which reflects the increasing amount of mixed-layer illite-smectite in the clay fraction. Size-fractions from MS1 and MS6, however, show enhancement of only Rb (due to illite) in the finer fractions, accompanied by a small decrease in Sr content.

The significance of the Sr-isotope data, and its interpretation by model-age computations (Table 2.6 lists these model-ages) will be discussed in Chapter 3.

Sample	Rb ppm	Sr ppm	Rb/Sr $\pm 2\sigma$	$^{87}\text{Rb}/^{86}\text{Sr}\pm 2\sigma$	$^{87}\text{Sr}/^{86}\text{Sr}\pm 2\sigma$	(2) Model age, my
DD9						
0.2-1 μm	228	260	0.876 \pm .008	2.54 \pm .03	0.7255 \pm 10	466
1-2 μm	220	185	1.193 \pm .012	3.46 \pm .03	0.7332 \pm 10	501
2-5 μm	201	139	1.446 \pm .015	4.19 \pm .04	0.7404 \pm 10	537
5-10 μm	147	98	1.503 \pm .015	4.36 \pm .04	0.7438 \pm 20	572
(1) >10 μm	145	119	1.218 \pm .012	3.53 \pm .03	0.7363 \pm 10	554
(1) W.R.	186	155	1.202 \pm .016	3.49 \pm .05	0.7341 \pm 4	516
MS 1						
0.2-1 μm	259	47	5.462 \pm .050	15.93 \pm .16	0.7845 \pm 8	334
1-2 μm	205	44	4.668 \pm .046	13.61 \pm .14	0.7796 \pm 5	366
2-5 μm	163	43	3.809 \pm .038	11.09 \pm .11	0.7681 \pm 2	374
5-10 μm	114	49	2.303 \pm .024	6.69 \pm .07	0.7485 \pm 5	408
(1) >10 μm	108	53	2.023 \pm .020	5.87 \pm .06	0.7415 \pm 3	379
(1) W.R.	115	52	2.224 \pm .032	6.46 \pm .09	0.7445 \pm 6	378
MS 6						
0.2-1 μm	274	52	5.334 \pm .050	15.54 \pm .16	0.7790 \pm 7	317
1-2 μm	240	52	4.623 \pm .046	13.46 \pm .13	0.7733 \pm 9	336
2-5 μm	186	62	2.992 \pm .030	8.70 \pm .09	0.7570 \pm 18	383
5-10 μm	151	70	2.146 \pm .020	6.23 \pm .06	0.7458 \pm 10	407
(1) >10 μm	128	76	1.682 \pm .016	4.88 \pm .05	0.7387 \pm 16	414
(1) W.R.	145	74	1.956 \pm .026	5.68 \pm .07	0.7406 \pm 3	380

Notes: (1) W.R. = Whole rock: Rb & Sr estimates & Rb/Sr ratio by XRF, $^{87}\text{Sr}/^{86}\text{Sr}$ ratio obtained on unspiked sample.
(2) Model ages calculated assuming initial $^{87}\text{Sr}/^{86}\text{Sr}$ ratios of 0.709 (DD9) and 0.7105 (MS1 & 6).

Table 2.6. Isotope dilution analytical data for size-fractionated samples from Buildwas and Marloes; also shown are model ages (see Chapter 3).

2.6.2. Between-Sample Clay Fractions

The susceptibility of relevant nuclides in fine-grained particles to continued mobilisation or remobilisation during a period of metamorphic re-heating, subsequent to closure of the whole-rock system, has been demonstrated by several isotopic investigations (e.g. O'Nions et al. 1969; Jäger, 1970; Clauer & Bonhomme, 1970). A redistribution of Sr-isotopes over short distances (i.e. within distances corresponding to hand-specimen size) will not have affected the whole-rock Rb-Sr system, though it may be detected with data from within-sample fractions (section 2.6.1). However, the grain-size effect mentioned above suggests that studies of the Rb-Sr system between the clay-fractions separated from a number of the whole-rock samples might be of interest. The two suites of Llandovery sediments in the present study provide an opportunity to compare the results of such investigations on rocks of differing metamorphic histories.

The clay-fractions (<2 μ m e.s.d.) of five samples from the Buildwas suite, and of seven samples from the Marloes suite, were separated by gravitational separation at CNRS, Strasbourg (see Appendix A). This method has the advantage over the centrifugal technique used elsewhere in this study of enabling larger amounts of material to be separated at one time.

The samples were analysed for Rb, Sr and $^{87}\text{Sr}/^{86}\text{Sr}$ by isotope dilution procedures as outlined previously (section 2.6.1), and the analytical results on these samples are presented in Table 2.7.

2.7. Intercalated Bentonites

The occurrence of many thin, laterally persistent 'bentonite' bands in the sections at Marloes Sands and Deadman's Bay has already been mentioned (Section 2.2.2). Six of these bentonites at Marloes Sands (MS) and seven at Deadman's Bay (RS) were sampled.

Whole-rock mineralogical analysis (Appendix B) revealed no qualitative difference from the assemblages observed in the subjacent terrigenous

Sample No.	Rb ppm	Sr ppm	Rb/Sr $\pm 2\sigma$	$^{87}\text{Rb}/^{86}\text{Sr}\pm 2\sigma$	$^{87}\text{Sr}/^{86}\text{Sr}\pm 2\sigma$
DD 8B (CLAY)	211	297	0.710 \pm .007	2.066 \pm .02	0.72473 \pm 20
DD 30 (CLAY)	158	204	0.775 \pm .008	2.254 \pm .02	0.72871 \pm 11
DD 34 (CLAY)	247	249	0.992 \pm .01	2.887 \pm .03	0.73074 \pm 5
DD 38 (CLAY)	212	232	0.914 \pm .009	2.660 \pm .03	0.72803 \pm 9
DD 39 (CLAY)	89	136	0.654 \pm .007	1.904 \pm .02	0.72357 \pm 28
MS 3 (CLAY)	215	50	4.30 \pm .04	12.52 \pm .12	0.77498 \pm 20
MS 4 (CLAY)	219	55	4.00 \pm .04	11.63 \pm .12	0.77053 \pm 16
MS 5 (CLAY)	226	53	4.23 \pm .04	12.32 \pm .12	0.77398 \pm 10
MS 7 (CLAY)	215	57	3.75 \pm .04	10.91 \pm .12	0.76498 \pm 20
MS 10 (CLAY)	201	72	2.80 \pm .03	8.14 \pm .09	0.75004 \pm 16
MS 15 (CLAY)	250	135	1.85 \pm .02	5.38 \pm .06	0.73604 \pm 20
MS 17 (CLAY)	248	118	2.10 \pm .02	6.09 \pm .06	0.73959 \pm 16

Table 2.7. Isotope dilution analytical data for clay-fractions (<2 μm e.s.d.) from Buildwas (DD) & Marloes (MS) samples.

sediments: quartz and plagioclase are the sole coarse-grained phases (i.e. the diagnostic high-temperature K-feldspar (sanidine) found in many bentonites is absent).

Clay-fraction mineralogical analyses, including illite crystallinity indices (Appendices B & C), are presented in Table 2.8. Once again, the similarity between assemblages of clay phases in the terrigenous sediments (Fig. 2-8) and in the bentonites (Table 2.8) is noteworthy, though the latter have a markedly higher proportion of illite in the clay-fraction. The predominance of illite and the absence of montmorillonite, the clay mineral generally associated with bentonites, suggests that the term 'metabentonite' (Dunoyer de Segonzac 1970, p.301) might better describe these rocks.

The results of XRF determinations of Rb/Sr ratios, and mass-spectrometric determinations of $^{87}\text{Sr}/^{86}\text{Sr}$ ratios, for these samples are presented in Table 2.9. The higher proportions of illite are reflected in the greater range of Rb/Sr ratios in these metabentonites compared to the normal sediments.

The detailed discussion of the data presented in this chapter, together with isochron diagrams etc., forms the subject of the subsequent chapter.

Sample No.	Chlorite,% ⁽¹⁾	Illite,% ⁽¹⁾	Illite Crystallinity Index ⁽²⁾
Deadman's Bay section:			
RS 1B	20	80	5.7
RS 16B	10	90	6.0
RS 17B	10	90	5.9
RS 18B	10	90	5.4
RS 19B	15	85	5.5
RS 20B	10	90	5.9
RS 21B	10	90	5.7
Marloes Sands section:			
MS 8B	10	90	5.7
MS 23B	10	90	4.9
MS 24B	10	90	4.9
MS 25B	2	98	4.9
MS 26B	2	98	5.9
MS 27B	5	95	5.5

Notes: (1) Semi-quantitative estimates of abundances by weight; see Appendix B.

(2) See Appendix C for measurement technique; also Fig. 2-6 for comparison with other samples on Kubler scale.

Table 2.8. Clay-fraction (<2 μ m) mineralogy of 'Bentonite' bands from Upper Llandovery of Marloes, Pembrokeshire.

Sample No.	Rb ppm*	Sr ppm*	Rb/Sr±2σ	⁸⁷ Rb/ ⁸⁶ Sr±2σ	⁸⁷ Sr/ ⁸⁶ Sr±2σ
Deadman's Bay section:					
RS 1B	265	71	3.75±.05	10.89±.15	0.75878±16
RS 16B	258	115	2.24±.07	6.49±.20	0.74142±4
RS 17B	263	95	2.77±.08	8.06±.24	0.74725±14
RS 18B	257	48	5.36±.17	15.61±.48	0.78095±6
RS 19B	241	47	5.18±.15	15.10±.45	0.77871±12
RS 20B	266	49	5.41±.17	15.78±.49	0.78080±8
RS 21B	267	39	6.92±.22	20.18±.65	0.79843±10
Marloes Sands section:					
MS 8B	245	118	2.07±.03	6.01±.09	0.73957±6
MS 23B	283	43	6.58±.20	19.21±.58	0.79404±8
MS 24B	272	45	6.03±.18	17.58±.52	0.78770±16
MS 25B	355	53	6.67±.20	19.47±.59	0.79507±6
MS 26B	351	47	7.47±.23	21.80±.68	0.80228±10
MS 27B	240	70	3.45±.10	10.01±.30	0.75591±8

* Rb & Sr concentrations estimated independently of Rb/Sr ratio;
 estimated precision ± 5%

Table 2.9. Rb-Sr Analytical Data for 'Bentonite' Bands from Upper Llandovery sections in Marloes District, Pembrokeshire.

CHAPTER 3

THE BEHAVIOUR OF Rb AND Sr IN ARGILLACEOUS SYSTEMS -
AN INTERPRETATION OF THE ISOTOPIC AND MINERALOGICAL DATA

3.1. Introductory Comment

The purpose of this chapter is to assess and interpret the preceding Rb-Sr isotope data obtained from Lower Silurian sediments. The data will be interpreted and discussed in the context of available information concerning the physical and chemical processes occurring during burial and compaction of sediments. Much of our appreciation of these processes is derived from observations on sedimentary successions considerably younger than those involved in this study, and it will be assumed that these are equally applicable in the Palaeozoic.

It is worthwhile at this stage to reemphasise the conditions which must be met in order that a series of rock samples yield a Rb-Sr isochron. These are, that samples (with a range of Rb/Sr ratios) shall have remained closed systems with respect to Rb and Sr subsequent to a time when the Sr-isotope composition was homogeneous throughout the samples. The problems which are fundamental to the understanding of Rb-Sr systematics in sediments are therefore posed:

- (i) What are the processes by which Sr-isotope homogenization takes place between the components of a sedimentary system prior to closure?
- (ii) What is the cause of closure of the system to further Sr-isotope exchange, in those systems where a Rb-Sr isochron is obtained?

In those cases where Sr-isotope homogenization over a large scale (i.e. greater than hand - specimen scale) at some time in the past is apparent from the Rb-Sr data, it seems certain that ionic transport in solution must have been involved. The minimum 'domain' size over which homogenization must have been effected is delimited by the smaller of either (a) the scale over which samples satisfying the Rb-Sr isochron

equation have been collected, or (b) the size of unit whose bulk Rb/Sr ratio represents that of the entire section. In this context, it may be reiterated that samples involved in this study were collected, in general, at different stratigraphic heights in a section (i.e. across bedding) and therefore do not represent lateral variations (cf. section 2.2).

3.2. Buildwas - an Example of Unmetamorphosed Palaeozoic Argillites

3.2.1. Interpretation of Rb-Sr data from whole-rock samples

If the Rb-Sr data obtained from Buildwas mudstones (Table 2.3) are plotted on a conventional isochron diagram, a non-linear array is obtained (Fig. 3-1). A linear regression through all points is possible, but in order that each point fits the line within error, an error expansion factor of three must be applied (i.e. mean square of weighted deviates - MSWD - is 9. Refer to program P2CHRON and explanation of MSWD in Appendix E.5). Since the analytical errors on $^{87}\text{Sr}/^{86}\text{Sr}$ ratios are already somewhat higher than those considered acceptable in later parts of this study, it is concluded that the samples represented by these data do not satisfy the conditions for an isochron. The slope of the best-fit line represents an age of 510 ± 25 m.y. (2σ) ($\lambda = 1.39 \times 10^{-11} \text{ yr}^{-1}$) - an age considerably higher than the estimated age of 420 ± 15 m.y. (using the same decay constant for ^{87}Rb) for the Upper Llandovery (Fullager & Bottino 1968). (Another estimate for the age of the Upper Llandovery is 445 ± 7 m.y. (Bofinger et al. 1970). Recently, a computerised scheme of data selection and weighting has produced an estimate of >436 m.y. for the age to the base of the Silurian (Armstrong & McDowall 1974).).

It is clear from Fig. 3-1 that the data points at low Rb/Sr, i.e. those from calcareous samples, 'anchor' the regression line in such a way that they induce a steeper slope than would otherwise obtain. This is borne out by the mean value of 0.7089 ± 6 obtained for the $^{87}\text{Sr}/^{86}\text{Sr}$ ratio

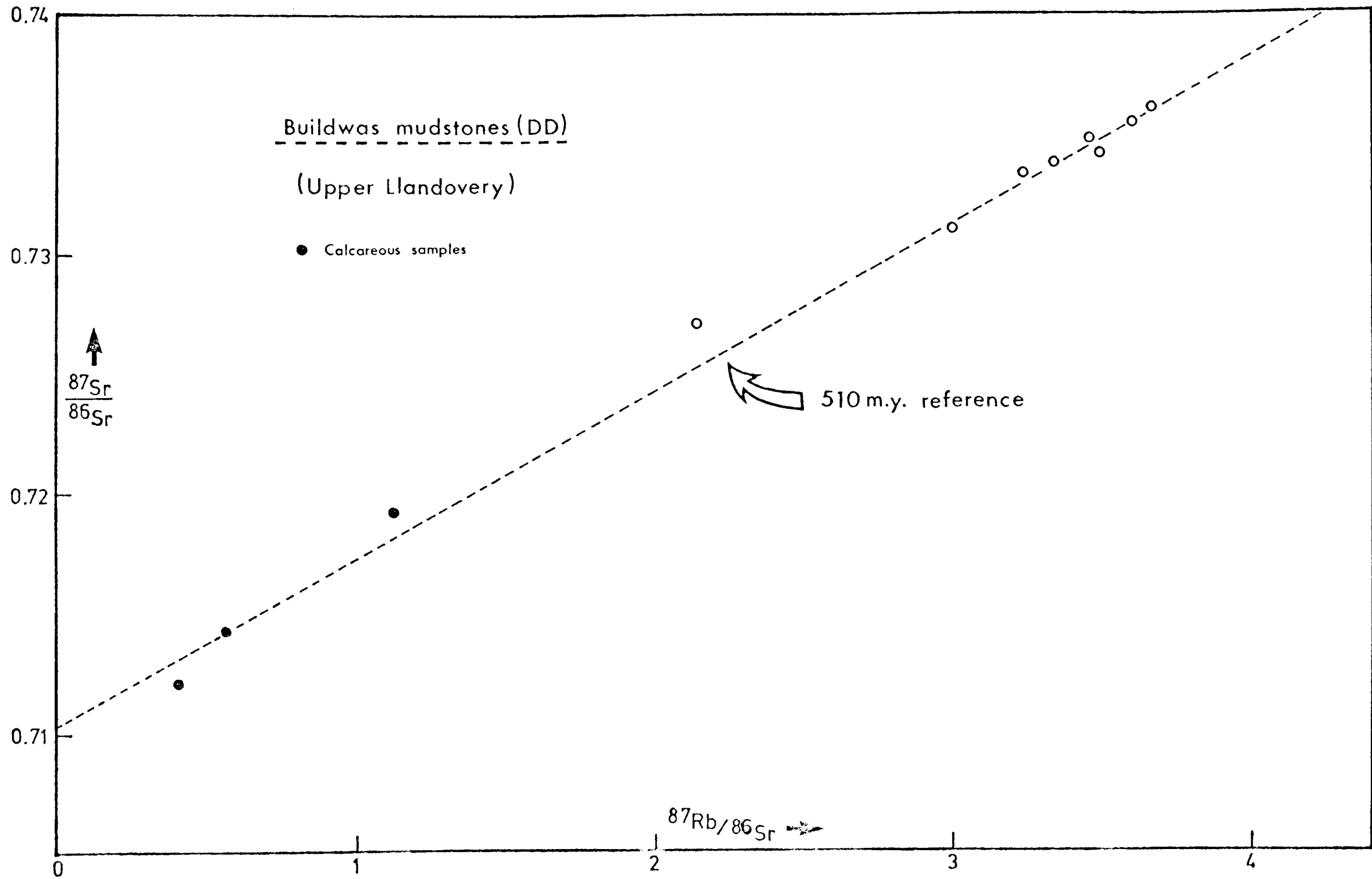


Fig. 3-1. Rb-Sr data from Buildwas mudstones plotted against isochron coordinates. Best-fit line to points is shown, representing date of 510 ± 25 m.y. ($\lambda = 1.39 \times 10^{-11} \text{ yr}^{-1}$).

of calcite leachates from these calcareous samples (Table 2.4). This value may be compared with the initial ratio of 0.7103 ± 9 on the 510 m.y. regression line. If all samples in which calcite is detected (solid circles in Fig. 3-1, see also Table 2.1) are omitted from the regression, a date of c.450 m.y. is represented, though with a correspondingly greater uncertainty owing to the reduction in Rb/Sr range.

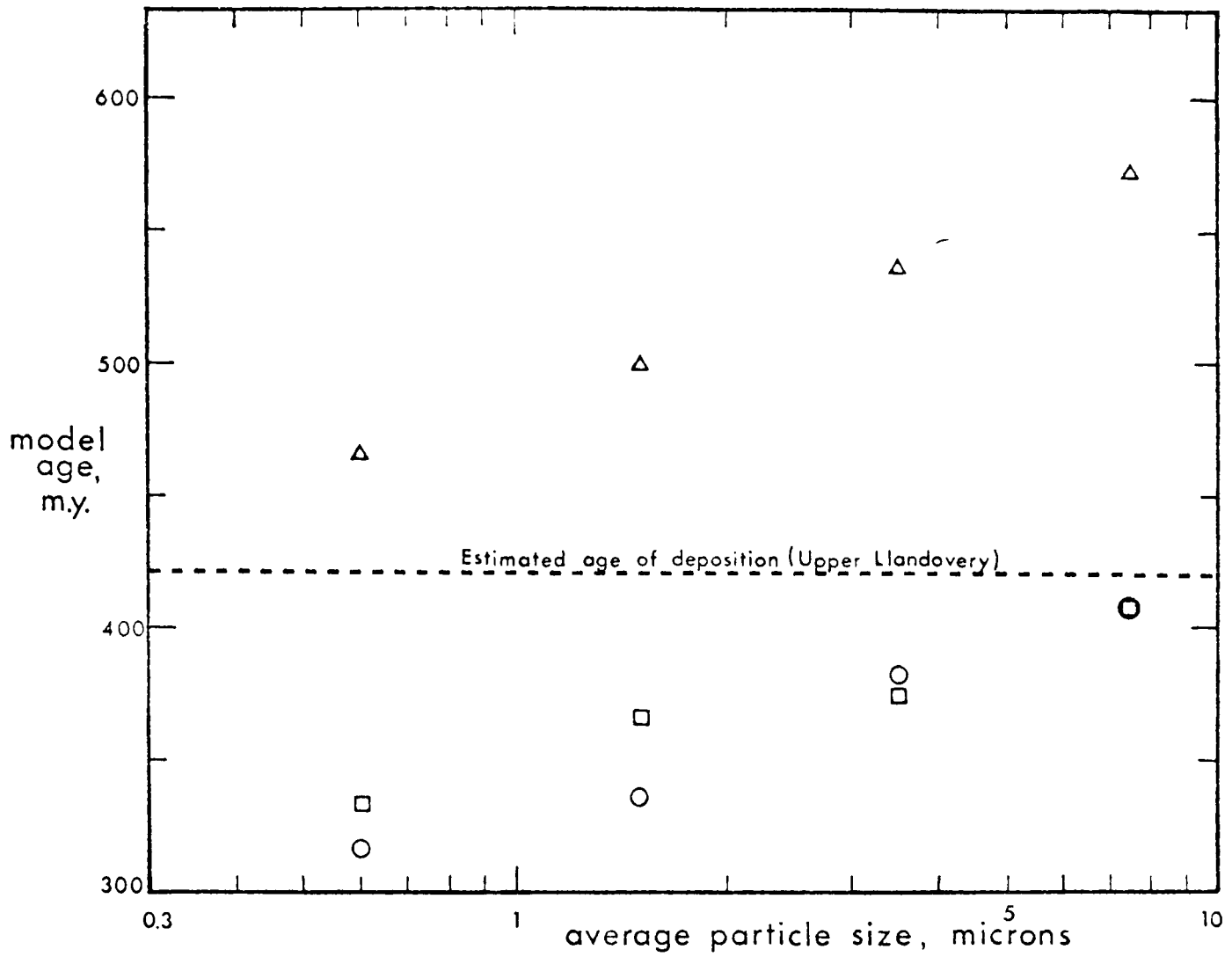
It is deduced from these observations that the samples collected from Buildwas represent a multi-component Rb-Sr system. Calcite, where present, is a component which has crystallized subsequent to deposition and, on the above evidence, in a state of isotopic disequilibrium with respect to the bulk strontium contained within the silicate phases.

The strontium-bearing silicates comprise two or more components in terms of Rb-Sr systematics. Clearly, there is a component of the Rb-Sr system arising from the presence of detrital material: possibly mica which has not been completely transformed during the weathering and degradation process. However, the degraded nature (cf. Millot 1970) of the clays present in these sediments (Section 2.3) suggests that Rb and/or Sr representative of environments other than provenance might be incorporated in these clays, e.g. in the exchangeable cation sites.

3.2.2. Within-sample size fractions

Further evidence of the genetic complexity of Sr in clays is provided by the array of data given by size-fractions from sample DD9 (Table 2.6). Model ages for each fraction, which have been calculated with an assumed initial $^{87}\text{Sr}/^{86}\text{Sr}$ ratio of 0.709 (the mean value for calcite leachates, considered to be a minimum for the initial ratio), are graphically represented in Fig. 3-2. The model ages are seen to decrease with average particle size, although the minimum age (that for the 0.2- μm fraction) is nevertheless greater than the estimated age of deposition.

Decreasing average particle size is found, by reconnaissance X-ray



<u>key:</u>		<u>$(^{87}\text{Sr}/^{86}\text{Sr})_0$ value</u>
DD 9	△	0.7090
MS 1	□	0.7105
MS 6	○	

Fig. 3-2. Plot of Rb-Sr model ages against mean particle size for size-fractions from samples DD9, MS1, & MS6. See text for discussion of selection of initial ratio values.

powder photograph studies, to correlate with an increasing proportion of the mixed-layer illite-smectite phase. The trend of increasing proportions of the mixed-layer phase is accompanied by increases in both Sr and Rb contents in the finer fractions (cf. Table 2.6; compare this pattern with that for MS 1/6 where illite is the fine-grained phase and consequently only Rb increases as size decreases). This demonstrates the importance of the smectite-type layers in providing sites for Sr, whereas Rb replaces the interlayer K in the illite layers.

3.2.3. Between-sample clay fractions

The Rb-Sr data from the clay (<2 μ m) fractions separated from five Buildwas samples (section 2.6.2.) are plotted on an isochron diagram in Fig. 3-3. This diagram reiterates the point made previously concerning the complex Rb-Sr systematics due to the various component clay phases. The five data points scatter around a reference line corresponding to an age greater than that of deposition, and clearly at least two components to the Rb-Sr system are present.

3.3 Marloes - an Example of Folded and Slightly Metamorphosed Palaeozoic Shales

3.3.1. Interpretation of Rb-Sr data from whole-rock samples

The Rb-Sr data from whole-rock samples from Marloes Sands (MS) and Deadman's Bay (RS) (cf. Table 2.4) are plotted on isochron diagrams in Figs. 3-4 and 3-5 respectively. Overall, the precision of $^{87}\text{Sr}/^{86}\text{Sr}$ measurements is better than for Buildwas (DD) samples, and in Fig. 3-4 only the data points of higher precision (<0.005% error on the mean for $^{87}\text{Sr}/^{86}\text{Sr}$) are represented.

These nine data points (MS 3, 5, 7, 10, 12, 13, 14, 15, 20) yield a best-fit line with a MSWD value of 11 (program P2CHRON - see Appendix E.5). The slope of this line corresponds to a date of 382 ± 12 m.y. (2σ)

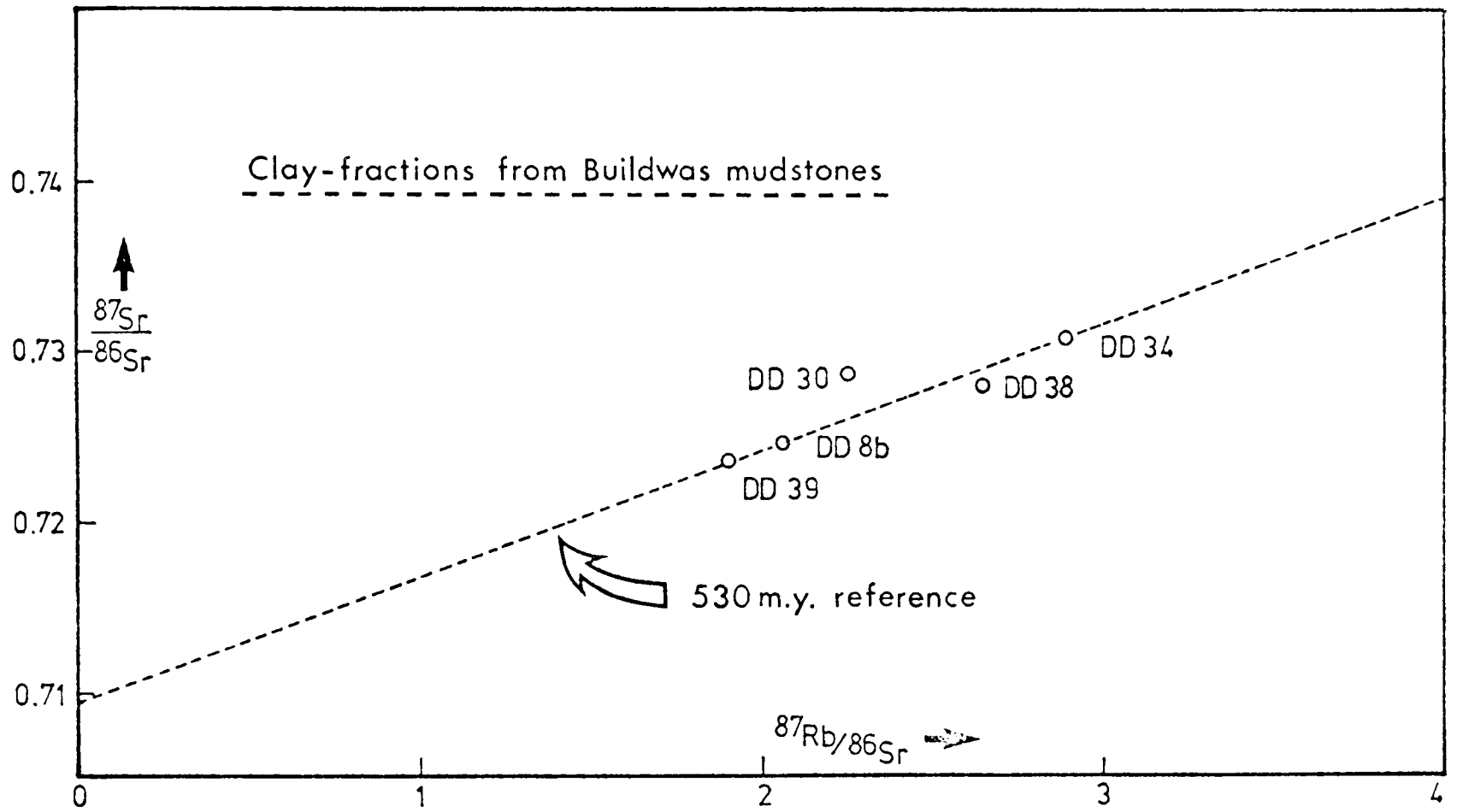


Fig. 3-3. Rb-Sr data from clay (<2 μm) fractions of five Buildwas samples, plotted against isochron coordinates.

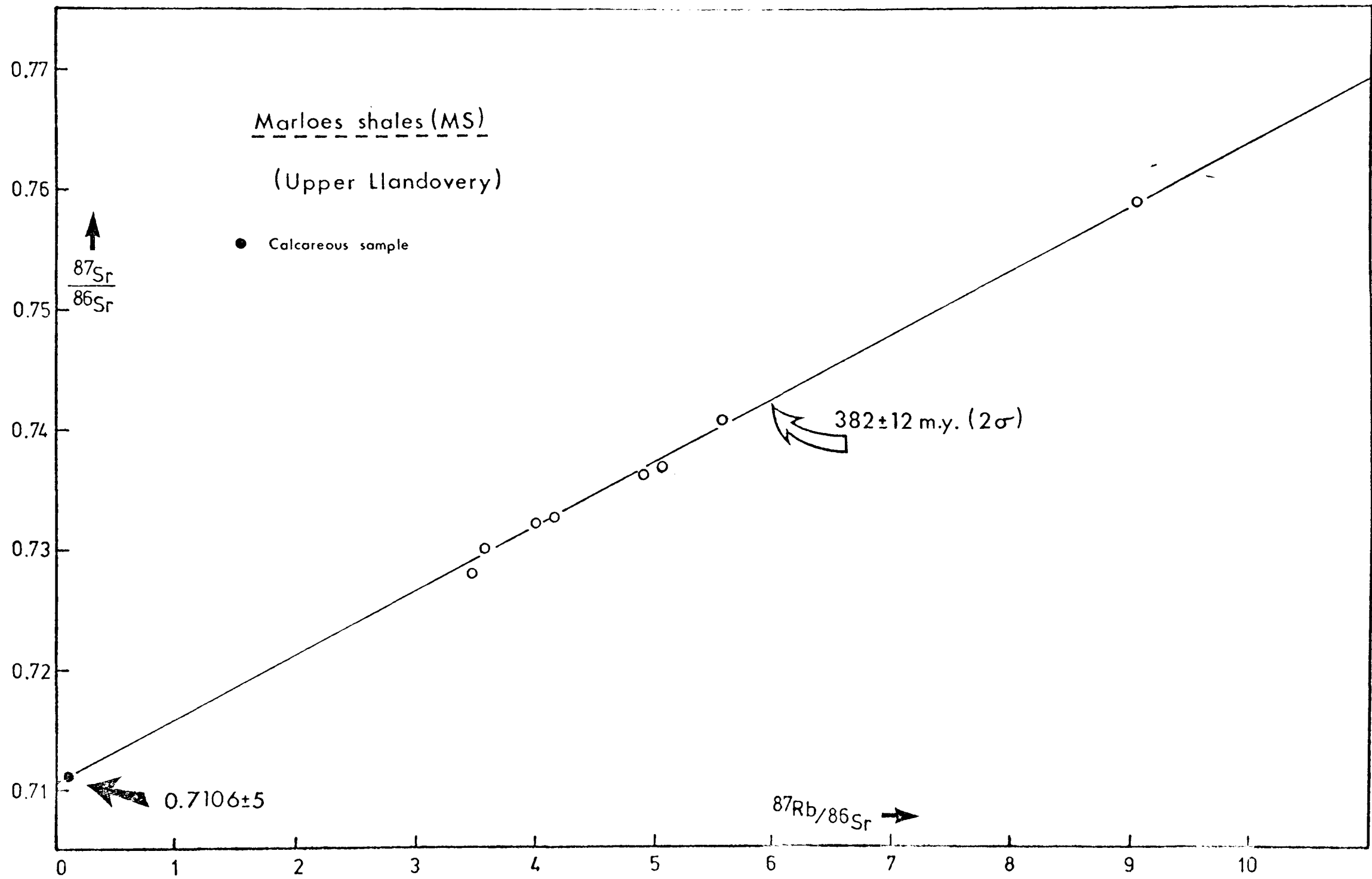


Fig. 3-4. Rb-Sr data from Marloes Sands shales plotted on an isochron diagram. Only the most precise data from Table 2.4 has been plotted. Best-fit age is 382 ± 12 m.y. (MSWD = 11). ($\lambda = 1.39 \times 10^{-11} \text{ yr}^{-1}$)

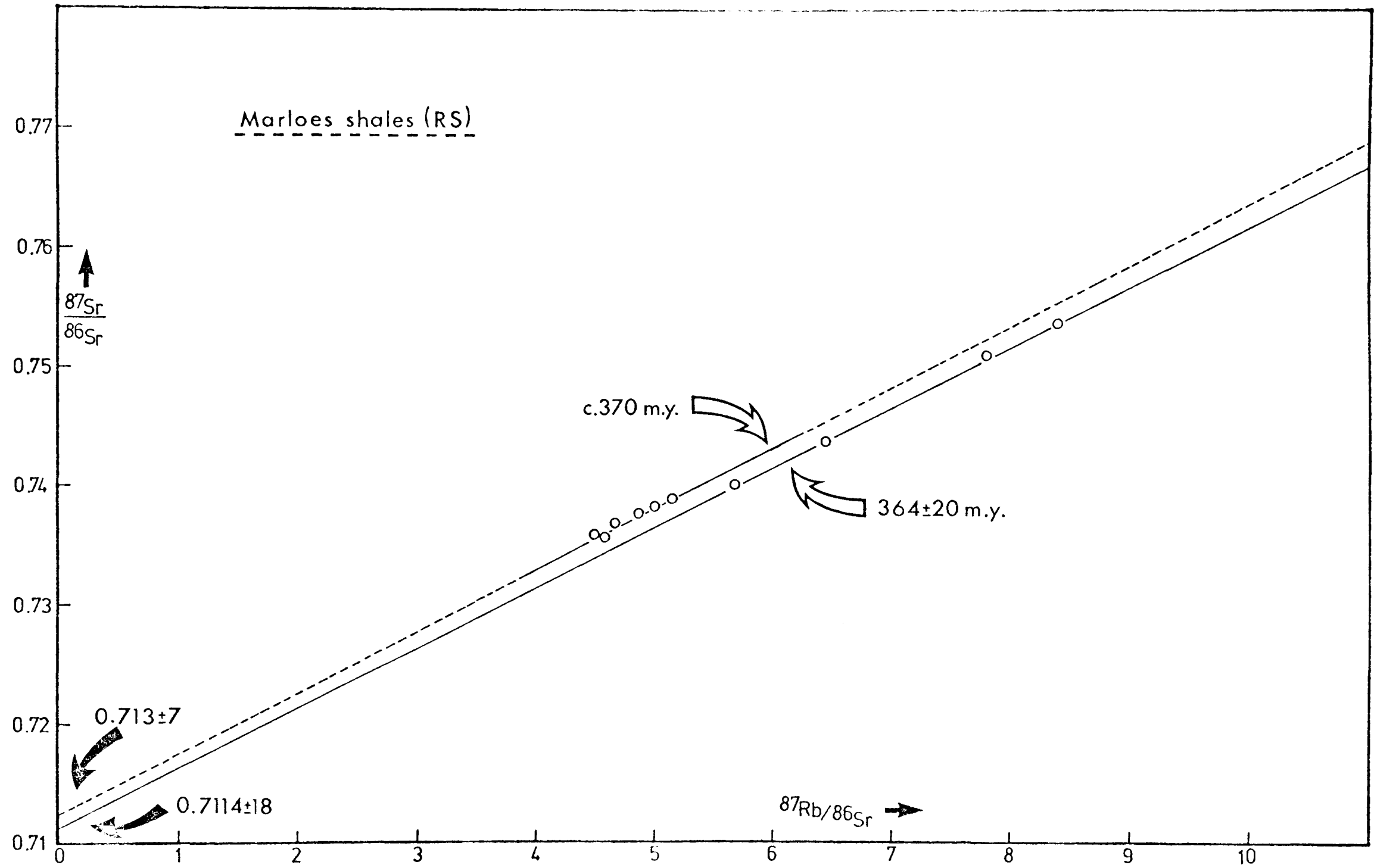


Fig. 3-5. Rb-Sr data from Deadman's Bay shales plotted on an isochron diagram. Two parallel best-fit lines give ages of 364 ± 20 m.y. and ca.370 m.y.

($\lambda = 1.39 \times 10^{-11} \text{ yr}^{-1}$) and an initial $^{87}\text{Sr}/^{86}\text{Sr}$ ratio of 0.7106 ± 5 . Although the MSWD value is similar to that for Buildwas samples (Fig. 3-1), this factor and the considerably lower errors (up to an order of magnitude smaller) in $^{87}\text{Sr}/^{86}\text{Sr}$ measurements on Marloes samples imply that these samples come close to satisfying the conditions for an isochron. Regression of all MS data contained in Table 2.4 changes the date and initial ratio values only insignificantly, as does regression of data from non-calcareous samples only.

Rb-Sr data from Deadman's Bay samples clearly fall into two groups (Fig. 3-5). Samples RS 3, 4, 5, 7 represent an isochron age of 364 ± 19 m.y. (MSWD = 0.5) with an initial ratio of 0.7114 ± 18 . Samples RS 10, 11, 12, 13, 14, 15 represent an age of 370 ± 103 m.y. (MSWD = 4) with an initial ratio of 0.713 ± 7 . The large errors, particularly in the latter case, are caused by a poor spread of Rb/Sr ratios due to the absence of any calcareous samples. The two groups of samples are from quite distinct locations, the former group (RS 3, 4, 5, 7) having been collected at the western side of Deadman's Bay and the latter group from the cliffs to the east, separated by a stratigraphic height of about 40m. Such a grouping of data may provide evidence concerning the extent of Sr-isotope homogenization 'domains'; this matter will be discussed subsequently.

It is clear that these three whole-rock isochron dates, all within error of each other, are significantly younger than the independently adduced depositional age for Upper Llandovery sediments of 420 ± 15 m.y. (Fullager & Bottino, 1968). Therefore, it is concluded that the Sr-isotopic composition within each group of samples was uniform just prior to an 'event', around 380 m.y., at which time the Rb-Sr system became closed to homogenization over domains of this scale (i.e. over stratigraphic intervals of 50-100m).

Two alternatives may be proposed to explain this behaviour:

- (a) Prior to ~380 m.y., each section had uniform Rb/Sr and $^{87}\text{Sr}/^{86}\text{Sr}$ values at the hand specimen level; immediately prior to the ~380 m.y. closure, Rb mobilisation alone need have taken place, resulting in differentiation with respect to Rb/Sr values yet leaving $^{87}\text{Sr}/^{86}\text{Sr}$ temporarily uniform
- or (b) Prior to ~380 m.y., differentiation with respect to Rb/Sr values already obtained within each section. Just prior to closure at 380 m.y., Sr (both common and radiogenic Sr, $\pm\text{Rb}$) mobilisation occurred, resulting in a uniform $^{87}\text{Sr}/^{86}\text{Sr}$ at the time of closure.

The former alternative, (a), is unlikely on several counts. Uniformity of Rb/Sr and $^{87}\text{Sr}/^{86}\text{Sr}$ ratios implies mechanical homogenization at the time of deposition; such homogenization is not apparent in the case of the Buildwas mudstones (Section 3.2.). Rb mobilisation would be expected to be exhibited in a greater range of observed Rb concentrations than of Sr: the reverse trend is apparent from Table 2.4. In addition, the association of radiogenic $^{*87}\text{Sr}$ with Rb implies mobilisation of the former with the latter; a uniform $^{87}\text{Sr}/^{86}\text{Sr}$ ratio would be maintained only if subsequent distribution of $^{*87}\text{Sr}$ was proportional to the distribution of common Sr (i.e. uniform). Lastly, the mineral associations of Rb and Sr in rocks containing degraded clays (cf. Section 3.2.2.) argue strongly for the mobilisation of Sr (some of which is resident in exchange cation sites in smectite layers) to be more facile than that of Rb. However, this last point has been investigated in detail - see Chapter 4.

Therefore, it is suggested that the ~ 380 m.y. date represents the culmination of a period of Sr ($\pm\text{Rb}$) mobilisation, as described in (b) above.

The 382 ± 12 m.y. Rb-Sr date obtained from Marloes shales may be compared with similar K-Ar dates obtained by Harper (1965) on Lower

Palaeozoic slates from the Southern Caledonides fold belt. In the Harlech Dome area of N. Wales, Harper measured K-Ar ages of 405 m.y. and 385 m.y. on the ? Lower Cambrian Llanbedr slates and an Ordovician slate from the edge of the Dome, respectively. Slates from N.W. Galway and the Isle of Man also gave ages in the range 360-385 m.y., and Harper considered these to date the F1 fold movements of the southern extension of the Caledonian orogeny. The younger dates obtained by Harper correspond with the older K-Ar dates from slates of south-west England obtained by Dodson & Rex (1971), which they assign to an early phase of Hercynian (Variscan) movements.

Bearing in mind, therefore, the allocthonous nature of the block in which the Marloes sections occur (Section 2.1) it is concluded that the 382 m.y. Rb-Sr date from the Marloes Sands argillites (and the 364 ± 20 m.y. date from those from Deadman's Bay) record a regional event of late Caledonian/early Variscan nature. This is concordant with the unconformity observed in Pembrokeshire at the top of the lower O.R.S. (Section 2.1), although the presence of other, localized unconformities throughout the Silurian (Fig. 2-3) should be noted.

3.3.2. Within-sample size fractions

Evidence for a post-380 m.y. episode of Sr-mobilisation over small (i.e. intergranular) distances is provided by the Rb-Sr data from size-fractions of MS1 and MS6 (Table 2.6), which are plotted on an isochron diagram in Fig. 3-6.

As the grain-size decreases, the data points are seen to fall progressively further below the whole-rock line, producing a decrease of slope. This trend is more clearly shown in a plot of model age against average particle size (the latter on a log scale, Fig. 3-2). These model ages are calculated with the minimum possible initial $^{87}\text{Sr}/^{86}\text{Sr}$ ratio, 0.7105, which is the mean value for Sr leached from calcite and

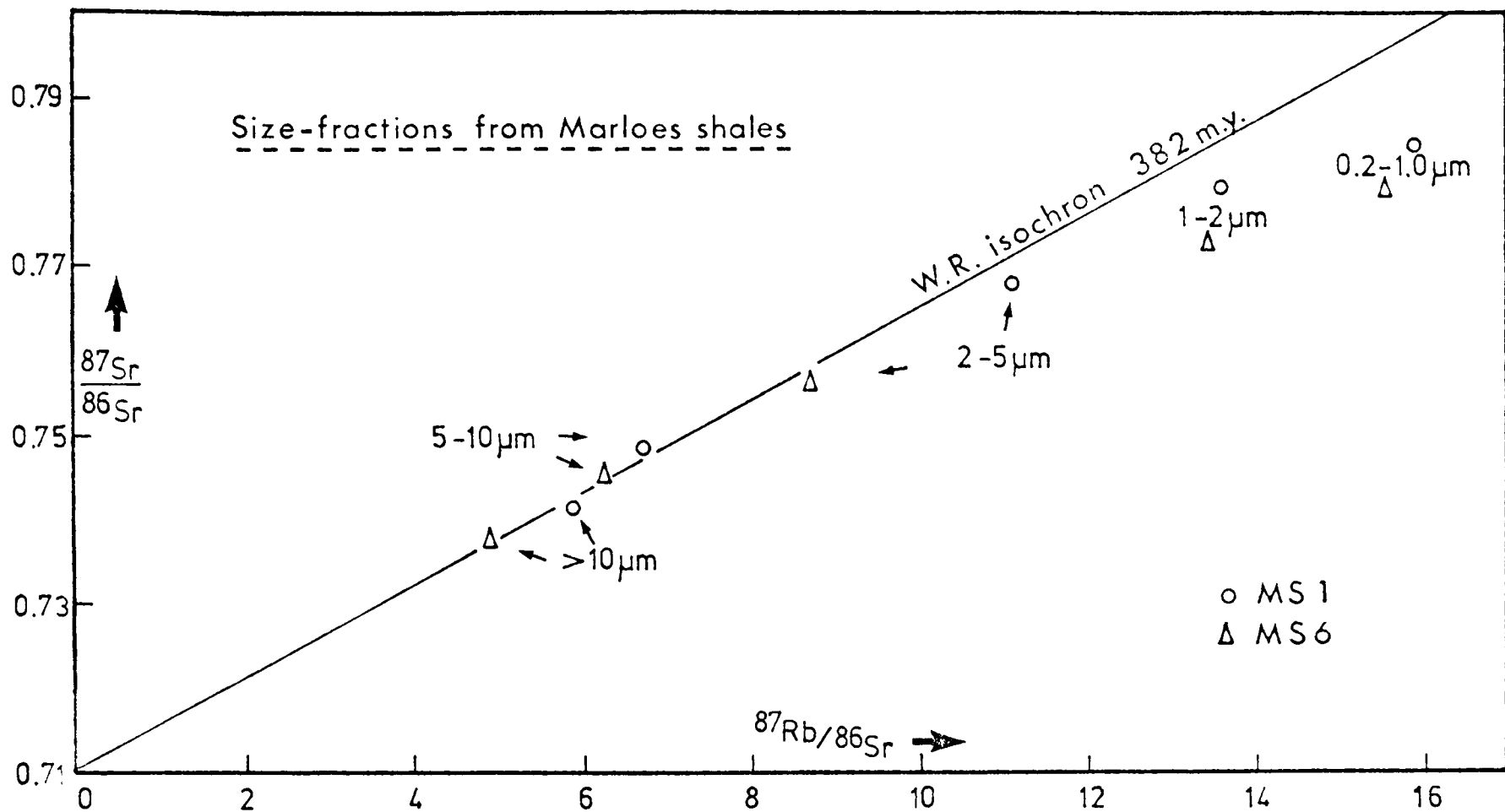


Fig. 3-6. Rb-Sr data from size-fractions from two Marloes shales plotted against isochron coordinates. Note progressive lowering of data below whole-rock isochron as size decreases.

is taken as the initial ratio value on the whole-rock isochron. A decrease in model ages is observed as grain-size decreases, the finest fractions (0.2-1 μm) of MS1 and MS6 yielding model ages of 334 m.y. and 317 m.y. respectively. These data represent a situation quite different to that represented by size-fractions from a Buildwas sample (section 3.2.2.), in which the youngest model-age is still pre-depositional.

The pattern of model-ages for Marloes size-fractions is interpreted as the result of a period of partial remobilisation of Sr over intergranular distances. Either continuous loss or episodic loss of radiogenic ^{87}Sr from the finer fractions may account for the observed pattern. The latter is supported by the trend of model ages towards a minimum close to 300 m.y. K-Ar dates in the region of 300 m.y. from north Cornwall slates (Dodson & Rex 1971) have been attributed to a period of late Carboniferous deformation (i.e. Hercynian). Since the folding and thrusting which are observed in the Marloes area have been considered to be Hercynian (Section 2.1), it therefore seems reasonable to suggest that thermal effects associated with these regional movements may account for the partial remobilisation of Sr.

3.3.3. Between-sample clay fractions

The absence of any large-scale remobilisation, even partial, subsequent to ~ 380 m.y. is reiterated by the data from clay fractions separated from seven Marloes shales (Table 2.7). These yield a best-fit age of 394 ± 12 m.y. (MSWD = 4.7) with an initial ratio value of 0.7061 ± 14 (Fig. 3-7). This age is indistinguishable from the whole-rock age of 382 ± 12 m.y. (Fig. 3-4); the age given by only those whole-rock samples from which the clay fractions were separated is 390 ± 11 m.y. with an initial ratio of 0.7098 ± 6 .

Although the clay fraction and whole-rock isochron ages are indist-

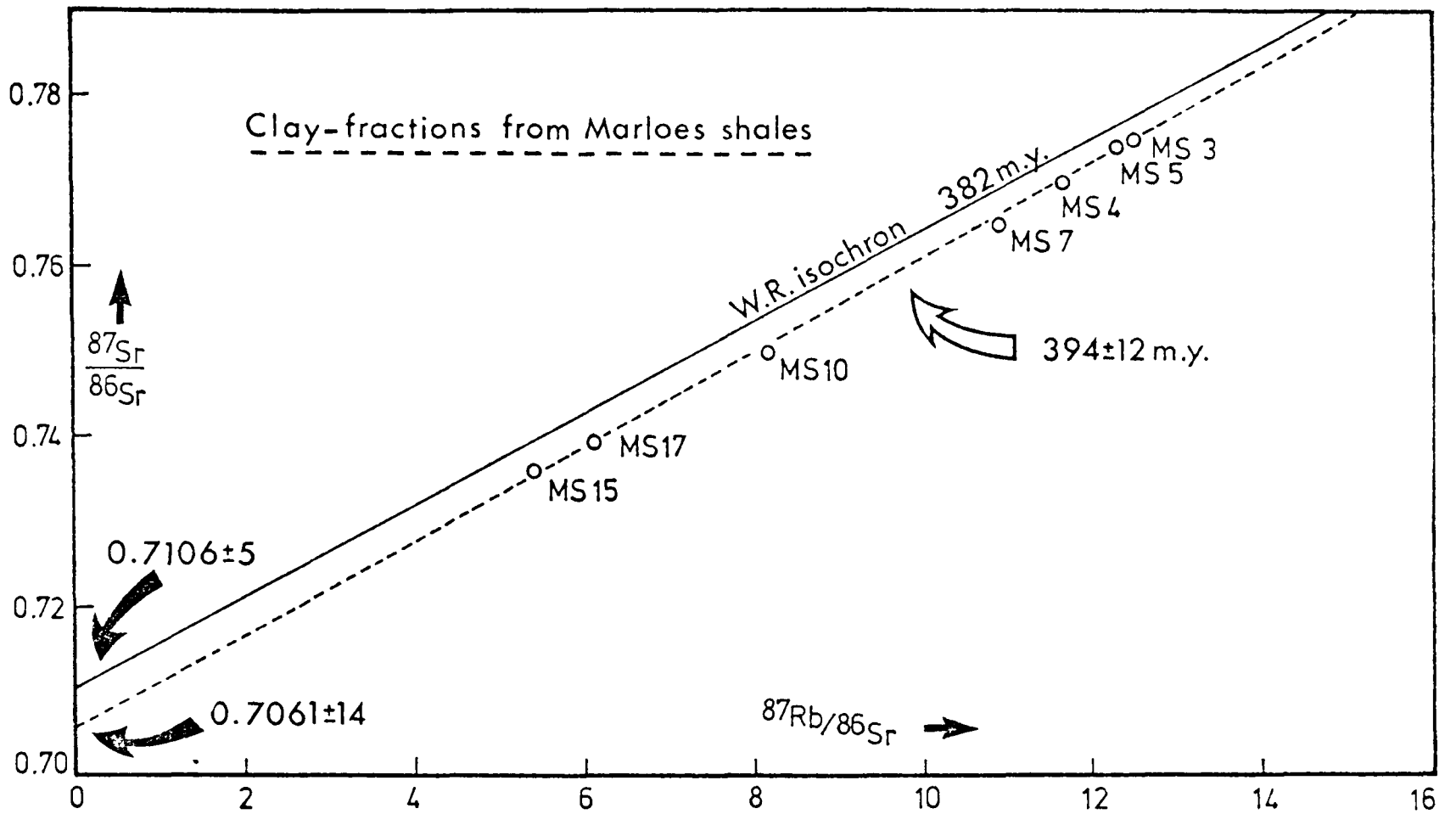


Fig. 3-7. Rb-Sr data from clay-fractions (<2 μm) of seven Marloes samples plotted on an isochron diagram. Whole-rock isochron is shown for comparison. Note indistinguishable ages, but significantly different initial $^{87}\text{Sr}/^{86}\text{Sr}$ ratios.

inguishable, the initial ratio values of the two are significantly different. This difference reflects the depletion of radiogenic ^{87}Sr in the fine-fractions which has already been observed in data from size-fractions (Section 3.3.2). (The alternative explanation to ^{87}Sr depletion is one of Rb metasomatism or loss of common Sr, i.e. increase of Rb/Sr ratio. However, the observed linear array in Fig. 3-7 would require that a uniform change in Rb/Sr had taken place, independent of the absolute value - this is considered most improbable). The mechanism by which this episodic depletion of ^{87}Sr in the clay fractions might take place, and a simple model to explain the observed relationship between whole-rock and clay fraction isochrons, will be discussed subsequently (Section 3.4.3).

3.3.4. Whole-rock data from bentonites

Rb-Sr data from all thirteen bentonite samples (Table 2.9), both from Deadman's Bay (RS) and Marloes Sands (MS), plot on a good isochron (MSWD = 1.8). The slope of this isochron (Fig. 3-8) represents a date of 298 ± 7 m.y. ($\lambda = 1.39 \times 10^{-11} \text{ yr}^{-1}$) with an initial $^{87}\text{Sr}/^{86}\text{Sr}$ ratio of 0.7146 ± 8 . When divided according to locality, the ages and initial ratios are:

MS bentonites : 295 ± 7 m.y. (MSWD = 0.6), $(^{87}\text{Sr}/^{86}\text{Sr})_0 = 0.7150 \pm 7$

RS bentonites : 306 ± 14 m.y. (MSWD = 2.2), $(^{87}\text{Sr}/^{86}\text{Sr})_0 = 0.7132 \pm 20$

The well-defined 298 m.y. date from the bentonites is considerably younger than the ca. 380 m.y. dates given by the shales in which the bentonites are intercalated. The former age, 298 m.y., is similar to those K-Ar dates obtained from slates folded during the Hercynian (Dodson & Rex 1971; see section 3.3.2). It is also concordant with estimates of ages for the Upper Carboniferous (e.g. Armstrong & McDowall 1974), at which time Hercynian uplift and folding is inferred in the Marloes section (cf. section 2.1.2 and Fig. 2-3).

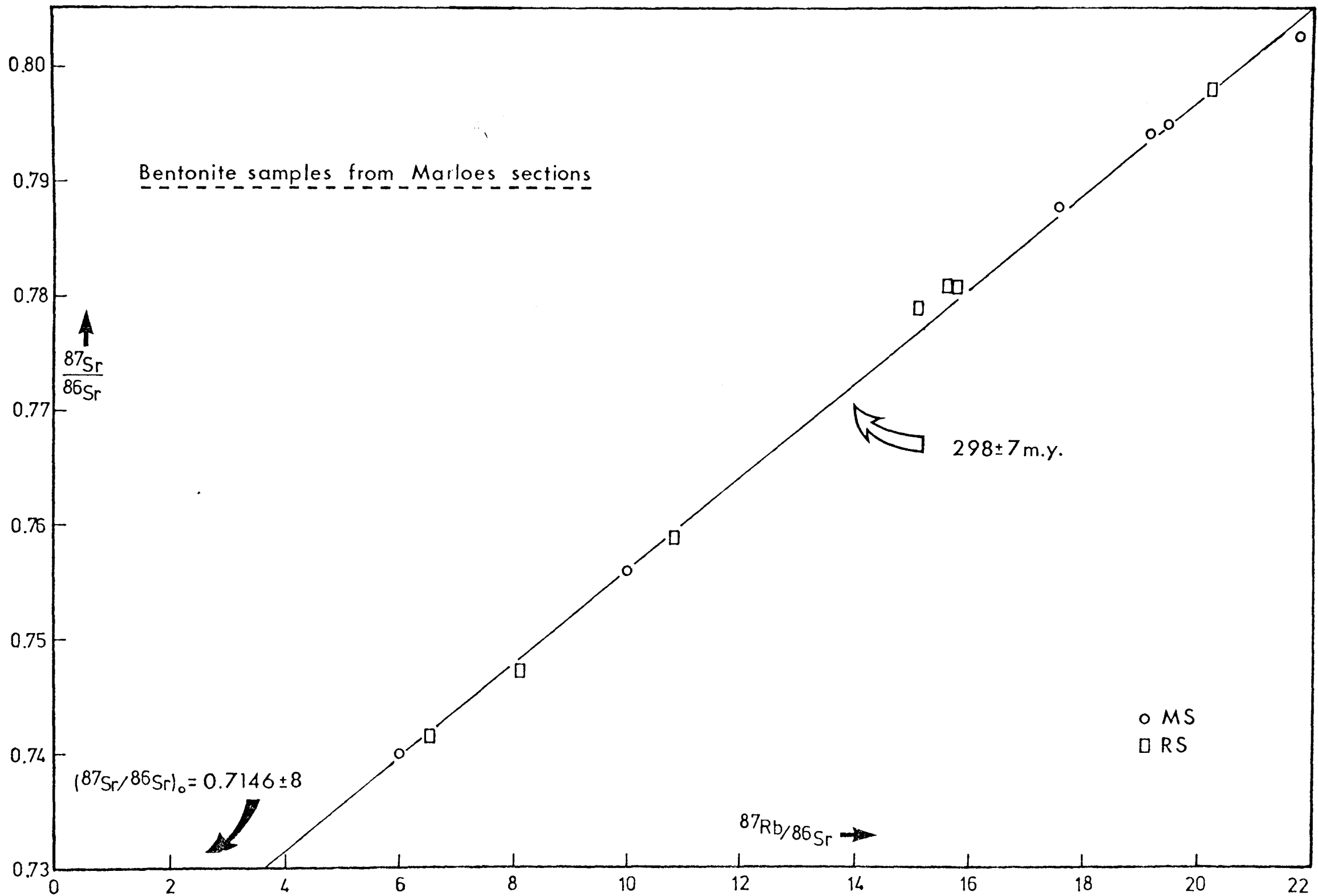


Fig. 3-8. Whole-rock Rb-Sr data from 14 bentonite samples from Marloes Sands and Deadman's Bay sections plotted on isochron diagram. Slope corresponds to $298 \pm 7 \text{ m.y.}$ (MSWD = 1.8). ($\lambda = 1.39 \times 10^{-11} \text{ yr}^{-1}$).

3.4 Discussion of Behaviour of Sr and Rb in Sediments

3.4.1 Weathering, halmyrolysis and deposition

The establishment of chemical equilibrium between percolating solutions and weathering products is, naturally, dependent on the residence time of the waters within the weathering profile, as well as many other factors. Dasch (1969), by demonstrating a lack of equilibration between Sr-isotopes in igneous and metamorphic rocks and in their weathering profiles, has also shown that Sr-isotope equilibration does not obtain between the components of the weathering profile and the percolating waters.

No direct investigation has yet been carried out into the effect of halmyrolysis (rapid reaction between clays and sea-water at the fluvial-marine interface) on the Rb-Sr system in clay minerals. However, certain conclusions may be inferred from a recent study of changes in major element chemistry during halmyrolysis by Russell (1970). Russell found that the extent of such reaction in the area studied (Rio Ameca, Mexico) is limited simply by the cation exchange capacity of the clays being transported. The major changes are the loss of exchangeable Ca^{2+} from clays and the uptake of K^+ , Na^+ and Mg^{2+} from the marine environment. To a first approximation, we may consider Sr^{2+} to follow Ca^{2+} in its behaviour, and Rb^+ to follow K^+ . The net decrease in cation exchange capacity following uptake of K^+ supports the view that the 'smectite' component of these clays may be no more than a highly degraded illite. (Berner 1971, p.180). Indeed, many occurrences of expandable clay phases (including that in the Buildwas mudstones in the present study) may well be better described as degraded illites (i.e. K^+ -depleted during weathering), in contrast to occurrences of smectites derived from alteration of volcanic products.

It has been shown in the case of the unmetamorphosed Buildwas mudstones (Section 3.2) that Sr-isotope equilibrium between the various

mineral phases did not obtain at or subsequent to deposition. This conclusion concerning unmetamorphosed sediments is in agreement with the findings of Dasch (1969). In a study of modern deep-sea sediments, isotopic equilibration between sea-water strontium and the clay phases (smectite, illite and kaolinite) was not observed by Dasch, even in the finest ($<0.08\mu\text{m}$) fraction studied. There was noted, however, a trend towards lower $^{87}\text{Sr}/^{86}\text{Sr}$ ratios in the finer fractions of a sample, which may be correlated with an increasing proportion of smectite (i.e. of cation exchange sites) as particle size decreases.

It is concluded that, under normal conditions, weathering products do not experience complete Sr-isotopic homogenization at any stage of the weathering and depositional régimes. However, various components, particularly those with relatively high cation exchange capacity, may undergo varying degrees of modification to their Rb and Sr contents and Sr-isotopic composition.

3.4.2 Burial and early diagenesis

Before considering the specific problem of Rb and Sr behaviour during burial of argillaceous sediments, it will be useful to summarise briefly the present state of information concerning the major chemical and mineralogical changes accompanying burial.

The decrease in proportion of expandable layers in mixed-layer phases is a well-established feature of diagenetic progress (Burst, 1969; Perry & Hower 1970; Dunoyer de Segonzac 1970; Weaver & Beck 1971; van Moort 1971). This has been interpreted as the reconstitution of illite-type layers from a mixed-layer illite-smectite (cf. earlier note in Section 3.4.1. concerning the questioned validity of describing these expandable clays as illite-smectite). Clearly, such an evolution requires the fixation of K^+ into interlayer sites, and there is observed, indeed, an increase in K^+ content of clay fractions with depth (Perry & Hower 1970).

However, this trend is not reflected in whole-rock analyses, from which Perry and Hower concluded that a redistribution of K^+ due to breakdown of discrete (detrital) mica is occurring, rather than uptake of externally-derived K^+ from pore-fluids. Weaver and Beck (1971) made similar conclusions from studies of cores from oil wells in the Gulf of Mexico, although in this case they consider the source of K^+ to be the breakdown of detrital K-feldspar.

The mineral associations of Rb and Sr in sediments have already been mentioned in various parts of this chapter. However, it is worthwhile to review them here, both in the light of the diagenetic changes mentioned above and in the light of the observations made on the Rb-Sr system in the Buildwas mudstones.

Radiogenic ^{87}Sr is, in the first instance, associated with its parent element, Rb, as a substituent in K-containing minerals. The significant minerals in sediments, in this respect, are K-feldspar and mica/illite derivatives. Clearly, in a disequilibrium situation such as that observed in the Buildwas mudstones (Section 3.2), no mechanism for complete K^+ (and consequently Rb^+ and $^{87}\text{Sr}^{2+}$) release and redistribution has obtained since deposition. These mudstones have been buried to an estimated depth of less than 2000 m. (Section 2.1.1) and the clays have undergone little diagenetic modification. In particular, detrital illite clearly persists to some extent (Section 3.2), although K-feldspar is not detected in these rocks.

The mineral associations of Sr in sediments are more difficult to delineate. Its behaviour as a substituent for Ca^{2+} indicates that associations with calcite, plagioclase and clays with cation exchange capacity must be considered. The $\text{Sr}^{2+}/\text{Ca}^{2+}$ ratio in exchange sites on clays may be predicted to be higher than that in solution with which it is in equilibrium, due to the preferential incorporation of the larger cation in exchange sites. Since Weaver and Beck (1971; p.35) have

observed an increasing replacement of exchangeable Mg^{2+} by Ca^{2+} with depth, leading to a very high (exchangeable Ca^{2+})/(interstitial Ca^{2+}) ratio at depths below 4000m., one may infer an even greater trend in Sr^{2+} uptake.

The transformation of carbonate, initially deposited as aragonite, to calcite is expected to result in a relative depletion of Sr^{2+} in the lattice and loss of Sr^{2+} to pore fluids. Considerable evidence has accrued which demonstrates the relative rapidity with which calcite recrystallizes and preserves equilibrium with the environment (Berner 1971; p.146). It therefore seems reasonable to deduce that the isotopic composition of Sr in calcite leachates from Buildwas mudstones (mean $^{87}Sr/^{86}Sr$ ratio 0.7089 ± 6 ; cf. Table 2.5) reflects the composition of Sr residing in exchange sites in the clays. Since it has been noted previously (Section 3.2.1) that the Sr contained in these calcite leachates has never been in isotopic equilibrium with the bulk Sr contained in the silicate components, it may be concluded that there is a significant Sr content in the silicate phases which is out of equilibrium with that in exchange sites.

Plagioclase is ubiquitously present in the coarser size-fractions from Buildwas samples, though it occurs in minor amounts (Table 2.1). This may be an authigenic or detrital phase, though the complete absence of K-feldspar (generally more resistant in the weathering cycle than plagioclase) suggests that it is probably authigenic. This conclusion is supported by the small crystallite size-discrete particles are not visible in thin section - though this characteristic in itself prevents optical determination of the plagioclase. Authigenic plagioclase is generally of the low-Ca, albite end of the solid solution series (Degens 1965; p.49), thus one might expect it to account for only a very small proportion of the bulk Sr. Rb^{+} does not substitute to any appreciable extent into Na^{+} sites in plagioclase, on account of its size, thus the

question of ^{87}Sr content and its behaviour does not arise.

A distinct correlation between the recrystallization of a mixed-layer phase and the progress towards Sr-isotope homogenization between the various components of a shale has been reported by Perry and Turekian (1974). In studies of a diagenetic sequence of Miocene well-core samples from the Gulf Coast of Louisiana, these authors have observed a steady progression towards Sr-isotope homogeneity between the size-fractions within a shale sample as the depth of burial increases. The corresponding decrease in the percentage of smectite-type layers in the mixed-layer phase had already been demonstrated by Perry and Hower (1970). Although at the greatest depth sampled, 5523 m., there is still 20% expandable layers present in the mixed-layer phase, Perry and Turekian predict that elimination of the expandable component at depth coincides with complete homogenization of Sr-isotopes.

The conclusions of Perry and Turekian (op. cit.) may be extended from Sr-isotope homogenization on a small, within-sample scale to homogenization on a large scale similar to that represented by the suite of whole-rock samples from Buildwas. In such poorly compacted sediments, sufficient pore fluids remain to provide a continuous aqueous medium by which large-scale ionic transport may take place. The rate-determining step in the process of large-scale Sr-isotope homogenization is the exchange process between crystallite and pore-fluid rather than the subsequent transport of ions in solution. This latter statement may be justified by comparing the tracer diffusion coefficient for Sr^{2+} in aqueous solution at infinite dilution, $7.94 \times 10^{-6} \text{ cm}^2 \text{ sec}^{-1}$ at 25°C (Li & Gregory 1974), with the empirical diffusion coefficients determined in this study for the solid-fluid exchange process, which are at least ten orders of magnitude smaller (see Chapter 4). Therefore, it is seen that the absence of Sr-isotope equilibration between whole-rock samples from Buildwas (maximum burial depth 2000 m.) is concordant with

the persistence of disequilibrium beyond 5000m. in the Gulf Coast succession. This assumes, of course, a similarity in physico-chemical gradients during burial of the Palaeozoic Buildwas and the Tertiary Gulf Coast successions, particularly with respect to geothermal gradients ($\sim 31^{\circ}\text{C km}^{-1}$ for the latter case, Perry & Hower 1972). Several other examples demonstrating lack of Sr-isotope equilibration between components of ancient unmetamorphosed sedimentary rocks are now in the literature (e.g. Chaudhuri & Brookins 1969; Spears 1974).

Finally, the pattern of Rb-Sr model ages from size-fractions of a Buildwas mudstone sample (Fig. 3-2) may be compared directly with a similar pattern of both Rb-Sr model ages and K-Ar ages obtained from size-fractions of Pennsylvanian argillites from Ohio and Pennsylvania by Hofmann et al. (1974). These argillites underlie coal-seams, and contain mixed-layer clays, as well as discrete mica (described as the $2M_1$ polytype of illite) in the coarser fractions. The age pattern in both cases is one of a regular decrease in model age with decreasing mean particle size (plotted on a logarithmic scale, cf. fig. 3-2). The influence of detrital clay components is clear from the model ages exceeding the estimated age of deposition (cf. Section 3.2.2). However, Hofmann and co-workers suggest that the grain-size effect on model ages is specifically a consequence of the reconstitution of the 1Md polytype of illite from the degraded mixed-layer species which dominate the finer fractions. From the proximity of the Rb-Sr model ages for the finest fractions to the estimated age of deposition, the authors infer that this reconstitution or recrystallization takes place close to the time of deposition. The data may be equally well-explained as being a consequence of Rb loss and Sr uptake during the degradation process leading to the mixed-layer phase, particularly since it is this phase, rather than 1Md illite, which predominates in the fine-fractions both of the clays described by Hofmann and co-workers (*op. cit.*) and of the Buildwas mudstones in the present study.

It is concluded that Rb and Sr redistribution in sediments may occur prior to, or shortly after, deposition to a limited extent, this extent being very variable and depending largely on the severity of weathering and degradation of the clays. There is no a priori reason to expect complete Sr-isotope homogenization in any situation at this stage, and, indeed, no evidence from the present study or from other investigations supports this. Therefore Rb-Sr ages, including model ages, obtained from sediments with mixed-layer clay mineralogies, or from size-fractions of these samples, must be regarded, at best, as poorly defined maxima for the true age of the sediment. Any such Rb-Sr ages will merely be derived from best-fit lines to non-linear data scatter, since no evidence suggests that isochron conditions might have been fulfilled in such sediments.

3.4.3 Low-grade metamorphism

The distinction between advanced diagenesis and low-grade metamorphism is not a clear one, and rests on a contrast between thermal régimes: in the latter case a perturbed geothermal gradient is recognised as the cause of the metamorphic changes, whilst in the former case these result from the changing physico-chemical conditions encountered during progressive burial.

Before discussing the behaviour of Rb and Sr in the sedimentary rocks sampled at Marloes, it is necessary to attempt to outline the physico-chemical conditions to which the observed Rb-Sr systematics are a response. The phases present in the argillaceous sediments from Marloes (Section 2.3) suggest that at least some of them are products of post-depositional modification. The development of a moderate cleavage in these shales, and the appearance of other tectonic features (Section 2.2.2), suggest that this tectonisation may be the direct cause of the observed assemblage. However, this must be established by further evidence, since it

has been shown that the development of such an assemblage (i.e. the illite-chlorite paragenesis) may result simply from advanced diagenetic (as opposed to metamorphic) reactions (e.g. Dunoyer de Segonzac 1970).

The maximum overburden thickness at any time on the Llandoverly sediments at Marloes has been estimated at 4000 m. (Section 2.1.2). A comparison of this with the figure of 2000 m. for sediments of similar age at Buildwas (and presumably of similar depositional mineralogy, both being situated in the Lower Palaeozoic Welsh Basin), and which are unaltered, suggests that the Marloes assemblage is indeed a product of distinct metamorphic conditions. This conclusion is further supported by the observations by other authors of the depths to which mixed-layer phases persist under non-metamorphic conditions (summarised by Dunoyer de Segonzac 1970, p.296), and also by the anchizonal range of illite crystallinity indices measured on Marloes samples (Section 2.3.2).

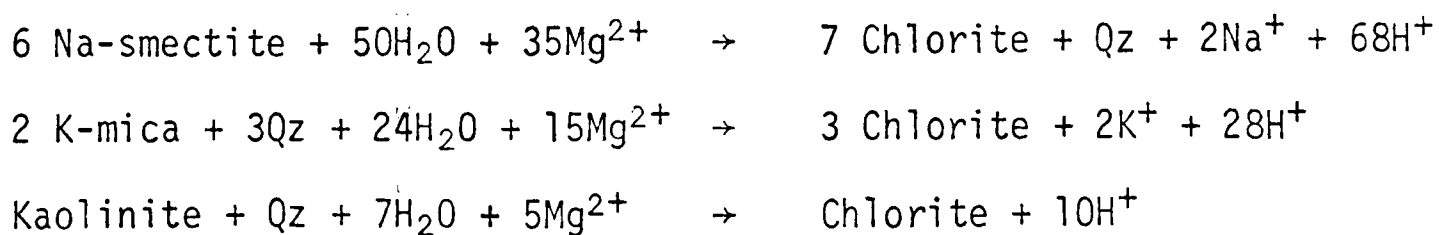
The most complete study of the formation of the illite-chlorite paragenesis in argillites is that of the active metamorphism associated with the Salton Sea geothermal system in south-eastern California (Muffler & White 1969). The geothermal gradients measured in wells in the Salton Sea geothermal field range up to ca. $270^{\circ}\text{C km}^{-1}$, which may be compared with the present-day average in non-orogenic regions of ca. $30^{\circ}\text{C km}^{-1}$ (for example, in the Gulf Coast succession studied by Perry & Hower 1972). Muffler and White observed the disappearance of mixed-layer illite-smectite by 210°C , and a rapid increase in abundance of chlorite after about 180°C . Although the authors suggest reactions which may explain these phase changes independently of any metasomatising influence of the hypersaline brine, nevertheless the stability fields of individual phases will be dependent on the composition of this fluid phase.

Helgeson (1967) has used independently determined equilibrium data

and the observed phase relations and fluid compositions in the Salton Sea system, to construct activity diagrams for the phases in the system $\text{Na}_2\text{O}-\text{K}_2\text{O}-\text{Al}_2\text{O}_3-\text{SiO}_2-\text{K}_2\text{O}$ with coexisting calcite. Three of Helgeson's activity diagrams for this system at 300°C are shown in Fig. 3-9; cation activities are plotted as the logs of their ratios to a_{H^+} . These diagrams show clearly that the average composition of sea-water (depicted by the solid square in Figs. 3-9 (a) and (b)) falls within the chlorite stability field at 300°C ; despite expansion of the stability fields of kaolinite, etc. as the temperature is lowered (see Helgeson, 1970; p.158), chlorite remains the stable silicate phase at all relevant temperatures below 300°C . It may be noted that any increases in the activities of relevant pore-water cations (by cation-selective membrane filtration, for instance) relative to marine values, will tend to stabilize chlorite further (Kharaka & Berry 1973, have shown that membrane filtration by clays enriches $a_{\text{Mg}^{2+}}$ relative to a_{Na^+} or a_{K^+} in the residual fluids).

The most important conclusion suggested by the activity diagrams in Fig. 3-9 is that a mixed-layer illite-smectite clay assemblage existing in a fluid of sea-water composition is unstable with respect to chlorite at all relevant temperatures. The persistence of a mixed-layer clay under such conditions is therefore a metastable phenomenon, and the question of disappearance of expandable smectite interlayering becomes one of kinetics rather than thermodynamics.

Making the assumption of a mixed-layer illite-smectite starting material, the production of the observed illite-chlorite paragenesis may be expressed by the reactions:



and similar reactions by K-feldspar (if present) and albite. The

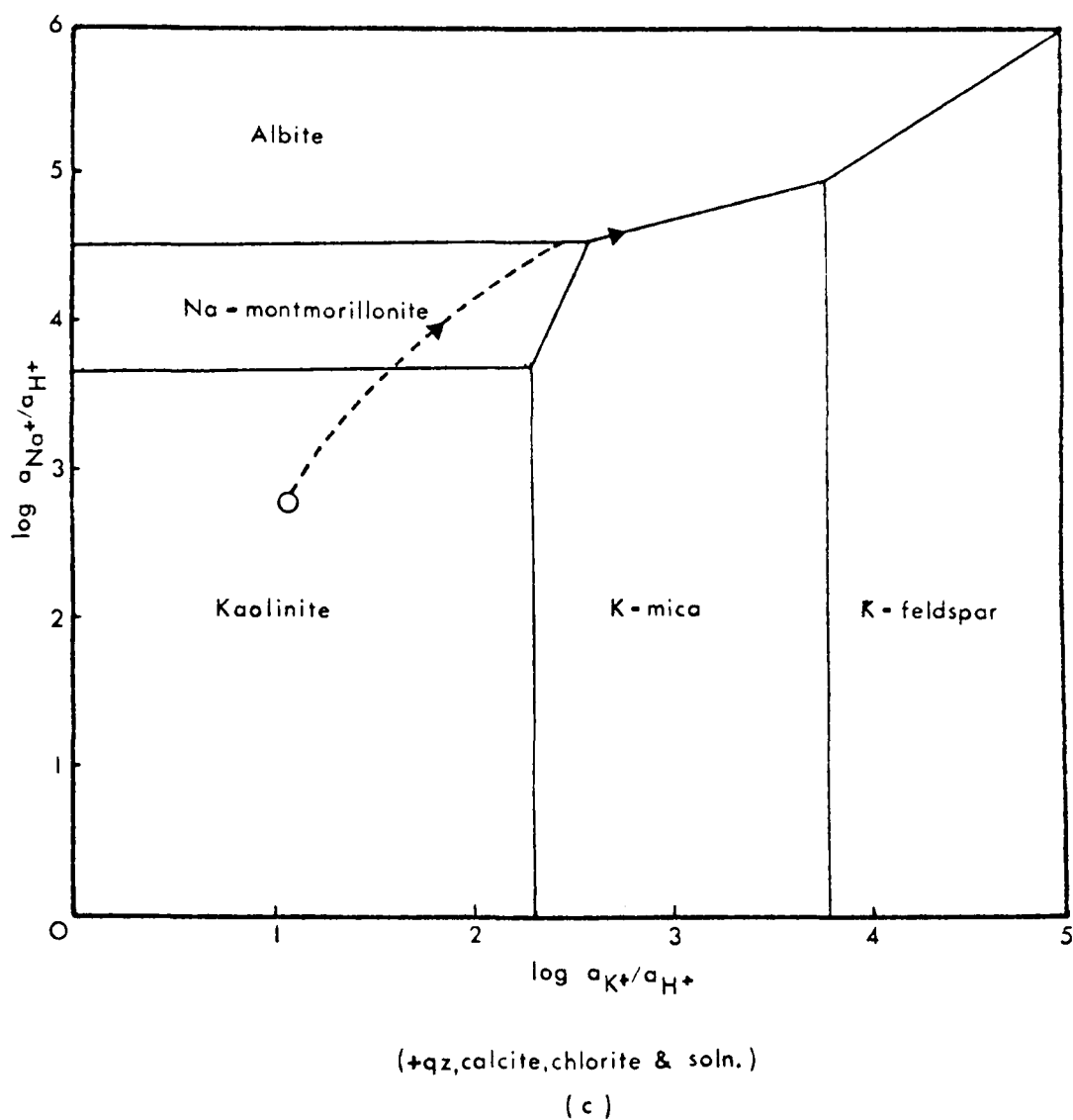
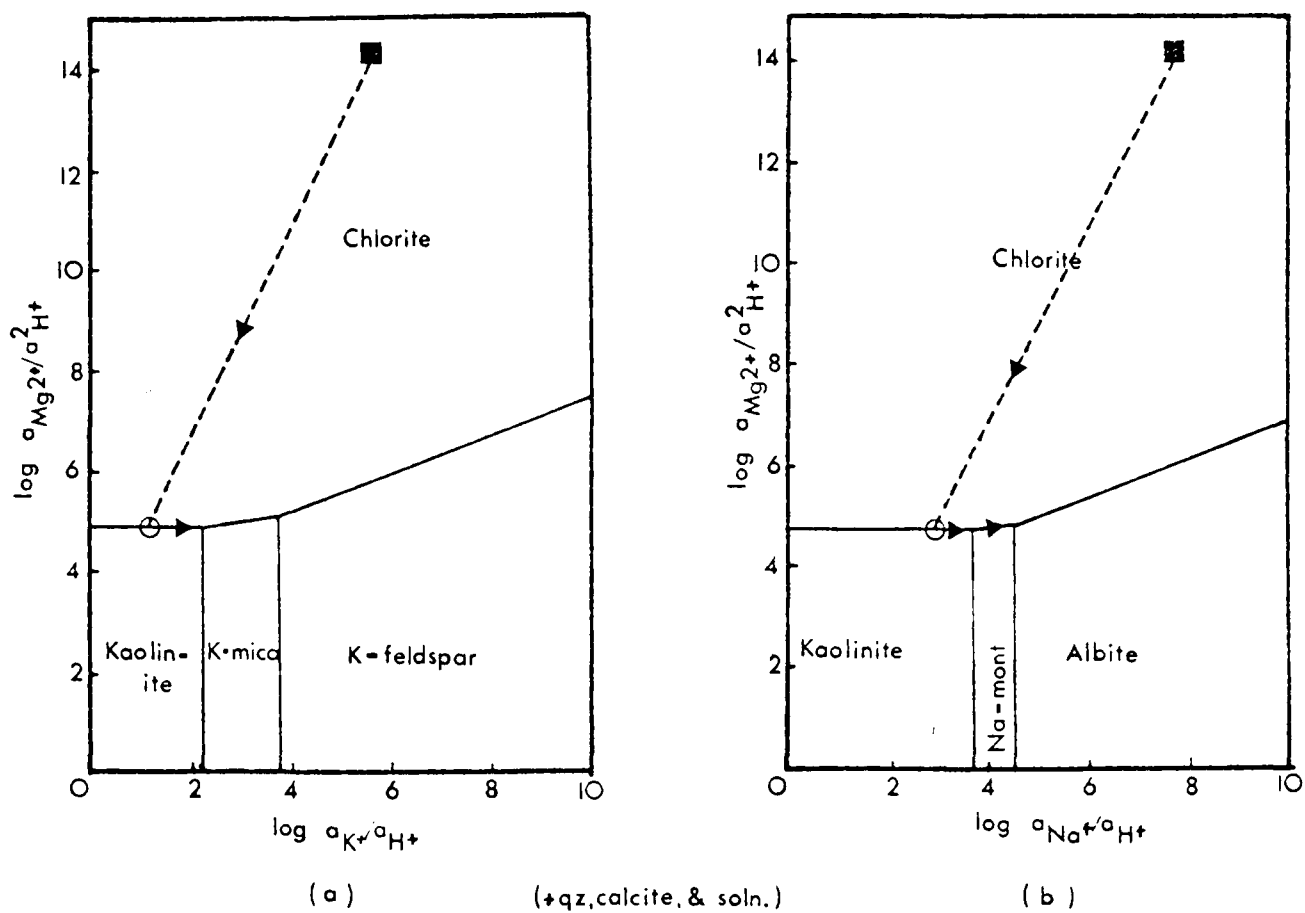


Fig.3-9. Activity diagrams depicting phase relationships between components of argillaceous sediment at 300°C. ■ represents composition of average sea-water, and broken lines represent reaction paths of fluid composition for reactions producing chlorite (see text). Open circle O in (c) represents arbitrary transposition into changed coordinates (maintaining $a_{Mg^{2+}}$ constant) of fluid of composition represented by O in (a) & (b). After Helgeson (1967).

reaction whereby degraded (K^+ -depleted) illite takes up K^+ and approaches stoichiometric K-mica must also be considered. The reactions described above represent reaction paths for fluid composition denoted by the dotted lines in Fig. 3-9. In the present case of the Marloes shales, the reaction path has culminated along the phase boundaries of the assemblage K-mica + chlorite + albite (\pm Na-smectite, cf. Fig. 2-8).

In the present case, that of an illite-chlorite paragenesis, it appears from the above evidence that thermodynamic considerations tell us little concerning the conditions under which the transition from a degraded clay assemblage takes place. However, it should be noted that the important problem of fluid compositions at depth is very much an unknown factor. Examples have been described where certain cation activities, e.g. those of Mg^{2+} , K^+ , Fe^{2+} , have been augmented at depth, apparently by the influx of brines derived from external sources (e.g. Muffler & White 1969; Weaver & Beck 1971). Indeed, the occurrence of abundant chlorite in Marloes shales argues for its development during a regional metamorphic episode, when the injection of such brines might be expected. (It is estimated that a shale with an initial porosity of 80% containing average sea-water with 1200 ppm Mg^{2+} , has sufficient supply of Mg^{2+} to convert only ca. 1% by weight of its component silicates to chlorite).

Two whole-rock Rb-Sr isochron dates have emerged from this study on Llandovery shales from Marloes: 382 ± 12 m.y. from the terrigenous sediments, and 298 ± 7 m.y. from the composite isochron given by samples from different bentonite bands (Sections 3.3.1 and 3.3.4). Both dates have been tentatively correlated with the two major disturbances experienced by these strata: the Caledonian and Hercynian orogenic episodes respectively. It is suggested that the 382 m.y. isochron represents the homogenization of Sr-isotopes (cf. Section 3.3.1) over a sufficiently

large-scale to satisfy whole-rock isochron conditions; this was due to the recrystallization of Sr-bearing phases to a more stable assemblage in the presence of fluid phase (by which ionic transport over large distances is facilitated). Such a recrystallization might have followed the reaction path described above and in Fig. 3-9. It is interesting to note that a major part of the Sr in deep geothermal brines from the Salton Sea region has been shown, by $^{87}\text{Sr}/^{86}\text{Sr}$ measurements, to have originated from the leaching of nearby sediments (Doe et al. 1966). The reactions occurring within these sediments under the influence of the enhanced geothermal gradient have already been described in this discussion (Muffler & White 1969). A similar process is envisaged for the 382 m.y. Sr-isotope homogenization in Marloes sediments.

The interpretation of the Rb-Sr systematics leading to the 298 ± 7 m.y. Hercynian date from bentonite bands is certainly more problematical. The excellence of the fit of data to an isochron leaves little doubt as to the reality of a 298 m.y. 'event'. Indeed, the comparative improvement over the linearity of data from the terrigenous sediments may well reflect the greater severity of Hercynian metamorphic conditions over those previously encountered in the Caledonian orogeny.

Two problems of interpretation arise from these observations:

- (i) How has the isotope homogeneity of Sr amongst all the bentonite bands at 298 m.y. originated?
- (ii) Why do bentonite samples give a whole-rock isochron age of 298 m.y., whereas the subjacent shales have retained a closed whole-rock Rb-Sr system since ca. 382 m.y.?

Two solutions to (i) are possible:

- (a) The bulk chemical composition (at least with respect to Rb and Sr) of each bentonite band is identical. Prior to ca. 298 m.y., total Sr mobilisation laterally throughout each individual band was in

operation, so that at the cessation of homogenization at 298 m.y. the isotopic composition of Sr was uniform throughout each band and amongst bands. This interpretation does not require communication of Sr between bands, and therefore the presence of a continuous fluid phase within the intervening argillites is not necessary.

or (b) Total Sr was homogenized between bentonite bands, which need not have similar bulk chemistry, throughout the section (or as far as demanded by bulk chemical inhomogeneity). This homogenization operated prior to closure at 298 m.y., although no significant exchange of Sr with the subjacent shales took place subsequent to ca. 382 m.y.

Evidence against alternative (a) is very strong. The colinearity and high precision of all the data demands a remarkable degree of homogeneity between bands if (a) obtained. Whilst noting the relatively low variation in Rb concentrations (Table 2.9), the variability in Sr contents leading to the very favourable spread of Rb/Sr ratios argues against this.

The acceptance of alternative (b) above, which demands the presence of a continuous fluid phase up to 298 m.y. at least, then raises the problem outlined in (ii) above. One possible explanation of the more recent Sr-isotope homogenization amongst the bentonites lies in a distinction between the starting materials in the two cases. It has already been assumed that the initial material comprising the Marloes sediments was a degraded mixed-layer clay, similar to that observed in the Buildwas mudstones. On the other hand, the bentonites (or metabentonites) might be expected to have originally comprised an assemblage predominated by montmorillonite, which is commonly found as the alteration product of volcanic material. It is tempting to speculate that the delay in recrystallization of the bentonite material until 298 m.y., the date at which Sr-isotope homogenization last occurred, may have been a kinetic

effect. This is justified by the evidence already presented for the metastability of both the mixed-layer clay and montmorillonite with respect to illite + chlorite.

It is clear from the above that, if recrystallization is accepted as the mechanism by which Sr-isotope homogenization takes place, then the same recrystallization must also be proposed as the cause of the closure of the system to further Rb or Sr redistribution. This follows from the necessity to maintain sufficient connate fluids to permit widespread Sr transport at least to 298 m.y., whilst closing the Rb-Sr system of the normal sediments to further homogenization subsequent to ca. 382 m.y. The cause of dewatering of a sediment during induration is not well understood. It is not possible, therefore, to infer the relative importance of fluid movement and cation transport through fissures and that due to the intrinsic permeability of the compacted sediment, subsequent to the initial metamorphism at ca. 382 m.y. A significant factor influencing permeability may be the distribution of recrystallized calcite as a cement. The Sr-isotope data on calcite leachates shows that the Sr contained in calcite was in equilibrium with that in silicate phases no later than 382 m.y. (a further example of closed system behaviour by calcite concordant with that of the silicates is given by Clauer 1973).

Although no widespread homogenization of Sr-isotopes in the sediments occurred after ca. 382 m.y., a perturbation to the Rb-Sr system on an intergranular scale has been observed (Sections 3.3.2 & 3.3.3). The pattern of Rb-Sr data from clay-fractions of several Marloes shales, and its relationship to the whole-rock isochron, are particularly interesting (Section 3.3.3 and Fig. 3-7). Table 3.1 lists the Rb-Sr data for both the whole-rock samples and the clay-fractions for seven Marloes shales (cf. Tables 2.4 & 2.7). It also shows, in the last column, the difference between the $^{87}\text{Sr}/^{86}\text{Sr}$ ratio predicted from the WR isochron

Sample No.	WR	Rb/Sr		$\Delta(\text{Clay-WR})$	$(^{87}\text{Sr}/^{86}\text{Sr})_{\text{meas}}^{\text{clay}}$	$(^{87}\text{Sr}/^{86}\text{Sr})_{\text{predict}}^{\text{clay}}$	$\delta(^{87}\text{Sr}/^{86}\text{Sr})$
		Clay					
MS 3	3.11	4.30		1.19	0.7750	0.7779	0.0029
4	2.84	4.00		1.16	0.7699	0.7729	0.0030
5	1.92	4.23		2.31	0.7740	0.7766	0.0026
7	1.70	3.75		2.05	0.7650	0.7689	0.0039
10	1.20	2.80		1.60	0.7500	0.7539	0.0039
15	1.38	1.85		0.47	0.7360	0.7390	0.0030
17	0.34	2.10		1.76	0.7397	0.7428	0.0031
$(^{87}\text{Sr}/^{86}\text{Sr})_0$	0	0			0.7061	0.7098 (WR)	0.0037

Table 3.1. Comparison of Rb-Sr data for WR and clay fractions of MS samples. Also shown are $^{87}\text{Sr}/^{86}\text{Sr}$ ratios predicted from WR isochron corresponding to clay Rb/Sr, and δ value i.e. difference between predicted and measured $^{87}\text{Sr}/^{86}\text{Sr}$ ratios for clay fractions.

for the clay Rb/Sr ratio and the $^{87}\text{Sr}/^{86}\text{Sr}$ ratio actually measured on the clay fraction. These $\delta(^{87}\text{Sr}/^{86}\text{Sr})$ values do not show a great variation, and this explains why the slope (i.e. age) of the regression line through clay-fraction data is indistinguishable from that through the corresponding whole-rock data, although a different intercept is given. (Table 3.1, bottom line).

It may also be noted from Table 3.1 that the small variations in $\delta(^{87}\text{Sr}/^{86}\text{Sr})$ do not correlate with variations either in Rb/Sr of clay fractions or in Δ Rb/Sr (Clay - WR). The former rules out a simple model of episodic or continual loss of radiogenic $^{*87}\text{Sr}$ from the fine-fractions, which would produce a drop in $^{87}\text{Sr}/^{86}\text{Sr}$ which was proportional to the Rb/Sr ratio. The latter rules out a simple model of exchange of Sr between the clay-fractions and the adjacent residual phases (i.e. a partial rehomogenization of Sr-isotopes on an intergranular scale), which would produce a lowering of $^{87}\text{Sr}/^{86}\text{Sr}$ which was proportional to Δ Rb/Sr (Clay - WR). However, some sort of redistribution of Sr on a very small scale, rather than an absolute loss of $^{*87}\text{Sr}$, is supported by the close approach to fulfillment of isochron conditions by the whole-rock samples (giving ca. 382 m.y.). This is also supported by the pattern of model-ages from size-fractions of MS 1 & 6 (Table 2.6), in which the coarse-fractions give model-ages slightly greater than those of the W.R. samples, suggesting that they have a slight excess of $^{*87}\text{Sr}$ corresponding to the depletion of $^{*87}\text{Sr}$ observed in the finer fractions.

The small scale over which partial Sr-isotope homogenization subsequent to 382 m.y. in Marloes shales is observed, suggests that a fluid phase need not have been involved as a transporting medium. The mechanism may be more closely described by a volume diffusion model through crystal lattices and across intergranular boundaries.

CHAPTER 4

AN EXPERIMENTAL INVESTIGATION OF FACTORS INFLUENCING Rb-Sr SYSTEMS
DURING DIAGENESIS

4.1. Introduction

It is clear from the preceding chapter that no direct and complete observation has yet been made of the progressive homogenization of Sr-isotopes which, from the Rb-Sr isotope data on shales such as those from Marloes, does occur at some stage during late diagenesis or low-grade metamorphism. In the Marloes shales in the present study, it has been concluded (Chapter 3) that this homogenization was provoked by a distinct metamorphism and, that in all probability was the direct result of recrystallization of the original depositional phases. To date, the only field study of the systematic progress towards Sr-isotope homogeneity, albeit incomplete, has been that of Perry & Turekian (1974).

However, it has emerged from the evidence of Helgeson (1967) which was considered in Section 3.4.3, that the homogenization, even though it may be linked to recrystallization phenomena, may be defined entirely as a problem of kinetics.

In order to investigate more fully the rate processes involved in Sr-isotope homogenization between the components of a sediment and the connate fluids, a hydrothermal experimental apparatus has been used to simulate natural conditions during burial.

The dependences of the rates of Sr and Rb loss from the reactant assemblage on three parameters have been investigated in this preliminary study. These three parameters are:

- (a) Time, i.e. length of experimental run;
- (b) Temperature;
- (c) Fluid phase composition.

A reactant assemblage comprising clay of a degraded nature has been chosen in order to simulate more closely the phases present in sediments prior to recrystallization. Since it is not possible to obtain pure separates of such clays, a well-documented fine-fraction with a multi-component assemblage was used.

4.2. Experimental Details

4.2.1. Starting material

A fine-grained fraction (particle size range 0.2-1 μm) from one of the Lower Silurian mudstone samples from Buildwas, Shropshire (DD9) was chosen as the starting material for all experiments. These mudstones have already been described in Chapter 2 as unmetamorphosed sediments, containing degraded mixed-layer clays which have undergone very little diagenetic modification. The conclusions from these mineralogical observations are amplified by the Sr-isotope results (Section 2.4), which also demonstrate the presence of detrital components. The model age given by the 0.2-1 μm fraction of DD9 is 466 m.y. (Fig. 3-2) which is greater than the 420 m.y. estimated depositional age.

The clay fraction (<2 μm) mineralogy of sample DD9 is depicted in Fig. 2-8. The predominant phase is an illitic mixed-layer clay (the expandable I/M and non-expandable I phases being grouped together). Other phases present are kaolinite (5-10%) and chlorite (ca. 5%), as well as small amounts of quartz and plagioclase. The mineral composition of the 0.2-1 μm fraction is very similar. A diffractogram of an oriented specimen shows a predominance of mixed-layer clays.

The strontium and rubidium concentrations in DD9 (0.2-1 μm) have already been determined by isotope dilution analysis (Section 2.6.1 and Table 2.6), as well as the strontium isotopic composition. These analyses are:

Rb : 228 ± 1 ppm
Sr : 260 ± 1 ppm
 $^{87}\text{Sr}/^{86}\text{Sr} = 0.7255 \pm 10$

About 0.05-0.1g of this reactant was used in each experiment. This amount is limited by the reactor capsule size, but is sufficient to make an oriented specimen mounting after each experiment for X-ray diffraction investigation.

4.2.2. Fluid composition

In order to investigate the effects of fluid composition on exchange rates, the fluid chemistry was dominated by the addition of Na^+ , K^+ or Mg^{2+} as the chlorides. 'Specpure' or 'Analar' salts were used, and the quantities used were such that their contributions to total blanks in each experiment were:

1M NaCl solution : 1.5 ng Sr, Rb not measured
1M KCl solution : 0.3 ng Sr, 80 ng Rb
1M MgCl_2 solution : 0.5 ng Sr, 0.3 ng Rb

4.2.3. Reactor assembly

Reaction capsules were made from gold tubing (0.20 ins o.d. x 0.004 ins wall x 1.2 ins length), by sealing the ends by carbon-arc welding. The gold tubing was cleaned by immersion in hot conc. nitric acid and washed in deionised water. Subsequently, it was dried and annealed in a muffle furnace at 600°C. The Sr blank contributed by the reactant capsule was approximately 1 ng.

About 0.1g of starting material (Section 4.2.1) was weighed accurately into a gold reactant capsule, sealed at one end. Small amounts of ^{84}Sr - and ^{87}Rb -enriched 'spike' solutions (ca. 0.1 g of AB-2 and ca. 0.05g of AB-1 respectively, see Table D.1 in Appendix D) were added to the capsule by means of dropping pipette. Considerable care was taken to ensure that the drops

of solution were placed at the base of the capsule without trapping an air bubble. The weights of 'spike' solutions added were measured by the gains in weight of the capsule + contents (rapid measurement was necessary to eliminate loss by evaporation). Finally, about 0.1g of 2.5M saline solution (NaCl, KCl, MgCl₂) were added, such that the final concentration of the cation in the reactant fluid was close to unit molarity (deviation from this never greater than $\pm 10\%$).

The capsule was closed by crimping, and sealed by welding. The problem of boiling of reactant fluid during welding was overcome by immersing the lower part of the capsule in a small insulated beaker of liquid nitrogen. The sealed capsule was tested by heating it to 100°C in an oven and checking for constant weight.

The loaded capsule was placed in the 'hot-spot' region of a cold-seal René bomb, and maintained there by means of a stainless steel spacer rod. The bomb was attached to a high-pressure water line (commercial equipment supplied by Tem-Pres Research Inc., model HR-1B), and the hydrothermal pressure was maintained at approximately 1 kilobar during each run. This pressurisation served not only as a simulation of burial (1 kilobar lithostatic pressure corresponds to about 4000m of overburden) but also as a constraining force against the internal pressure developed within the capsules.

The bomb was heated externally, the temperature being controlled within $\pm 1-2\%$ of the desired setting. (Temperature control was improved for the later experiments by replacing the mechanically-activated controllers by Eurotherm thyristor-driven control units). In addition, the bomb temperature was monitored continuously by a chromel-alumel thermocouple located within the wall of the bomb close to the 'hot-spot', and recorded on a calibrated multi-point recorder.

4.2.4. Analytical Techniques

On completion of an experiment, the reactor assembly was allowed to cool and de-pressurize. Rapid quenching was not necessary, since the presence of Sr- and Rb-'spike' solutions throughout each run eliminated interference from cooling phenomena. The reactor capsule was rinsed in de-ionised water, immersed in liquid N₂ to freeze the contents, and cut open. After thawing, the contents, a muddy slurry, were squeezed out into an ultraclean P.T.F.E. beaker.

Two techniques of obtaining a particle-free solution were tried. Initially, the slurry was squeezed through a 'Millipore' cellulose ester microfilter (pore size 0.05 µm). This method was satisfactory with respect to contamination (<1 ng Sr blank was measured), however fast centrifugation was found to give an improved recovery of residual solids, and is a simpler operation.

The solid residue was disaggregated ultrasonically into an aqueous suspension, and mounted by the suction-onto-ceramic tile method (Appendix B.2) for clay minerals' analysis.

The amounts and concentrations (AB-1 : 28.50 ppm Rb; AB-2 : 29.06 ppm Sr) of the 'spike' solutions added during reactor assembly (Section 4.2.3) were sufficient to ensure that the extract after the hydrothermal run contained a measurable quantity of each element. The supernatant solution from the centrifuge treatment was divided into aliquots, from which Sr and Rb were separated for mass-spectrometric analysis of isotope compositions (Appendix D and Section 2.6.1).

The presence of 'spike' Sr and Rb (for isotopic compositions, see Table D.1 in Appendix D) in the experimental fluid permits the calculation, directly from the measured isotopic compositions after each experiment, of the quantities of Sr and Rb exchanged by the solid with the fluid, as well as the ⁸⁷Sr/⁸⁶Sr ratio (Appendix E.3 and E.4). The errors associated with these Sr and Rb analyses are similar to those by isotope dilution analysis

discussed elsewhere (Section 2.6.1). However, in many cases, the small amount of Sr recovered did prohibit precise determinations of $^{87}\text{Sr}/^{86}\text{Sr}$ (i.e. some $^{87}\text{Sr}/^{86}\text{Sr}$ ratios may be quoted with confidence only to the third decimal place).

4.2.5. Hydrothermal Experimental Conditions

The ideal simulation of burial conditions, with respect to temperature and time, is obviously not available in the laboratory. Therefore, temperatures used are somewhat higher than would obtain in nature - generally in the range 300-360°C - in order that observable changes occur during the run-time available (maximum 300 hours in this study).

The stability fields of clay phases as a function of temperature and fluid composition has already been discussed (Section 3.4.3) in the light of the data from Helgeson (1967). It was concluded that under normal marine conditions, and conditions which may be predicted to obtain during burial, the mixed-layer clay is unstable with respect to illite + chlorite (Fig. 3-9). Similarly, the reaction material in the present experiments may be shown to be unstable under the experimental conditions. Values of log (activity ratios) for the starting fluid in each experiment are as follows (assuming pH = 7).

$$1\text{M NaCl} \quad , \quad \log a_{\text{Na}^+}/a_{\text{H}^+} \approx 7,$$

$$1\text{M KCl} \quad , \quad \log a_{\text{K}^+}/a_{\text{H}^+} \approx 7,$$

$$1\text{M MgCl}_2 \quad , \quad \log a_{\text{Mg}^{2+}}/a_{\text{H}^+}^2 \approx 14$$

It is clear from Fig. 3-9 that under these conditions, the starting phases are unstable with respect to albite, microcline and chlorite respectively for each of the three initial cation concentrations. The activity diagrams also show that even for quite large decreases in brine cation activity or decreases in pH during the course of an experiment, this conclusion holds.

Experiments were conducted at temperatures from room temperature to

360°C, with fluids of each of the three major cations. In addition, experiments were carried out under virtually identical conditions, but for different durations, in order to investigate the change with time of the rates of Sr and Rb exchange.

4.3. Results

4.3.1. Post-experiment solid phases

After some experiments, insufficient clay was recovered to permit full, semi-quantitative mineralogical analysis. However, it was possible to obtain diffractograms of air-dried and glycollated specimens from most experiments. Remarkably little change was detected in the majority of experiments in the X-ray intensity of the 10Å reflection from the mixed-layer illite-smectite clay, which is the major phase. The crystallinity index of illite, inferred from the 10Å peak, was monitored on the glycollated specimens, and show little change from the >12 value for the starting material (cf. Fig. 2-9), except in the experiment with 1M MgCl₂ at 360°C (Fig. 4-1). In this case, a distinct change in crystallinity index from >12 to approx. 8 was detected. This change coincides with the appearance in the diffractogram from the air-dried specimen of a high background intensity from the 10Å peak to higher d-spacings; superimposed on this are broad peaks at ca. 12Å and ca. 14Å. The 12Å peak was found to disappear on glycollation. This behaviour correlates with that observed by Weaver and Beck (1971, p.14) in deeply buried (5000-8000m) Carboniferous shales. The authors attributed their observations to the presence of a mixed-layer 10Å/14Å illite-chlorite phase, the 12Å peak representing a regular interstratification though its behaviour with glycol suggests the presence of some expandable smectite layers as well.

A slight shift in the 10Å peak to ca. 10.4Å was detected in the experiments with NaCl at 360°C (Fig. 4-1). This possibly indicates a trend towards regular interstratification within the mixed-layer illite-smectite

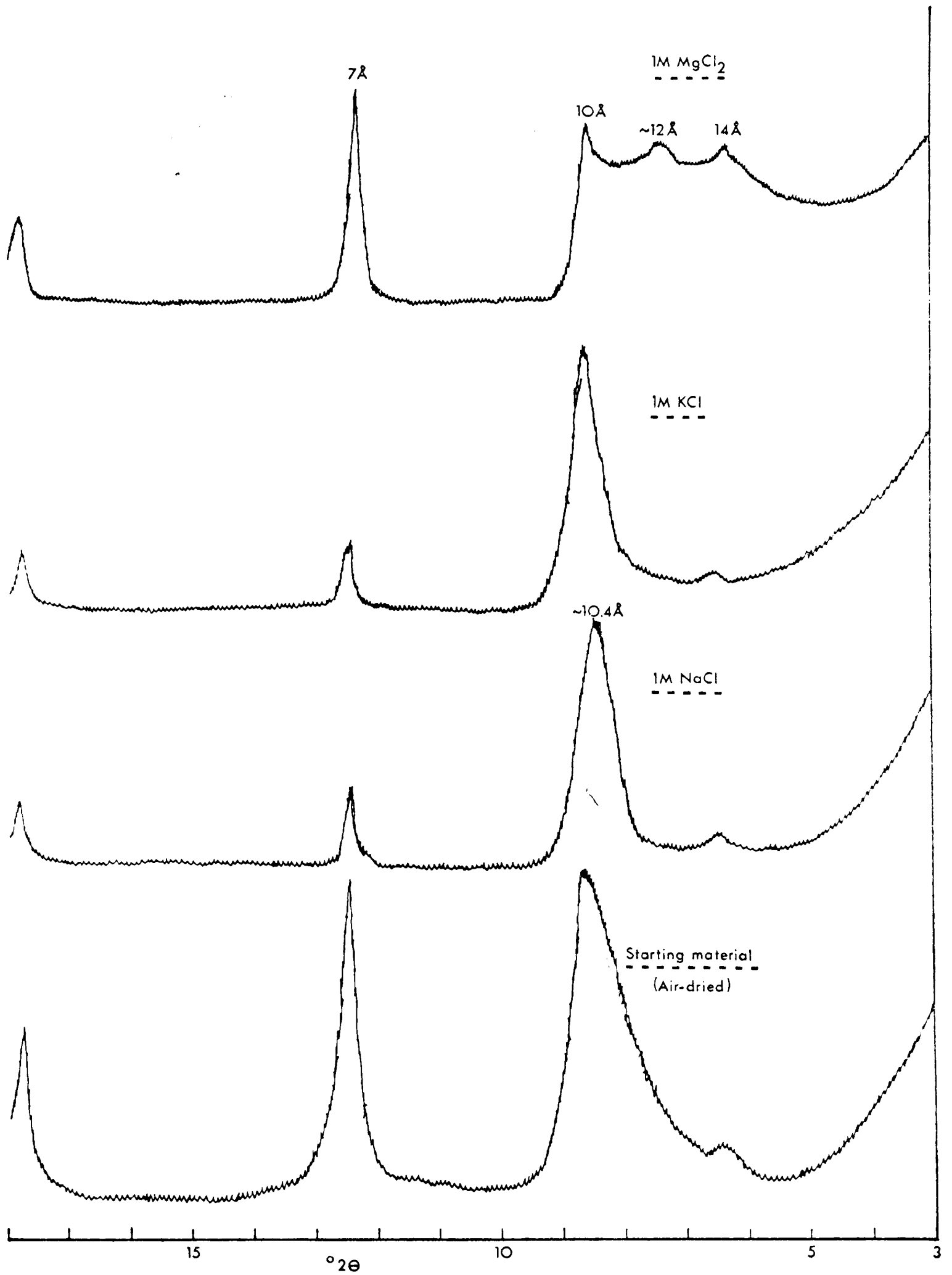


Fig. 4-1. Diffractogram traces of air-dried oriented clay mounts of (a) experimental starting material, and the same material after heating at 360°C for 12 hours with (b) 1M NaCl soln., (c) 1M KCl soln., (d) 1M MgCl₂ soln..

phase.

In all experiments except those with $MgCl_2$ present, a marked decrease in intensity of the 7\AA peak was observed (Fig. 4-1). This is attributed to reaction of kaolinite with the fluid, though the products of the reaction are not apparent, probably due to the small proportion of kaolinite originally present. In all cases, the residual intensity at 7\AA is due to the chlorite (002) reflection, which, with $MgCl_2$ present at 360°C , is enhanced by the production of chlorite and illite-chlorite interstratifications as previously noted.

A summary of these observed and inferred phase changes is given in Table 4.1.

4.3.2. Rb and Sr exchanged with fluid

The data from the isotope dilution analyses for Rb, Sr, and $^{87}\text{Sr}/^{86}\text{Sr}$ appear in Table 4.2. The amounts of Sr and Rb lost from the substrate to the fluid are tabulated as micrograms of the respective element per gram of reactant. It was found that experimental runs conducted at up to 100°C in the case of Rb, and up to 200°C for Sr, displayed a consistent amount of elemental loss irrespective of the duration of run. These quantities of Sr and Rb (remarkably reproducible in the former case) are attributed to cations labile to exchange due to surface-adsorption or some such process, and will be referred to as 'blank' quantities. Their mode of incorporation is clearly different from the majority of the Sr and Rb, and therefore the analytical results have been 'blank corrected' by subtraction of $29\ \mu\text{g/g}$ of Sr and $6\ \mu\text{g/g}$ of Rb (See Table 4.2). Mean rates of loss (in $\mu\text{g hr}^{-1}$) have been calculated from these 'blank-corrected' quantities. These parameters do not represent actual rates, since to do so would be to assume implicitly no dependence of actual rate of loss on time elapsed since the start of an experiment. Indeed, the experimental results demonstrate that such an assumption is not valid.

Experiment no.	Temp, °C	Time, hrs	Fluid composition
V	20	100	Brine cations absent
IV	100	48	" " "
VII	215	48	" " "
II	215	234	0.96M NaCl
XII	215	309	0.66 "
X	315	306	1.09 "
I	315	306	1.00 "
XXIII	340	308	0.94 "
XXV	360	2	0.72 "
XXI	360	5	0.76 "
XX	360	12	1.02 "
XXXIV	360	24	1.05 "
XXXIII	360	186	1.05 "
XVIII	20	100	0.86M KCl
XVI	315	306	1.06 "
XXII	340	306	1.03 "
XIV	360	12	1.03 "
XXXV	360	24	1.05 "
XXVI	20	100	1.00M MgCl ₂
XXXI	315	306	1.02 "
XXXII	340	306	1.13 "
XVII	360	11	1.10 "
XXIX	360	24	1.15 "

Table 4.2(a) List of experimental conditions (all at 1 kilobar pressure) for each run.

Equipment no.	Measured, $\mu\text{g/g}$	Sr exchange		Mean rate, $\mu\text{g/hr}$	$^{87}\text{Sr}/^{86}\text{Sr}$
		'Blank corrected'			
V	29	-		-	0.716
1V	31	-		-	0.716
V11	30	-		-	0.717
11	30	-		-	0.718
X11	29	-		-	0.718
X	48	19		0.062	0.722
1	44	15		0.049	0.719
XX111	55	26		0.084	0.720
XXV	55	26		13	0.7165
XX1	37	8		1.6	0.719
XX	53	24		2	0.718
XXX1V	44	15		0.63	0.7210
XXX111	104	75		0.40	0.7169
XV111	29	-		-	0.716
XV1	105	76		0.25	0.713
XX11	124	95		0.31	0.7134
X1V	133	104		8.7	0.712
XXXV	155	126		5.3	0.7120
XXV1	44	-		-	0.7164
XXX1	60	31		0.10	0.720
XXX11	88	59		0.19	0.7190
XV11	95	66		6	0.716
XX1X	95	66		2.75	0.7170

Table 4.2(b) Analytical data for Sr exchange under experimental conditions listed in Table 4.2(a). Reactant material has 260 $\mu\text{g/g}$ Sr with $^{87}\text{Sr}/^{86}\text{Sr} = 0.7255$.

Experiment no.	Measured, $\mu\text{g/g}$	Rb exchange		Mean rate, $\mu\text{g/hr}$	^{87}Sr $\times 10^{-2} \mu\text{g/g}$
		'Blank corrected'			
V	6	-	-	-	1.44
1V	6	-	-	-	1.54
V11	11	-	-	-	1.79
11	13	7		0.030	2.08
X11	11	5		0.016	2.01
X	23	17		0.056	5.23
1	29	23		0.075	3.49
XX111	37	31		0.101	4.91
XXV	22	16		8	3.01
XX1	26	20		4	2.94
XX	29	23		2	3.68
XXX1V	36	30		1.3	4.50
XXX111	48	42		0.23	6.10
XV111	3	-		-	1.44
XV1	15	9		0.029	2.12
XX11	19	13		0.042	2.99
X1V	13	7		0.58	1.37
XXXV	17	11		0.46	2.00
XXV1	14	-		-	2.36
XXX1	42	36		0.12	5.40
XXX111	55	49		0.16	6.98
XV11	37	31		2.9	4.73
XX1X	50	44		1.8	5.66

Table 4.2(c). Analytical data for Rb & radiogenic ^{87}Sr exchange under experimental conditions listed in Table 4.2(a). Reactant material has 228 $\mu\text{g/g}$ Rb. ^{87}Sr exchange is calculated from $^{87}\text{Sr}/^{86}\text{Sr}$ in Table 4.2(b).

It is also possible to estimate the amount (y $\mu\text{g/g}$) of radiogenic ^{87}Sr which has been exchanged with the fluid in each experiment. The approximation is made that the gross amount of Sr lost (x $\mu\text{g/g}$) comprises solely 'common' Sr, the $^{87}\text{Sr}/^{86}\text{Sr}$ ratio of which is estimated from the measured $^{87}\text{Sr}/^{86}\text{Sr}$ ratios of those experiments with high Sr loss / Rb loss values (i.e. experiments XIV and XXXV in Table 4.2). The $^{87}\text{Sr}/^{86}\text{Sr}$ ratio of 'common' Sr has been estimated in this way at ~ 0.711 (compare with $^{87}\text{Sr}/^{86}\text{Sr}$ intercept at 0.7103 of best-fit line on Fig. 3-1). If the measured $^{87}\text{Sr}/^{86}\text{Sr}$ ratio for Sr added to the fluid is R , then, by applying the above approximations and the known isotopic composition of Sr (Chapter 1.3) it can be shown that

$$\frac{0.0701x + y}{0.0986x} = R$$

from which y can be calculated. The computed values for y are in Table 4.2(c).

The dependence of radiogenic $^{*87}\text{Sr}$ exchange on Rb exchange is demonstrated in Fig. 4-2, in which these two parameters are plotted on the ordinate against an arbitrary order of experiments on the abscissa. The amount of $^{*87}\text{Sr}$ exchanged with the fluid is directly proportional to the amount of Rb exchanged, as is to be expected from the association of $^{*87}\text{Sr}$ with the parent ^{87}Rb lattice sites. It has therefore been established that in the subsequent discussion of results, we may extend the conclusions concerning the behaviour of Rb to include that of $^{*87}\text{Sr}$.

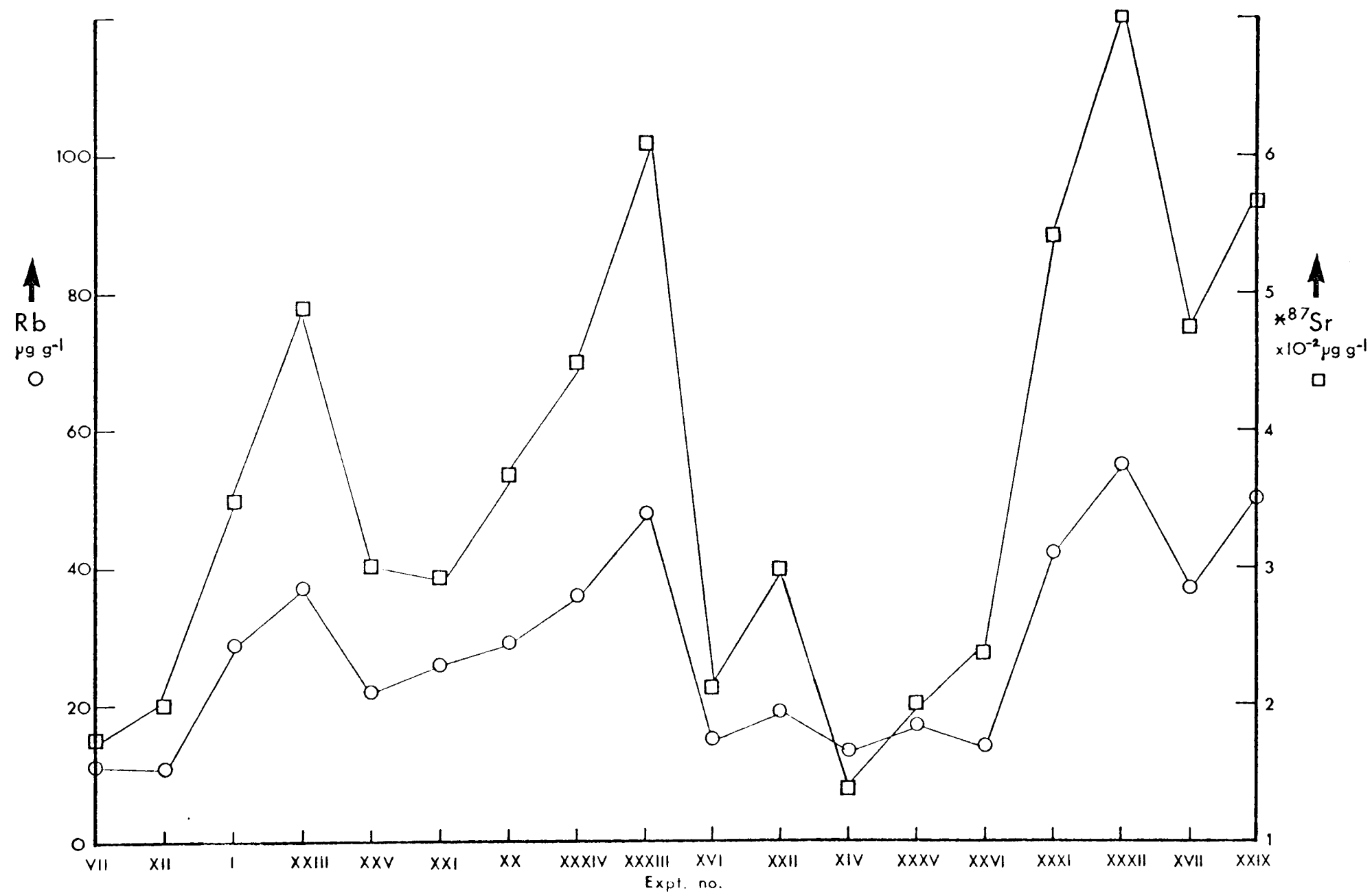


Fig. 4-2. Graph demonstrating the correlation between amount of radiogenic ⁸⁷Sr exchanged (open squares) and amount of Rb exchanged (open circles) from clays to fluid.

4.4. Discussion of Results

4.4.1. Time-dependence

It is clear from the data in Table 4.2 (e.g. experiments XXV, XXI, XX, etc.) that the mean overall rates of exchange of both Sr and Rb with the fluid decrease as the duration of experiment increases. This is demonstrated in Fig. 4-3, in which the mean rates of all experiments at 360°C are plotted against duration. The irregular pattern for rates of Sr exchange against duration in Fig. 4-3 is probably indicative of poor precision for the data from runs of short duration. Nevertheless, the trend apparent in Fig. 4-3 is undoubtedly genuine, and has been observed also in investigations of Rb loss from biotite (Hofmann & Giletti 1970). These authors suggest that it may be caused by early facile loss from low-energy sites, and for the present substrate of degraded clay phases this explanation seems very probable.

The greater proportion of total Sr than of total Rb which is exchanged during this period of rapid loss, suggests that exchange sites associated with 'smectite-type' interstratifications may be responsible. Whatever the cause, this amplifies the earlier cautionary note (Section 4.3.2) concerning the use of mean overall rates of exchange. In order to eliminate as far as possible the influence of this initially high rate on the significance of any conclusions for the overall Sr or Rb content, the exchange rates from runs of greatest duration for any given set of conditions, have been used in subsequent calculations.

4.4.2. Dependence on fluid composition and temperature

The data plotted in Fig. 4-3 hints at a consistent influence by the nature of the brine cation on the rate of Sr or Rb loss. If measured overall rates of Sr and Rb exchange are plotted (as logs) against temperature, a pattern of dependence on fluid composition emerges (Fig. 4-4). At any given temperature, the rates of exchange are in the following order

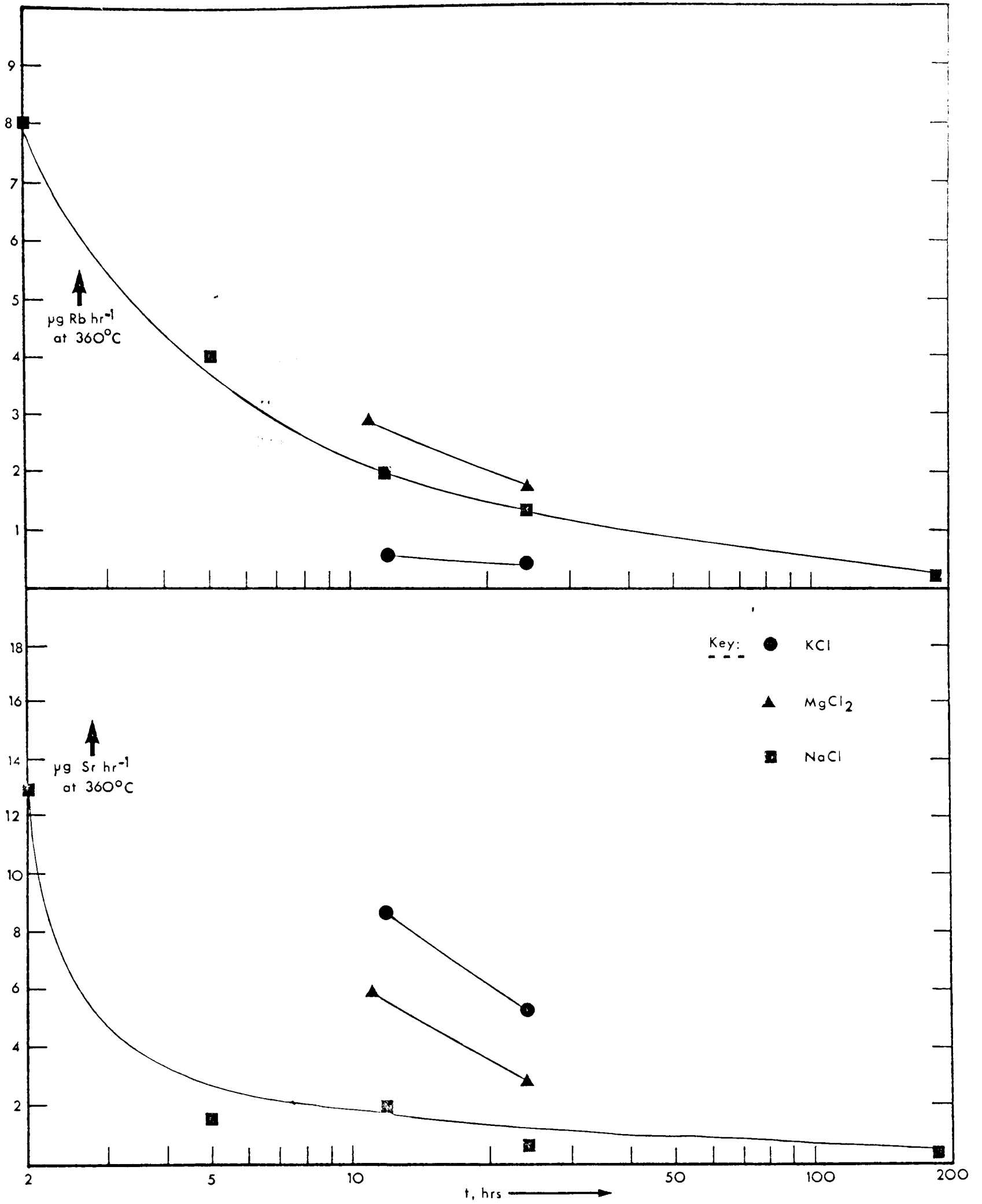


Fig. 4-3. Mean rates of Rb & Sr exchange from clays to fluid at 360°C , plotted against duration of experimental run.

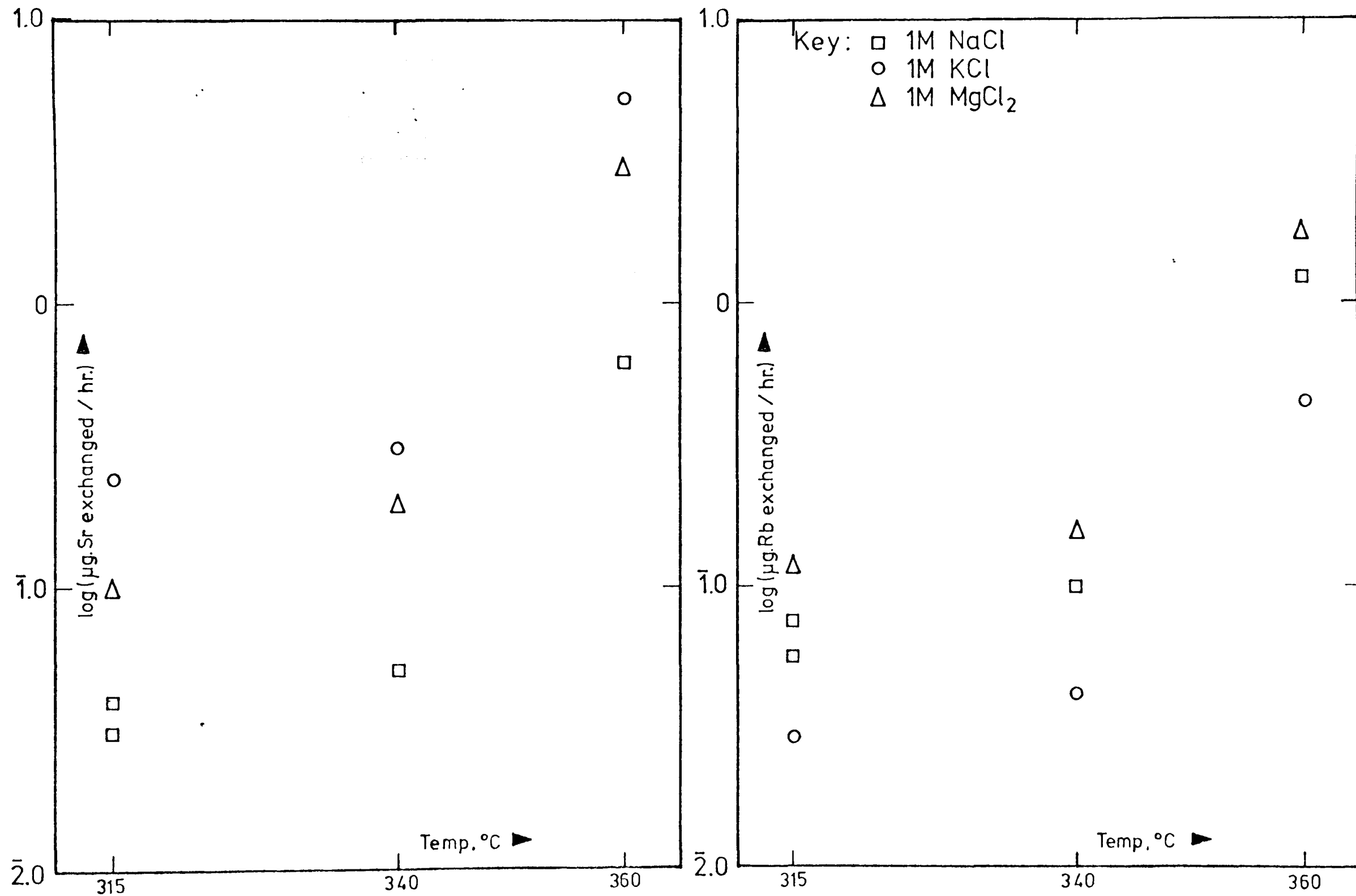


Fig. 4-4. Diagrams showing rates of exchange of Sr & Rb (plotted on a log scale) as a function of temperature, for experimental runs with varying brine composition.

of brine cations:

Sr exchange : $K^+ > Mg^{2+} > Na^+$

Rb exchange : $Mg^{2+} > Na^+ > K^+$

Such a rate dependence on fluid composition has not previously been observed quantitatively, and will be discussed subsequently in the context of interpretational models.

4.5. Discussion of Interpretational Models

The exchange of Sr and Rb contained in a complex natural assemblage, such as employed in these experiments, cannot be described by any unique mechanistic model. Indeed, Hofmann and Giletti (1970) consider the same problem in relation to the multicomponent nature of mica solid solutions. Nevertheless, models may be examined in the light of empirical data, and also compared with conclusions reached from field studies.

The apparently small extent to which phase changes have occurred, despite the metastable nature of the substrate (Section 4.2.5), and the high proportions of total Sr and Rb which have been exchanged, suggest that this exchange is not directly related to phase changes.

Two models may be proposed to describe the exchange of cations between solid phases and fluid; these are:

(i) volume diffusion of species through the lattice to the solid-fluid interface,

and

(ii) dissolution kinetics and equilibria.

Each of these models will be considered in the following sections.

4.5.1. Volume diffusion from lattice

Empirical diffusion coefficients may be computed from the Sr and Rb exchange data by the method adapted from Crank (1956) and described in Appendix F. These coefficients are listed (as D/a^2) in Table 4.3. It

Expt. No.	Temp, °C	Time, hrs	Fluid comp.	D/a ² (Sr)sec ⁻¹	D/a ² (Rb)sec ⁻¹
X	315	306	~1M NaCl	9.6 x 10 ⁻¹⁰	8.4 x 10 ⁻¹⁰
I	315	306	"	5.6 x 10 ⁻¹⁰	1.4 x 10 ⁻⁹
XXIII	340	308	"	1.7 x 10 ⁻⁹	2.6 x 10 ⁻⁹
XXV	360	2	"	2.5 x 10 ⁻⁷	1.0 x 10 ⁻⁷
XXI	360	5	"	9.9 x 10 ⁻⁹	6.7 x 10 ⁻⁸
XX	360	12	"	3.9 x 10 ⁻⁸	3.9 x 10 ⁻⁸
XXXIV	360	24	"	7.5 x 10 ⁻⁹	3.3 x 10 ⁻⁸
XXXIII	360	186	"	2.8 x 10 ⁻⁸	9.5 x 10 ⁻⁹
XVI	315	306	~1M KCl	1.6 x 10 ⁻⁸	2.4 x 10 ⁻¹⁰
XXII	340	306	"	2.3 x 10 ⁻⁸	4.7 x 10 ⁻¹⁰
XIV	360	12	"	7.9 x 10 ⁻⁷	3.9 x 10 ⁻⁹
XXXV	360	24	"	5.4 x 10 ⁻⁷	4.5 x 10 ⁻⁹
XXXI	315	306	~1M MgCl ₂	2.7 x 10 ⁻⁹	3.9 x 10 ⁻⁹
XXXII	340	306	"	1.1 x 10 ⁻⁸	7.8 x 10 ⁻⁹
XVII	360	11	"	3.2 x 10 ⁻⁷	7.7 x 10 ⁻⁸
XXIX	360	24	"	1.6 x 10 ⁻⁷	7.7 x 10 ⁻⁸

Table 4.3. Empirical diffusion coefficients (quoted as D/a²) for experimental runs

is to be stressed that these are purely empirical values, and that calculation of them does not imply the acceptance of a diffusive mechanism.

The values calculated for the diffusion parameter, D/a^2 , have been listed in Table 4.3 because these are the most convenient expressions of rate constant from which activation energies may be determined. Since the effective particle radius for diffusion, a , is not easily determined, and may be highly variable, the computed value of the diffusion coefficient, D , is not entirely reliable. However, for the purposes of comparison with other investigations, D may be calculated using the estimated spherical diameter (e.s.d.) based on settling rates as an estimate for $2a$.

In the present experiments, the values obtained for D/a^2 (for Sr or Rb) are in the range from $5 \times 10^{-10} \text{ sec}^{-1}$ for Sr with a NaCl brine at 315°C to about $5 \times 10^{-7} \text{ sec}^{-1}$ for Sr with a KCl brine at 360°C . Assuming a value of $0.3\mu\text{m}$ for the parameter a (mean e.s.d. = $0.6\mu\text{m}$), these values correspond to a range for values of D from $5 \times 10^{-19} \text{ cm}^2 \text{ sec}^{-1}$ to $5 \times 10^{-16} \text{ cm}^2 \text{ sec}^{-1}$. These may be compared with a value for D of $2 \times 10^{-15} \text{ cm}^2 \text{ sec}^{-1}$ obtained by Hofmann and Giletti (1970) for Rb diffusion out of biotite at 550°C , and a similar value by McNutt (1964) for ^{87}Sr diffusion out of biotite. Therefore it is seen that the empirical values for D for the clays in the present study are generally compatible with those obtained elsewhere for micaceous structures, when the higher temperatures in the latter cases are taken into account.

These data also stress the importance of the grain size effect. The effective rate constants, D/a^2 , in the present experiments are greater than those measured by Hofmann and Giletti (op. cit.) and by McNutt (op. cit.). However the computed D values are in the reverse order as a consequence of very small grain size in the present study.

Despite the general agreement with a diffusion model, a simple diffusion model is invalidated by the strong dependence of D/a^2 on fluid composition (Table 4.3). Examination of the temperature dependence of D/a^2

also supports this view.

The Arrhenius equation, which describes the temperature dependence of rate constants by the general form:

$$k = Ae^{-E_a/RT}$$

where k = rate constant,

A = a constant, called the 'frequency factor',

E_a = activation energy,

and T = temperature, $^{\circ}\text{K}$,

may be applied to the specific case of diffusion coefficients:

$$\frac{D}{a^2} = Ae^{-E_a/RT}$$

From this equation, it is seen that a plot of $\ln (D/a^2)$ against $1/T$ should yield a straight line with slope $-E_a/R$, from which an empirical value of E_a may be obtained. Such a plot also serves as a test of the validity of interpretation in terms of a single mechanism operating at all temperatures, since only in such a case would a linear Arrhenius plot be observed.

Arrhenius plots ($\log D/a^2$ against $1/T^{\circ}\text{K}$) for a cylinder-diffusive loss model of Sr and Rb exchange between the mixed-layer clay reactant and a NaCl brine are shown in Fig. 4-5. It is clear from this figure that data points for neither Sr nor Rb are colinear, i.e. the simple model does not hold. The maximum slopes of Sr and Rb data correspond to activation energies of 108 and 51 kcal/mole respectively, whereas the minimum slopes correspond to 25 and 27 kcal/mole respectively. Clearly the first two values are far in excess of any realistic estimates and as such are meaningless, though they do suggest a new mechanism for loss of Sr and Rb at the higher temperatures (possibly recrystallization of substrate and formation of new phases?). The minima values for the empirical E_a , 25 and 27 kcal/mole for Sr and Rb respectively, are more comparable in magnitude with that estimated by Hofmann and Giletti (1970) for Rb-diffusion

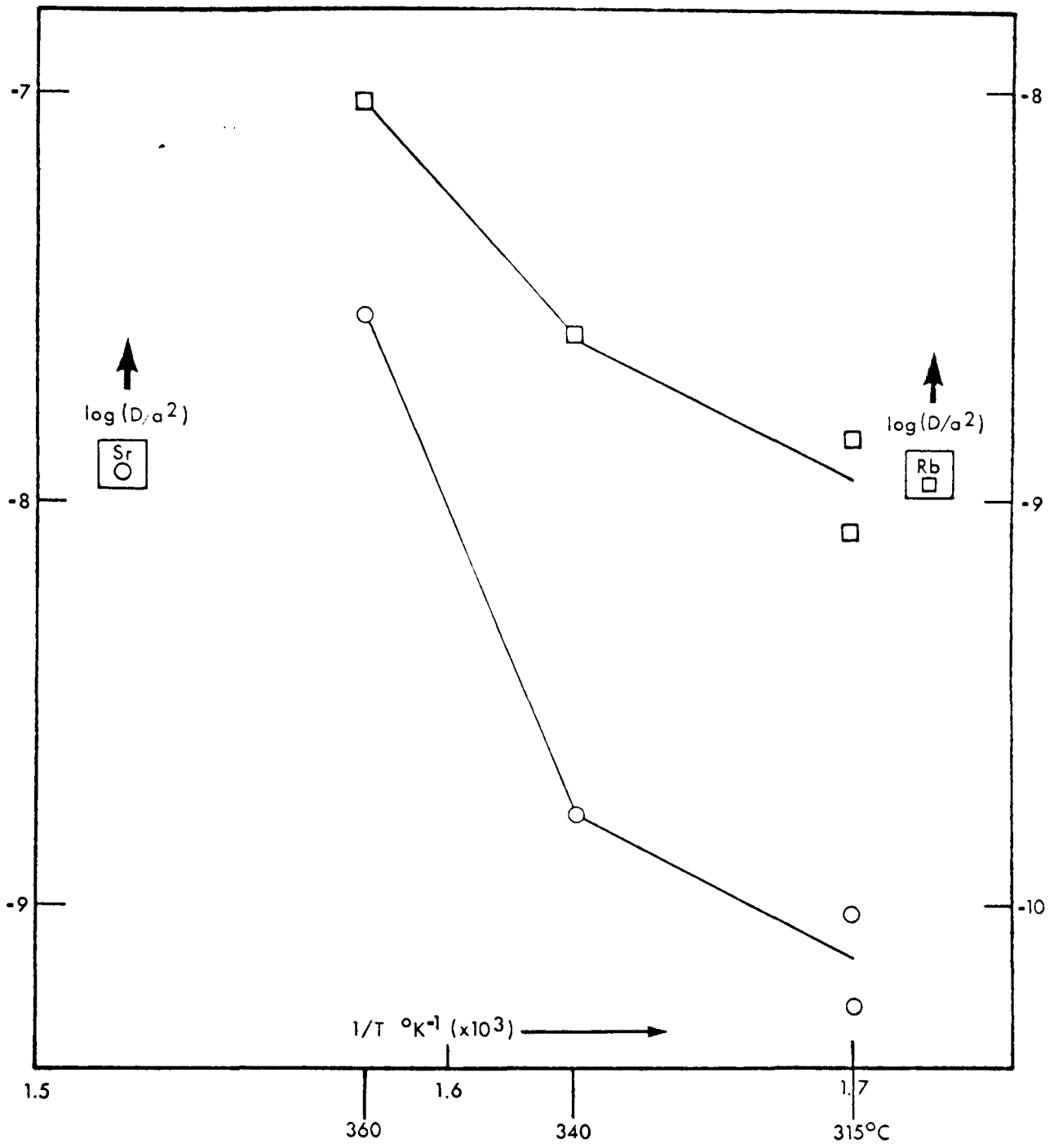


Fig. 4-5. Arrhenius plots ($\log D/a^2$ against $1/T^\circ\text{K}$) for a cylinder diffusive loss model of Sr (O) and Rb (\square) exchange between reactant and 1M NaCl brine.

from biotite (21 kcal/mole⁻¹).

In conclusion, it has been shown that an interpretation of the exchange characteristics of the present clay reactant, based on a simple volume diffusion model, leads to diffusion coefficients in some cases several orders of magnitude greater than those previously measured for well crystalline micas. In addition, analysis of the temperature dependence of these empirical diffusion coefficients may yield unrealistically high activation energy values. Both these observations suggest that simple volume diffusion is not the sole mechanism by which Sr and Rb exchange takes place, and in some cases (e.g. higher temperatures) is not the dominant mechanism.

4.5.2. Dissolution kinetics and equilibria

The many processes associated with the overall phenomenon of dissolution are not well understood for silicate minerals. The most comprehensive treatment of the kinetics of transfer of ionic species between silicates and unequilibrated aqueous solutions has been by Helgeson (1971). Helgeson has suggested that, for both congruent (dissolution) and incongruent (e.g. hydrolysis) reactions, the rate determining step is diffusional transfer of species through a surface layer (or layers) of intermediate reaction products. This leads to the overall reaction rate being described by the equation:

$$\frac{dm_i}{dt} = k_i t^{-\frac{1}{2}}$$

(a parabolic rate law). A plot of reaction progress parameter (m_i) against $t^{\frac{1}{2}}$ should be linear. Unfortunately, data from the present investigations is insufficient to test this rigidly. However, a preliminary plot of the five data points for Rb loss in NaCl brine at 360°C (expts. XXV, XXI, XX, XXXIV, XXXIII) suggests that the above equation does not adequately describe the observations.

The possibility of dissolution equilibrium having been rapidly achieved, and therefore the rate of exchange being described by the kinetics of a dynamic equilibrium (which Helgeson, op.cit., suggested would not necessarily follow a parabolic rate law) must also be considered. Huang and Keller (1973) found that at room temperature, clay minerals had almost achieved equilibration with solutions after 100 days. It is also worth noting that these authors observed an initially rapid rate of dissolution, similar to the pattern of Sr and Rb release with time observed in the present study (Fig. 4-3). At the elevated temperatures of these investigations, it seems probable that dissolution equilibrium has been achieved in many, if not all, experiments.

However, a strong argument against exchange kinetics between equilibrated solid and solution being the dominant mechanism by which Sr and Rb are released, is the absence of major phase changes in experiments. It may be reasonably predicted that a dissolution process, i.e. dislocation of the silicate lattice, should be the rate determining step in an overall silicate phase change. Therefore by this mechanism, one would expect the observed Rb and Sr release to be paralleled by phase transformation to stable assemblages, which apparently does not occur (Section 4.3.1).

4.5.3. Conclusions

It is clear from these attempts to assign distinct interpretational models to experimental observations that the response of Rb and Sr in the system is governed not only by the simple processes described (diffusion, dissolution) but by many other complex properties as yet not understood. Indeed, such a situation is predictable by the complex and poorly-understood nature of clay mineral structures themselves.

Nevertheless, the results of such studies on naturally-occurring clay assemblages are of intrinsic value themselves. The metastable state of these degraded clays, and therefore the necessity to consider Rb-Sr system-

atics as a kinetic as well as a thermodynamic problem, has already been noted. These studies have clearly demonstrated the dependence of rate-determining processes, not only on directly related parameters such as temperature and grain size, but also on the less easily related parameter of fluid composition.

Finally, one comparison of conclusions from experimental and field studies may be noted. The previously described experiments suggest that exchange of Rb and Sr with the fluid is not directly related to, and dependent on, phases changes to a stable assemblage. On the other hand, the studies of Perry and Turekian (1974) suggest that exchange and consequent homogenization of Sr amongst Sr-bearing phases during progressive diagenesis in nature is paralleled by a recrystallization of mixed-layer phases. Such a discrepancy may be attributed to the necessity for use of unrealistic temperatures in laboratory simulations in order to make observable changes occur in the finite time available. It also underlines the caution with which experimental observations may be extrapolated to natural systems.

CHAPTER 5

Rb-Sr STUDIES ON SEDIMENTS FROM THE LONG MYND, SHROPSHIRE

5.1. Introduction

Studies on shales of independently adduced depositional age have shown that such rocks can yield Rb-Sr isochron ages (Chapter 3). Furthermore, these isochron ages are significantly lower than the estimated age of deposition. In the present study, such an age from Silurian shales from Pembrokeshire has been interpreted as the date of a distinct metamorphic episode at which time transformation of metastable clay phases took place (Section 3.4.3).

In order to test further the applicability of the Rb-Sr dating method to argillaceous sediments, shale samples were collected from several stratigraphic levels in the Longmyndian succession and were subjected to Rb-Sr isotope investigations. The Longmyndian succession poses an interesting stratigraphic problem: it has been considered at various times to have been deposited in the late Proterozoic or the early Phanerozoic. It was hoped that considerations based on Rb-Sr data might enable constraints to be put on the age of the Longmyndian. Previous estimates of the age of the succession have made use of rather tenuous correlations based predominantly on lithological evidence.

5.2. The Longmyndian Succession

5.2.1. Geological setting and structure

The Long Mynd comprises an elongated plateau, extending roughly N.E.-S.W., situated in the west of Shropshire in the Welsh Borderland (see inset, Fig. 5-1). The sediments of which the Long Mynd is composed form a succession at least 5000m thick, the stratigraphy of which has been described in detail by James (1956).

The overall structure of the Long Mynd is synclinal (James, op.cit.).

In the west, in an inverted sequence, the Longmyndian is seen to be unconformably overlain by Uriconian volcanics, which have a faulted western contact with Tremadoc shales. To the east, the Long Mynd outcrop is unconformably overlain by Silurian strata, which are separated from an eastern outcrop of Uriconian volcanics by the main Church Stretton Fault (CSF, see Fig. 5-1). Thus there has been little direct evidence from the type outcrop of Longmyndian to support an accurate assessment of the succession's stratigraphical position.

In addition to the main occurrence west of CSF, there are several faulted inliers to the east, which have been inferred, on grounds of lithology and thickness, to belong to the same succession. It is on stratigraphical relationships inferred between these inliers and the surrounding Uriconian volcanics and Lower Palaeozoic sediments that a Precambrian age has been assigned to the Longmyndian.

Prior to the discovery of the Olenellus fauna (Lapworth, 1888) in the Comley sandstone (overlying the Wrekin quartzite, which is unconformable upon the Uriconian volcanics east of CSF), the Long Mynd succession had been included in the Cambrian system (see Cowie et al. 1972). Subsequently, the Longmyndian, which has been considered to be a little younger than, and partly derived from, the Uriconian (James 1956; Greig et al. 1972), was placed in the Precambrian. Some authors have considered the contact between the inferred Longmyndian and the Uriconian east of CSF to be conformable (Cobbold & Whittard 1935; James 1956).

5.2.2. Previous Geochronological Evidence

The only previous radiometric age measurements made directly on Longmyndian rocks are two unpublished K-Ar age determinations (S. Moorbath, pers. comm.). Coarse-grained muscovite separated from a siltstone collected from the Synalds Group in the lower part of the succession (Table 5.1), gave a K-Ar age of ca. 537 m.y. Similar muscovite from a sample collected

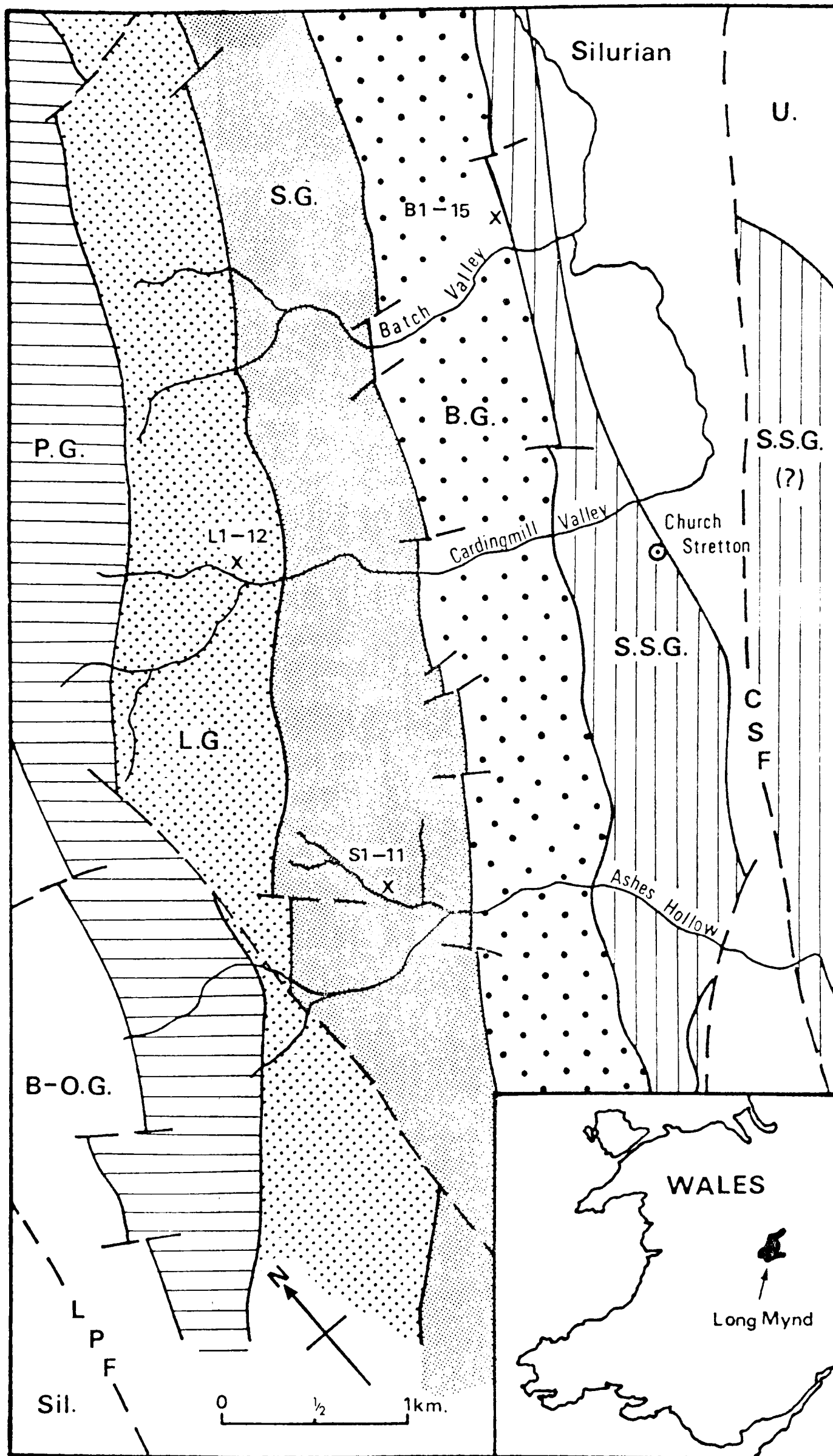


Fig.5-1. Geological sketch-map of part of the Long Mynd, west of Church Stretton, Shropshire, showing sample locations.
 B-O.G. Bayston-Oakswood Group, P.G. Portway Gp., L.G. Lightspout Gp., S.G. Synald's Gp., B.G. Burway Gp., S.S.G. Stretton Shale Gp., U Uriconian volcanics.
 CSF Church Stretton Fault, L.P.F. Linley-Pontesford Fault.
 (Adapted from Greig et al., 1968).

WENTNOR SERIES

BRIDGES GROUP: purple laminated siltstones and
sandstones 600-1200m.

BAYSTON-OAKSWOOD GROUP: massive purple and
greenish grey sandstones with
thick conglomerate bands 1200-2400m.

Probable unconformity

STRETTON SERIES

PORTWAY GROUP: green and purple siltstones and
sandstones with a conglomerate
at the base 200-1000m.

LIGHTSPOUT GROUP: greenish grey flaggy silt-
stone with sandstone bands, thin
tuffs near top 500-800m.

SYNALDS GROUP: purple silty shales with sand-
stone bands, tuff bands 500-800m.

BURWAY GROUP: greenish grey sandstones and
siltstones with a grit at the
top and a silicified tuff at
the base 600m.

STRETTON SHALE GROUP: greenish grey shales with
a grit at the base ?1000m.

Table 5.1. Lithologic Succession of the Longmyndian.

(after Greig et al., 1968)

in an inlier, which is inferred to be Longmyndian, near Old Radnor gave a K-Ar age of ca. 570 m.y. The possibly detrital origin of these coarse-grained muscovites, combined with the uncertainty concerning the behaviour of the Ar daughter product during metamorphic events, makes an interpretation of these dates difficult.

K-Ar ages of 677 ± 72 to 632 ± 32 m.y. have been obtained on three samples of Uriconian volcanics, but have been interpreted as minimum ages only for these severely altered rocks (Fitch et al. 1969).

The correlation of the uppermost series in the Longmyndian succession, the Wentnor Series (Table 5.1), with the Torridonian in Scotland has been suggested on lithological and sedimentological grounds (Lapworth & Watts 1910). This has received support from palaeomagnetic work, which shows similarity between remanent magnetization axes of Wentnor and Upper Torridonian rocks (Creer 1957). An Rb-Sr isochron age of 805 ± 17 m.y. (recalculated to $\lambda = 1.39 \times 10^{-11} \text{ yr}^{-1}$) for red shales from the Upper Torridonian (Moorbath 1969) was interpreted by the author as that of diagenesis closely following deposition and compaction. Accepting this age to be at least a minimum age for Upper Torridonian deposition, the tentative correlation between this succession and the Wentnor Series had led to an assumed age for the Longmyndian in excess of 600 m.y. (Greig et al. 1968).

A possible correlation of the Mona metamorphic rocks of Anglesey with the Longmyndian has been suggested by Dewey (1969). He has interpreted the two successions as offshore and nearshore facies respectively and considers them to have been formed on the eastern boundary of a Precambrian Proto-Atlantic Ocean. K-Ar dates of 580-600 m.y. on muscovites, and Rb-Sr ages of 609 ± 13 , 613 ± 18 , and 614 ± 14 m.y. (recalculated to $\lambda = 1.39 \times 10^{-11} \text{ yr}^{-1}$) on whole rock-muscovite pairs were obtained from the Coedana granite and its hornfels in the Mona complex (Moorbath & Shackleton 1966). These ages were interpreted by the authors as representative of some late

event in the metamorphic history of the complex, an opinion with which Fitch et al. (1969) are in general agreement. However these data give no direct information concerning the primary age of the complex, except in placing a lower limit on this age. Therefore, on the basis of Dewey's (1969) hypothesis, the Longmyndian should have an age exceeding 600 m.y.. Dewey's correlation between Longmyndian and Monian has been revised recently by Baker (1973), who has reinterpreted the two successions as eastern and western borders respectively of a marginal Late Proterozoic ocean basin. However, evidence has also been presented against any chronological equivalence of these two successions. A detailed petrographic study of lithic fragments in the Longmyndian (Greig et al. 1968) has suggested that they are derived in part from Mona-type schists, supporting the contention that the Monian predates the Longmyndian.

The present study has been undertaken in an attempt to resolve some of these problems of correlation.

5.3. Sample Description

Fine-grained rock samples were collected from single sections (maximum 100m stratigraphical height) of each of the Burway, Synalds and Lightspout Groups (these divisions being based on lithological characteristics), which lie within the older part of the Longmyndian succession (Table 5.1). The locations of these three sampling sites are shown on a geological sketch-map of part of the Longmyndian outcrop west of the Church Stretton fault in Fig. 5-1.

Samples were cleaned of weathered portions, crushed, and portions fractionated to obtain the clay (<2 μ m) fractions, according to the techniques described in Appendix A. Mineralogies of total rock samples were investigated by XRD studies on cavity-mounted powders, and those of clay-fractions by XRD studies of oriented specimen mounts (See Appendix B). Illite crystallinity indices were also determined for standardised con-

ditions as described in Appendix C.

Fifteen samples were collected from the stratigraphically lowest group sampled, the Burway Group (sample numbers prefixed by B), at a small quarry section in the Batch Valley (Grid ref. S0 459956) north of Church Stretton (Fig. 5-1). Lithologically, these samples comprise greenish shales; the coarse-grained mineralogy is estimated at 65-75% quartz and 35-25% plagioclase. The clay fraction is 60-70% illite and 40-30% chlorite, with the illite crystallinity index in the range 6-7.5 (i.e. the anchizone, cf. Fig. 2-9). One sample (B7), however, was collected from a cherty horizon (the so-called 'Buxton rock'), and this was found to have a markedly higher proportion of plagioclase (50%), whilst the clay-fraction displays a higher percentage (60%) of chlorite.

Eleven samples were collected from the Synalds Group at an exposure in Ashes Hollow (S0 430934). They comprise greyish-green or purple (S2/3/5/6/7/10/11) shales and siltstones. Two of the siltstones, S4 and S8, have distinct mica flakes visible in hand-specimen. The coarse-grained mineralogy is monotonously 80-85% quartz and 20-15% plagioclase, whilst the clays are 60-75% illite (CI range 7.5-8.5, i.e. anchizone) and 40-25% chlorite.

Twelve samples of the Lightspout Group were collected in the Cardingmill Valley (S0 436952), 2 km west of Church Stretton. These purple shales were found to comprise 75-85% quartz and 25-15% plagioclase in the coarse-grained fraction, whilst the clays are 70-80% illite (CI range 9-11, i.e. non-metamorphic zone) and 30-20% chlorite.

It may be noted that none of the samples collected contained any detectable traces of K-feldspar or of calcite. A summary of these semi-quantitative mineralogical analyses is presented in Table 5.2.

Sample Nos.	Coarse-grained fraction		Fine-grained fraction		Illite CI
	Quartz %	Plagioclase %	Illite %	Chlorite %	
Lightspout Group					
LM/73/L1-12	75-85	25-15	70-80	30-20	9-11
Synalds Group					
LM/73/S1-11	80-85	20-15	60-75	40-25	7.5-8.5
Burway Group					
LM/73/B1-6,8-15	65-75	35-25	60-70	40-30	6-7.5
LM/73/B7	50	50	40	60	6

Table 5.2. Summary of relative proportions of coarse-grained minerals and of clay minerals in samples collected from the Longmyndian

5.4. Whole-rock Rb-Sr isotope data

Rb/Sr ratios were determined in duplicate on pressed pellets of rock powders by X-ray fluorescence techniques, employing a single standard (Pankhurst & O'Nions 1973). The method has been described in detail in Section 2.4, though in this instance the PW 1410 spectrometer in Oxford was used; an outline of the correction and computation program is given in Appendix E.1. Estimates of Rb and Sr concentrations ($\pm 5\%$) appear in Table 5.3, as well as the direct determinations of Rb/Sr ratios.

Strontium was extracted from aliquots of whole-rock powders by conventional dissolution and ion-exchange techniques (Appendix D). The isotopic composition of the strontium was determined on the 30m radius mass-spectrometer in the Oxford laboratory, as previously described in Section 2.4 (correction and normalization program in Appendix E.2). The Eimer and Amend SrCO_3 standard was measured twice during the course of this study, and gave a mean value for $^{87}\text{Sr}/^{86}\text{Sr}$ of 0.70830 ± 4 . $^{87}\text{Sr}/^{86}\text{Sr}$ values (normalized to $^{86}\text{Sr}/^{88}\text{Sr} = 0.1194$) for the Longmyndian samples are listed in Table 5.3.

Using a ^{87}Rb decay constant of $\lambda = 1.39 \times 10^{-11} \text{ yr}^{-1}$, the data from the Burway Group define an isochron (MSWD = 1.2) corresponding to an age of 529 ± 6 m.y. (2σ), with an initial $^{87}\text{Sr}/^{86}\text{Sr}$ ratio of $0.7061 \pm .0001$ (Fig. 5-2). Those from the Synalds Group define an isochron corresponding to an age of 452 ± 31 m.y. (MSWD = 0.9), with $(^{87}\text{Sr}/^{86}\text{Sr})_0$ of $0.7100 \pm .0012$ (Fig. 5-3). The large error in this case is due to the poor spread in Rb/Sr ratios. However, the age given does appear to be significantly younger than that from the Burway Group. The stratigraphically highest group sampled, the Lightspout Group, yielded data giving an age of 529 ± 23 m.y. (MSWD = 4.4), with an $(^{87}\text{Sr}/^{86}\text{Sr})_0$ of $0.7075 \pm .0005$ (Fig. 5-4). The latter age is statistically indistinguishable from that from the Burway Group.

Sample Nos.	Rb ⁽¹⁾	Sr ⁽¹⁾	Rb/Sr ⁽²⁾	⁸⁷ Sr/ ⁸⁶ Sr ⁽²⁾
Lightspout Group				
LM/73/L1	105	147	0.712±.020	0.72314±6
L2	111	128	0.868±.024	0.72633±7
L3	92	282	0.326±.010	0.71478±3
L4	113	113	1.005±.028	0.72866±16
L5	101	210	0.483±.014	0.71767±4
L6	101	240	0.422±.012	0.71597±4
L7	115	71	1.622±.048	0.74130±4
L8	115	162	0.711±.020	0.72266±5
L9	129	217	0.593±.016	0.72059±7
L10	115	126	0.918±.026	0.72723±6
L11	103	107	0.961±.028	0.72776±4
L12	94	273	0.346±.010	0.71480±10
Synalds Group				
LM/73/S1	105	123	0.856±.022	0.72576±9
S2	116	132	0.877±.022	0.72584±5
S3	110	121	0.913±.024	0.72669±10
S4	113	126	0.896±.024	0.72639±18
S5	124	162	0.765±.020	0.72391±5
S6	109	103	1.069±.028	0.72999±6
S7	98	88	1.106±.030	0.73000±10
S8	85	90	0.940±.026	0.72712±9
S10	111	100	1.111±.030	0.72993±6
S11	112	102	1.097±.030	0.72984±12
Burway Group				
LM/73/B1	114	114	0.997±.028	0.72733±4
B2	109	105	1.033±.028	0.72793±6
B3	93	105	0.901±.026	0.72516±10
B4	112	120	0.941±.026	0.72634±18
B5	102	104	0.975±.028	0.72648±14
B6	105	110	0.954±.026	0.72620±12
B7	21	177	0.119±.004	0.70857±4
B9	84	103	0.814±.024	0.72349±6
B10	122	93	1.311±.036	0.73353±8
B12	136	94	1.461±.040	0.73708±6
B13	125	108	1.162±.032	0.73083±4
B15	105	117	0.898±.026	0.72598±6

(1) Estimates only, errors ± 5%;

(2) Errors quoted are 2σ.

Table 5.3. Analytical data for Longmyndian samples

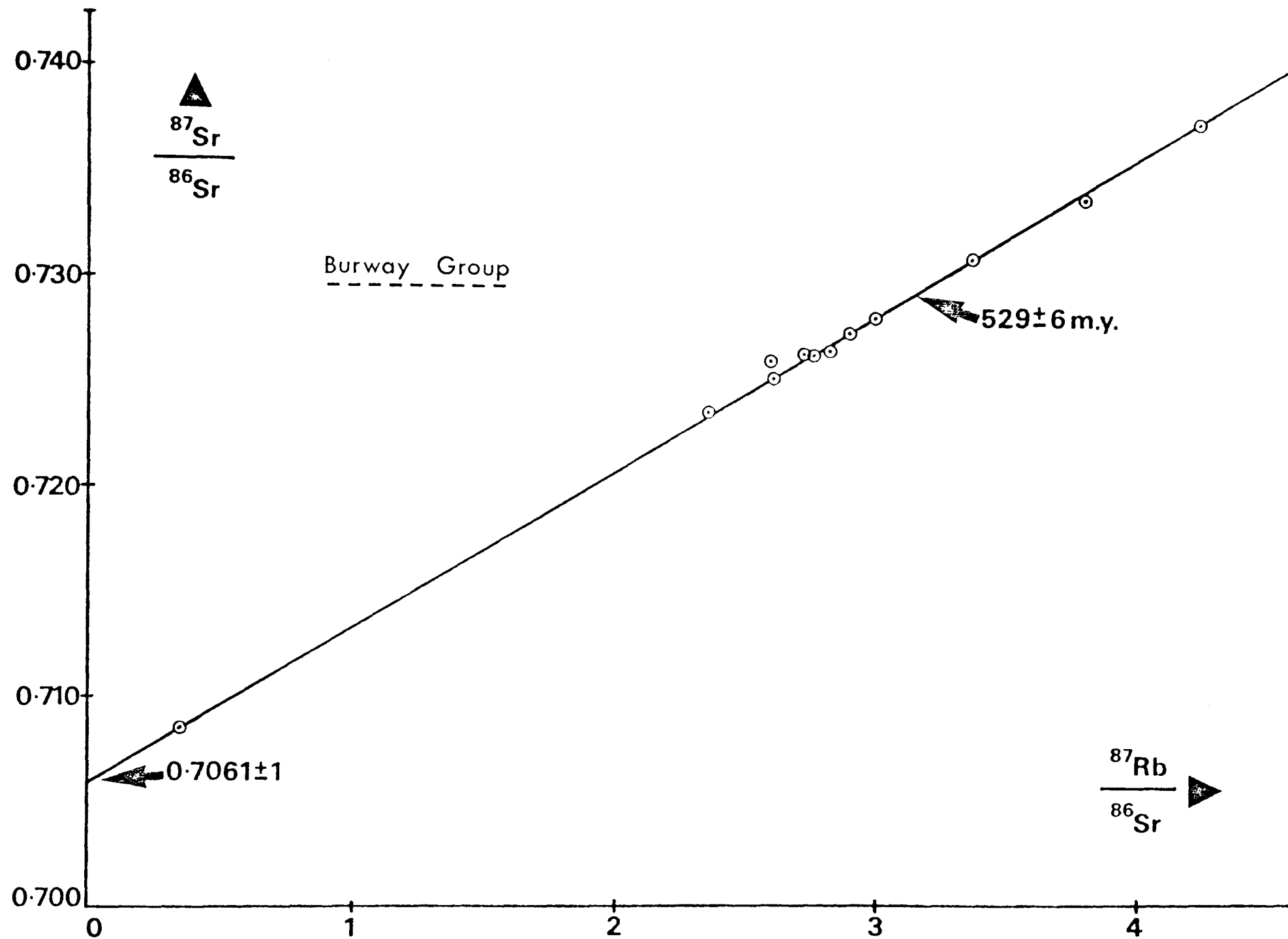


Fig.5-2. Whole-rock Rb-Sr isochron diagram of data from Burway Group, Longmyndian.

MSWD = 1.2; $\lambda = 1.39 \times 10^{-11} \text{ yr}^{-1}$.

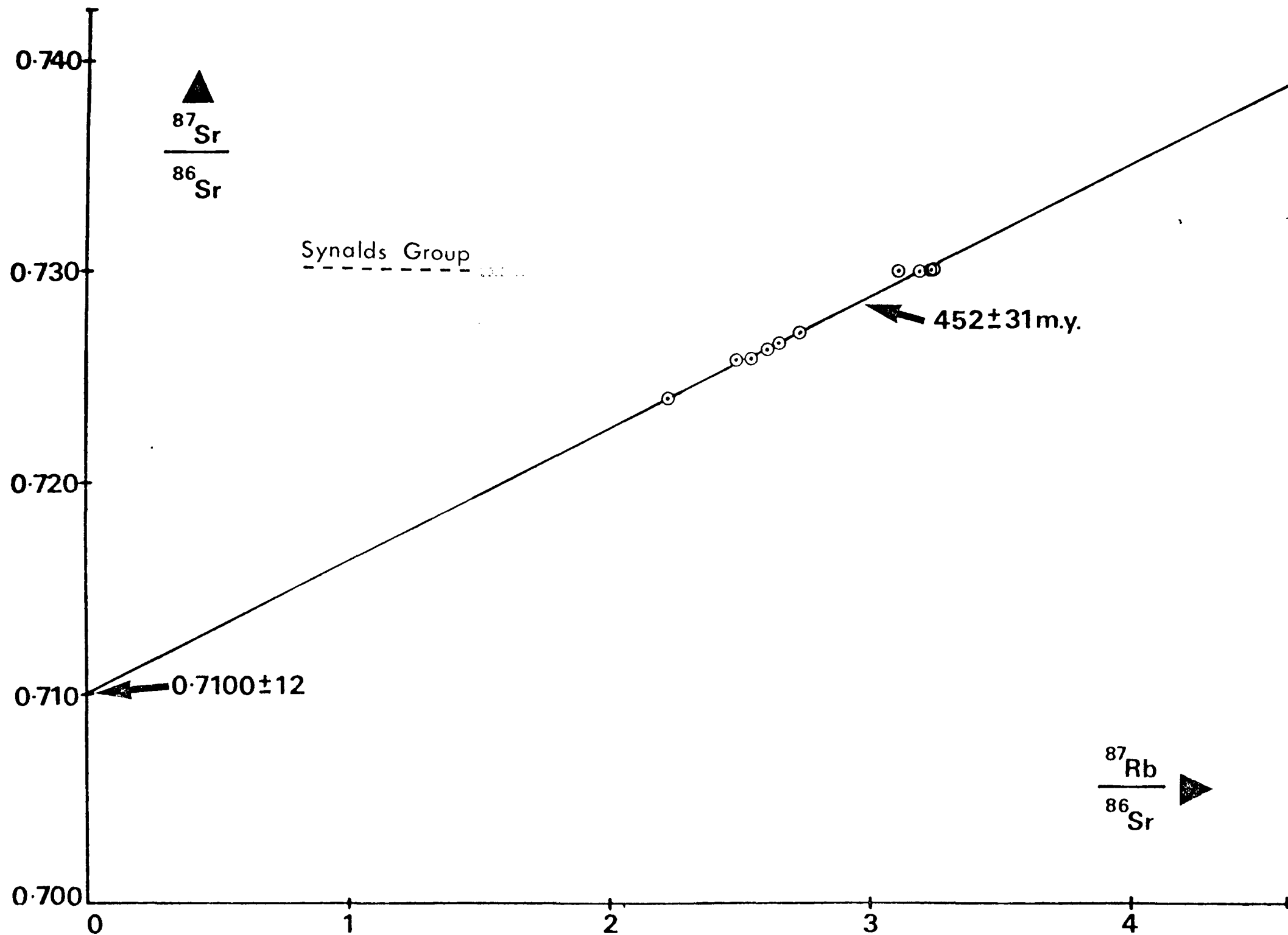


Fig. 5-3. Whole-rock Rb-Sr isochron diagram of data from Synalds Group, Longmyndian.
 MSWD = 0.9; $\lambda = 1.39 \times 10^{-11} \text{ yr}^{-1}$.

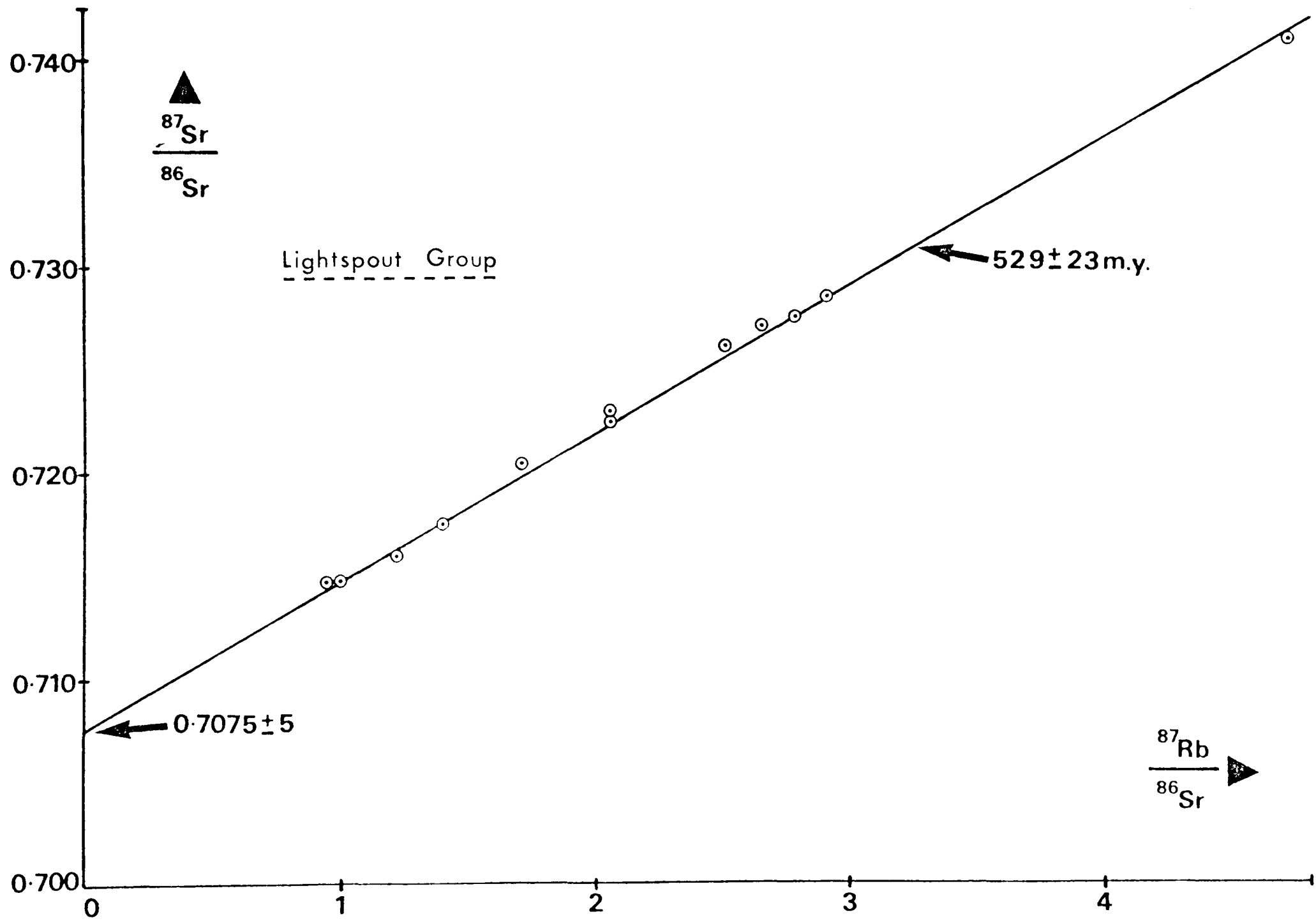


Fig.5-4. Whole-rock Rb-Sr isochron diagram of data from Lightspout Group, Longmyndian.
 MSWD = 4.4; $\lambda = 1.39 \times 10^{-11} \text{ yr}^{-1}$.

5.5. Interpretation

5.5.1. Isochron ages

It is clear from the proximity to linearity (represented by the MSWD values) of the above three sets of Rb-Sr data, that the three systems have fulfilled the conditions for isochrons. This implies that at the dates given by the respective isochrons, the Sr-isotope composition was homogeneous within each group, and that subsequent to this date the individual samples behaved as closed systems with respect to Rb and Sr.

In the discussion of the Rb-Sr data from Upper Llandovery shales from Pembrokeshire (Section 3.4), it was concluded that the isochron ages given by such shales represent the transformation of degraded clays to a stable assemblage (illite + chlorite). Homogenization of Sr-isotopes was a result of the transformation, whilst closed system behaviour was induced by the stability of the final assemblage. In the previous study (Chapter 3) it was possible to attribute the dates of these transformations to distinct metamorphic episodes. However, the possibility must also be admitted that such transformations might also result from progressive diagenetic phenomena, as has been demonstrated by Perry & Turekian (1974) in a succession which has undergone rapid burial.

Evidence for the involvement of a distinct metamorphic episode is provided by the concordance of ages from two of the groups, the Burway and the Lightspout Groups which give 529 ± 6 and 529 ± 23 m.y. respectively. That these two groups give independent isochrons is proven by the distinct difference between initial $^{87}\text{Sr}/^{86}\text{Sr}$ ratio values (0.7061 ± 7 and 0.7075 ± 5 respectively), and also by the intervention between the two of the Synalds Group which gives a considerably younger age (452 ± 31 m.y.). On the other hand, the illite crystallinity indices shown in Table 5.2 support the contention that no metamorphism has affected the Longmyndian to any marked extent. These indices were found to be remarkably high (in the range 6 to 10 on the Kubler, 1968, scale shown in Fig. 2-9), i.e.

representative of very low grade illite. Furthermore, the illite crystallinity index increases with stratigraphical height (Table 5.2), suggesting that the illite crystallinity is a remnant of burial diagenesis, and has not been subsequently recrystallized under metamorphic conditions.

The significance of the younger age from the Synalds Group is somewhat obscured by the large error incorporated in the age. It is tempting to suggest that the apparent preservation of open system behaviour in this group beyond ca. 529 m.y. might be accounted for by considerations such as those suggested for the meta-bentonites at Marloes (Section 3.3.4). Indeed, the generally siltier lithology of Synalds Group samples, and the appearance of distinct mica flakes in at least two samples (Section 5.3), may be indicative of a depositional assemblage which differed from those of the other two groups, at least with respect to the major Rb- and Sr-bearing phases. The speculative nature of any such interpretation must be stressed; at present there is no unique explanation for this observation, and further, more detailed investigation is required. However, the general observation that the lithological divisions of the Longmyndian (i.e. the groups in Table 5.1) accord with the grouping of Rb-Sr data into sets yielding distinct isochrons, at least on the limited evidence presented here, is of interest. This observation further supports the

suggestion made previously (Section 3.4.3) that the initial assemblage at deposition may be of great importance in determining the response of the sedimentary Rb-Sr system to metamorphic (or diagenetic) conditions. A similar argument has been put forward by Clauer (1973), when he stated that, for Sr-isotope homogenization to occur, "it is necessary that the clay material is susceptible to diagenetic transformation."

An alternative hypothesis to explain at least the youngest Rb-Sr isochron age (i.e. the most recent closure of a whole-rock Rb-Sr system, at ca. 452 m.y.) is that of a dewatering phenomenon. It could be proposed that such an age represents the advancement of dewatering such that

ionic transport in solution (the process by which large-scale isotopic homogenization takes place) ceases to operate over the required scale. Possible causes of dewatering include both compaction associated purely with burial, or folding and uplift. However, this provides a model only for closure of the Rb-Sr system, and implicitly assumes that the conditions necessary for Sr-isotope homogenization have already obtained. In this respect, the recrystallization model which may explain both Sr-homogenization and system closure phenomena, is favoured.

5.5.2. Maximum depositional age - discussion

It has been established, therefore, that the isochron ages from shales represent phenomena occurring in the sediments subsequent to deposition (Section 3.3.1). Although these ages are only minima for the age of deposition, it is possible to define within reasonable certainty a maximum age of deposition, by consideration of the initial $^{87}\text{Sr}/^{86}\text{Sr}$ ratios for each isochron - a method which has been used elsewhere (O'Nions et al., 1973). The Rb-Sr data from the oldest group sampled, the Burway Group, has been shown to define an isochron corresponding to 529 ± 6 m.y. with $(^{87}\text{Sr}/^{86}\text{Sr})_0$ of 0.7061 ± 1 (Fig. 5-2). If this $(^{87}\text{Sr}/^{86}\text{Sr})_0$ ratio is projected backwards in time, assuming an average Rb/Sr of unity (cf. Table 5.3), it is found that at ca. 600 m.y., the average $^{87}\text{Sr}/^{86}\text{Sr}$ would have been ca. 0.704. Similar considerations applied to the Synalds and Lightspout Groups' data also yield maximum ages close to 600 m.y. at which the mean $^{87}\text{Sr}/^{86}\text{Sr}$ values could have been as low as 0.704. This value of 0.704 for $^{87}\text{Sr}/^{86}\text{Sr}$ is a reasonable minimum value for the source materials of the Longmyndian sediments, particularly in view of the evidence for these sources being the Uriconian calc-alkaline suite and, perhaps, Mona-type metamorphics (Greig et al., 1968). An age greater than ca. 600 m.y. can be derived only by Rb-metasomatism subsequent to deposition, or by reaction with a fluid with

an $^{87}\text{Sr}/^{86}\text{Sr}$ ratio less than the initial ratios on the isochrons, i.e. less than ca. 0.706. The former possibility is not suggested by the Rb contents of the shales, which are compatible with values from unaltered shales, and furthermore it is unlikely that shales could yield an isochron after such a process. The latter possibility is ruled out because, although connate fluids clearly contribute some Sr during equilibration, present knowledge of early marine Sr isotopic composition for which the earliest figure is 0.7078 for Palaeozoic seawater (Peterman et al. 1970) indicates that such fluids would not have a ratio falling below 0.706. No evidence, therefore, suggests any model for the systematics other than the simple closed system model proposed above.

Further evidence for deposition of the Longmyndian subsequent to 600 m.y. is provided by a series of K-Ar ages for various minerals from metamorphic rocks in the Malverns and also in Anglesey. Fitch et al. (1969) collate eleven such K-Ar ages in the range 590-615 m.y., and attribute them to a period of widespread metamorphism and subsequent uplift in this region. If indeed the Longmyndian deposition predated this metamorphic episode, one would predict that this metamorphism might have induced the recrystallization of clay minerals (which has been suggested as the mechanism for Sr-homogenization and subsequent closure of the Rb-Sr system). It is clear that the Longmyndian Rb-Sr isochron ages do not relate to this 590-615 m.y. metamorphism, and this strongly implies deposition subsequently.

5.6. Stratigraphical Implications

Therefore it is proposed that the Longmyndian sediments were deposited no earlier than ca. 600 m.y., i.e. in the Cambrian or the very late Precambrian. Lambert (1971) recommended an age of ~ 610 m.y. ($\lambda = 1.39 \times 10^{-11} \text{ yr}^{-1}$) for the Cambrian-Precambrian boundary, whilst Armstrong & McDowell (1974)

has suggested that this be revised to ~585 m.y.

Correlation of the Longmyndian with the Upper Torridonian (Lapworth & Watts 1910) is thus ruled out completely, as is correlation with the Mona complex, both these latter successions having been shown by radiometric ages to be >600 m.y. old. It is of interest to note that the Ingletonian succession of Northern England, previously attributed to the Precambrian, has been shown (by Rb-Sr methods) to have an early Palaeozoic time of deposition, between 505-555 m.y., i.e. Cambrian or very early Ordovician (O'Nions et al. 1973).

In terms of local stratigraphy (i.e. in the proximity of the Long Mynd), the significance of this age constraint may be interpreted in two ways:

- (a) The outcrop east of the Church Stretton Fault (cf. Fig. 5-1) has been incorrectly correlated with the basal Longmyndian (i.e. west of CSF). Therefore stratigraphical inferences, drawn from the occurrence of Lower Cambrian sandstones east of CSF (Section 5.2.1) may not be extended to the stratigraphy west of CSF.
- or (b) The Longmyndian succession represents a previously unrecognised period of very rapid sedimentation, occurring close to the Cambrian-Precambrian boundary and prior to deposition of the recognised, fossiliferous Cambrian strata of the Welsh Borderland. Such sedimentation might possibly have followed upon the already mentioned period of metamorphism and uplift inferred to have taken place in Anglesey and elsewhere between 615-590 m.y. This would accord with the observation of Mona-type metamorphic fragments in the Longmyndian sediments (Greig et al. 1968).

It would be speculative at present to favour one alternative over the other, though it may be pointed out that in the first case, (a), the out-

crop (previously inferred to be Longmyndian) east of CSF would still remain as an unsolved stratigraphical problem.

CHAPTER 6

Rb-Sr STUDIES ON CAMBRIAN SLATES FROM NORTH WALES

6.1 Introduction

The two major occurrences of Cambrian strata in North Wales are the anticlinal Harlech Dome and, to the north, the Caernarvonshire Slate Belt; these are separated by the Ordovician igneous and sedimentary synclinal complex of Snowdon (Fig. 6-1). Both occurrences comprise sequences of alternating coarse- and finer-grained beds, enabling stratigraphical divisions to be established on a lithological basis.

The greater parts of both successions are unfossiliferous, and it is only in the uppermost beds that fossil occurrences - predominantly of a trilobite fauna - enable tentative stratigraphic identifications to be made. Below these fossiliferous beds are in excess of 2000m of sediments in the Harlech Dome succession, and some 1700m of sediments at Nantlle (Caernarvonshire Slate Belt), which are inferred to be Cambrian on the evidence from the overlying strata. The base of this succession is not seen in the Harlech Dome (except in a recent bore-hole, see Section 6.2.1), and only in the Nantlle-Llanberis outcrop are these sediments observed in contact with the rhyolitic lavas of the ? Late Precambrian Clogwyn Volcanic Group which forms the Padarn Ridge.

Therefore two stratigraphic problems present themselves. Firstly, the question of the ages of the lower parts of both of these very considerable thicknesses of sediments, i.e. whether the inference of rapid sedimentation and Cambrian ages for the entire successions is justified. Secondly, and very much related to the first, is the problem of correlation between the two successions. Despite the well-established lithological divisions within each succession, it has not been possible to deduce an unambiguous correlation between the lower parts of the two groups on this basis, if indeed any such correlation is justified. The present study has been under-

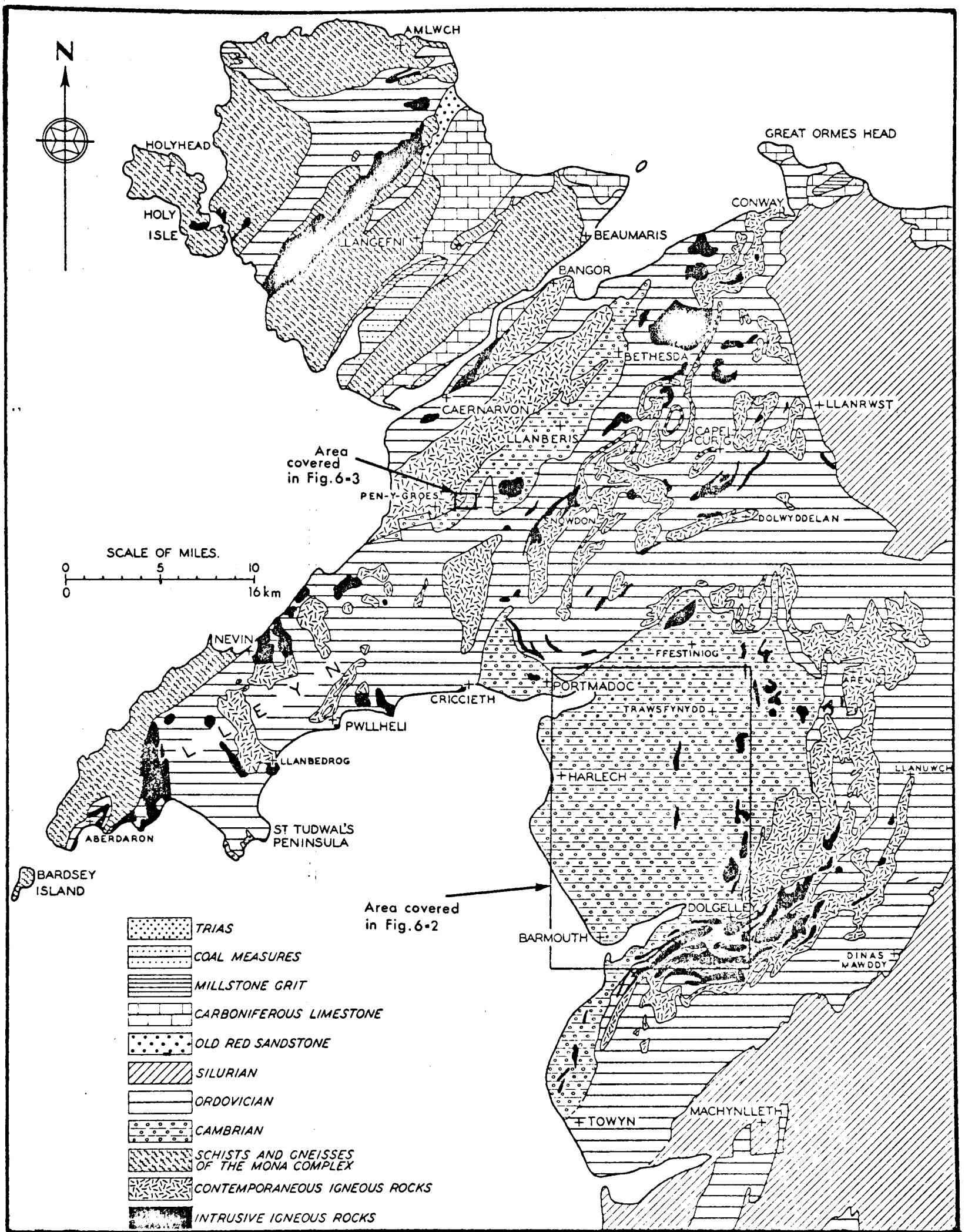


Fig. 6-1. Geological sketch-map of North Wales, showing Cambrian outcrops of the Harlech Dome and the Caernavonshire Slate Belt. Areas enclosed by rectangles are shown in more detail in Figs. 6-2 & 6-3. After Smith & George (1961).

taken in an attempt to provide further independent evidence towards the solution of these problems.

The well-developed slaty cleavage exhibited in the finer-grained beds of both outcrops, but particularly in the Caernarvonshire Slate Belt where the uniformity of lithology and the severe compression has produced slates of excellent commercial quality, is indicative of the severity with which Caledonian folding has affected this region. This study has therefore served the additional purpose of investigating further the perturbation, if any, of the whole-rock Rb-Sr system caused by folding and metamorphism of this nature.

6.2. Geological Setting

6.2.1. Harlech Dome

The Harlech Dome comprises a thick succession, in excess of 2000m, of sediments which has undergone complex compression leading to a broadly anticlinal domed structure. The predominant structural trend is roughly north-south, leading to an elongation of the core of the dome (Fig. 6-2). It has been generally accepted (Smith & George 1961; Rushton 1974) that an unconformity separates the Cambrian strata of the Dome from the surrounding Ordovician beds, though this is not exhibited as an angular discordance, and in several localities the complete transitional sequence through Tremadoc beds is observed (e.g. south of the Harlech Dome and Mawddach Estuary, cf. Fig. 6-2). The rim of the Harlech Dome is extensively faulted, many of the faults trending approximately north-south, and these are considered to have originated at a late stage in the development of the anticlinal structure (Matley & Wilson 1946). In many places, particularly to the south and east of the Dome, these result in faulted contacts between beds in the upper part of the Harlech Dome succession and the Ordovician volcanics (and some intrusives) of the Cader Idris - Arenig centres.

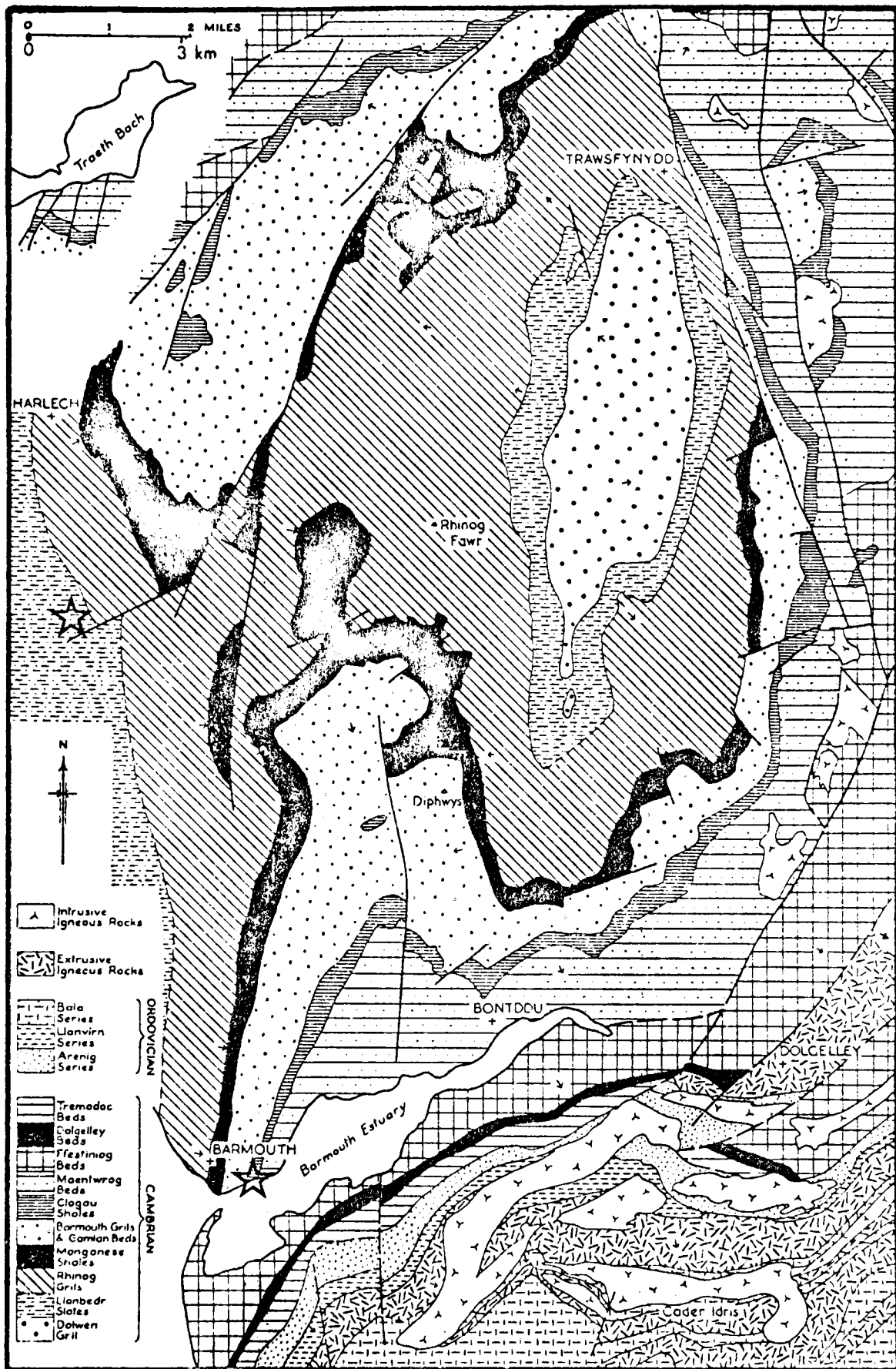


Fig. 6-2. Geological sketch map of Harlech Dome area. Sampling localities in Clogau Shale and Llanbedr Slate are depicted by ☆.

After Matley & Wilson (1946) and Smith & George (1961).

The lithological divisions and the structure of the Harlech Dome sequence have been well-documented by Matley and Wilson (1946) and Rushton (1974); the lithological sequence and the stratigraphical interpretation of the former authors is reproduced in Table 6.1. It may be noted that the lowest indisputable faunal evidence in the succession occurs in the Clogau Shales, where the diagnostic trilobite fauna includes Paradoxides. The overlying beds, the Maentwrog Flags and upwards, have sporadic occurrences of a trilobite fauna including Olenus, as well as the brachiopod Lingulella davisii which has prompted the alternative name for this group of 'Lingula Flags'. Since the ~2000m. of strata underlying the Clogau shales are unfossiliferous, the position of the Middle-Lower Cambrian boundary is questionable, being based on somewhat dubious lithological correlations. The position of this boundary shown in Table 6.1 was suggested by Matley & Wilson (1946) on the basis of previous correlations with manganese-bearing horizons in other Cambrian sequences, notably with that in Warwickshire where the ore-beds are closely associated with the Hartshill Quartzite, above which the Lower Cambrian Olenellid fauna is found. Rushton (1974) has, however, rejected any such correlation.

A recent bore-hole put down in the core of the Dome passed through 283m of Dolwen Grits before intersecting volcanic rocks which have been tentatively correlated with the Clogwyn Volcanic Group which forms the Padarn Ridge and underlies the Cambrian of the Caernarvonshire Slate Belt (Ann. Rep. Inst. Geol. Sci., 1972, p.33).

As mentioned previously, the domed structure is dominated by folding along roughly north-south axes. This folding is, however, less severe than that observed further north in the Caernarvonshire Slate Belt (Section 6.2.2), and Matley and Wilson (op. cit.) have observed the dip to be generally in the range of 30-40°. The same authors consider the cleavage, well-developed with a northerly strike in the argillaceous beds, to represent a late phase in the structural development of the Dome. Indeed,

	(Tremadoc Beds)	
UPPER CAMBRIAN		
(<u>Olenus</u> Series)	Dolgellau Shales	60-180m
	Ffestiniog Flags	520-800m
	Maentwrog Beds	Penrhos Shales 340m
		Vigra Flags 310m
MIDDLE CAMBRIAN		
(<u>Paradoxides</u> Series)	Clogau Shales	75-100m
	Cefn Coch Grit	2-15m
	Gamlan Flags & Grits	220-300m
	Barmouth Grits	100-200m
? LOWER CAMBRIAN		
	Upper Manganese Shales	90-180m
	Manganese Group Manganese Grit	2-60m
	Ore-bed Shales	15-18m
	Rhinog Grits	400-800m
	Llanbedr Slates	90-200m
	Dolwen Grits	>150m

(Base not exposed, but a bore-hole has intercepted
? Arvonian volcanics at 283m)

Table 6.1. Stratigraphic Sequence of the Harlech Dome.

(After Matley & Wilson 1946; Smith & George 1961
and Rushton 1974)

Matley & Wilson (op. cit.) attribute both this cleavage development and the major phase of faulting (north-south trend) to the Caledonian orogeny.

In the argillaceous beds, no metamorphic assemblage of higher grade than muscovite-chlorite has been observed, although in the manganese-rich horizons, spessartite-garnet commonly occurs as a metamorphic mineral. A petrological study of detrital grains from the coarse-grained beds has led to the suggestion that they may, at least in part, be derived from the Mona complex in Anglesey (Appendix by A.W. Woodland in Matley & Wilson 1946).

6.2.2. Caernarvonshire Slate Belt

The Cambrian outcrop north of Snowdon comprises a belt of steeply dipping strata, striking roughly NE-SW. The outcrop has been considered by some to be bounded on both the NW and SE extremities by strike-faults (Morris & Fearnside 1926; Smith & George 1961), though the former contact - that with the Clogwyn Volcanic Group - is considered by Wood (1969) to be conformable. In addition to strike faulting, normal faulting is a dominant feature of the outcrop (Fig. 6-3). Due to the intense folding, faulting and compression to which these strata have been subjected during the Caledonian orogeny (and probably also earlier to some extent), the thicknesses are somewhat uncertain. However, the most detailed study of the succession has been that of Morris and Fearnside (op. cit.), and their lithological divisions and estimated thicknesses are presented in Table 6.2.

The earliest faunal occurrence in this succession is in the Green Slates, in which Pseudatops viola and other trilobites have been reported (Howell & Stubblefield 1950), on which evidence a Lower Cambrian age is suggested. No further biostratigraphic evidence is available to correlate strata between this succession and that of the Harlech Dome, and

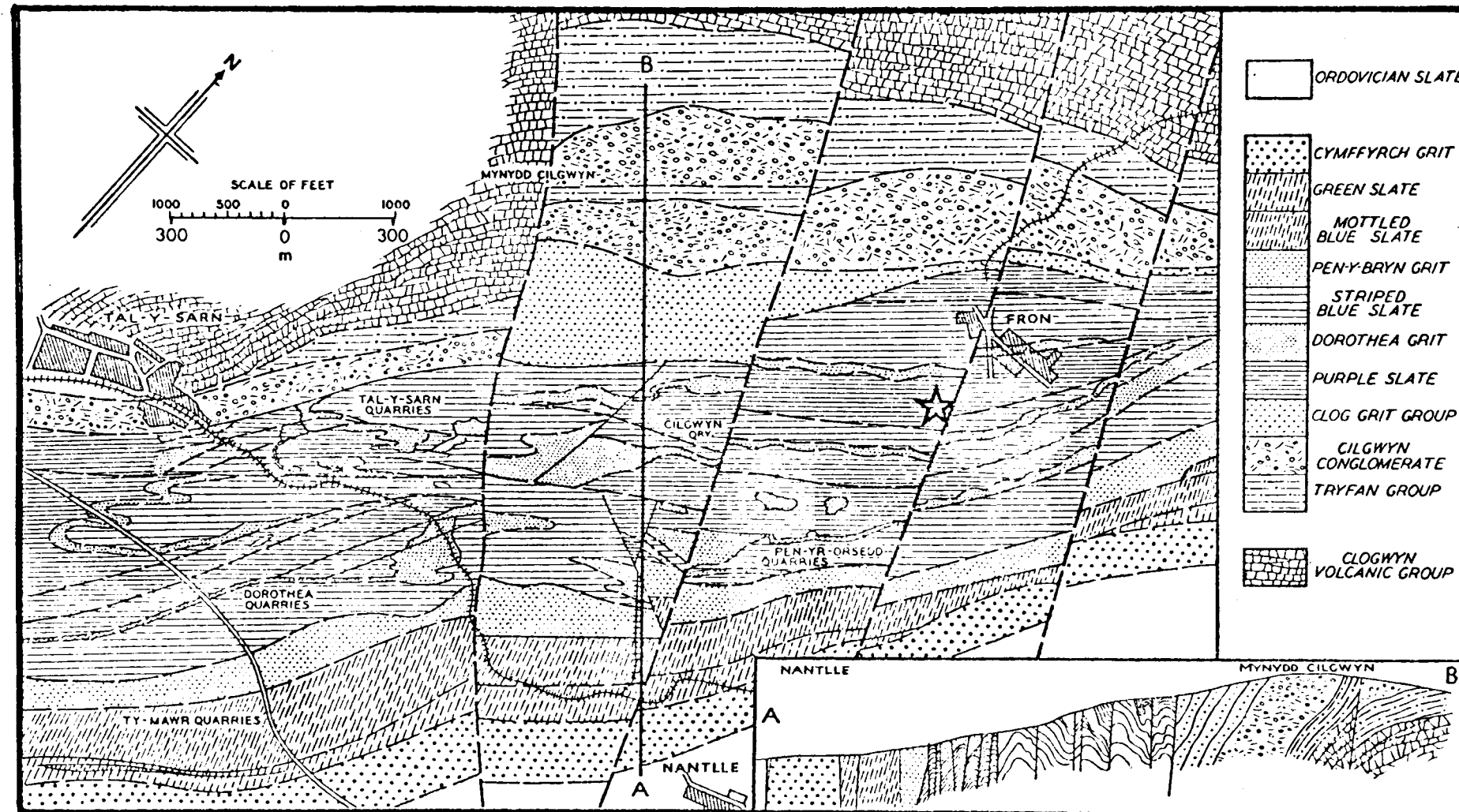


Fig. 6-3. Simplified geological map and section of Slate Belt outcrop near Nantlle, Caernavonshire. See Fig. 6-1 for regional location. Sampling locality is marked thus ☆. After Morris & Fearnside (1926) and Smith & George (1961).

	Cymffyrch Grits	>180m
? LOWER CAMBRIAN		
	Green Slates	40-100m
	Mottled blue Slates	~300m
	Pen-y-bryn Grits	60-100m
	Striped blue Slates	200-400m
	Dorothea Grit	30m
	Purple Slates	~250m
	Glog Grits	>600m
	Cilgwyn Conglomerate	150m
	Tryfan Grits	300m

? Unconformity

? PRECAMBRIAN

Clogwyn Volcanic Group (Arvonian)

Table 6.2. Stratigraphic Sequence of the Caernarvonshire Slate Belt at Nantlle. (After Morris & Fearnside 1926).

therefore lithological criteria have been applied. Morris & Fearnside (1926) proposed the equivalence of the Llanbedr Slates of the Harlech Dome with the Purple Slates at Nantlle, but more recently Wood (1969) has suggested a correlation of the Llanbedr Slates with the Green and Mottled Blue Slates. On the basis of the bore-hole intersection of volcanics beneath the Dolwen Grits in the Harlech Dome (Section 6.2.1), the former correlation is the favoured alternative, if, indeed, lithological correlation is justified.

6.3 Sample Collection and Description

6.3.1. Harlech Dome

Sixteen samples of grey to dark grey shales were collected from an outcrop 1 km east of Barmouth (Grid ref. SH 623158) (Fig. 6-1). According to Matley and Wilson (1946), these shales belong to the Clogau Shales (Table 6.1) of probable Middle Cambrian age. At this locality, the beds dip relatively steeply, at 50-60° to ESE, and exhibit a well-developed cleavage approaching slate quality in some samples. The samples were collected across beds over a stratigraphic height of about 30m.

A further sixteen samples were taken from an outcrop of the Llanbedr Slates in a disused quarry about 300m. east of Llanbedr (Grid ref. SH 590268) (Fig. 6-1). These slates are stratigraphically lower than the Clogau Shales, but as mentioned previously no biostratigraphic evidence is available (Table 6.1). These beds dip at 30-50° to the east, and possess a cleavage with similar strike but generally a more pronounced dip (Matley & Wilson 1946). The extent of cleavage development has led to the commercial exploitation of these slates in the past. Several dolerite dykes (presumably of Ordovician age) are present at this locality; sampling was not carried out in close proximity to these disturbances.

The mineralogy of these shales is very similar to previously studied samples, quartz, muscovite (sericite), chlorite and minor plagioclase

being the only phases detectable by X-ray diffractometry techniques (see Appendix B). A reconnaissance study of the fine-fractions using oriented specimens for XRD, showed about 70% muscovite and 30% chlorite in both the Clogau and Llanbedr samples. The values of illite crystallinity index inferred from the 10\AA diffraction peak are in the ranges 2.8-3.0 and 3.6-4.0 for the Clogau Shales and Llanbedr Slates respectively. Both these ranges fall well within the Epizone (See Fig. 2-9), and suggest a slightly more severe degree of metamorphism than in argillites studied previously in the present investigation.

6.3.2 Caernarvonshire Slate Belt

Twelve samples of purple slates and one of pale green slate (sample no. SB/N13) were collected from the Pen-yr-Orsedd slate quarries (now abandoned) at Nantlle (Grid ref. SH 507542 and Fig. 6-3). Sampling was on a small scale, being carried out over total distances of about 20m across and along the direction of maximum cleavage development. As far as can be determined from their map, the section lies in the Purple Slate Group of Morris and Fearnside (1926), which these authors tentatively correlated with the Llanbedr Slates of the Harlech Dome succession (Section 6.2.2).

Quartz, muscovite (sericite), and minor amounts of chlorite and plagioclase comprise the whole-rock mineralogy of all the Nantlle Slates except for sample SB/N13, the green slate, which was found to contain a greater proportion of chlorite. The fine-fractions of the twelve purple slates comprise 85-90% muscovite and 15-10% chlorite, the illite crystallinity index being in the range 4.8-5.0. This places these slates at the base of the Epizone on Kubler's Crystallinity Index scale (Fig. 2-9), suggesting a lower degree of metamorphism than has been suffered by the Harlech Dome shales (Section 6.3.1), despite the more severe compression and folding in the former.

6.4 Whole-Rock Rb-Sr Data

Rb/Sr ratios of all whole-rock samples were determined by X-ray fluorescence spectrometry, using the previously described method of Pankhurst & O'Nions (1973) (Section 2.4). About six samples from each suite was selected to represent the optimum spread of Rb/Sr ratios. For the five Clogau Shale samples chosen, unspiked Sr was extracted by the usual cation exchange technique for mass-spectrometric analysis (Appendix D.1). However, in the case of the seven Llanbedr Slate samples and six Nantlle Slates, quantities of ^{87}Rb - and ^{84}Sr -enriched 'spike' solutions (AB-1 and NBS-988 respectively, see Table D.1 in Appendix D) were added at the dissolution stage, prior to extraction of Rb and Sr (Appendix D.2). This enabled Rb and Sr concentrations, as well as $^{87}\text{Sr}/^{86}\text{Sr}$ ratios, to be accurately measured for these samples by isotope dilution computations (reducing the error on Rb/Sr to about half that obtained by XRF - see Pankhurst & O'Nions, op.cit.).

Sr isotope compositions, of both spiked and unspiked samples, were measured on either the 30cm radius mass spectrometer or the Vacuum Generators Micromass.30 spectrometer, both in the Oxford laboratory. Refer to Sections 2.4 and 2.6 for technical details of the measurements, and O'Nions & Pankhurst (1973) for details of the Micromass 30. In both cases, the ion currents were recorded on Keithley 640 vibrating reed amplifiers across 10^{10} ohm resistors. Eimer and Amend standard SrCO_3 was determined on both instruments during the course of the measurements, giving the values:

30 cm. mass spec.:	$0.70810 \pm 5 (2\sigma)$
Micromass 30	0.70807 ± 4

These values are indistinguishable, and no correction was applied to sample measurements made on either spectrometer.

The Rb/Sr and $^{87}\text{Sr}/^{86}\text{Sr}$ values for the selected samples are presented in Tables 6.3 and 6.4. This data is presented on isochron diagrams in

Sample No.	Rb ppm'	Sr ppm'	Rb/Sr±2σ	⁸⁷ Rb/ ⁸⁶ Sr±2σ	⁸⁷ Sr/ ⁸⁶ Sr±2σ
Clogau Shales:					
HD/C5	208	112	1.847±.036	5.365±.104	0.74804±4
C7	116	96	1.209±.024	3.508±.069	0.73736±4
C8	117	102	1.144±.022	3.319±.063	0.73659±10
C11	202	121	1.674±.034	4.861±.098	0.74540±4
C14	157	107	1.466±.030	4.256±.087	0.74158±6
Llanbedr Slates:					
HD/LL3	176	106	1.684±.034	4.892±.099	0.74842±18 ⁺
LL6	175	112	1.560±.031	4.531±.093	0.74676±6
LL7	176	143	1.233±.012 [*]	3.579±.035	0.73976±12 ⁺
LL8	176	113	1.557±.031	4.522±.093	0.74668±8
LL9	176	101	1.739±.017 [*]	5.052±.052	0.74926±8
LL14	178	138	1.291±.013 [*]	3.747±.041	0.74139±6 ⁺
LL15	178	129	1.380±.014 [*]	4.006±.041	0.74158±4 ⁺

1. Rb & Sr concs. estimated independently of Rb/Sr ratio except for *;
estimated precision ± 5%.

* Rb/Sr ratios from isotope dilution analyses for Rb & Sr; others by XRF.

+ ⁸⁷Sr/⁸⁶Sr ratios measured on Micromass 30; others on 30cm mass spec.

Table 6.3. Rb-Sr data for whole-rock samples from Harlech Dome succession.

Sample No.	Rb ppm'	Sr ppm'	Rb/Sr $\pm 2\sigma$	$^{87}\text{Rb}/^{86}\text{Sr}\pm 2\sigma$	$^{87}\text{Sr}/^{86}\text{Sr}\pm 2\sigma$
Purple Slates, Nantlle:					
SB/N1	190	194	0.979 \pm .010*	2.838 \pm .029	0.72867 \pm 10 ⁺
N3	168	216	0.781 \pm .016	2.264 \pm .046	0.72556 \pm 8 ⁺
N4	191	213	0.895 \pm .009*	2.594 \pm .026	0.72715 \pm 12 ⁺
N6	200	175	1.140 \pm .020	3.306 \pm .058	0.73121 \pm 12 ⁺
N9	168	206	0.815 \pm .008*	2.362 \pm .023	0.72588 \pm 4 ⁺
N12	102	141	0.718 \pm .007*	2.081 \pm .020	0.72456 \pm 12 ⁺

1. Rb & Sr concs. estimated independently of Rb/Sr ratio except for *;
estimated precision \pm 5%.

* Rb/Sr ratios from isotope dilution analyses for Rb & Sr; others by XRF.

+ $^{87}\text{Sr}/^{86}\text{Sr}$ ratios measured on Micromass 30.

Table 6.4. Rb-Sr data for whole-rock samples from Caernarvonshire Slate Belt

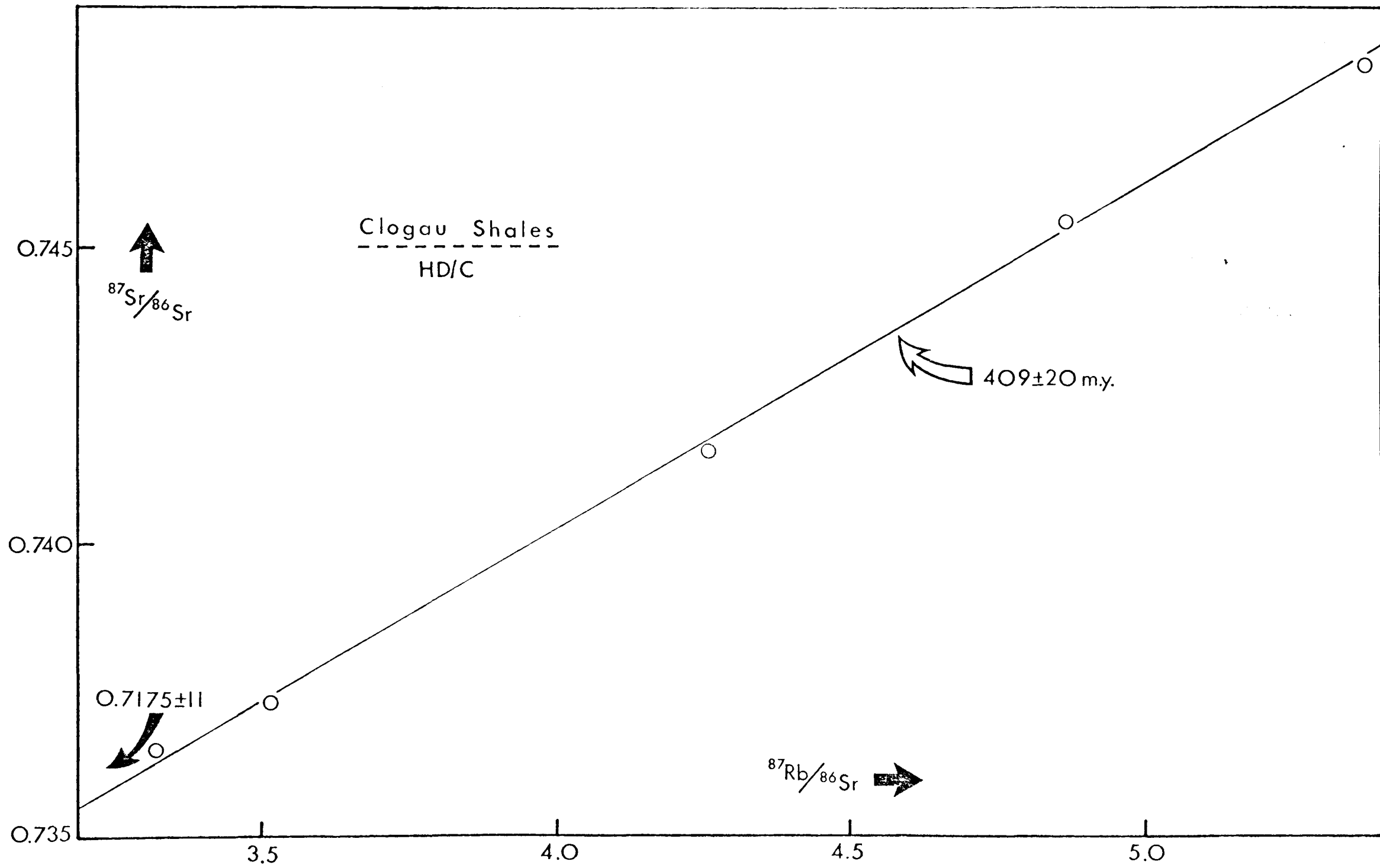


Fig.6-4. Whole-rock Rb-Sr data from Clogau Shale group in Harlech Dome succession.
 Isochron corresponds to an age of 409 ± 20 m.y. (MSWD = 4.5).

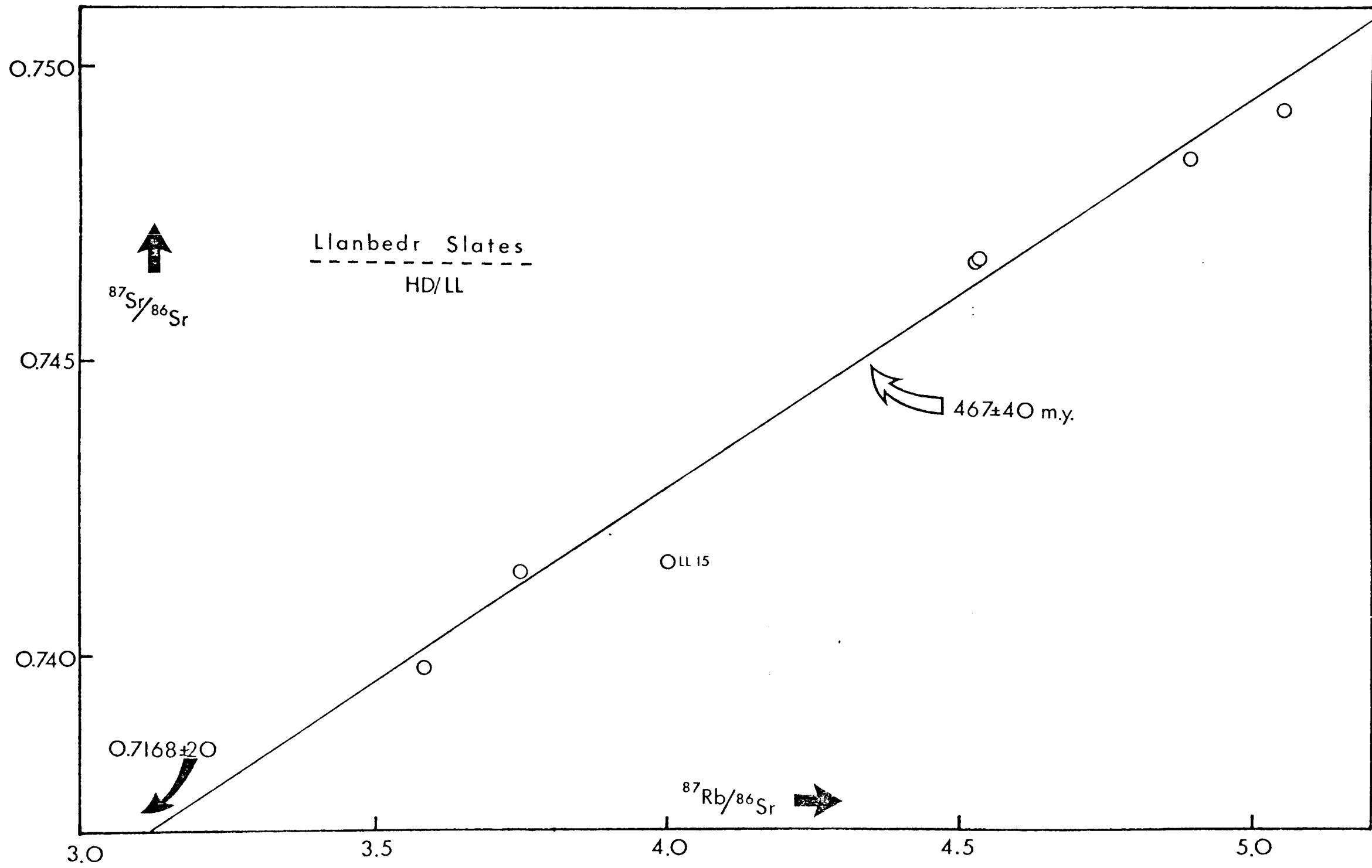


Fig.6-5. Whole-rock Rb-Sr data from Llanbedr Slate group in Harlech Dome succession. All points give best-fit age of 482 ± 75 m.y. (MSWD = 15), but omitting LL15 gives 467 ± 40 m.y. (MSWD = 4.5).

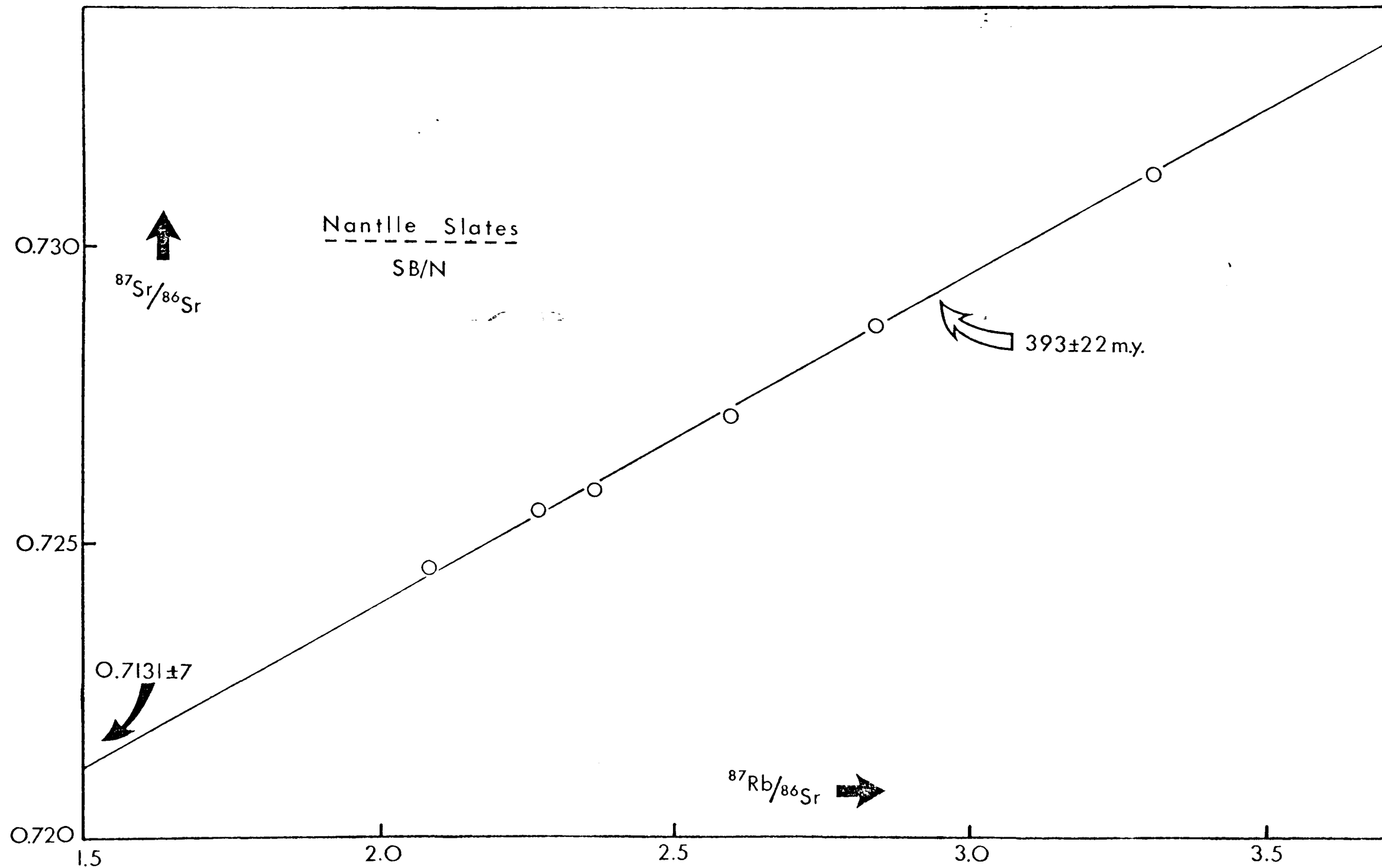


Fig.6-6. Whole-rock Rb-Sr data from Purple Slate group, Nantlle in Caernavonshire Slate Belt. Isochron corresponds to an age of $393 \pm 22 \text{ m.y.}$ (MSWD = 1.8).

Figs. 6-4 to 6-6.

The ages obtained from these isochrons (using $\lambda = 1.39 \times 10^{-11} \text{ yr}^{-1}$), and the corresponding initial $^{87}\text{Sr}/^{86}\text{Sr}$ values are listed below, with the MSWD values which indicate the colinearity of data (cf. Appendix E.5).

Clogau Shale (Fig. 6-4): $409 \pm 20 \text{ m.y. (}2\sigma\text{)}$, $0.7175 \pm .0011$, (MSWD 0.7);

Llanbedr Slates (Fig. 6-5): $482 \pm 75 \text{ m.y.}$, $0.7157 \pm .004$, (MSWD 15);

Ditto (omitting LL15): $467 \pm 40 \text{ m.y.}$, $0.7168 \pm .002$, (MSWD 4.5);

Nantlle (Purple) Slates (Fig. 6-6): $393 \pm 22 \text{ m.y.}$, $0.7131 \pm .0007$, (MSWD 1.8).

Clearly, the Clogau Shale samples and the Nantlle Slate samples yield good whole-rock isochrons. However, there is considerably more scatter from the Llanbedr Slate samples, although omission of one discrepant data point (sample HD/LL15) from the regression does lower the MSWD to a more acceptable figure. No explanation for the discrepancy of LL15 is apparent from either the quality (freshness) of sample or the mineral assemblage.

6.5 Interpretation and Discussion

The isochron ages from the Clogau Shales and from the Nantlle Slates are statistically indistinguishable, and clearly represent distinct 'events', around 400 m.y., which have induced isotopic homogenization within, and subsequent closure of, the Rb-Sr system. The recrystallization of clay minerals to a stable assemblage under very low-grade metamorphic conditions has already been suggested as a mechanism by which this isotopic event might take place (Section 3.4.3). The fact that indistinguishable Rb-Sr dates have been obtained from these two geographically distinct successions supports a conclusion that the dated event is a regional metamorphism, which in this case is clearly Caledonian, accompanying the folding movements. These Rb-Sr dates correlate with a range of K-Ar ages, from various rock-types in Wales, representing several thermal maxima in that region between 390-430 m.y. (Fitch et al. 1969).

The Rb-Sr age of 467 ± 40 m.y. from the Llanbedr Slates is of great interest, since the Clogau Shales from the same succession have been shown above to yield a Caledonian age of 409 ± 20 m.y. Two possible explanations for this earlier age are suggested:

- (a) Deep diagenesis alone was able to bring about complete recrystallization of clays, prior to any metamorphic event as such. Consequently, the Sr-isotope system would not record a single geological event, and might be predicted to give a poorly-defined 'isochron' (cf. Discussion of work by Perry & Turekian, 1974, in Section 3.4.2). Therefore this could also explain the lack of data colinearity, which is apparent from the MSWD value of 4.5. However, the estimated maximum thickness of only 4000m, and probably considerably less, of strata overlying the Llanbedr Beds by middle Ordovician times argues against this explanation.
- (b) The intrusion of the dolerite dykes which occur in the sampling locality (cf. Section 6.3.1) provided a temporary heat source of sufficient magnitude to induce local recrystallization of clay minerals in the host sediments. (N.B. None of the present samples were collected less than 10m from outcrops of these dykes). The probable Ordovician age of the numerous intrusions in the Harlech Dome has already been mentioned, and, within the Ordovician, igneous activity was virtually continuous in North Wales (viz. the extrusive centres of Rhobell Fawr, Cader Idris and Snowdon with major activities during the Arenig, Llanvirn and Bala periods respectively). Therefore, a ca. 470 m.y. age (i.e. mid-Ordovician) for dyke intrusion is quite plausible. However, confirmation of this alternative would be possible only by an investigation accompanied by systematic sampling at increasing distances from intrusive activity in this locality, and also sampling at other outcrops of the same horizon.

Whatever the explanation for the earlier age, it is clear that this first isotopic 'event' has closed the whole-rock Rb-Sr system to further redistribution of nuclides, even during the Caledonian metamorphism detected by Rb-Sr data from other strata. It is of interest to note that a K-Ar age of 405 m.y. (i.e. Caledonian) has been measured on a sample of Llanbedr Slate (Harper 1965). A comparison of this age with the Rb-Sr age from the same horizon exemplifies the differing behaviours of the two parent-daughter systems.

The initial $^{87}\text{Sr}/^{86}\text{Sr}$ ratio values on the three isochrons above are not low enough to permit the estimation, by projecting them backwards in time, of maximum depositional ages of any new stratigraphic significance (cf. a similar calculation for Longmyndian strata in Section 5.5.2). However, they do provide a simple means of comparing strata for correlative purposes between the two successions. Use of this parameter for comparison makes two assumptions: (i) that equivalent beds in the two successions would have had similar average depositional $^{87}\text{Sr}/^{86}\text{Sr}$ ratios (i.e. similar source areas and degrees of weathering, etc; see Section 3.4.1), and (ii) that the bulk sediment Rb-Sr system remains closed to any major changes subsequent to deposition (discussed more fully in Section 5.5.2).

At roughly the same time (ca. 400 m.y.), it is seen that the Clogau Shales and Nantlle (Purple) Slates had significantly different $^{87}\text{Sr}/^{86}\text{Sr}$ ratios: $0.7175 \pm .0011$ and $0.7131 \pm .0007$ respectively. Therefore, a correlation between these two horizons is not supported by the Sr-isotope data. This accords with previous conclusions made on lithological and other criteria.

The suggested correlation between the Llanbedr Slates and the Nantlle (Purple) Slates (Section 6.2.2) is challenged by the $(^{87}\text{Sr}/^{86}\text{Sr})_0$ values on the respective isochrons, though it may be noted that the precision on this value from Llanbedr Slates (Fig. 6-5) is poor. Projection backwards

(correcting for ^{87}Sr growth) of the $(^{87}\text{Sr}/^{86}\text{Sr})_0$ value from Nantlle Slates from 393 m.y. to 467 m.y. (the isochron age from Llanbedr Slates), and assuming a mean Rb/Sr ratio of 0.9 for the former, gives an average $^{87}\text{Sr}/^{86}\text{Sr}$ of about 0.7105 at this time for the Nantlle Slates. This value is clearly very significantly different from the $^{87}\text{Sr}/^{86}\text{Sr}$ value of $0.7168 \pm .002$ for Llanbedr Slates at the same time. A discussion of areal variability of Sr-isotopic compositions in recent deep-sea sediments has been given by Biscaye & Dasch (1971), who have concluded that isotopic variability due to physical processes (e.g. differential sedimentation) may operate over very substantial distances. In the present case, it is considered that this could not account for a large difference in $^{87}\text{Sr}/^{86}\text{Sr}$ ratios between two relatively close deposits. Therefore, it is concluded that contemporaneous deposition of these two argillaceous horizons is plausible only if two source regions of significantly different Sr-isotope compositions are postulated.

6.6 Conclusion

Rb-Sr whole-rock ages from samples of the Clogau Shale division of the Harlech Dome succession and of the Purple Slates at Nantlle, reiterate the conclusion that such ages represent recrystallization of clay minerals under metamorphic conditions. In these cases, the isochrons date the occurrence of this process during Caledonian metamorphism and folding.

Although in this study it has not been possible to deduce maxima for depositional ages of any new significance, new evidence which challenges the suggested correlation between Llanbedr Slates (Harlech Dome) and the Purple Slates (Nantlle) has been deduced by consideration of their contemporaneous $^{87}\text{Sr}/^{86}\text{Sr}$ ratios.

CHAPTER 7

CONCLUDING SUMMARY

7.1 The Significance of Rb-Sr Isotope Data from Sediments

The detailed nature of this study has permitted further conclusions to be drawn concerning the response of the Rb-Sr system in sediments to the physico-chemical changes encountered during burial and low-grade metamorphism. The present study, in combination with the investigations of other authors, now enables us to place more confident interpretation on the Rb-Sr data obtained from sediments than has hitherto been the case. A summary follows of the major points concerning the behaviour of such Rb-Sr systems, and the implications these have on the significance of Rb-Sr data.

- (a) There is no evidence from this and many other studies to suggest that complete Sr-isotope equilibration between the components of sedimentary detritus takes place prior to, or at the time of, deposition. This period covers the régimes of weathering and transport, halmyrolysis, and deposition. Partial isotopic equilibration of Sr may occur to a limited extent between Sr contained in an aqueous phase and that in sites which are labile to cation exchange (i.e. those occurring in some clay minerals).
- (b) The failure of detrital material to equilibrate isotopically with its environment is continued into the régime of burial and early diagenesis. This is demonstrated by the lack of Sr-isotope equilibration which is apparent between authigenic minerals and those which have some detrital component (e.g. mixed-layer clay minerals). This implies that an 'isochron' obtained from whole-rock samples such as those from Buildwas (Chapter 2) is fortuitous, being a mixing-line of several components; the slope of such a line is not simply

related to any single event. This situation may be detected by (i) high-precision Rb/Sr and $^{87}\text{Sr}/^{86}\text{Sr}$ data, by which the non-colinearity becomes apparent, and (ii) investigation of mineralogy, and in particular the clay mineralogy.

- (c) In sections of argillaceous sediments which have undergone diagenesis and low-grade metamorphism (e.g. Marloes, Longmyndian, Harlech Dome, etc. suites in the present study), it is clear that the conditions for Rb-Sr whole-rock isochrons have been satisfied. These sediments have a mineralogy comprising illite + chlorite in the clay fraction and may be further described by their illite crystallinity indices. Moreover, the variation in Rb/Sr ratios over distances of a few metres across a shale sequence is often favourable for the isochron method.
- (d) The general quality of such Rb-Sr isochrons implies that specific geological events are responsible for Sr-isotope homogenization. In situations where independent stratigraphical evidence is available (e.g. Marloes), it is clear that the age represented by the isochron is significantly younger than the inferred depositional age, i.e. it represents a minimum age for deposition. The process responsible for isotope homogenization therefore occurs during diagenesis or low-grade metamorphism. It is tentatively suggested that the dated event is a distinct recrystallization of metastable degraded clay minerals to a stable assemblage, this serving both as a process for Sr-isotope homogenization and also as a means of closing the system to further large-scale Sr mobilization. In the present study, the dated events in most cases may be identified with well-documented metamorphic-deformational episodes (e.g. Caledonian, Hercynian), though it is predicted that recrystallization may also take place by diagenesis alone without the intervention of a regional metamorphic event. Although in some cases the dated event

may occur soon after deposition, and therefore the age represents a good approximation to that of deposition, isochron ages have also been obtained which are considerably less (~ 100 m.y. or more) than the estimated age of deposition. Therefore, the position of the dated event in the post-depositional history of the sediment is still problematical for the direct stratigraphical application of the age. The unsupported assumption that a Rb-Sr isochron age from sediments is 'close to depositional age' is clearly unjustified.

- (e) However, a maximum age for deposition may be deduced from the isochron information, by consideration of the initial $^{87}\text{Sr}/^{86}\text{Sr}$ ratio for the sediments at the dated event. Projection of this ratio backwards in time, using an average Rb/Sr ratio representative of the bulk sediment, to a reasonable minimum $^{87}\text{Sr}/^{86}\text{Sr}$ for provenance rocks permits a constraint to be placed on the length of time between deposition and the dated event. Assumptions concerning the absence of metasomatic perturbations on the Rb-Sr system are implicit in this approach. For example, a 529 m.y. isochron from Longmyndian shales has a sufficiently low initial $^{87}\text{Sr}/^{86}\text{Sr}$ ratio (0.7061) that considerations as mentioned above enable a maximum age of ca. 600 m.y. to be deduced, significantly younger than had previously been considered.
- (f) The size of domain over which Sr-isotope mobilisation has occurred is difficult to define from field observations, since this may be obscured by the scale of bulk chemical homogeneity within a shale sequence. However, in all the sections studied (with the exception of that at Deadman's Bay, Marloes in Chapter 2), samples taken over stratigraphical intervals of up to 100m were found to plot on single Rb-Sr whole-rock isochrons, i.e. they each possessed single, uniform (within error) $^{87}\text{Sr}/^{86}\text{Sr}$ ratios at the events dated by the respective isochrons. From consideration of the magnitudes of

ionic diffusion coefficients in an aqueous phase compared to those for volume diffusion through crystalline lattices, one might predict that ionic transport over large distances in the presence of a fluid phase would be permitted. Furthermore, the scale of mobilisation is expected to show strong dependence on diverse physical parameters, such as time, temperature, and fluid continuity (i.e. permeability), and therefore might vary considerably between sequences. Systematic sampling on a large scale (i.e. >100m intervals), both across and along bedding, might yield more information on this matter.

7.2 Isotope Techniques in Experimental Investigations

The technique of Rb and Sr isotope dilution as 'tracers' for the Sr-isotope homogenization process during experimentally induced diagenesis, has been developed. This has revealed a great deal of information about the diagenetic changes in sediments:

- (a) The kinetics of Sr-isotope homogenization between clays and fluid show strong dependences on both temperature and fluid composition, i.e. $\text{rate} = f(T, X)$. The temperature dependence is very much as expected on the basis of previous work, although an Arrhenius relationship (i.e. $\log \text{rate}$ versus $1/T^{\circ}\text{K}$ is linear) does not obtain. This might be explained by the complexity of the clay reactant material. The dependences of both Rb (and radiogenic ^{87}Sr) and Sr exchange rates on fluid composition have not previously been observed, and they throw new light on the mechanisms involved. Furthermore, these dependences are cation-specific (i.e. rate of Sr-exchange in order $\text{K}^+ > \text{Mg}^{2+} > \text{Na}^+$ as brine cations, whereas Rb-exchange rate is in order $\text{Mg}^{2+} > \text{Na}^+ > \text{K}^+$). A simple volume diffusion model for the rate determining process is therefore dismissed, although it must be admitted that diffusion kinetics still offers the best

quantitative expression of the observations. A correlation between isotope exchange and recrystallization of clay minerals is not as clearly defined by these experimental studies as the field observations would suggest. This may reflect the caution which must be applied in extrapolating experimental observations into the geologically-significant régimes of lower temperatures and considerably longer reaction times. Further work in all aspects of this experimental approach is called for.

7.3 Future Work

The capability of Rb-Sr isotope data from sediments for dating geological events is now well-established. Conversely, it is also clear that investigation of the Rb-Sr system by isotopic analytical techniques offers a sensitive method of tracing the chemical and mineralogical changes in sediments during burial and metamorphic processes.

Further investigations are required into the precise nature of the response of sedimentary mineral assemblages to the dated events. Such investigations may clarify why some rocks (e.g. Marloes bentonites, Longmyndian Synalds Group) apparently remain open systems to Sr-isotope homogenization, beyond the closure of the Rb-Sr system in adjacent sediments. It might then be possible for the geologist to identify with more confidence the position of a dated event in the post-depositional evolution of a sedimentary rock.

APPENDIX A

TECHNIQUES FOR CRUSHING AND SIZE FRACTIONATION OF
ARGILLACEOUS ROCKS

A.1. Crushing

All the rock samples collected in this study required some reduction by mechanical means prior to aqueous dispersion and size fractionation. Mechanical reduction also homogenized samples, necessary for X-ray fluorescence analysis of Rb/Sr ratios and extraction of Sr for mass-spectrometric analysis.

Initially, samples were broken up manually (with cold-chisel and hammer) under clean conditions, and weathered portions discarded. (Percolation of meteoric waters along planes of fissility or cleavage resulted in "staining" in some specimens, and the stained portion could not be removed completely).

The selected specimen chips were passed through a jaw-crusher, producing an aggregate suitable for grinding by swing-mill. A Tema swing-mill, with agate or tungsten carbide grinding elements reduced the aggregate to a fine-powder after 5-10 mins. grinding. It is unlikely that such a short period of grinding would have an effect on the crystalline state of the clay minerals. (Both Takahishi (1959) and Yoder & Eugster (1955) have investigated by electron microscopy the effects of dry-grinding on crystallinity of clay minerals, showing that short grinding times have little effect). In the present investigation, electron micrographs of some of the clay mineral separates show that re-aggregation has not occurred.

A.2. Size-Fractionation

There are two methods of size-fractionation commonly available to clay mineralogists: (i) particle settling under gravitational force, or (ii) forced sedimentation under the influence of 'centrifugal' forces. Both methods are usually carried out in a liquid medium. In the present study de-ionised water was used; however, recent developments in particle size analysis have involved the use of air as the viscous medium in high-speed fractionation. All these fractionation techniques are described by the Stokes' Law formulation of the force acting on a spherical particle passing through a viscous medium:

$$f = 3\pi d\eta v$$

where f = force acting on particle,

d = diameter of particle,

η = viscosity of medium,

v = limiting velocity of particle.

In this work, most separations were carried out by centrifugal sedimentation, with the exception of twelve clay fractions produced by CNRS, Strasbourg. This technique was selected for the following reasons:-

(a) small amount of sample required,

(b) comparatively small volume of water involved, thereby reducing problems of contaminants in this medium,

and (c) speed of separation compared to gravity settling, reducing the period of exposure to airborne contaminants.

Tanner & Jackson (1947) used an integrated form of Stokes' Law, applicable to centrifugal sedimentation, to determine plots of minimum particle size sedimented at a given speed of rotation against a parameter dependent on time and rotational radii of top and base of the liquid column. This integrated equation is:

$$t = \frac{K_c \ln(R/S)}{N^2 d^2}$$

where t = time of rotation,

K_c = constant for system, incorporating viscosity of medium and densities of medium and particles ($K_c = 2.52$ in present work),

R = radius of rotation to base of liquid column,

S = radius of rotation to top of liquid column,

N = speed of rotation,

d = mean diameter (estimated spherical diameter, esd) of particles.

Such a plot, for particles of specific gravity 2.65 (taken as an average for material in this study) in water at room temperature is shown in fig. A-1.

5-10 g. of powdered sample was subjected to ultrasonic disaggregation in deionised water. After this treatment, the $>10\mu\text{m}$ (esd) fraction was removed by gravitational settling. The residual suspension was transferred to centrifuge tubes and spun in an IEC centrifuge, time and speed being determined from fig. A-1.

Obviously, fractionation under these conditions is far from perfect - the assumption that the particles may be represented by a spherical diameter is an obvious shortcoming for minerals of platy morphology. Also, sidewall retardation effects in a small centrifuge tube may not be negligible. However, it is considered that a reproducible separation, on the order of 90% effective, may be obtained after three such treatments for each fraction.

Aliquots of the separated clay fractions, in suspension, were mounted for clay mineralogy determination (see Appendix B) if required. Excess water was removed from the remaining separates by high-speed centrifuging, and they were then dried at $60-70^\circ\text{C}$ and stored.

Clay-fractions were separated from twelve Marloes and Buildwas samples in the Centre de Sédimentologie et Géochimie de la Surface, CNRS, Strasbourg (with the co-operation of Dr. N. Clauer). These separations were

carried out by gravitational sedimentation under clean conditions. In this case, the force acting on the particles is that of gravity alone. A suspension of whole-rock powder in a large settling column was allowed to fractionate, the supernatant suspension being removed after the calculated length of time and centrifuged at high-speed to obtain the clay (<2 μ m) fraction. The advantage of this method over the centrifugal technique is that it permits production of much larger quantities of clay separate from a single fractionation.

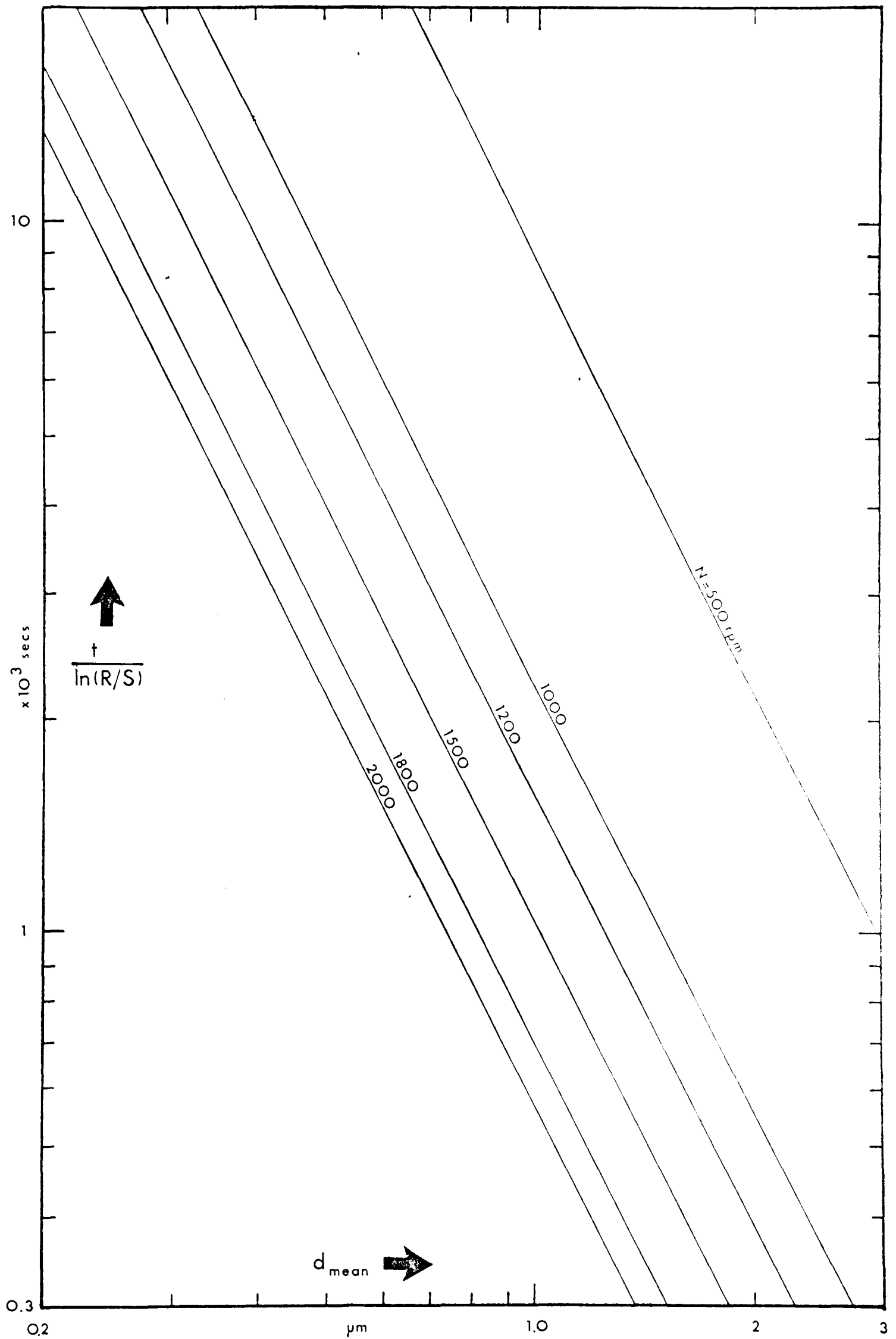


Fig. A-1. Sedimentation nomographs, after Tanner & Jackson (1947). Linear plots, representing different centrifuge rotational speeds, relate minimum particle size sedimented (d_{mean}) with function of time and centrifuge parameters ($t/\ln(R/S)$).

APPENDIX B

X-RAY DIFFRACTION TECHNIQUES OF DETERMINATIVE MINERALOGY

The diffraction of X-rays by a crystal lattice is described by the Bragg Law:

$$n\lambda = 2d\sin\theta$$

where n = integer,

λ = X-ray wavelength,

d = lattice spacing,

θ = Bragg angle, between incident beam and lattice plane.

Thus peaks in diffracted X-ray intensity at different values of θ , will be related to d , a parameter representative of the crystal structure of the phase(s) under irradiation. This forms the basis of qualitative and quantitative methods in mineralogical determination. It is not intended to give here a detailed description of the theory and interpretation of X-ray diffraction phenomena from mineral phases - the subject is adequately dealt with by Zussman (1967) and Nuffield (1966). However, it should be emphasised that it is only a semiquantitative method at the present time, particularly when used as a rapid analytical tool, as in the present study.

The quantitative estimation of mineral mixtures by X-ray powder diffractometry relies upon a relationship between the intensity of reflection from specified lattice planes in a mineral and the amount of that phase in the mixture:

$$I_{i(hkl)} \propto \frac{Kx_i}{\rho \sum_{i=1}^n x_i \mu_i}$$

where $I_{i(hkl)}$ = intensity of reflection from hkl plane of i th component,

K = 'constant' (see below),

x_i = weight fraction of i th component in mixture,
 μ_i = mass-absorption coefficient for i th component.

Thus $I_{i(hkl)}$ is inversely proportional to the overall mass-absorption coefficient for the mixture which, of course, varies with composition. However, the intensity of a reflection from a component phase is also dependent upon less easily controlled or defined parameters, which must be accounted for in the so-called 'constant', K , in the above relationship. Crystallite size and degree of preferred orientation are the two most important of these parameters, particularly when dealing with argillaceous rocks (see, for example, Parrish, 1958). Crystallite size may affect the distribution of particle orientations, causing it to deviate either from the random distribution required for whole-rock mineralogy determinations, or from the preferred orientation of 001 planes parallel to the specimen surface required for clay determinations. In addition, homogeneity of sample is necessary in order that average mass-absorption coefficient is experienced in the paths of X-rays. Degree of preferred orientation is the variable most difficult to control, depending on crystallite size (see above), particle morphology (minerals with platy morphology obviously present the biggest problem in this respect), and mode of specimen preparation and mounting. This problem will be discussed further in the sections dealing with determination of whole-rock and clay-fraction mineralogies.

B.1. Whole-Rock Mineralogy

Finely powdered samples, produced by swing-mill grinding (Appendix A), were packed into rectangular cavity mounts, thereby preserving random particle orientation to a large extent. However, compression inevitably leads to some orientation of platy minerals with their basal 001 planes normal to the direction of compression. Therefore, in analyses of argillaceous samples using these 'random orientation' mounts, reliable estimates

of the proportions of clay minerals, based on the intensities of basal reflections, relative to the non-platy minerals (e.g. quartz, calcite, plagioclase) are not possible.

X-ray diffractograms were measured on a Philips PW 1050 diffractometer, using Ni-filtered Cu K α radiation. 1° divergence and anti-scatter slits were employed, with a 0.1 mm. receiving slit. The goniometer speed was 1°2 θ per minute, the diffracted X-rays being detected by a scintillation counter (Tl-activated NaI) and passed through a pulse-height analysing unit prior to recording on a strip-chart.

Estimates of the proportions of minerals present were made according to the method adopted by Schultz (1964). Since all the relevant peaks were sharp and well-defined, the peak heights (background corrected) were taken as proportional to the integrated intensities and used in all calculations. The specific reflections used for estimation of each mineral, their d-spacings and corresponding positions in degrees 2 θ for Cu K α radiation, and the relevant intensity factors, are shown in Table B-1. Relative proportions of minerals are calculated by dividing measured peak heights by the relevant intensity factors.

B.2. Clay-fraction Mineralogy

The determination and classification of clay minerals is a complex, and often controversial, subject, which is dispersed through the literature of disciplines as diverse as pedology and petroleum geology. There is broad agreement among clay mineralogists on the classification of clay minerals on structural and compositional criteria (Grim, 1953 and Millot, 1970). Figure B-1 shows the mineral groups referred to in this study. However, the complexity of physicochemical conditions obtaining during weathering, transportational, and depositional regimes is evidenced by the different views on clay genesis held by various authors. Weaver (1959) and Millot (op. cit.) are examples of opposing emphases, the former pro-

TABLE B-1. Data for estimation of mineral composition (except clays) of cavity mounted samples

Mineral phase	Reflection (hkl)	d(hkl), Å	Degrees 2θ (CuKα)	Intensity factor
Quartz	101	3.34	26.66	2
Calcite	104	3.04	29.36	1
Plagioclase	040	3.18	28.04	1
K-feldspar	20 $\bar{2}$;040	3.24	27.50	1

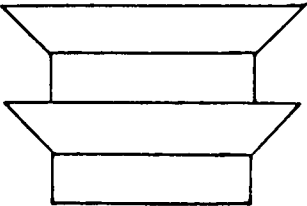
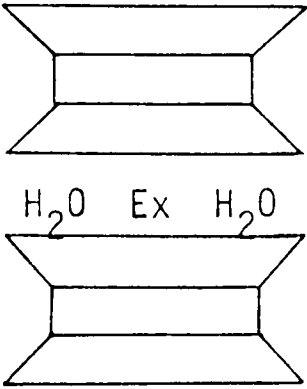
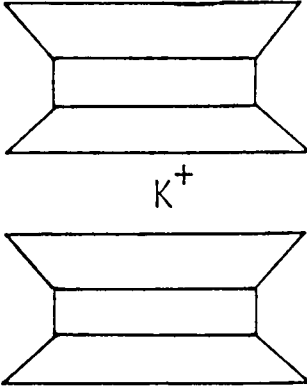
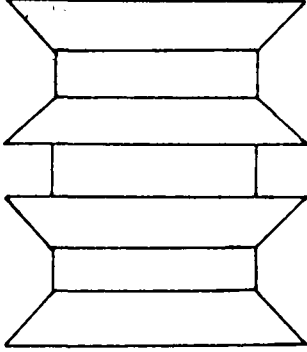
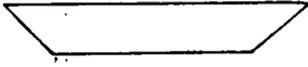
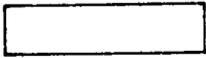
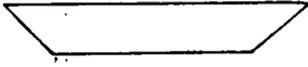
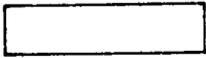
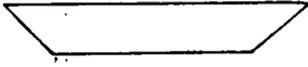
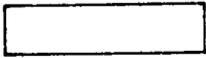
MINERAL	STRUCTURE	COMPOSITION (Idealized)				
Kaolinite		$Al_2Si_2O_5(OH)_4$				
Montmorillonite		$Ex_x\{Al_{2-x}Mg_x\}\langle Si_4 \rangle_0^{10}(OH)_2$				
Illite		$K_{1-x}\{Al_2\}\langle Al_{1-x}Si_{3+x} \rangle_0^{10}(OH)_2$				
Chlorite		$\{Mg,Al\}_3(OH)_6\{Mg,Al\}_3\langle Si,Al \rangle_4^{10}(OH)_2$				
<table border="1" style="width: 100%; border-collapse: collapse;"> <tr> <td style="text-align: center; width: 150px;">  </td> <td>Tetrahedral layer < ></td> </tr> <tr> <td style="text-align: center;">  </td> <td>Octahedral layer { }</td> </tr> </table>				Tetrahedral layer < >		Octahedral layer { }
	Tetrahedral layer < >					
	Octahedral layer { }					

Fig. B-1. Structural and compositional characteristics of clay mineral groups involved in this study. 'Ex' indicates hydrated exchangeable cations. (After Berner, 1971).

pounding a detrital dominance whilst the latter considers a transformational and authigenic dominance in clay genesis in sediments. Indeed, the diversity of sediments is such that examples supporting all shades of opinion may be found.

The application of X-rays to the elucidation of clay minerals present in a sample is treated in depth by Brown (1961). The scheme used in the present study is that used by Shaw (1971, 1973), which involves the use of glycollation, acid- and heating-treatments to aid in discrimination between clay mineral groups.

B.2.1. Sample Mounting

Since clay minerals all have structures consisting of stacked 2-dimensional aluminosilicate layers (i.e. phyllosilicate class of minerals), their basal reflections in the X-ray diffraction pattern may be enhanced by alignment of their 001 planes parallel to the face of the mounted specimen. The many methods of mounting clay minerals for XRD analysis have been critically assessed by Gibbs (1965, 1968), with the aim of eliminating those methods which may produce segregation of clay minerals according to particle size and morphology. Such methods yield an inhomogeneous specimen and consequently erroneous XRD analytical results. The technique for sample mounting chosen for the present study is the suction-onto-ceramic disc method described by Shaw (1972). In this method, a ceramic filter disc (produced from unglazed biscuit tiles with a 1.5 inch diameter corer) is mounted between gaskets in a cylindrical filter funnel attached to a Buchner flask (fig. B-2). A small volume of aqueous suspension of dispersed clay (see Appendix A for clay fractionation) is rapidly sucked onto the ceramic filter, depositing a thin layer of oriented clay particles. This has the advantages of producing, rapidly and reproducibly, a well-oriented clay mineral mount in a form suitable for immediate use in a Philips diffractometer without any modification to the

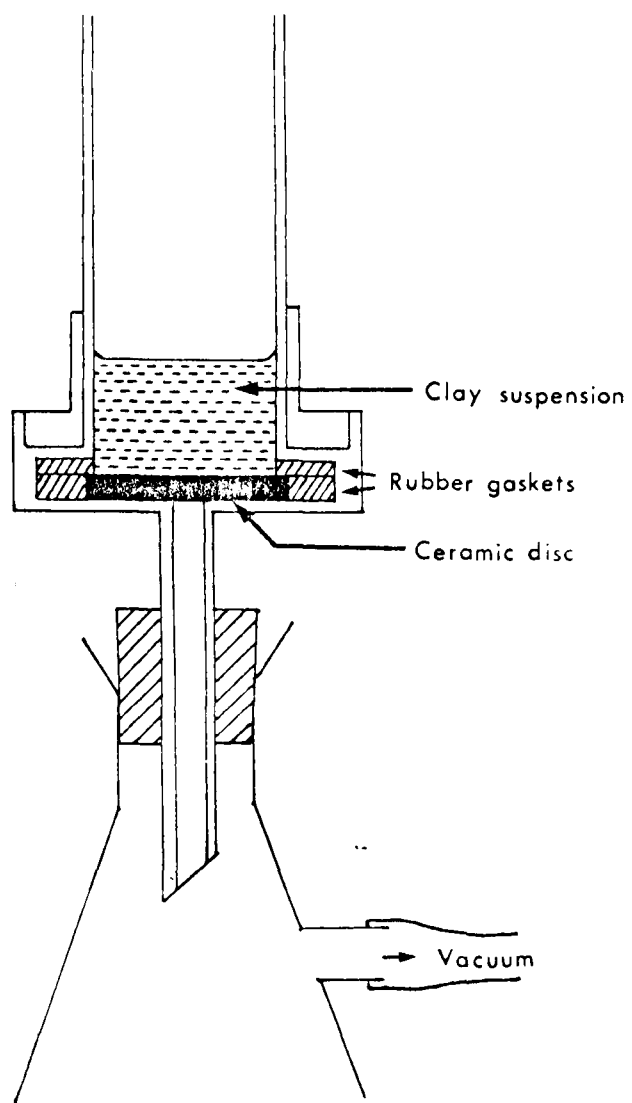


Fig. B-2. Apparatus for producing oriented clay mineral mounts for X-ray diffractometry, by suction-onto-ceramic tile method of Shaw (1972).

latter. The problem of particle segregation, caused by slow settling, is eliminated by this method. The ceramic discs themselves give poorly defined diffraction patterns, with quartz and feldspar peaks - consequently their possible contribution to a clay XRD pattern in the unlikely event of insufficient thickness of clay is of little importance.

B.2.2. Classification and Estimation of Clay Mineralogy

X-ray diffractograms of the oriented clays were recorded between 3° and $20^{\circ}2\theta$ for the air-dried specimen, and also for that after treatment with ethylene glycol. (Another advantage of the ceramic mounts is that glycol liquid may be applied directly, the excess being absorbed by the ceramic base; for many other mounting techniques, glycollation must be carried out by the vapour). In some cases, diffractograms were also recorded of clays after boiling in 10% hydrochloric acid for 15 mins, or after heating the glycollated specimen at 400°C and 550°C for 1 hour in each case. The effects of these various treatments on intensities, shapes, and positions of diffraction maxima is an aid in assigning all or part of the maxima to specific clay mineral types (Table B-2).

Treatment with ethylene glycol displaces the interlayer water from smectites, replacing it with the organic molecule, and shifting the (001) peak to $\sim 17\text{\AA}$. However, as Weaver (1967) pointed out in a lucid summary of determinative clay mineralogy, mixed-layer clays containing a smectite component may produce a peak-shift to less than 17\AA upon glycollation. The complex matter of interlayering in mixed-layer illite-smectite clays - the estimation of relative amounts of components and the distinction between random- and regular-interstratification - has been dealt with by Reynolds and Hower (1970), who used mathematical models to predict positions of diffraction maxima. In the present study, the nature of any mixed-layer clays present has not been investigated in great detail - a simple identification being considered sufficient. Boiling with hydrochloric

Air dry basal spacing	Glycerated sample	Heated at 400°C for one hour	Heated at 550°C for one hour	Boiled in 10% HCl	MINERAL
~ 14 Å	No change	No change	Increase in intensity	All reflections vanish	CHLORITE
~ 14 Å	Expands to 18 Å	Collapses to ~10 Å	No change or slight collapse	May dissolve in HCl	SMECTITE
≥10-14 Å	No change	No change	No change or slight increase in intensity	No change	Regular interstrat. ILLITE-CHLORITE
≥10-14 Å	No change	No change	No change	May dissolve in HCl	Random interstrat. ILLITE-CHLORITE
≥10-14 Å	Expands to higher spacing	Collapses to ~ 10 Å	No additional collapse	No change	ILLITE-SMECTITE
~ 10 Å	Unsymmetrical peak with perhaps slight shift	No change	No change except slight sharpening of reflection	No change	ILLITE (MUSCOVITE)
~ 7 Å	No change	No change	Destroyed	No change	KAOLINITE

Table B.2. Identification of Clay Minerals by X-ray Diffraction (Adapted from Shaw, 1971)

acid completely destroys the chlorite structure, the octahedral site cations (i.e. Fe^{2+} , Mg^{2+} , etc.) passing into solution. Heating at 400°C causes the collapse of expandable lattices to their basal spacing, by expelling the interlayer water or glycol molecules. Heating at 550°C destroys the kaolinite lattice, thereby causing the 7\AA diffraction maxima due to kaolinite (001) to be lost.

Biscaye (1964) suggested that kaolinite and chlorite in recent sediments may be differentiated (both having maxima at $\sim 7\text{\AA}$ - the 001 and 002 reflections respectively) by resolving the 3.58\AA (kaolinite 002) and 3.54\AA (chlorite 004) peaks respectively. This necessarily involves both a very slow scan speed to produce the required resolution, and also good calibration of the chart record unless both 3.5\AA peaks are present. The acid-treatment method of differentiation (Table B-2) is preferred in the present study, thus by-passing the troublesome and often unreliable task of accurate chart calibration.

Quantification in clay mineral studies has been, and remains, a field in which the inherent problems are compounded by the diversity in methods adopted by different groups. The use of synthetic standards, made up from known proportions of standard pure clay minerals, where available, is inappropriate. The variability of composition among samples of the same clay mineral type from different naturally occurring clay assemblages is well known: the relevance of standard clays, which necessarily occur in unusual environments, to the determination of natural clay mixtures must therefore be doubted. Gibbs (1967) attempted to overcome this problem by using, as standards, clay minerals extracted from the samples to be analysed, and thereby producing calibration curves from known mixtures of these standards. To obtain montmorillonite, kaolinite, chlorite and illite fractions, Gibbs used modified heavy-liquid mineral separation techniques. It seems probable that only in a few cases will the density differentials between the relevant minerals enable separations of suff-

icient efficiency to be achieved - the presence of mixed-layer minerals would exacerbate this problem. Johns et al. (1954), on the other hand, applied considerations of structure and the variation in scattering with diffraction angle to the estimation of inter-peak intensity factors. Schultz (1964), Biscaye (1965), Weaver (1967), and Shaw (1971) have all resorted to computation based on estimated intensity factors; Table B-3 lists the inter-peak intensity factors used by these authors. All four authors have estimated that different clay phases at the same diffraction angle will have roughly the same intensity factor, i.e. collapsed smectite, mixed-layer illite-smectite, and illite at 10\AA all have the same reflection efficiency, as do kaolinite and chlorite at 7\AA .

Pierce and Siegel (1969) suggested that, in the absence of any one method of calculation being shown to be more accurate than others, at least a unified approach should be agreed upon in order that results be comparable on an inter-laboratory basis. No such unified approach has been forthcoming, and therefore the significance of the semi-quantitative results in the present study should be confined strictly to the relative compositions of samples within this study.

The computation method adopted for this investigation is that described above, in which estimated intensity factors are utilised to correct the intensities of diffraction maxima and thus produce values which may be compared quantitatively. Although there is some diversity in the actual factors used (Table B-3), this is the most widely used technique, and has the advantage of rapidity.

Initially, in the study of clay mineralogies of Buildwas and Marloes argillites (Chapter 2), a scheme of goniometer slit adjustment suggested by Shaw (1971) was adopted. Shaw varied sizes of divergence and anti-scatter slits with diffraction angle in an attempt to equalize the beam intensity experienced by the sample over all diffraction angles. This practice was dropped for all subsequent samples, in order to simplify the

17Å peak area	10Å peak area	7Å peak area	Reference
1x	4x	2x	Biscaye (1965)
1x	4x	1.6x	Weaver (1967)
1x	4.5x	4.5x } to } * 2.2x }	Schultz (1964)
1x	4x	1.6x	Shaw (1971)
1x	4x	1.6x	This work

* Value depends on crystallinity of kaolinite.

Table B-3. Peak Intensity Factors used by various authors for quantification of clay mineral analyses.

method and bring it into line with the usual practice of maintaining constant slit width. The counting units (rate-meter, pulse-height analyzer, etc.) and the recorder were replaced during the study; the operating conditions under which diffractograms were measured are given below:

(i) Buildwas & Marloes samples:

Philips PW1051 amplifier, rate-meter, analyzer and recorder
 Rate-meter : x 8 (x 16)
 Time-constant : x 2
 Goniometer speed : $\frac{1}{2}^{\circ} 2\theta \text{ min}^{-1}$
 Receiving slit : 0.1 mm.
 Divergence and anti-scatter slits: $\frac{1}{4}^{\circ}(3^{\circ}-10^{\circ}2\theta)$, $\frac{1}{2}^{\circ}(10^{\circ}-20^{\circ}2\theta)$
 Chart speed : 1600 mm. hr⁻¹

(ii) All subsequent samples (Longmyndian, etc.):

J & P amplifier, single-channel analyzer and rate-meter
 Telsec type V horizontal-bed recorder
 Full-scale deflection: 10^3 (3×10^3) counts
 Time-constant : x 1
 Goniometer speed : $2^{\circ} 2\theta \text{ min}^{-1}$
 Divergence and anti-scatter slits: 1°
 Receiving slit : 0.1 mm.
 Recorder input : 100 mV
 Chart speed : 1 cm min⁻¹.

In the comparative study of Buildwas and Marloes samples, the integrated peak intensities were computed by measuring areas under peaks, some of which are broad and asymmetrical (fig. B-3). The intensity factors of Shaw (1971) were used (Table B-3); a sample calculation from the diffractograms shown in Fig. B-3 is given below:

Sample No. DD 7d (<2 μ m).

%(illite + illite-smectite + smectite)

$$= \frac{I(10\text{\AA}) @ 400^{\circ}\text{C} \times 2.5 \times 100}{[I(10\text{\AA}) @ 400^{\circ}\text{C} \times 2.5] + [I(7\text{\AA}) @ 400^{\circ}\text{C}]}$$

(NB. 2.5 is intensity factor for 10 \AA peak)

$$= \frac{1149 \times 2.5 \times 100}{[1149 \times 2.5 \times 100] + 543} = 84\%$$

%(kaolinite + chlorite)

$$= 100 - \% (\text{illite} + \text{illite-smectite} + \text{smectite})$$

$$= 100 - 84 = 16\%$$

%(illite)

$$= \frac{I(10\text{\AA})_{\text{gly}}}{I(10\text{\AA})_{@ 400^{\circ}\text{C}}} \times \%(\text{illite} + \text{illite-smectite} + \text{smectite})$$

(normalise 10 \AA peak areas between diffractograms by using unaffected 7 \AA peak areas)

$$= \frac{694/420}{1149/543} \times 84 = 66\%$$

%(kaolinite)

$$= \frac{I(7\text{\AA})_{\text{acid}}}{I(7\text{\AA})_{\text{A.D.}}} \times \%(\text{kaolinite} + \text{chlorite})$$

(normalise 7 \AA peak areas between diffractograms by using unaffected 4.95 \AA illite (002) peak areas)

$$= \frac{117/139}{554/591} \times 16 = 14\%$$

%(chlorite)

$$= \%(\text{kaolinite} + \text{chlorite}) - \%(\text{kaolinite})$$

$$= 16 - 14 = 2\%$$

The other suites of rocks studied contained sufficiently well crystalline clays (giving symmetrical peaks, e.g. fig.2-7) to eliminate the need to measure areas under peaks, and the peak heights at a fastscan speed were taken as proportional to the integrated peak intensities.

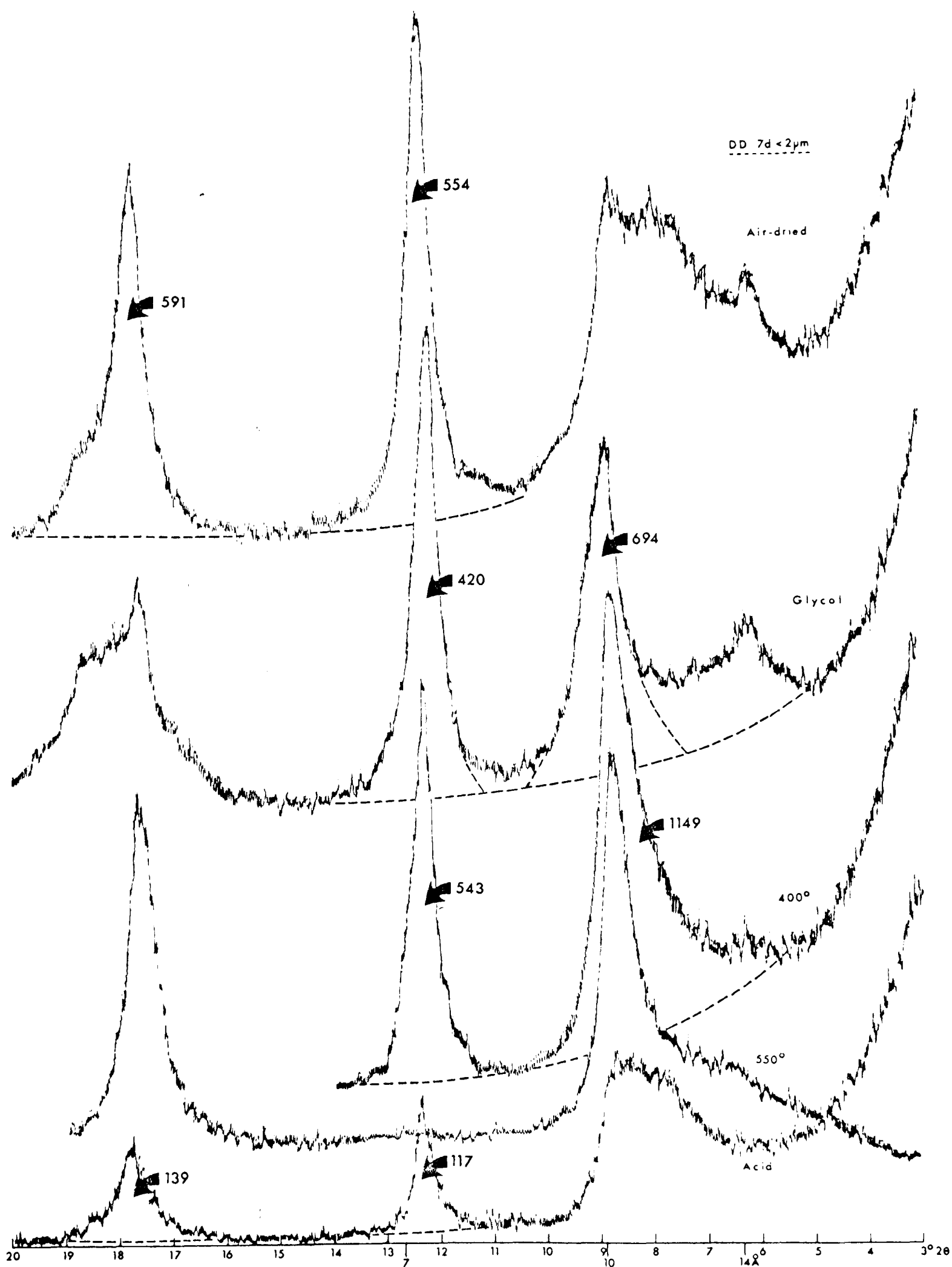


Fig. B-3. Diffractograms of oriented mount of clay-fraction of sample DD7d after various treatments. Figures represent integrated peak intensities in arbitrary units. See text for computation of clay mineral abundances from these measured intensities.

APPENDIX C

CRYSTALLINITY INDEX MEASUREMENTS AND STANDARDS

Illite crystallinity measurements were made on the oriented clay fraction ($<2\mu\text{m}$) mountings (Appendix B). A diffractogram of each sample in the region of the 10\AA peak was recorded under the same conditions used for clay mineralogy determination, except that a slow goniometer scan speed of $2^\circ 2\theta$ per minute with a fast recorder speed of 1600 mm hr^{-1} (Philips) or 3 cm min^{-1} (Telsec) were used. Similar diffractograms were also taken of three "crystallinity index standards" supplied by Professor B. Kubler (Institut de Géologie, Université de Neuchâtel, Switzerland). These standards are specimens from the same illite-chlorite slate, two of which are mounted on wedges of different angularity (Fig. C-1). The purpose of the wedges is to present the face of the sample at an angle to the X-ray beam rather than parallel as with normal samples. In this way, the diffraction peaks are artificially broadened to an extent depending on the angularity of the wedge. In addition, the humidity-dependence and fragility of standards with genuinely low crystallinity are by-passed.

The width of the 10\AA peak at its half-height was measured for each sample and corrected back to the recorder speed of 1600 mm/hr used by Kubler (1968) in his definitive paper on the crystallinity index for illite. A calibration curve was established, each time a set of measurements was made, using the standards of known crystallinity index supplied by Prof. Kubler.

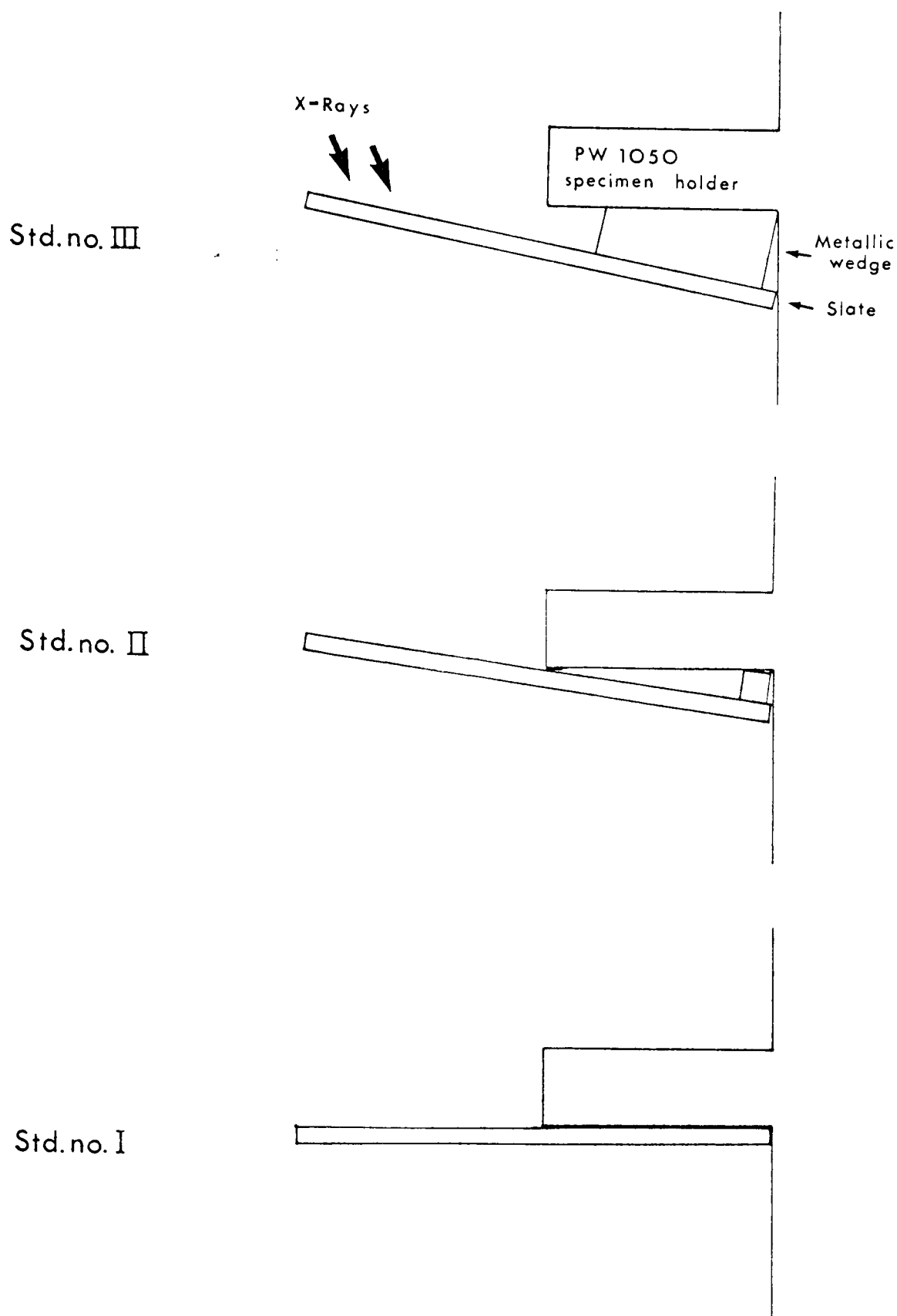


Fig. C-1. Illustration of mode in which the three illite crystallinity standards are mounted in diffractometer goniometer. Use of wedges to offset the sample from the focus of the X-ray beam permits the manufacture of all three standards from a single slate.

APPENDIX D

CHEMISTRY OF Rb & Sr SEPARATIONS FOR MASS-SPECTROMETRIC ANALYSIS

D.1. Extraction of unspiked Sr for isotopic analysis

A small amount of sample was taken into solution by acid digestion, and Sr isolated by ion exchange techniques.

Approximately 0.1-0.2g of powdered sample (i.e. sufficient to contain $\sim 30\mu\text{g}$ of Sr) was placed in a covered Pt dish. 1 ml. of redistilled HClO_4 (Frederick Smith Company, Chicago; Sr-blank ~ 0.1 ng/ml) and 10 ml. of HF (Merck Suprapur; Sr-blank ~ 0.02 ng/ml) were added, refluxed for several hours, and then taken to dryness. The residue was taken up in a small amount of 6M HCl (redistilled Analar, ~ 0.03 ng/ml Sr), and once again evaporated to dryness. The resulting residue was leached with deionised water, centrifuged, and an aliquot of the supernatant solution (sufficient for 5-10 μg Sr) loaded onto a 16 x 1 cm. Bio-Rad AG 50W-X8 ion exchange column (all-quartz construction). (Between samples, the columns were washed twice with 60 ml 6M HCl, and resettled after each wash with H_2O and 2.5M HCl respectively.) Elution was by 2.5M HCl, the Sr-fraction being collected at approximately 45-60 ml, and subsequent to the Rb elution peak. The Sr-cut was evaporated to dryness in a PTFE beaker under PTFE evaporation covers provided with an overpressure of filtered air. The residue was dissolved in a few drops of water and transferred to a quartz micro-beaker, in which it was evaporated to dryness, covered with 'Parafilm' and stored for analysis.

Total Sr blank for the overall process was consistently low, due to the use of clean-room facilities, ultra-pure reagents, quartz or PTFE vessels, and use of the overpressured evaporators. Total Sr blank in this laboratory, using the method outlined here, has been measured at values generally lower than 10 ng. (Pankhurst and O'Nions, 1973). This blank

was further reduced, in the more recent parts of this work, by the introduction of a decomposition step carried out in PTFE beakers under the evaporators. HClO_4 was replaced in this step with 1-2 ml. of quartz-distilled nitric acid. Correction to measured $^{87}\text{Sr}/^{86}\text{Sr}$ ratios for blanks at this level are negligible, being only one or two in the fifth decimal place.

D.2. Extraction of spiked Rb and Sr for isotope dilution analysis

About 0.1-0.2g. of sample were weighed accurately into a Pt-dish. To this were added accurately weighed quantities of ^{84}Sr - and ^{87}Rb -enriched 'spike' solutions. The amounts of 'spikes' added were such that the precision of isotope ratio measurements might be optimised, i.e. final $^{86}\text{Sr}/^{84}\text{Sr}$ or $^{87}\text{Rb}/^{85}\text{Rb}$ ratios in the range 1-2. The isotopic compositions and concentrations (determined by calibration against solutions of 'normal' strontium/rubidium of known concentrations) for the 'spike' solutions used in this study are listed in Table D-1. It may be noted that the more heavily ^{84}Sr -enriched 'spikes' were used in the later parts of this study, enabling less total 'spike' strontium to be added and therefore reducing the correction that must be applied to obtain the $^{87}\text{Sr}/^{86}\text{Sr}$ ratio of the unspiked sample.

After 'spike' addition, acid decomposition was carried out as described before, taking additional precautions to guard against any loss of solution prior to complete homogenization of sample and 'spike' strontium and rubidium. After centrifuging, the resulting solution was divided into aliquots for Sr- and Rb-extraction respectively.

Spike conc.	$^{84}/_{86}$	$^{88}/_{86}$	$^{87}/_{86}$	$^{84}/_{88}$	Sr
0.9112 $\mu\text{g/g}$	22.662	3.3538	0.42139	6.7579	
1.310 $\mu\text{g/g}$	237.92	1.4801	0.2455	160.67	
29.06 $\mu\text{g/g}$	242.39	1.4586	0.2428	166.02	(AB-2)
1.898 $\mu\text{g/g}$	1715.1	0.7411	0.1558	2315	(NBS-988)

Spike conc.	$^{87}/_{85}$	Rb
10.46 $\mu\text{g/g}$	161	
23.60 $\mu\text{g/g}$	161	
28.50 $\mu\text{g/g}$	111.4	(AB-1)
-	0.3829	(Normal Rb)

Table D-1. Concentrations and isotopic compositions of Sr and Rb 'spike' solutions used in isotope dilution analyses during this study.

D.2.1. Sr-extraction was carried out using the ion exchange procedure previously described above.

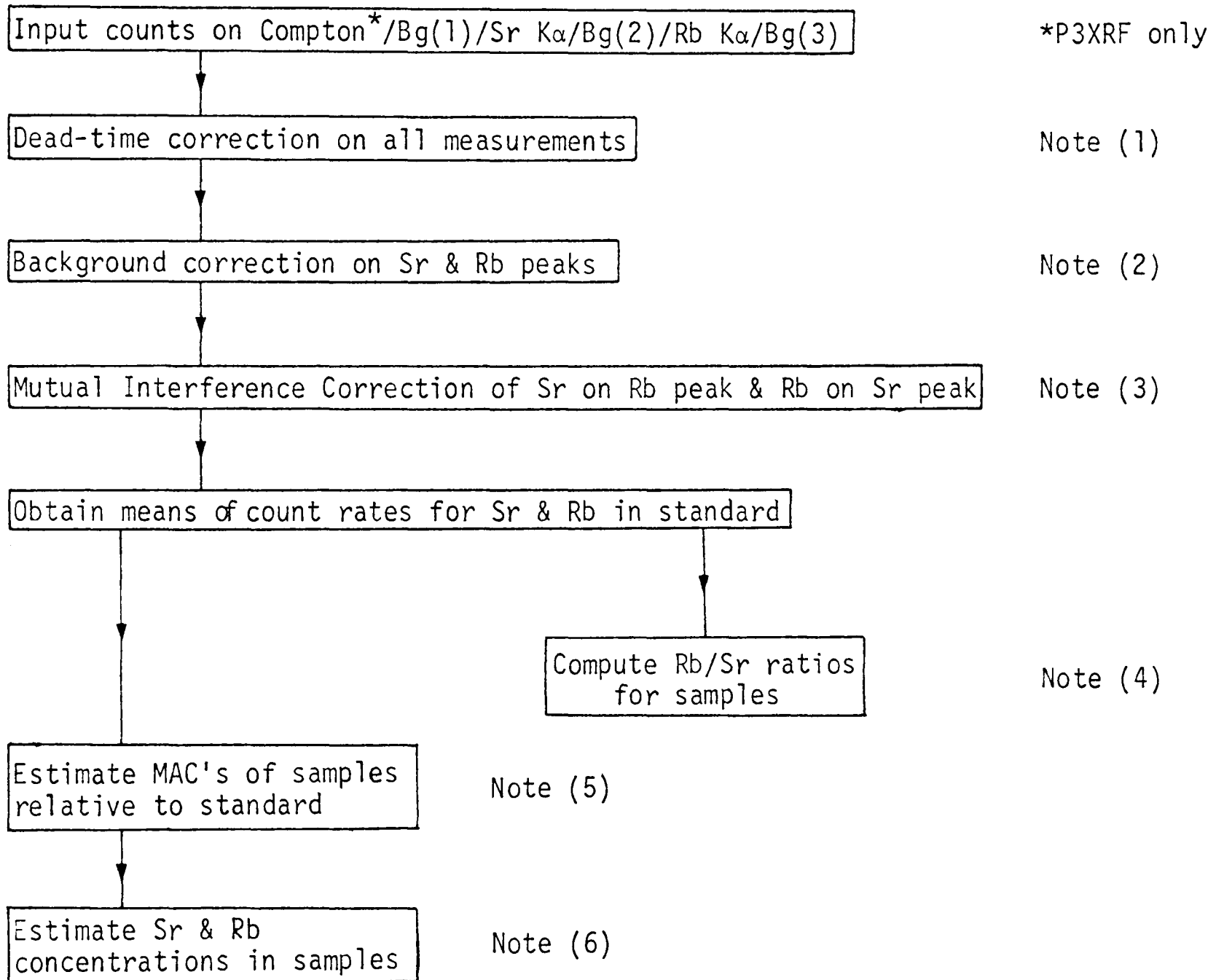
D.2.2. Rb-extraction was achieved by ion-exchange procedures on zirconium phosphate. An aliquot (~2 ml) of sample solution sufficient to contain 3-5 μg Rb was acidified to 2.5M HCl and loaded onto a 4 x 0.5 cm. column of zirconium phosphate (Bio-Rad ZP-1). The column had been washed with 10 ml 2M NH_4Cl -HCl solution (prepared from HCl and isothermal NH_4OH) and acidified with 3 ml 2.5M HCl. Elution was with 12 ml 2.5M HCl, removing all cations except Rb^+ and Cs^+ . Rb was stripped with 2 ml. 2M NH_4Cl -HCl. Ammonium salts were destroyed by slow evaporation of the eluate with 1 ml. conc. HNO_3 (redistilled B.D.H. Aristar); the resulting Rb concentrate was transferred to a quartz micro-beaker, evaporated to dryness, and stored for mass spectrometric analysis. The Rb blank for this process has been measured at less than 2 ng. total (Pankhurst and O'Nions, op.cit.).

APPENDIX E
COMPUTATIONS

(Programs written by Dr. R.J. Pankhurst)

E.1. Rb/Sr RATIOS BY XRF

Program P2XRF (P3XRF with Compton peak):-



Note (1): $\text{Real time} = \text{Count time} - (\text{counts} \times \text{dead time})$

$\text{True count rate} = \text{Counts}/\text{real time}$

Note (2): $\text{Corrected Sr count rate} = \text{Measured Sr count rate} - \text{Bg}(2) - \text{Background factor (Sr)} \times (\text{Bg}(1) - \text{Bg}(2))$

$\text{Corrected Rb} = \text{measured Rb} - \text{Bg}(3) - \text{Bg. fac. (Rb)} \times (\text{Bg}(2) - \text{Bg}(3))$

Note (3): $\text{Corrected Sr count rate} = \text{Measured Sr count rate} + \text{Interference factor (Sr)} \times \text{Rb count rate}$

$\text{Corr. Rb} = \text{Measured Rb count rate} + \text{Int. fac. (Rb)} \times \text{Sr count rate}$

$$\text{Note (4): } \left[\frac{\text{Rb}}{\text{Sr}} \right]_{\text{sample}} = \frac{(\text{Corr. Rb count rate})_{\text{sample}}}{(\text{Corr. Sr count rate})_{\text{sample}}}$$

$$\times \frac{(\text{Rb/Sr})_{\text{standard}}}{\text{Mean} \left(\frac{(\text{Corr. Rb count rate})}{(\text{Corr. Sr count rate})} \right)_{\text{standard}}}$$

$$\text{Note (5): } \frac{\text{MAC (sample)}}{\text{MAC (standard)}} = \frac{[\text{Bg}(1) + \text{Bg}(2) + \text{Bg}(3)]_{\text{standard}}}{[\text{Bg}(1) + \text{Bg}(2) + \text{Bg}(3)]_{\text{sample}}}$$

or with P3XRF only:

$$\frac{\text{MAC (sample)}}{\text{MAC (standard)}} = \frac{\text{Compton (standard)}}{\text{Compton (sample)}}$$

$$\text{Note (6): } \text{ppm Sr (sample)} = \frac{\text{Corr. Sr count rate (sample)}}{\text{Count rate per ppm Sr (standard)}} \times \frac{\text{MAC (sample)}}{\text{MAC (standard)}}$$

$$\text{ppm Rb (sample)} = \frac{\text{Corr. Rb count rate (sample)}}{\text{Count rate per ppm Rb (standard)}} \times \frac{\text{MAC (sample)}}{\text{MAC (standard)}}$$

Overall errors are calculated on the basis of those arising from the reproducibility of both sample and standard data, incorporating the estimated errors in dead-time, background, and mutual interference correction factors.

Error propagation is computed by the normal methods:

(i) Where sum or difference of two terms, each incorporating errors, is concerned:

$$S_{a \pm b}^2 = S_a^2 + S_b^2 \quad (S = \text{standard deviation})$$

(ii) Where product or quotient of two terms, each incorporating errors, is concerned:

$$e_{axb}^2 = e_a^2 + e_b^2$$

$$\text{or } e_{a/b}^2 = e_a^2 + e_b^2 \quad (e = \text{relative st. deviation; i.e. } e_a = S_a/a)$$

E.2. $^{87}\text{Sr}/^{86}\text{Sr}$ RATIOS FROM MASS-SPECTROMETRIC MEASUREMENTS

Program P2ZSR:-

Input counts on mass values 88/87/86/85½(bg)/85(Bg + Rb)

Calculate mean counts & variance for 85½ & 85 peaks over 10 cycles

If 85½ & 85 are significantly different, contribution of Rb to 85 peak, and therefore to 87 peak, calculated

88, 87, 86 peak counts corrected for mean background

Peak counts interpolated back to single moment (at measurement of 86 peak) in each cycle to correct for growth

$^{86}/^{88}$, $^{87}/^{86}$ (corrected for Rb interference) & $^{87}/^{86}$ (Rb-corrected & normalised to $^{86}/^{88} = 0.1194$ to correct for fractionation) ratios calc.

Program PIMEAN

Input N values of $^{87}/^{86}$ ratio, X_n , each from set of 10 cycles

Calculate mean $^{87}/^{86}$ ratio, $\sum_n X_n / N = \bar{X}$

Calculate root mean square deviation of X values in distribution
$$\sigma = \left\{ \frac{\sum_n (X_n - \bar{X})^2}{(N-1)} \right\}^{\frac{1}{2}}$$

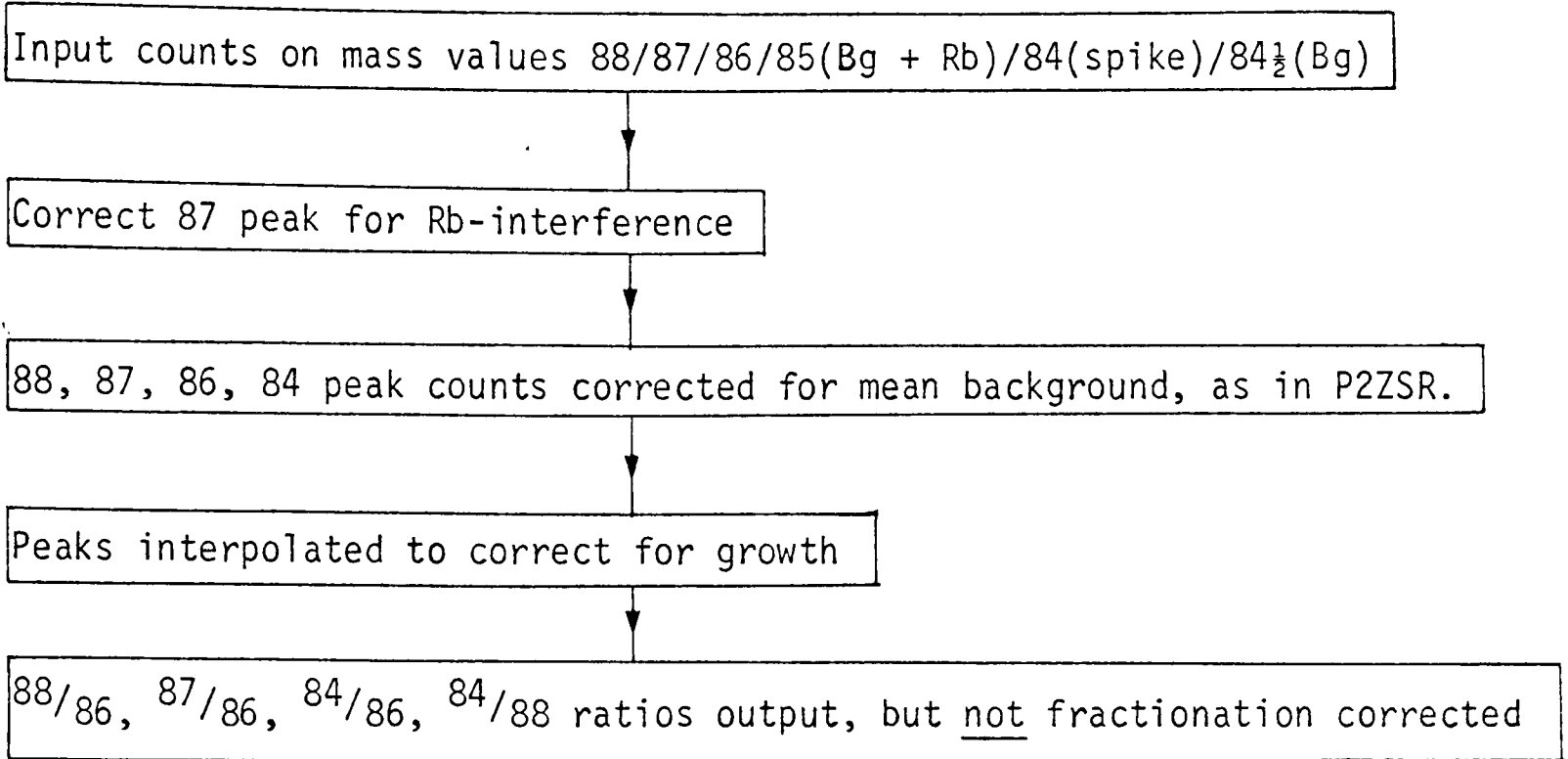
Estimated standard error associated with \bar{X}

$$\sigma_{\text{mean}} = \frac{\sigma}{N^{\frac{1}{2}}} = \left\{ \frac{\sum_n (X_n - \bar{X})^2}{N(N-1)} \right\}^{\frac{1}{2}}$$

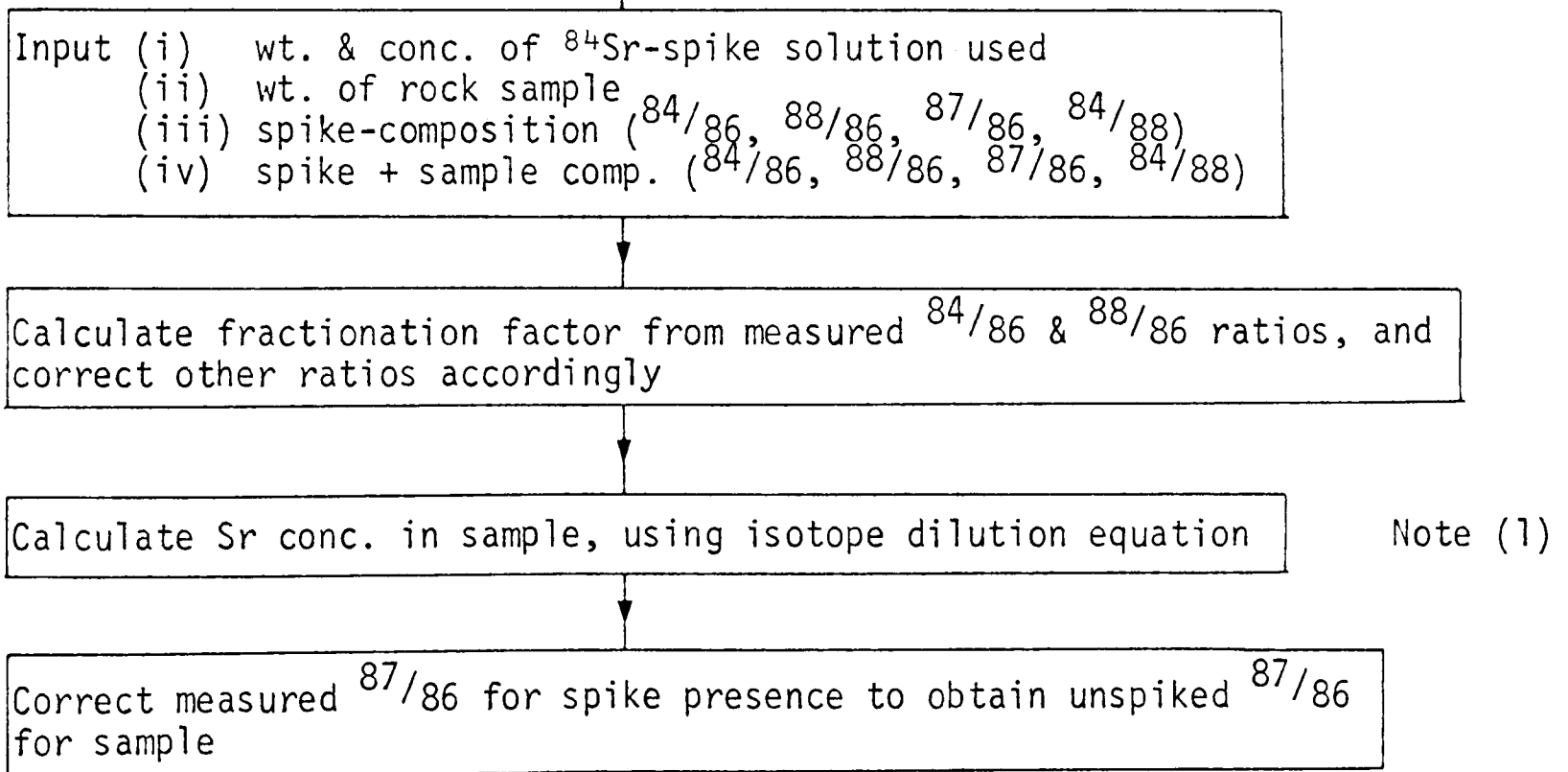
Output \bar{X} , σ , σ_{mean} values

E.3. Sr CONCENTRATIONS & $^{87}\text{Sr}/^{86}\text{Sr}$ RATIOS BY ISOTOPE DILUTION

Program PMZ84SR:-



Program PS841D:-



Note (1)

Note (1): General equation for isotope dilution analysis:-

$$\mu\text{g}(\text{Sr})_{\text{sample}} = \mu\text{g}(\text{Sr})_{\text{spike}} \times \frac{[(^{84}/^{88})_{\text{spike}} - (^{84}/^{88})_{\text{meas}}]}{[(^{84}/^{88})_{\text{meas}} - (^{84}/^{88})_{\text{normal}}]}$$

$$\times \frac{(\text{At. wt. Sr})_{\text{normal}}}{(\text{At. wt. Sr})_{\text{spike}}}$$

E.4. Rb CONCENTRATIONS BY ISOTOPE DILUTION

Program P87RBID:-

Input (i) wt. & conc. of ^{87}Rb -spike solution used
(ii) wt. of rock sample
(iii) $^{87}/^{85}$ ratios of spike & normal
(iv) measured $^{87}/^{85}$ (corrected for background)

Calculate Rb conc. in sample, using isotope dilution equation

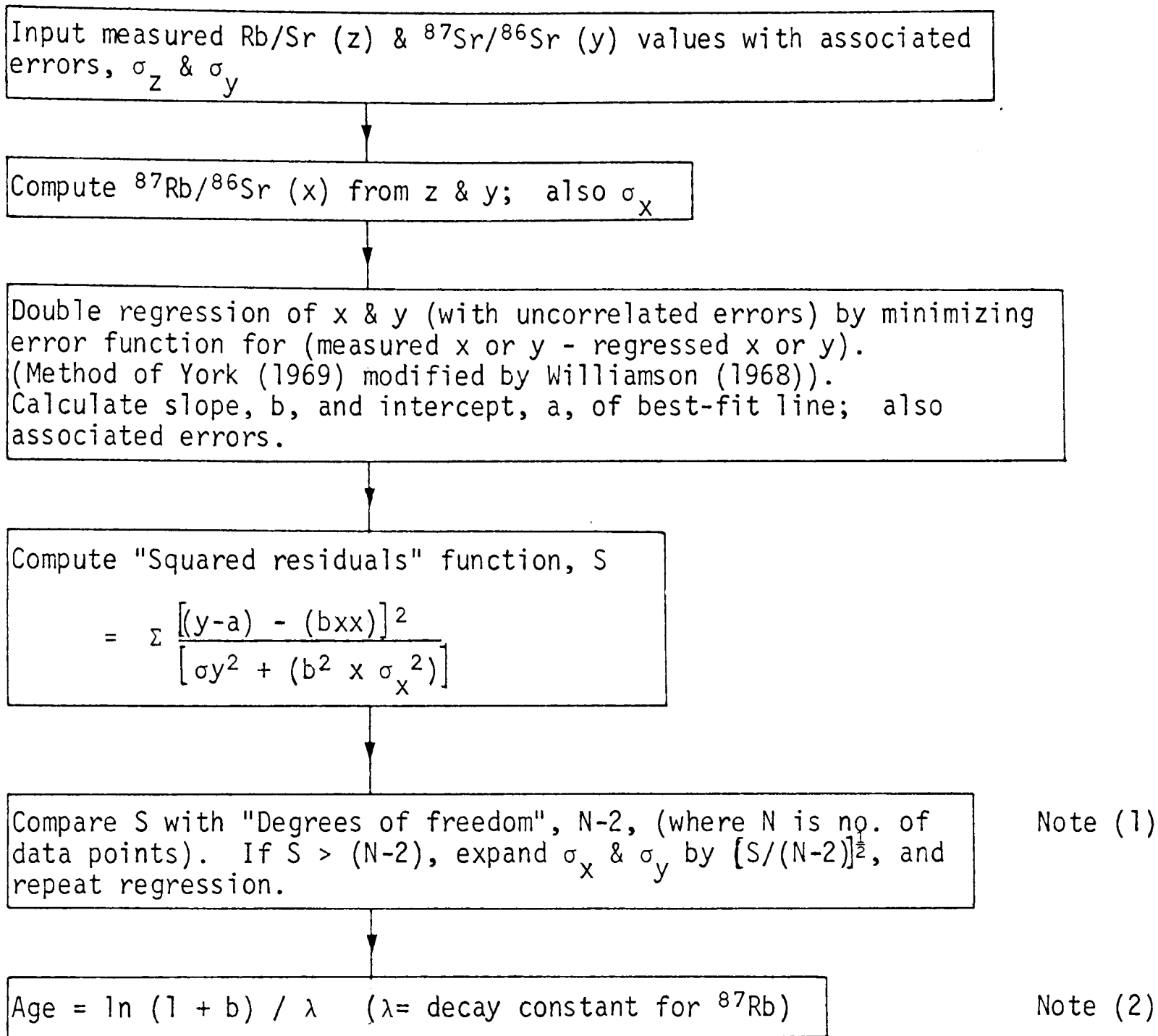
Note (1)

Note (1): Equation for isotope dilution analysis:-

$$\mu\text{g(Rb)}_{\text{sample}} = \mu\text{g(Rb)}_{\text{spike}} \times \frac{[(^{87}/^{85})_{\text{spike}} - (^{87}/^{85})_{\text{meas}}]}{[(^{87}/^{85})_{\text{meas}} - (^{87}/^{85})_{\text{normal}}]} \times \frac{(\text{At. wt. Rb})_{\text{normal}}}{(\text{At. wt. Rb})_{\text{spike}}}$$

E.5. ISOCHRON REGRESSION

Program P2CHRON:-



Note (1): Mean source of weighted deviates, MSWD, = S/(N-2).
When MSWD < 1, clearly there is a complete linear fit.
However, MSWD > 1 may still represent isochron behaviour
(see, for instance, MacIntyre et al., 1966).

Note (2): In this study, $\lambda = 1.39 \times 10^{-11} \text{ yr}^{-1}$
Other commonly used value is $1.47 \times 10^{-11} \text{ yr}^{-1}$ (i.e.
giving ages ~ 6% lower), see Chapter 1.

APPENDIX F

DIFFUSION COEFFICIENT COMPUTATIONS

Two idealized diffusion models may be applied to layer silicates: diffusion in a cylinder (i.e. radially in all directions perpendicular to the cylinder axis) and diffusion in a plate (i.e. perpendicular to the face of the plate). These two models are compared by Hofmann and Giletti (1970) and Hofmann et al. (1974), who show that, whilst absolute values for diffusion coefficients may differ significantly between the two geometries, the temperature dependence is little affected. For the purposes of computation in the present study, a cylindrical diffusion model is assumed.

Crank (1956, pp.70-73) has derived equations (based on Ficks Laws of diffusion) to describe diffusional transport out of an infinite cylinder into a stirred solution of limited volume, and approximations of his formulae will be applied in the present case to determine diffusion coefficients.

If the amount of Sr or Rb lost from the cylinder in time t is M_t , and the amount lost after infinite time (i.e. the equilibrium distribution) is M_∞ , then, to a first approximation:

$$\frac{M_t}{M_\infty} = \frac{4}{\alpha\pi^{\frac{1}{2}}} (1+\alpha) \left(\frac{Dt}{a^2}\right)^{\frac{1}{2}}$$

where α is the ratio of volumes of solution and cylinder

D is the cylindrical diffusion coefficient

and a is the radius of the cylinder

In the present case, we are dealing with a great number of particles, rather than a single infinite cylinder, but we may group them together as an infinite cylinder with radius half the estimated diameter of the particles. (This, of course, assumes that the contribution to net diffusional transport of movement across layers, parallel to the cylinder axis, is

small). In the present experiments, the size fraction used is in the range 0.2-1 μm , and therefore we may assign a mean value of 0.3 μm to a .

The ratio of solution to solid volumes, α , is calculated from the weights of solid and fluid used in each experiment. An approximate mean specific gravity for the solid phases of 2.5 is assumed.

A value is easily attributed to M_∞ for this form of experiment. Since the amount lost after time t , M_t , is effectively measured as the amount of Sr or Rb from the substrate which has homogenized with that in the fluid (i.e. the 'spike'), then M_∞ represents complete isotopic homogenization in the system. Therefore M_∞ would be measured as loss of the total Sr and Rb contents of the substrate to the fluid.

From the above formula, therefore, it is possible to compute a value for D/a^2 for the hypothetical case where all Sr or Rb loss is accounted for by volume diffusion out of an infinite cylinder. Assuming a to be adequately represented by the mean grain size, D may then be calculated.

REFERENCES

- Allsopp, H.L., Ulrych, T.J. & Nicolaysen, L.O., 1968. Dating some significant events in the history of the Swaziland System by the Rb-Sr isochron method. *Can. J. Earth Sci.*, 5, 605-619.
- Armstrong, R.L. & McDowell, W.G., 1974. Proposed refinement of the Phanerozoic time-scale. Abs., Intl. Meeting for Geochronology, Cosmochronology & Isotope Geology, Paris.
- Baker, J.W., 1971. The Proterozoic history of Southern England. *Proc. Geol. Assoc.*, 82, 249-266.
- _____ 1973. A marginal late Proterozoic ocean basin in the Welsh region. *Geol. Mag.*, 110, 447-455.
- Berner, R.A., 1971. *Principles of Chemical Sedimentology*. McGraw-Hill, N.Y., 240pp.
- Biscaye, P.E., 1964. Distinction between kaolinite and chlorite in recent sediments by X-ray diffraction. *Am. Mineralogist*, 49, 1281-1289.
- _____ 1965. Mineralogy and sedimentation of recent deep-sea clay in the Atlantic Ocean and adjacent seas and oceans. *Geol. Soc. Am. Bull.*, 76, 803-832.
- _____ & Dasch, E.J., 1971. The rubidium, strontium, Sr-isotope system in deep-sea sediments: Argentine Basin. *J. Geophys. Res.*, 76, 5087-5096.
- Bofinger, V.M., Compston, W. & Vernon, M.J., 1968. The application of acid leaching to the Rb-Sr dating of a Middle Ordovician shale. *Geochim. Cosmochim. Acta*, 32, 823-833.
- _____, _____ & Gulson, B.L., 1970. A Rb-Sr study of the Lower Silurian State Circle Shale, Canberra, Australia. *Geochim. Cosmochim. Acta*. 34, 433-445.
- Brookins, D.G. & Chaudhuri, S., 1973. Comparison of K-Ar and Rb-Sr age determinations for Eskridge and Stearns Shales (Early Permian), Eastern Kansas. *Bull. Am. Ass. Petrol. Geol.*, 57, 520-527.

- Brown, G. (ed.), 1961. X-ray identification and crystal structures of clay minerals. Mineralogical Society, London.
- Burst, J.F., 1969. Diagenesis of Gulf Coast clayey sediments and its possible relation to petroleum migration. Bull. Am. Ass. Petrol. Geol., 53, 73-93.
- Cantrill, T.C., Dixon, E.E.L., Thomas, H.H. & Jones, O.T., 1916. The Geology of the South Wales Coalfield - Part XII. The Country around Milford. Sheet 227, Mem. Geol. Surv. G.B., 185 pp.
- Chaudhuri, S. & Brookins, D.G., 1969. The Rb-Sr whole-rock age of the Stearns Shale (Lower Permian), Eastern Kansas, before and after acid leaching experiments. Bull. Geol. Soc. Am., 80, 2605-2610.
- Clauer, N., 1973. Utilisation de la méthode Rb-Sr pour la datation de niveaux sédimentaires du Précambrien Supérieur de l'Adrar Mauretarien (Sahara occidental) et la mise en évidence de transformations précoces des minéraux argileux. Geochim. Cosmochim. Acta, 37, 2243-2256.
- _____ & Bonhomme, M., 1970. Datations Rb/Sr dans les schistes de Steige et la Série de Villé (Vosges). Bull. Serv. Carte Géol. Alsace Lorraine, 23, 191-208.
- Cobbold, E.S. & Whittard, W.F., 1935. The Helmeth Grits of the Caradoc range, Church Stretton; their bearing on part of the Precambrian succession of Shropshire. Proc. Geol. Assoc., 46, 348-359.
- Cocks, L.R.M. & Walton, G., 1968. A large temporary exposure in the Lower Silurian of Shropshire. Geol. Mag., 105, 390-397.
- Compston, W. & Pidgeon, R.T., 1962. Rb-Sr dating of shales by the total rock method. J. Geophys. Res., 67, 3493-3502.
- Cowie, J.W., Rushton, A.W.A. & Stubblefield, C.J., 1972. A Correlation of Cambrian Rocks in the British Isles. Geol. Soc. Lond., Special Report No. 2, 42 pp.
- Crank, J., 1956. Mathematics of Diffusion. Oxford Univ. Press, 350 pp.

- Creer, K.M., 1957. Palaeomagnetic investigations in Great Britain - IV. The natural remanent magnetization of certain stable rocks from Great Britain. *Phil. Trans. R. Soc. (A)*, 250, 111-129.
- Dasch, E.J., 1969. Strontium isotopes in weathering profiles, deep-sea sediments, and sedimentary rocks. *Geochim. Cosmochim. Acta*, 33, 1521-1552.
- Degens, E.T., 1965. *Geochemistry of Sediments - a Brief Survey*. Prentice-Hall Inc., N.J., 342 pp.
- Dewey, J.F., 1969. Evolution of the Appalachian/Caledonian orogen. *Nature, Lond.*, 222, 124-129.
- Dodson, M.H. & Rex, D.C., 1971. Potassium-argon ages of slates and phyllites from south-west England. *Q. Jl. Geol. Soc.*, 126, 465-499.
- Doe, B.R., Hedge, C.E. & White, D.E., 1966. Preliminary investigation of the source of Pb and Sr in deep geothermal brines underlying the Salton Sea Geothermal area. *Econ. Geol.*, 61, 462-483.
- Dunoyer de Segonzac, G., 1970. The transformation of clay minerals during diagenesis and low-grade metamorphism: a review. *Sedimentology*, 15, 281-346.
- _____, Ferrero, J. & Kubler, B., 1968. Sur la cristallinité de l'illite dans la diagenèse et l'anchimétamorphisme. *Sedimentology*, 10, 137-143.
- Earp, J.R. & Hains, A., 1971. *British Regional Geology - The Welsh Borderland*. H.M.S.O., London, 118 pp.
- Evernden, J.F., Curtis, G.K., Obradovitch, J. & Kistler, R., 1961. On the evaluation of glauconite and illite for dating sedimentary rocks by the potassium-argon method. *Geochim. Cosmochim. Acta*, 23, 78-99.
- Faure, G. & Kovach, J., 1969. The age of the Gunflint Formation of the Animikie Series in Ontario, Canada. *Bull. Geol. Soc. Am.*, 80, 1725-1736.
- _____ & Powell, J.L., 1972. *Strontium Isotope Geology*. Springer-Verlag, N.Y., 188 pp.

- Fitch, F.J., Miller, J.A., Evans, A.L., Grasty, R.L. & Meneisy, M.Y., 1969. Isotopic age determinations on rocks from Wales and the Welsh Borders. In The Precambrian and Lower Palaeozoic Rocks of Wales, Wood, A. (ed.), Univ. of Wales Press, pp.23-45.
- Flynn, K.F. & Glendenin, L.E., 1959. Half-life and beta spectrum of ^{87}Rb . Phys. Rev., 116, 744-748.
- Frey, M., 1970. The steps from diagenesis to metamorphism in pelitic rocks during Alpine orogenesis. Sedimentology, 15, 261-280.
- Fullager, P.D. & Bottino, M.L., 1968. Rb-Sr whole-rock ages of Silurian-Devonian volcanics from Eastern Maine. Trans. Amer. Geophys. Union, 49, 346.
- Gebauer, D. & Gr"unenfelder, M., 1973. U-Pb zircon and Rb-Sr systems during progressive metamorphism. Abs., ECOG 72, Fortschritte der Mineralogie, 50, 76-78.
- George, T.N., 1970. British Regional Geology - South Wales. H.M.S.O., London, 152 pp.
- Gibbs, R.J., 1965. Errors due to segregation in quantitative clay mineral X-ray diffraction mounting techniques. Am. Mineralogist, 50, 741-751.
- _____ 1967. Quantitative X-ray diffraction analysis using clay mineral standards extracted from the samples to be analysed. Clay Minerals, 7, 79-90.
- _____ 1968. Clay mineral mounting techniques for XRD analysis. J. Sediment. Petrol., 38, 242-243.
- Greig, D.C., Wright, J.E., Hains, B.A. & Mitchell, G.H., 1968. Geology of the Country around Church Stretton, Craven Arms, Wenlock Edge and Brown Clee. Mem. Geol. Surv. G.B., 379 pp.
- Grim, R.E., 1953. Clay Mineralogy. McGraw-Hill, London, 368 pp.
- Hamilton, E.I., 1965. Applied Geochronology. Academic Press, London, 250 pp.
- Harland, W.B., Francis, E.H. & Evans, P., 1971. The Phanerozoic Time-scale - a Supplement. Special Publication of the Geol. Soc. No.5, London, 356 pp.
- Harper, C.T., 1964. K-Ar ages of slates and their geological significance. Nature, Lond., 203, 468-470.

- Harper, C.T., 1965. A K-Ar isotopic age study of the British Caledonides. Unpubl. D.Phil. thesis, Oxford Univ.
- Helgeson, H.C., 1967. Solution chemistry and metamorphism. In Researches in Geochemistry, Vol.2, Abelson, P.H. (ed.), J. Wiley, N.Y., pp. 362-404.
- _____ 1970. A chemical and thermodynamic model of ore deposition in hydrothermal systems. In 50th Anniv. Symposia, Min. Soc. of Am. Spec. Report, No.3, pp.155-186.
- _____ 1971. Kinetics of mass transfer among silicates and aqueous solutions. Geochim. Cosmochim. Acta, 35, 421-470.
- Herzog, L.F., Pinson, W.H. & Cormier, R.F., 1958. Sediment age determination by Rb/Sr analysis of glauconite. Bull. Am. Ass. Petrol. Geol., 42, 717-733.
- Hofmann, A.W. & Gilletti, B.J., 1970. Diffusion in minerals under hydrothermal conditions. Eclogae Geol. Helv., 63, 141-150.
- _____, Hart, S.R. & Hare, P.E., 1972. $^{87}\text{Sr}/^{86}\text{Sr}$ ratios of pore fluids from deep-sea cores. Ann. Rep. Dir. Geophys. Lab., Washington, 1971-72, pp.563-564.
- _____, Mahoney, J.W. & Gilletti, B.J., 1974. K-Ar and Rb-Sr data on detrital and postdepositional history of Pennsylvanian clay from Ohio and Pennsylvania., Bull. Geol. Soc. Am., 85, 639-644.
- Howell, B.F. & Stubblefield, C.J., 1950. A revision of the fauna of the north Welsh Concoryphe viola beds implying a Lower Cambrian age. Geol. Mag., 87, 1-16.
- Hower, J., Hurley, P.M., Pinson, W.H. & Fairbairn, H.W., 1963. The dependence of K-Ar age on the mineralogy of various particle size ranges in a shale. Geochim. Cosmochim. Acta, 27, 405-410.
- Huang, W.H. & Keller, W.D., 1973. Gibbs free energies of formation calculated from dissolution data using specific mineral analyses - III. Clay minerals. Am. Mineralogist, 58, 1023-1028.

- Hunziker, J.C., 1970. Polymetamorphism in the Monte Rosa, Western Alps. *Eclogae Geol. Helv.*, 63, 151-161.
- Hurley, P.M., Cormier, R.F., Hower, J. & Fairbairn, H.W., 1960. Reliability of glauconite for age measurements by K-Ar and Rb-Sr methods. *Bull. Am. Ass. Petrol. Geol.*, 44, 1793-1808.
- Jäger, E., 1970. Rb-Sr systems in different degrees of metamorphism. *Eclogae Geol. Helv.*, 63, 163-172.
- James, J.H., 1956. The structure and stratigraphy of part of the Precambrian outcrop between Church Stretton and Linley, Shropshire. *Q. Jl. Geol. Soc.*, 112, 315-337.
- Johns, W.D., Grim, R.E. & Bradley, W.F., 1954. Quantitative estimation of clay minerals by diffraction methods. *J. Sediment. Petrol.*, 24, 242-251.
- Kharaka, Y.K. & Berry, F.A.F., 1973. Simultaneous flow of water and solutes through geological membranes - I. Experimental investigation. *Geochim. Cosmochim. Acta*, 37, 2577-2603.
- Kubler, B., 1968. Évaluation quantitative du métamorphisme par la cristallinité de l'illite. *Bull. Centre Rech. Pau - SNPA*, 2, 385-397.
- Kulp, J.L., Turekian, K.K. & Boyd, D.W., 1952. Sr content of limestones and fossils. *Bull. Geol. Soc. Am.*, 63, 701-716,
- Lambert, R. St J., 1971. The pre-Pleistocene Phanerozoic time-scale - a Review. In Part I of The Phanerozoic Time-Scale - a Supplement, Harland, W.B. & Francis, E.H. (eds.). Spec. Pub. of Geol. Soc. No. 5, London, pp.9-31.
- Lapworth, C., 1888. On the discovery of the Olenellus fauna in the Lower Cambrian rocks of Britain. *Geol. Mag.*, 5, 484-487.
- _____ & Watts, W.W., 1910. Shropshire. *Geol. Assoc. Jubilee Vol.*, 739-769.
- Li, Y-H & Gregory, S., 1974. Diffusion of ions in sea-water and in deep-

- sea sediments. *Geochim. Cosmochim. Acta*, 38, 703-714.
- MacIntyre, G.A., Brooks, C., Compston, W. & Turek, A., 1966. The statistical assessment of Rb-Sr isochrons. *J. Geophys. Res.*, 71, 5459-5468.
- Matley, C.A. & Wilson, T.S., 1946. The Harlech Dome, north of the Barmouth Estuary. *Q. Jl. Geol. Soc.*, 102-1-140.
- McNutt, R.H., 1964. A study of strontium redistribution under controlled conditions of temperature and pressure. M.I.T. Dept. Geol. & Geophys., U.S.A.E.C., 12th Ann. Rep. AT (30-1), 1381, 125-157.
- Millot, G., 1970. *Geology of Clays*. Springer-Verlag, N.Y.
- Moorbath, S., 1969. Evidence for the age of deposition of the Torridonian sediments of N.W. Scotland. *Scottish J. Geol.*, 5, 154-170.
- _____ & Shackleton, R.M., 1966. Isotopic ages from the Precambrian Mona complex of Anglesey, North Wales (G.B.). *Earth Planet. Sci. Lett.*, 1, 113-117.
- _____, O'Nions, R.K. & Pankhurst, R.J., 1973. Early Archaean age for the Isua Iron formation, West Greenland. *Nature, Lond.*, 245, 138-139.
- van Moort, J.C., 1971. A comparative study of the diagenetic alteration of clay minerals in Mesozoic shales from Papua, New Guinea, and in Tertiary shales from Louisiana, U.S.A. *Clays & Clay Minerals*, 19, 1-20.
- Morris, T.O. & Fearnside, W.G., 1926. The stratigraphy and structure of the Cambrian slate-belt of Nantlle (Caernarvonshire). *Q. Jl. Geol. Soc.*, 82, 250-303.
- Muffler, L.J.P. & White, D.E., 1969. Active metamorphism of Upper Cenozoic sediments in the Salton Sea geothermal fluid and the Salton Trough, Southeastern California. *Bull. Geol. Soc. Am.*, 80, 157-182.
- Nicolaysen, L.O., 1961. Graphic interpretation of discordant age measure-

- ments of metamorphic rocks. *Ann. N.Y. Acad. Sci.*, 91, 198-206.
- Nier, A.O., 1938. The isotopic constitution of Sr, Ba, Bi, Tl and Mg. *Phys. Rev.*, 54, 275-278.
- _____ 1950. A redetermination of the relative abundances of the isotopes of neon, krypton, rubidium, xenon and mercury. *Phys. Rev.*, 79, 450-454.
- Nuffield, E.W., 1966. *X-ray Diffraction Methods*. J. Wiley, N.Y., 409 pp.
- Obradovitch, J.D. & Peterman, Z.E., 1968. Geochronology of the Belt Series, Montana. *Can. J. Earth Sci.*, 5, 737-747.
- O'Nions, R.K., Morton, R.D. & Baadsgaard, H., 1969. K-Ar ages from the Bamble sector of the Fennoscandian shield in South Norway. *Norsk Geol. Tidsskr.*, 49, 171-190.
- _____ & Pankhurst, R.J., 1973. Secular variation in the Sr-isotope composition of Icelandic volcanic rocks. *Earth Planet. Sci. Lett.*, 21, 13-21.
- _____, Oxburgh, E.R., Hawkesworth, C.J. & MacIntyre, R.M., 1973. New isotopic and stratigraphical evidence on the age of the Ingletonian: probable Cambrian of northern England. *Jl. Geol. Soc. Lond.*, 129, 445-452.
- Pankhurst, R.J. & O'Nions, R.K., 1973. Determination of Rb/Sr and $^{87}\text{Sr}/^{86}\text{Sr}$ ratios of some standard rocks and evaluation of X-ray fluorescence spectrometry in Rb-Sr geochemistry. *Chem. Geol.*, 12, 127-136.
- Papanastassiou, D.A., 1970. The determination of small time differences in the formation of planetary objects. Unpubl. thesis, Divn. of Geol. & Planet. Sciences, Cal. Inst. of Tech.
- Parrish, W., 1958. Advances in X-ray diffractometry of clay minerals. *Proc. 7th National Clay Conf.*, Washington, pp.230-259.
- Perry, E.A. & Hower, J., 1970. Burial diagenesis in Gulf Coast pelitic sediments. *Clays & Clay Minerals*, 18, 165-177.

- Perry, E.A. & Hower, J., 1972. Late-stage dehydration in deeply buried pelitic sediments. *Bull. Am. Ass. Petrol. Geol.*, 56, 2013-2021.
- _____ & Turekian, K.K., 1974. The effects of diagenesis on the redistribution of Sr-isotopes in shales. *Geochim. Cosmochim. Acta*, 38, 929-935.
- Peterman, Z.E., 1966. Rb-Sr dating of middle Precambrian metasedimentary rocks of Minnesota. *Bull. Am. Ass. Petrol. Geol.*, 77, 1031-1044.
- _____, Hedge, C.E. & Tourtelot, H.A., 1970. Isotopic composition of Sr in sea-water throughout Phanerozoic time. *Geochim. Cosmochim. Acta*, 34, 105-120.
- Pierce, J.W. & Siegel, F.R., 1969. Quantification in clay mineral studies of sediments and sedimentary rocks. *J. Sediment. Petrol.*, 39, 187-194.
- Pringle, I.R., 1973. Rb-Sr age determinations on shales associated with the Varanger Ice Age. *Geol. Mag.*, 109, 465-472.
- Reynolds, R.C. & Hower, Y., 1970. The nature of interlayering in mixed-layer illite-montmorillonite. *Clays & Clay Minerals*, 18, 25-36.
- Rushton, A.W.A., 1974. The Cambrian of Wales and England. In *Cambrian of the British Isles, Norden, and Spitsbergen*. Holland, C.H. (ed.). J. Wiley, London, pp. 43-121.
- Russell, K.L., 1970. Geochemistry and halmyrolysis of clay minerals, Rio Ameca, Mexico. *Geochim. Cosmochim. Acta*, 34, 893-907.
- Sanzen-Baker, I., 1972. Stratigraphical relations and sedimentary environments of the Silurian - Early Old Red Sandstone of Pembrokeshire. *Proc. Geol. Assoc.*, 83, 139-164.
- Schultz, L.G., 1964. Quantitative interpretation of mineralogical composition from X-ray and chemical data for the Pierre Shale. U.S.G.S. Prof. Paper 391-C.
- Shaw, H.F., 1971. The clay mineralogy of recent sediments in the Wash, Eastern England. Unpubl. Ph.D. thesis, Univ. of London.

- Shaw, H.F., 1972. The preparation of oriented clay mineral specimens for XRD analysis by a suction-onto-ceramic tile method. *Clay Minerals*, 9, 349-350.
- _____ 1973. Clay mineralogy of quaternary sediments in the Wash embayment, Eastern England. *Marine Geology*, 14, 29-45.
- Smith, B. & George, T.N., 1961. *British Regional Geology - North Wales*. H.M.S.O. London, 3rd Ed., 97pp.
- Spears, D.A., 1974. The Rb-Sr dating of some Carboniferous shales. *Geochim. Cosmochim. Acta*, 38, 235-244.
- Takahishi, H., 1959. Effects of dry grinding on kaolin minerals. *Bull. Chem. Soc. Japan*, 32, 235,263.
- Tanner, C.B. & Jackson, M.L., 1947. Nomographs of sedimentation times for soil particles under gravity or centrifugal acceleration. *Soil Sci. Soc. of Am. Proc. for 1947*, 60-65.
- Taylor, S.R., 1965. The applications of trace element data to problems in petrology. In *Physics & Chemistry of the Earth*. Ahrens, L.A., Press, F., Runcorn, S.K. & Urey, C. (eds.), Vol.6, Oxford: Pergamon Press, pp.133-214.
- Velde, B. & Hower, J., 1963. Petrological significance of illite polymorphism in Palaeozoic sedimentary rocks. *Am. Mineralogist*, 48, 1239-1254.
- Wasserburg, G.J., Hayden, R.J. & Jensen, K.J., 1956. ^{40}Ar - ^{40}K dating of igneous rocks and sediments. *Geochim. Cosmochim. Acta*, 10, 153-165.
- Weaver, C.E., 1959. The clay petrology of sediments. In *Clays & Clay Minerals*, Proc. 6th Natl. Conf. on Clay Minerals, pp.159-173.
- _____ 1967. Significance of clay minerals in sediments. In *Fundamental Aspects of Petroleum Geology*. Nagy, B & Columbo, U (eds.), Elsevier, Amsterdam, pp.37-75.
- _____ & Beck, K.C., 1971. Clay water diagenesis during burial: How mud becomes gneiss. *Geol. Soc. of Am. Spec. Paper 134*, 96 pp.
- Whitney, P.R. & Hurley, P.M., 1964. The problem of inherited radiogenic

Sr in sedimentary age determinations. *Geochim. Cosmochim. Acta*, 28, 425-435.

Wood, D.S., 1969. The base and correlation of the Cambrian rocks of North Wales. In *The Precambrian and Lower Palaeozoic Rocks of Wales*, Wood. A. (ed.), Univ. of Wales Press, pp.47-65.

Yoder, H.S. & Eugster, H.P., 1955. Synthetic and natural muscovites. *Geochim. Cosmochim. Acta*, 8, 225-280.

Ziegler, A.M., Cocks, L.R.M. & McKerrow, W.S., 1968. The Llandovery transgression of the Welsh Borderland. *Palaeontology*, 11, 736-782.

_____, McKerrow, W.S., Burne, R.V. & Baker, P.E., 1969. Correlation and environmental setting of the Skomer Volcanic Group, Pembrokeshire. *Proc. Geol. Assoc.*, 80, 409-439.

Zussman, J., 1967. X-ray Diffraction. In *Physical Methods in Determinative Mineralogy*, Zussman J. (ed.). Academic Press, London, pp.261-334.